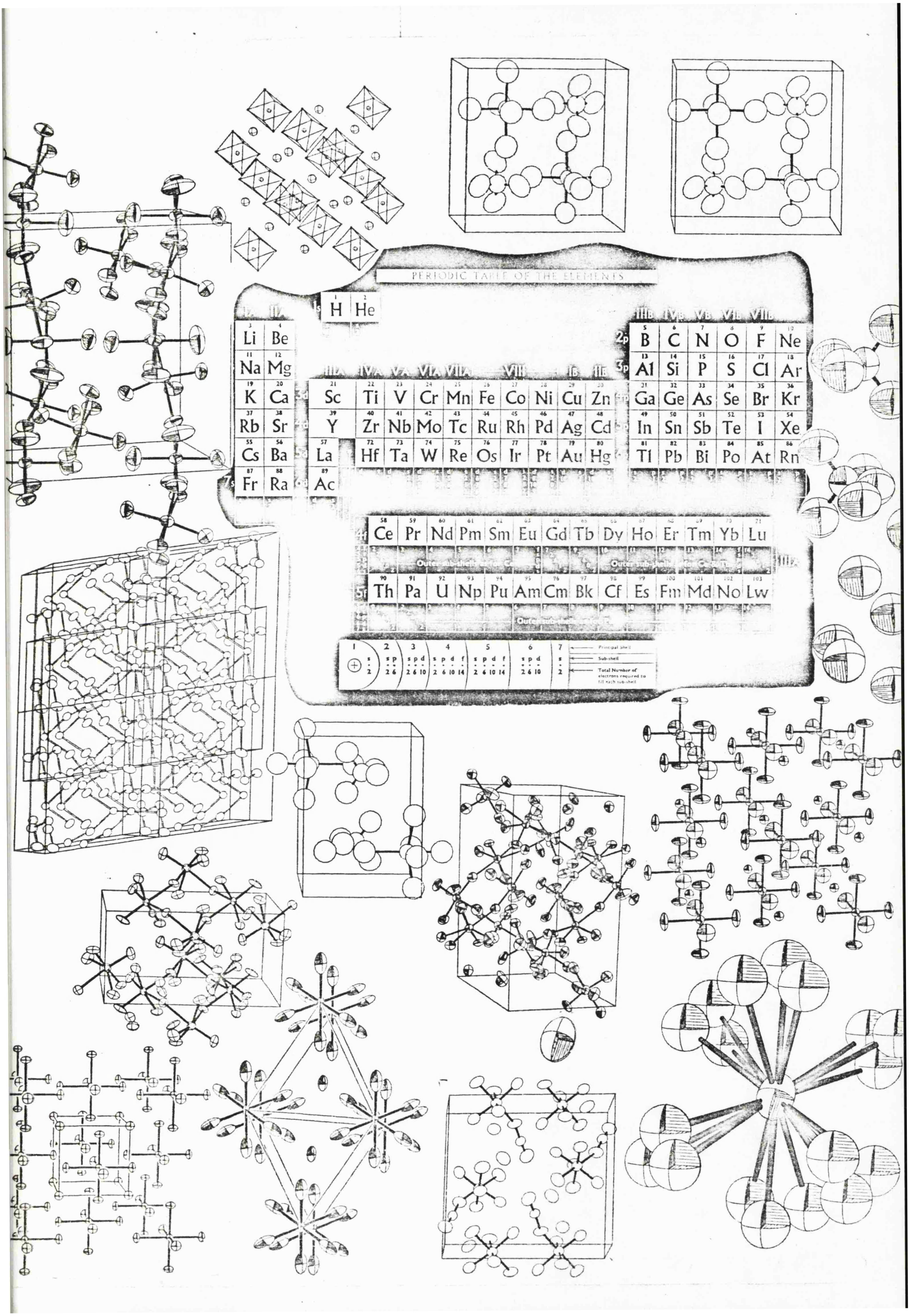
PERIODIC TABLE OF THE ELEMENTS
H He
Li Be B C N O F Ne
Na Mg Al Si P S Cl Ar
K Ca Sc Ti V Cr Mn Fe Co Ni Cu Zn Ga Ge As Se Br Kr
Rb Sr Y Zr Nb Mo Tc Ru Rh Pd Ag Cd In Sn Sb Te I Xe
Cs Ba La Hf Ta W Re Os Ir Pt Au Hg Tl Pb Bi Po At Rn
Fr Ra Ac
Ce Pr Nd Pm Sm Eu Gd Tb Dy Ho Er Tm Yb Lu
Th Pa U Np Pu Am Cm Bk Cf Es Fm Md No Lw

THE PREPARATION AND CRYSTAL STRUCTURES OF SOME METAL FLUORIDE COMPLEXES

A thesis presented for the degree of Doctor of Philosophy

in the

Faculty of Science

by

JOHN FAWCETT

University of Leicester

March 1980

STATEMENT

The experimental work described in this thesis has been carried out by the author in the Department of Chemistry of the University of Leicester between October 1975 and January 1980, except when otherwise stated. The work has not been submitted, and is not currently being submitted, for any other degree at this or any other university.

J. Fawcett

March 1980

Parts of this work have been published or are being submitted for publication as follows:

Sur L'exsistence de Nouveaux Composés D'addition de L'Oxytetrafluorure D'Uranium. Preparation des Composés $UF_4O.nSbF_5$ (n = 1, 2 ou 3) et structure crystalline de $UOF_4.2SbF_5$.
R. Bougon, J. Fawcett, J. H. Holloway, D. R. Russell, C.R. Acad. Sc. Paris, t. 287, 423, 1978.

Interaction between Uranium Oxide Tetrafluoride and Antimony Pentafluoride; Fluorine - 19 Nuclear Magnetic Resonance Investigations in solution; Preparation and characterization of the Adducts $UF_4O.nSbF_5$ (n = 1, 2 or 3) and Crystal Structure of $UF_4O.2SbF_5$.
R. Bougon, J. Fawcett, J. H. Holloway, D. R. Russell, J.C.S. Dalton, 1979, 12, 1881.

The Crystal Structure of Ammonium Hexafluoroplatinate.
J. Fawcett, J. H. Holloway, D. C. Puddick, D. R. Russell, submitted to Acta Cryst., January 1980.

The Preparation and Crystal Structure of Azidopentafluorotungsten.
J. Fawcett, R. D. Peacock, D. R. Russell, submitted to J.C.S. Dalton, February 1980.

Preparation and characterization of the adducts $MF_4O.SbF_5$ (M = Mo or W) and the Crystal Structure of $MoF_4O.SbF_5$.
J. Fawcett, J. H. Holloway, D. R. Russell, in preparation.

ACKNOWLEDGEMENTS

I wish to express my thanks to:

My Supervisor, Dr. David R. Russell, for his continual help and guidance, particularly in the early stages of this work;

Professor R. D. Peacock for his interest and advice, from which several structures in this thesis have arisen;

Dr. John H. Holloway for his continual interest and advice concerning all aspects of my work, and the provision of facilities for the preparative work involved;

The members of the inorganic teaching staff and technical staff of the Chemistry Department for their assistance;

My colleagues in the laboratory, most notably Drs. Boris Frlec and Gary Schrobilgen, from whose collective wisdom and advice I learnt a great deal;

Miss Vicky Orson-Wright and Mrs. Ann Crane for their skills in preparing respectively this typescript and several of the drawings;

Finally, my family for their help and support during this work.

ABSTRACT

The preparation of the adducts formed between antimony pentafluoride and the oxide tetrafluorides of uranium, molybdenum, tungsten and rhenium is described. Structural details from full single crystal X-ray investigations are reported for the adducts $UF_4O.2SbF_5$ and $MF_4O.SbF_5$ (M = Mo or Re). The rhenium adduct forms discrete fluorine bridged rings of the dimer $2(ReF_4O.SbF_5)$, the molybdenum adduct has a polymeric zig-zag chain arrangement, and the $UF_4O.2SbF_5$ structure contains both the ring and chain units in a three-dimensional network. Crystallographic and vibrational spectroscopic evidence indicate a small ionic contribution in the bridging bonds.

The structures of three complex fluorides of the form $A^{I}B^{V}F_6$, previously studied by X-ray powder diffraction, have been redetermined. $NaTaF_6$ and a new triclinic form of (β-) $CsNbF_6$ were studied by X-ray single crystal methods, and $NaWF_6$ by refinement of data from neutron diffraction of the microcrystalline powder. The $NaTaF_6$ structure is found to be consistent with the previously described face centred cubic ($NaSbF_6$) type, however, the $NaWF_6$ structure has been reassigned as primitive cubic (Pa3). Structures of two complex fluorides of the $A^{I}_2B^{IV}F_6$ general form are reported. $(NH_4)_2PtF_6$ was found to be of the face centred cubic (K_2SiF_6) type and K_2OsF_6 of the trigonal (K_2GeF_6) type.

Three structures are described that are considered as incomplete due to unsatisfactory refinement of the fluorine atom positions in apparently disordered structures. For $NF_4.SbF_6$, difficulty was encountered in the refinement of fluorine atom positional parameters about the antimony atom. Similar problems were encountered in the location of the fluorine atoms of the hydroxonium salts $H_3O.MF_6$ (M = Sb or Ta).

Finally the preparation and crystal structure of WF_5N_3, the first azide derivative of a transition metal fluoride are reported. Unsuccessful attempts to isolate MoF_5N_3 and $WF_{6-n}(N_3)_n$ (n ⩾ 2) are also described.

CONTENTS

LIST OF TABLES

LIST OF FIGURES

ABBREVIATIONS

[All temperatures quoted in the text are in ° centigrade]

Genetron 113	-	1,1,2 trichlorotrifluoroethane
Kel-F	-	polytrifluorochloroethylene
F.E.P.	-	tetrafluoroethylene/perfluoropropylene copolymer
P.T.F.E.	-	polytetrafluoroethylene
n.m.r.	-	nuclear magnetic resonance
i.r.	-	infrared
vs	-	very strong
s	-	strong
m	-	medium
w	-	weak
vw	-	very weak
br	-	broad
sh	-	shoulder
p.p.m.	-	parts per million
o.d.	-	outside diameter
i.d.	-	inside diameter
f.c.c.	-	face centred cubic
p.c.	-	primitive cubic
xs	-	excess of
Me	-	methyl

CHAPTER 1

X-ray and Neutron Diffraction

1.1 Introduction

This thesis is concerned with the preparation and structural characterisation of some metal fluoride complexes. Most of the structure determinations used data collected by single crystal X-ray diffraction, however attempts were made to refine data collected by the neutron diffraction of powders. With the improvements in equipment for data collection and the greater availability of computer programs for almost all aspects of refinement, structure determination by single crystal techniques has become increasingly routine. As a consequence, more complex problems may be studied and with greater accuracy than a few decades ago.

For many metal fluoride complexes the effort required to grow good single crystals is as time consuming as the structure determination. Where no single crystals can be grown the required data may be obtained by neutron diffraction and, increasingly, X-ray diffraction, of the micro crystalline powder. Both powder methods give relatively poor convergence of data, and the lack of suitable neutron sources and equipment, is also a disadvantage.

Many texts are available, which describe the theoretical and practical aspects of crystallography upon which this work depends; those found to be most useful are references 1-4.

1.2 Collection of X-ray Data

Intensity data was collected using a Stoe Stadi-2 diffractometer. This is a 2-circle instrument which uses Weissenberg geometry. All data sets were collected using molybdenum radiation, which allows more plane lines to be collected within the limiting sphere than copper.

The stabilised incident beam of X-rays passes through a suitably orientated graphite single crystal monochromator, and the diffracted beam is measured by a scintillation counter connected to a counting chain. The instrument was modified half way through this study and the earlier data sets were collected whilst the instrument was an off-line version. The instructions were then given by a punched tape which contained the information to record the intensities of the reflections for one layer. With the updated on-line instrument, the parameters required for data collection were stored in the memory of a PDP 8/A computer. In all cases, the intensity data collected was for a ω-scan through the reflection, with background scans at initial and final positions. The data was output on paper tape for later processing, chart recording and printout provided a visual check. Since the ω-width of a reflection in Weissenberg geometry is dependent on both μ and T, the ω-scan width was calculated for each reflection by the formula of Freeman _et al._,[5] or for the updated instrument by $\Delta w = A + B$. The diffractometer operations manual[6] gives full details of the equipment and its operation.

1.3 Collection of Neutron Diffraction Data

Neutron diffraction data was collected at A.E.R.E. Harwell, using either the H.R.P.D or P.A.N.D.A diffractometers. The variable wavelength of the neutron source was constant for a given data set and calibrated by a standard nickel sample before the run, typically a wavelength of 1.3 Å would be used. The samples were enclosed in standard 16 mm neutron diffraction cans constructed from vanadium. The can was fixed on a turntable which could be centred by 4 screws, correct slit settings and collimator were found photographically.

A bank of five (HRPD), or nine (PANDA) detectors move about an arc in the plane of 2θ to the sample and neutron beam. The 2θ step scan would normally take two days, and the step increment and time of count at each position may be adjusted to allow a scan of at least 100°. It was found desirable to split the scan into two parts, and allow longer count times for the weaker high-angle reflections. The data was output on paper tape for later processing.

1.4 Computer Programs

Structure determinations depended on a variety of computer programs at various stages. The paper tapes used for controlling data collection with the off-line diffractometer were generated by the program STOTP. The initial work-up of the intensity data was carried out by the program STOWK. This subtracted background intensities, scaled the data, and applied Lorentz[6] and polarisation corrections.[7] A modified version of the program, STOWK 2, applied these corrections to the data from the on-line diffractometer. Absorption corrections to the data were performed by the program ABSCR[8] before refinement or as an option of the full-matrix refinement program SHELX.[9] This was the program most important to this work since it performed all functions required for refinement of the structures. All of the cell-packing diagrams were drawn by the program ORTEP,[10] some ball and stick drawings of molecules used CRTPRJ, a program written by D. R. Russell.

The refinement of data from neutron diffraction involved several programs which performed similar functions to those outlined above. Intensity data from the out of step counters, was sorted and scaled by the program COLLAT.[11] It is then necessary to determine which reflections of the sample contribute to which part of the powder profile pattern. The program PREPRF[12] was used for this purpose before refinement was started, but any significant changes in the unit cell or profile parameters required that this stage should be repeated. The refinement of the structure was performed by the program REFINE[13] which is based on the work and program of Rietveld.[14]

The University main site computer, CDC Cyber 72, was used to run all the above programs. Numerous small programs were available for use on the Cyber 72 in both batch and interactive modes for less complex calculations or the editing and manipulation of files.

1.5 Solution of the Phase Problem and Refinement

Those structures in this study whose heavy atoms were not fixed on special positions were solved by the heavy atom method. The co-ordinates of heavy atoms were found using Patterson maps, an option of the SHELX refinement program, and this allowed sufficiently accurate phasing for the location of the remaining atoms by difference Fourier maps. Most structures had heavy atoms located on special positions with fixed co-ordinates of the appropriate space group, allowing location of the lighter atoms. All structures were refined by least squares and any special features of the solutions are discussed in the relevant chapter.

1.6 Scattering Factors, Dispersion Corrections and Absorption Coefficients

The scattering factors used in SHELX were obtained from International Tables Vol. IV,[15] as were the real and imaginary dispersion corrections. The atomic absorption coefficients were taken from tables of Cromer and Liberman,[16] and then corrected for ^{12}C base.

CHAPTER 2

Experimental Techniques

2.1 General Preparative Techniques

Many of the starting materials used and the majority of the compounds studied are sensitive to air or moisture and required handling either in vacuo or inert atmospheres to prevent decomposition. Metal, glass or fluoroplastic containers were used for reactions and storage. Metal reactors were pumped to 10^{-4} torr, hydrogenated, seasoned with fluorine and re-evacuated before use. All glass and fluoroplastic apparatus was pumped to 5×10^{-5} torr with heating, and seasoned with fluorine or chlorine trifluoride.

Transferences of volatile air sensitive materials were performed in vacuum systems, using either static vacuum conditions with a suitable temperature gradient, or dynamic vacuum. Non-volatile materials were manipulated under a dry nitrogen atmosphere in auto-recirculating positive pressure dry boxes (Lintott Mk III Glove box or VAC HE 42-2 Dri-lab). The atmospheres of both boxes circulated through columns of manganese oxide and molecular sieve to remove oxygen and water. The impurity levels were monitored by a Hersch oxygen meter (Mk II/L) and Elliot moisture meter (model 112). When transferring or particularly weighing small quantities of powders in the dry boxes, static electricity caused difficulties. This problem was alleviated by exposing samples and apparatus to a 4 mCi ^{210}Po α-emitter (type PDV 1 Radiochemical Centre, Amersham, Bucks). Weighings accurate to ±1 mg were performed in the dry box with a Oertling double-pan balance. Where greater accuracy was required the dry box balance was used for approximation, with more accurate weighings before and after dry box transfer on a laboratory balance (Stanton Unimatic CL41 ± 0.1 mg).

Samples not required for immediate use were sealed under vacuum or an argon atmosphere in glass ampoules or F.E.P. tubes. Thermally unstable samples were stored at -196° in a cryostat (British Oxygen Co. Ltd.). Whenever possible volatile samples were stored in glass ampoules with a break seal, in order to free valves for other operations.

2.2 Vacuum Systems

Vacuum line methods were used to prepare all but one of the compounds studied. A metal manifold with high and low vacuum facilities formed the basic system (Figure 1). This was constructed from $\frac{3}{8}$" o.d., $\frac{1}{8}$" i.d. nickel tubing (H. Wiggin and Co., Hereford) and argon arc welded nickel U-traps (~25 cm^3 capacity). AE-30 series, hard drawn stainless steel needle valves, crosses and tees (Autoclave Engineers Inc., Erie, Pennsylvania, U.S.A.) completed the manifold.

The low vacuum system (10^{-2} torr) consisted of a single stage rotary pump with a large metal trap containing soda-lime granules (5-10 mesh) between the pump and the manifold; this removed fluorine and volatile fluorides evacuated. The low vacuum system was used to remove large quantities of gases before opening the manifold to the high vacuum system. The main system vacuum (10^{-4} torr) was maintained by a single stage rotary pump (Genevac type G.R.S.2, General Engineering Co., Radcliffe, Lancs.), mercury diffusion pump and -196° cold trap. Argon and hydrogen could be admitted directly to the manifold from cylinders, and fluorine for seasoning apparatus was contained in welded nickel cans (~1 dm^3 capacity) fitted with AE-30 stainless steel needle valves.

Manifold pressures of plus or minus one atmosphere (0 to 1500 torr ± 5 torr) were measured by a stainless steel Bourdon-tube gauge (type 1F/66 Z, Budenberg Gauge Co. Ltd., Broadheath, Greater Manchester). The vacuum was monitored using a cold cathode Penning ionization gauge (Model 2A, Edwards High Vacuum Ltd., Crawley, West Sussex) measuring

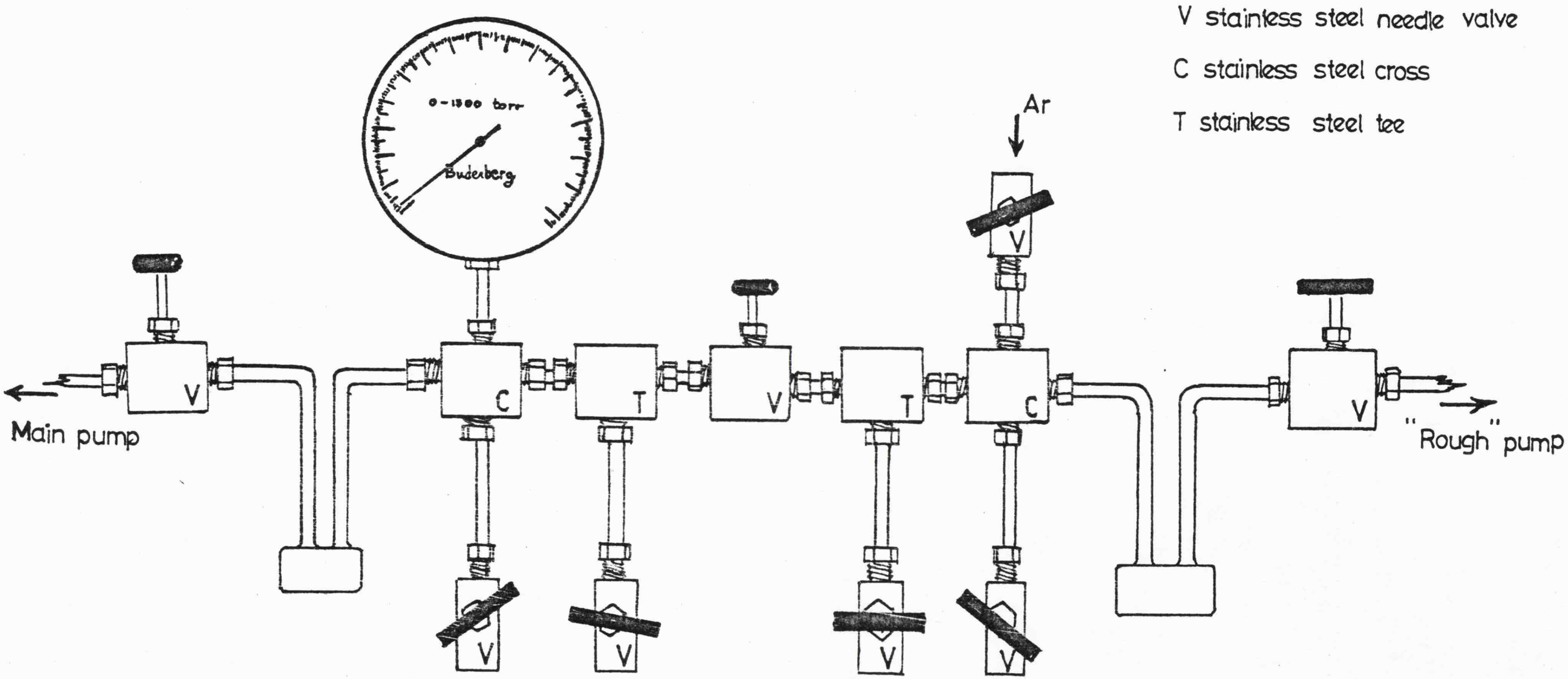

__Figure 1__

The Basic High Vacuum Metal Manifold.

pressures in the range 10^{-2} to 10^{-6} torr.

A variety of metal or fluoroplastic reactors could be attached to the manifold, and Pyrex or silica reactors were designed as required. Glass apparatus was attached to the manifold either by Kovar seals (glass to ¼" o.d. stainless steel) or by precision ¼" o.d. glass fitting into Swagelok compression unions (TFE-400-6, Techmation Ltd., Edgware, Middlesex). Greaseless 'Rotaflo' valves (Quickfit type TF2/13 or TF6/13) with PTFE stems were used where glass valves were required. Fluoroplastic apparatus attached to the manifold through two types of valve. Whitey (type B-1KS4) needle valves, constructed from brass with a PTFE compression seal on to a stainless steel stem. They were attached to the manifold and apparatus through ¼" i.d. compression seals. Kel-F valves were also used, constructed to a design developed at the Argonne National Laboratory, Chicago, Illinois, U.S.A., the body and stem of the valves were fabricated from Kel-F block (Pampus Fluoroplast Ltd., Stoke-on-Trent, Staffordshire). A PTFE packing disc formed a seal between the stem and body which was enclosed in a supporting aluminium case. Small fluoroplastic reactors were fabricated by heating and moulding either 6 mm o.d. Kel-F tubing (Voltalef - Paris) or ¼" o.d. FEP tubing (Trimflex Division, Teleflex Inc., Dover, New Jersey, U.S.A.). Larger reactors of ¾" o.d. Kel-F with approximately 30 cm^3 volume were also available (Argonne).

2.3 Preliminary Treatment of Crystals

Single crystals were all grown from solution of either anhydrous solvent or excess starting material. Most of the compounds studied were moisture sensitive. Having prepared and crystallised samples under rigorously dry conditions it was necessary to isolate and mount suitable single crystals in an inert atmosphere. Crystals were generally of poor quality with, typically, one well defined crystal in a hundred. A Pyrex capillary apparatus (Figure 2) was designed which, after evacuation to 10^{-5} torr and treatment with chlorine trifluoride, could be charged with a sample in a nitrogen atmosphere dry box. The sealed apparatus could then be manipulated under a microscope until selected single crystals were isolated and could be wedged in the capillaries. These were then sealed using a microtorch (model H164/1 Jencons, Hemel Hempstead, Herts).

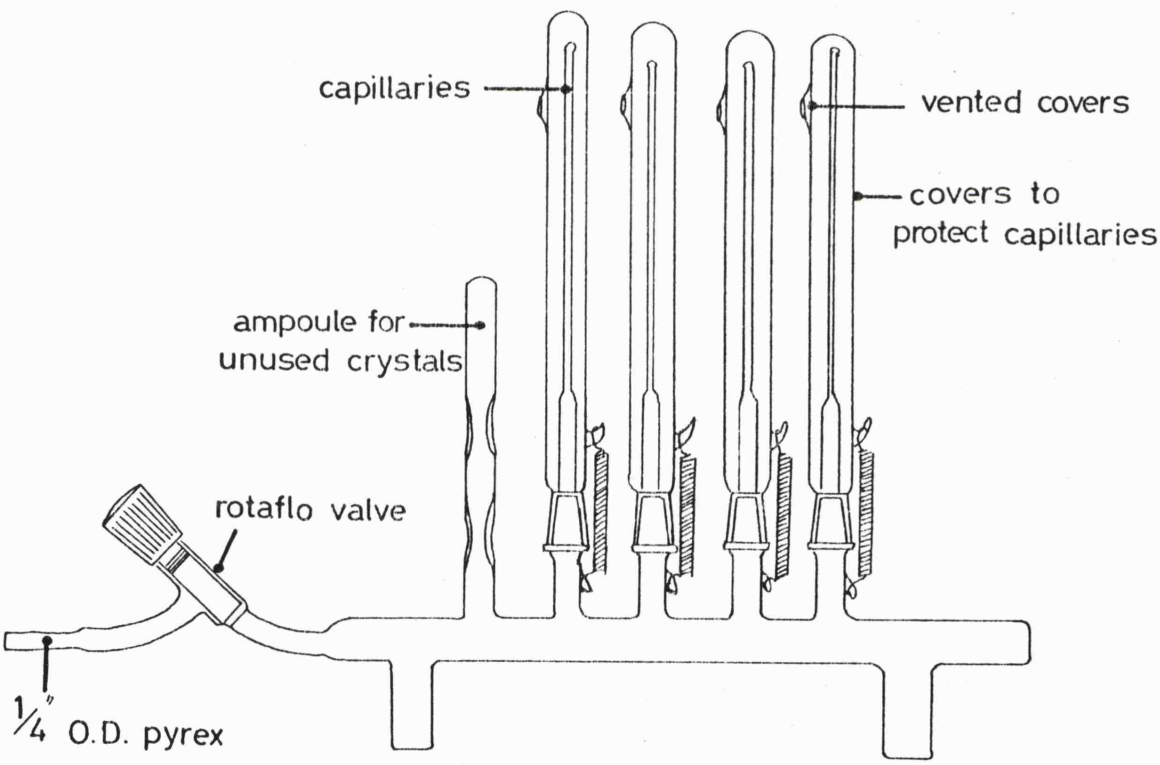

Figure 2

Capillary apparatus for the sorting of single crystals.

2.4 Characterisation of Products

The identity or purity of the products was established usually by three methods, X-ray powder photography, mass spectroscopy and Raman spectroscopy. Infra-red was used principally as a purity check of starting materials.

For X-ray powder diffraction, samples were ground to a fine powder in a dry box, and loaded into seasoned glass capillaries through a Rotaflo valve. The capillaries were re-evacuated and then sealed with a microtorch. The photographs were taken in a Philips 11.64 cm diameter camera using Kodirex KD 59 T film (Kodak Ltd.). For powder photographs Cu-$\underline{K}\alpha$ radiation was used with a nickel filter.

An AEI MS9 or V.G. Micromass 16 B were used to record mass spectra. Spectra of solid samples were frequently obtained from glass capillaries already used for X-ray powder diffraction. The capillaries could be inserted directly into the ionization chamber mounted on the end of a stainless steel probe (Figure 3). In order to minimise decomposition of the sample during passage through the mass spectrometer it was seasoned with small amounts of fluorine prior to use. Samples of liquids or gases were admitted from a glass ampoule fitted with a Rotaflo valve and $\frac{1}{4}$" o.d. compression fitting.

The Raman spectra were obtained using a Coderg T800 spectrometer, with either a 250 mW Ar^+ laser (Model 52, Coherent Radiation Laboratories) or 500 mW Kr^+ laser (Model 164, Spectra Physics Inc.). The Ar^+ laser provided 5145 Å (green) and 4880 Å (blue) radiation, the Kr^+ laser gave 6145 Å (red). Samples were contained in either glass ampoules or $\frac{1}{4}$" o.d. FEP tubes. Samples likely to be decomposed by the beam were cooled in a stream of cold nitrogen gas. The tubes were secured in an evacuated double-walled glass jacket (Figure 4) which, once positioned,

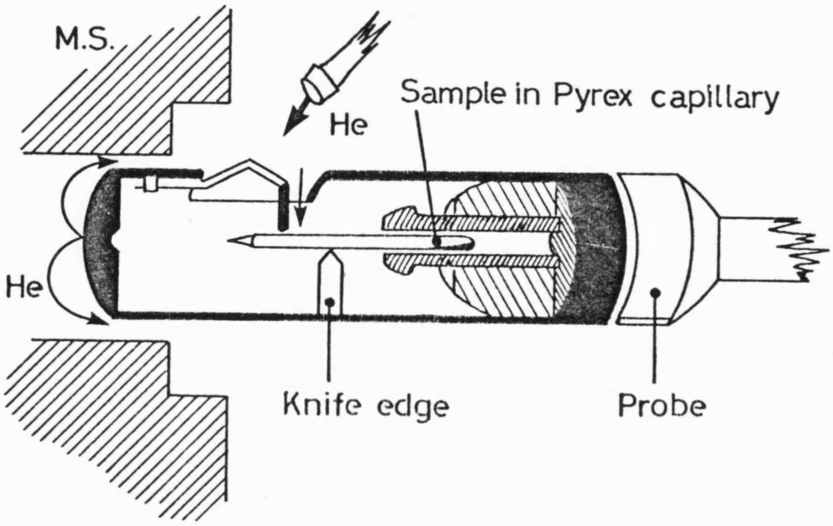

Figure 3

Mass Spectrometer Probe Attachment for air sensitive samples.

allowed several samples to be inspected without realignment. The nitrogen stream was generated from a 25 litre dewar of liquid nitrogen, with a controlled heat source allowing temperatures in the range 0° to -100° to be maintained. A copper-constantan thermocouple near the sample connected to an electric thermometer (model 1623, Comark Electronics Ltd., Littlehampton, Sussex) gave readings accurate to ±0.1°.

A Perkin Elmer 580 spectrometer was used to obtain infrared spectra. Solid samples were ground in a dry box and run as nujol mulls, between KBr windows (4000 – 350 cm^{-1}). A supply of sodium dried nujol was kept in the dry boxes. Gas-phase spectra were obtained using a 10 cm path length copper cell with AgCl windows (4000 – 400 cm^{-1}). PTFE gaskets

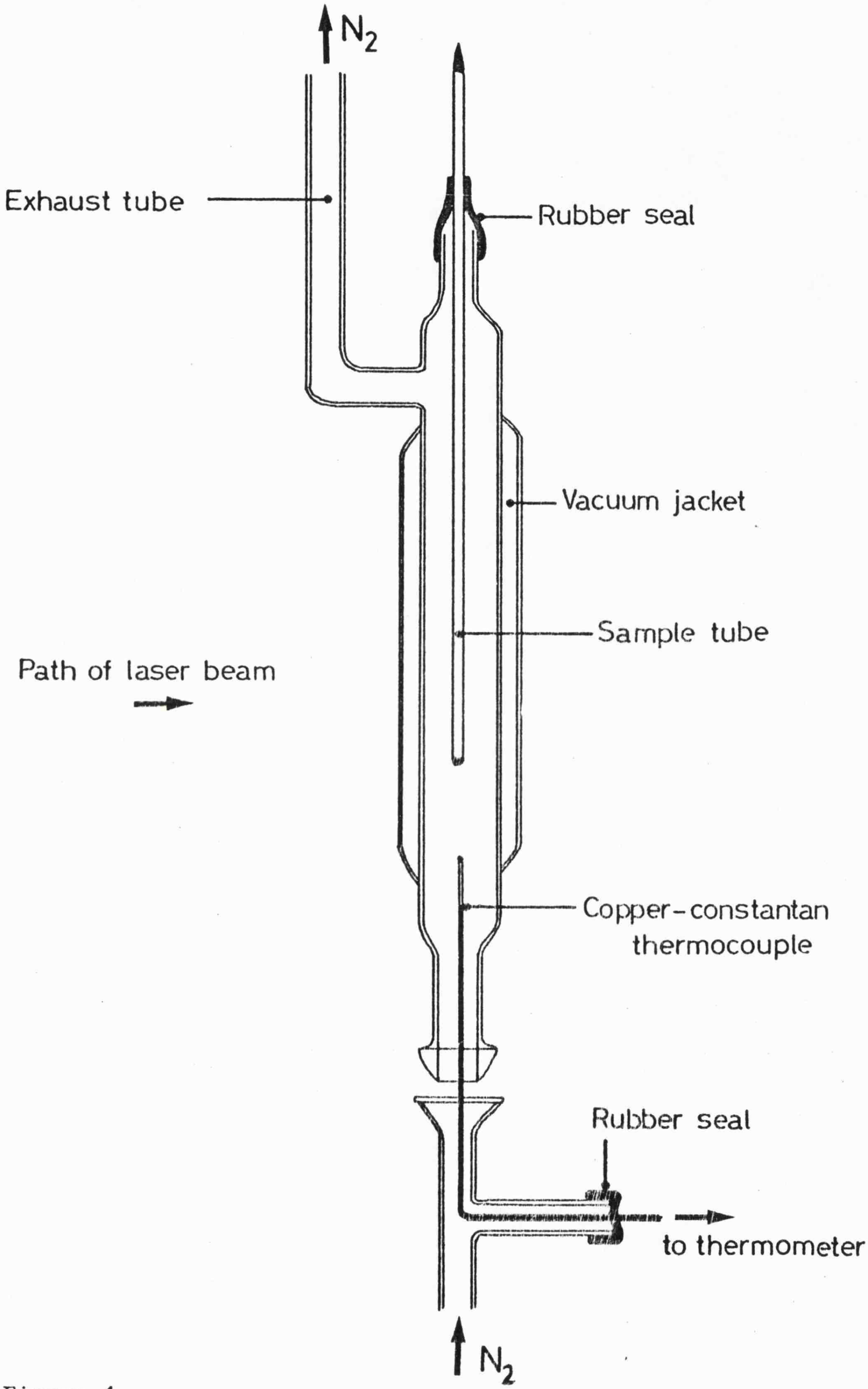

Figure 4

Low-Temperature Raman Apparatus.

were used as an air tight seal between the windows and the cell body. The cell attached to the manifold through a Hoke diaphragm valve (type 4171 M2B Hoke International Ltd., Barnet, Herts) and was pumped to 10^{-4} torr before approximately 40 torr pressure of sample was admitted.

2.5 Generation and Use of Fluorine in Flow Systems

Flow system reactions were used to prepare the metal pentafluoride and oxide tetrafluorides used as starting materials. Fluorine was produced by a medium temperature 60 amp fluorine generator (I.C.I. Ltd., General Chemical Division) with a maximum output of 40 g of fluorine per hour. The fluorine exit pipe of the generator led directly to an efficient fume hood and through two metal traps containing sodium fluoride pellets to remove hydrogen fluoride. Further impurities were removed by liquid oxygen traps built into the glass reaction systems, which were attached to the metal line through a ¼" i.d. neoprene compression seal. Dry nitrogen gas was used to purge the cathode compartment of the cell, and the reaction system before and after a preparation. For most reactions nitrogen was used as a diluant during fluorination and for the metal oxide tetrafluorides oxygen was admitted through a valve in the glass apparatus.

2.6 Starting Materials and Solvents

Fluorine; for reactions on the manifold fluorine was used without purification from a cylinder (Matheson Gas Products). For safety and convenience reasons only the fluorine was transferred to welded nickel cans (~1 dm^3 capacity).

Tantalum and niobium; the metals were obtained as powders (British Drug

Houses Ltd.) which were reduced at red heat in a stream of hydrogen before use.

Molybdenum (Hopkin & Williams Ltd.) and tungsten (BDH); metal powders were used without reduction for the preparation of the oxide tetra-fluorides.

Antimony (BDH); the metal powder was used without purification.

Sodium fluoride (BDH), potassium fluoride (Fisons Ltd.), caesium fluoride (Koch Light Ltd.) and rubidium fluoride (ROC/RIC Ltd.) were all heated at 120° to 150° in dynamic vacuum for 12 hrs, to remove adsorbed gases.

Caesium iodide (Koch Light), sodium iodide and potassium bromide (BDH); these compounds were heated at 110° in dynamic vacuum.

Bromine trifluoride (Matheson Gas Products Ltd.); was vacuum distilled from the cylinder into a silica ampoule, and the first and last fractions rejected.

Iodine pentafluoride (Cambrian Chemicals Ltd.); was vacuum distilled from the cylinder to a $\frac{3}{4}$" o.d. Kel-F tube where free iodine was converted to iodine pentafluoride by agitation with fluorine gas until the liquid was colourless.

Tungsten hexafluoride (Allied Chemicals Ltd.); was vacuum distilled from the cylinder to a $\frac{1}{4}$" o.d. Kel-F tube over sodium fluoride to remove hydrogen fluoride.

Osmium tetroxide (Johnson Matthey & Co. Ltd.); was used without purification, or prepared by burning osmium metal powder (Johnson Matthey) in a current of oxygen.

Anhydrous hydrogen fluoride (Imperial Chemical Industries Ltd.); was vacuum distilled from the cylinder to nickel storage cans or $\frac{3}{4}$" o.d. Kel-F tubes and degassed before use.

Sulphur dioxide (BDH); was vacuum distilled to storage ampoules over phosphorus pentoxide to remove traces of water.

Genetron 113 (Fluka A.G.); was purified by distillation from phosphorus pentoxide and stored over molecular sieve in glass ampoules.

In addition several pentafluorides and oxide tetrafluorides used as reactants were prepared by fluorination in flow systems.

Antimony pentafluoride; from the combination of antimony metal powder and fluorine, was vacuum distilled until the liquid was of a high viscosity.

Niobium and tantalum pentafluorides; obtained by heating the reduced metal powders in a fluorine stream were vacuum sublimed before use.

Molybdenum and tungsten oxide tetrafluorides; prepared by heating the metal powders in a stream of fluorine and oxygen (4:1). The products were then resublimed in vacuum to give colourless crystals.

CHAPTER 3

The Preparation of Uranium Oxide-Tetrafluoride-Antimony Pentafluoride Adducts and the Crystal Structure of $UF_4O.2SbF_5$

3.1 Introduction

Although uranium was first discovered in 1789 by Klaproth, it had little commercial importance until the discovery of nuclear fission by Hahn and Strassman in 1937. The increased importance of uranium as a nuclear fuel resulted in considerable interest in its chemistry. The halides have been studied in great detail and their chemical and structural properties are well established. However, the oxide fluoride compounds of uranium have had an uncertain history. Brooks et al.[17] first suggested the existence of UF_4O as the principal product of a gas-phase reaction between UF_6 and very low partial pressures of water. Further studies also suggested the existence of UF_4O[18] and $U_3F_8O_5$.[19] The first characterization of UF_4O was by Wilson.[20] The UF_4O was isolated from the reaction of UF_6 with dilute solutions of water in liquid HF. Paine et al.[21] confirmed the existence of α-UF_4O and determined its structure by X-ray diffraction. α-UF_4O is rhombohedral, space group $R\bar{3}m$, the uranium co-ordination being pentagonal bipyramidal. Three of the light atoms in the bipyramid are terminally bonded, the other four light atoms, which all lie in the plane of the pentagonal ring, each bridge two uranium atoms. Wilson et al. have also studied the α-UF_4O structure[22,23] and the polymorphic form β-UF_4O[24] which is the product of slow crystallization from HF solution.

The chemical properties of UF_4O have been the subject of numerous studies.[20,21,25-32] The acidic character of UF_4O has been demonstrated by its behaviour as a fluoride ion acceptor in reactions with monovalent alkali metal or ammonium fluorides, which give rise to compounds of the formulae MUF_5O and M_3UF_7O,[30-32] (M = NH_4, K, Rb or Cs). The Cs complex may be regarded as essentially ionic with an octahedral environment about the uranium atom. The NH_4, K and Rb compounds are less ionic with eight light atoms about the U forming dodecahedra which are fluorine bridged forming infinite chains. However, recent vibrational spectroscopic evidence[33-34] suggested the existence of the unlikely cation UF_3O^+. The reaction between $CsUF_5O$ and $XeF_2.2SbF_5$ in SbF_5, which was expected to yield the UF_5O^- anion in $XeF^+UF_5O^-$, resulted in a product, the Raman spectrum of which showed the peak associated with $\nu(U=O)$ shifted to higher frequency than in $CsUF_5O$ or even UF_4O. The implication that UF_4O might be behaving as a fluoride ion donor seems unlikely because of the low co-ordination number implied by the formulation for the UF_3O^+ ion. However, if cationic behaviour of the uranium was occurring it must result from an interaction with the strong Lewis acid antimony pentafluoride which is known to stabilise a number of unusual cations, such as $[I_2]^+$[35] and $[Br_2]^+$.[36] Antimony(V) fluoride is also capable of forming stable fluorine bridged adducts, or the hexafluoroantimonate anion, with fluoride ion donors. It is also self-associated _via_ fluorine bridges. The occurrence of either fluoride bridged adducts or complex fluorides appears to be dependent on the Lewis acidities of the component molecules.

In any consideration of bonding in complex fluorides the two extreme bond types, ionic and covalent, must be taken into account. Structures resulting from the interaction between complex ion donors and acceptors may be considered totally ionic if the fluorine atom completes a stable regular array about the metal atom of the anion, with all bond distances equal. The fluorine bridge bond is a type of covalent bond, where each of the bridged metal atoms effectively contributes half an electron to the bridging fluorine atom. However, in most complex fluorides, bonding may best be represented as a combination or hybrid of the extremes. In such cases the resulting bond energy will be greater than that of either contributing form. It would be convenient in discussing such structures to be able to make quantitative statements about their nature. Formulae for the degree of ionic character between two atoms are known, but for bonds between complex "ions" the case is less simple and depends upon bond length comparisons, with other adducts and the starting materials where these are polymeric.

The adducts formed between antimony(V) fluoride and the noble gas fluorides are of particular interest in comparing ionic contribution to bonding, since series of adducts are formed with variation of both stoichiometry and the oxidation state of the cation. In recent years the 1:1 adducts $M^+[SbF_6]^-$ (M = $[XeF]^+$;[37-41] $[XeF_3]^+$;[41-45] $[XeF_5]^+$;[41,46,47] $[XeOF_3]^+$;[41-44] $[XeO_2F_5]^+$;[41,42] $[KrF]^+$[42,48-51]) have been characterised by vibrational and n.m.r. spectroscopy. The ionic bonding contribution being determined by the number of electron pairs in the bonding shell such that $[XeF]^+$ > $[XeF_3]^+$ > $[XeF_5]^+$ and $[XeOF_3]^+$ > $[XeOF_5]^+$.

The series of adducts of 2:1, 1:1 and 1:2 composition of the noble gas difluoride/antimony(V) fluoride system have been studied for both xenon and krypton. The series $[Xe_2F_3]^+[SbF_6]^-$,[37-43] $[XeF]^+[SbF_6]^-$ and $[XeF]^+[Sb_2F_{11}]^-$[37-40,52-54] and the analogous $[Kr_2F_3]^+[SbF_6]$[48-51] $[KrF]^+[SbF_6]^-$ and $[KrF]^+[Sb_2F_{11}]^-$[42,48-51,55] compounds have been shown to exhibit a large ionic contribution to the bonding and a gradation of ionic character, 1:1 > 1:2 > 2:1 but with no adduct wholly fluorine bridged or ionic.

There are numerous examples of 1:1 and 1:2 adducts of antimony(V) fluoride with the halogen fluorides. The well defined (1:1) adducts with ClF_3,[56,57] IF_3,[58] BrF_3[59,60] and $ClFO_3$[61] have been characterised as largely ionic structures having some fluorine bridged character, as for example in the $BrF_3.SbF_5$ adduct where fluorine bridging between the ions gives an endless helical chain. Similarly the 1:2 adducts of SbF_5 with BrF_5[62] and BrF_7[63] may be represented by the formulations $[BrF_4]^+[Sb_2F_{11}]^-$ and $[BrF_6]^+[Sb_2F_{11}]^-$ with infinite chains of discrete $[BrF_x]^+$ and $[Sb_2F_{11}]^-$ ions coupled by relatively weak fluorine bridges. Adducts formed between antimony(V) fluoride and the pentafluorides of niobium[64,65] and tantalum,[65] are reported as essentially neutral fluorine bridged compounds. Nuclear magnetic resonance[65,66] and conductivity measurements[65] are consistent with the adducts being fluorine bridged with a small degree of ionic character coming from the resonance forms $[MF_4]^+[SbF_6]^-$. Complex fluorides of antimony(V) fluoride with nitrogen containing cations represent the opposite extreme and may be regarded as purely ionic species. The 1:1 adducts of FNO_2 and FNO, and the 1:2 adducts of F_3NO and F_4N_2[67] can thus be formulated as $[NO_2]^+[SbF_6]^-$, $[NO]^+[SbF_6]^-$, $[F_2NO]^+[Sb_2F_{11}]^-$ and $[F_3N_2]^+[Sb_2F_{11}]^-$ respectively with no appreciable anion-cation interaction.

It was decided, in view of the spectroscopic evidence already obtained for the UF_4O-SbF_5 system, that an X-ray single crystal study would be helpful in understanding the bonding in the adducts, and to establish from the uranium environment whether there is any evidence for the UF_3O^+ cation.

3.2 Preparation of uranium oxide-tetrafluoride-antimony pentafluoride adducts

Uranium oxide tetrafluoride was prepared as described by Wilson[20] and its purity was monitored by X-ray diffraction and vibrational spectroscopy. The $CsUF_5O$ was prepared by the reaction of UF_4O and CsF in liquid SO_2,[18] and $XeF_2.2SbF_5$ by the reaction of excess of SbF_5 with XeF_2.[53] Single crystals of the adduct $UF_4O.2SbF_5$ were prepared at the

Centre d'Etudes Nucleaires de Saclay by J. H. Holloway and R. Bougon. The crystals were obtained from the reaction of $CsUF_5O$ with $XeF_2.2SbF_5$ in liquid SbF_5 solvent. Stoichiometric quantities of the reactants were taken in F.E.P. tubes. Reaction occurred at room temperature with the evolution of gas, when no further gas was evolved the SbF_5 was removed by pumping in dynamic vacuum, initially at room temperature then at approximately 70°C. During this stage orange single crystals separated from the orange/yellow solid product. X-ray powder photographs of the crystals and bulk product showed that UF_4O, $CsUF_5O$, CsF and $CsSbF_6$ were not major constituents of the product. The Raman spectra of the bulk material (Table 1) showed, in addition to the ν(U=O) band of UF_5O^- (825 cm^{-1}) and UF_4O (875 cm^{-1}), a peak at 910 cm^{-1} which might be tentatively assigned to ν(U=O) of UF_3O^+.

The series of adducts UF_4OnSbF_5 (n = 1, 2 or 3) were prepared by the reaction of UF_4O with SbF_5 in preseasoned and weighed Kel-F reactors. Powdered UF_4O was added in a drybox and the reactor evacuated before re-weighing. The manifold and reactor were then pumped to good vacuum, $\leqslant 5 \times 10^{-5}$ torr, before SbF_5 was added in static vacuum. A large excess of SbF_5 was used to prepare the 1:3 and 1:2 adducts and complete solution obtained by gentle warming. Excess SbF_5 removed initially in static vacuum and later in dynamic vacuum yielded the 1:3 adduct at room temperature or the 1:2 adduct at 60-70°C. The 1:1 adduct required the addition of a stoichiometric quantity of SbF_5 and the use of anhydrous HF as solvent. The mixture was gently warmed and an orange solution obtained but at no time was complete solution achieved. On removal of the solvent an orange crystalline solid remained.

The solid adducts have been characterized by observations of the

TABLE 1

UF_4O		SbF_5 (1)	$UF_4O.3SbF_5$		$UF_4O.2SbF_5$		$UF_4O.SbF_5$	
R	R	R	I.R.	R	I.R.	R	I.R.	R
			1013		1010		1005	
			920s	921s		931m		
					912s	912s	907s	906s
895vs	896vs							
889vs	889vs							
882vs	882vs							
			740sh		732sh			
		717		721m	722vs	725sh	715vs	
					710sh	716m		
			700vs br	704s		702m		700m
		670				672sh		669vs
665s	665s		660sh	662vs	657s	655vs	650sh	649m
				612m				620w
			604s			607w		
						603w		
					596s	590m	590	589m
550m	548m				546sh	544m	540m	560m
				534m br			531m	534m
			525m br		526s			522m
					518sh	512sh		
					502sh			
			475m br				480	
					457m	461m		
						441sh		
							420w	
		345					365m	
345vw	345vw			337w				292m
276m	275m			284sh				287sh
		268		270m		275m	270m	
		231						
				221m		198m		
201m	202m							204s
		190		188m				185sh
148s	148s			149m		158m		158sh
		140		146m				142s
				139w				
117m	116	116		119w				123sh
				95w				96w

Vibrational data (cm^{-1}) of the adducts of UF_4O with SbF_5 compared with those of pure UF_4O and SbF_5.

reaction stoichiometry, chemical analysis, vibrational spectra and X-ray powder diffraction techniques. Chemical analyses for each adduct were in good agreement with the calculated mole ratios. The vibrational spectra obtained for the adducts (Table 1) were distinctly different from UF_4O and SbF_5. The band associated with $\nu(U{=}O)$ is shifted to higher frequency as the proportion of highly acidic SbF_5 increases, suggesting progressive withdrawal of electron density from UF_4O. However, no corresponding peaks are found characteristic of the anionic species of antimony, SbF_6^- or $Sb_2F_{11}^-$.[43,68,69] The X-ray powder diffraction pattern of the 1:3 adduct is similar to that of crystalline SbF_5, though not perfectly iso-structural. As soon as the composition 1:3 is passed in the pump curve, the rate of loss of SbF_5 increases and the powder pattern changes to a new form which is maintained until the 1:2 composition is reached. This implies that the 1:3 form changes to 1:2, and that excess of SbF_5 is present as a liquid which can be readily removed. The identity of the single crystals obtained from the $CsUF_5O$ and $XeF_2.2SbF_5$ reaction was confirmed by the equivalence of X-ray powder photographs with those of the 1:2 adduct.

3.3 Single Crystal X-ray Investigation of $UF_4O.2SbF_5$

Crystals of the adduct were transferred in an inert-atmosphere dry-box into short lengths of thin-walled preseasoned Pyrex capillaries and sealed. The crystal used for the investigation was rectangular block-shaped and had adhered to the wall of a capillary. It had the approximate dimensions 0.168 mm × 0.083 mm × 0.076 mm. Approximate cell dimensions were obtained from Weissenberg photographs taken using Cu-$\underline{K}_\alpha$ (nickel filtered) radiation and precession photographs using Mo-$\underline{K}_\alpha$ (Zr filtered) radiation. Final cell dimensions were determined from an oscillation photograph for the rotation axis a, and from its optimised counter angles for zero and upper layer reflections on a Weissenberg diffractometer. Chosen reflections were maximised by ω-scan and then 2θ scan using an asymmetric half slit.

3.4 Crystal Data

$F_{14}OSb_2U$; M = 764

Monoclinic a = 7.864(16), b = 14.704(8), c = 9.980(8)Å,

β = 99.8(1)°, U = 1137 $Å^3$, Dc = 4.46 g cm^{-3}, z = 4,

μ(MoKα) = 181.4 cm^{-1}, F(000) = 1311.9, MoKα radiation,

λ = 0.71069 Å.

Space group $P2_1/c$ (C_{2h}^5 No. 14). Neutral atomic scattering factors were used with anomalous dispersion corrections.

3.5 Collection of Intensity Data

Data were collected from layers 0kl to 8kl using the Stadi-2 diffractometer, in the +h, +k, +l quadrant only for the 0kl layer and in the two quadrants ±l for the remaining layers. Data were collected using an ω-scan technique, the counter angle (2θ) remaining fixed at the calculated value for each reflection, whilst the crystal rotates in the X-ray beam with a count time of 0.5 second at 0.01° increments of ω. The ω-scan angle was determined for each reflection to ensure that counts were not lost from broad reflections at high 2θ angles.

The intensities of reflections with $0.08 < \sin\theta/\lambda < 0.7$ $Å^{-1}$ were collected at 22-25°C, and a total of 1170 unique reflections were obtained with $I/\sigma I \geqslant 3$. Monitoring of check reflections throughout each layer indicated no significant deterioration of the crystal during the data collection. Between the collection of data for layer 5kl and 6kl it was necessary to realign the X-ray tube, and this resulted in an increase in beam intensity. It was therefore required to establish a scale factor for layers 6kl to 8kl. The check reflections monitored for layers 0kl to 5kl were recollected at the higher intensity and a scale factor calculated and applied to the data, no significant trend of deviant reflections resulted from the correction.

Lorentz, polarisation and absorption corrections were made to the data. The accurate measurement of the crystal for the absorption correction was difficult as the crystal was small by comparison with the tube diameter and observation of the crystal down the 011 axis was obscured.

3.6 Solution of the structure

The program system SHELX was used. A Patterson summation was used to locate the uranium and antimony atoms. Three cycles of least squares refinement gave an R factor of 0.15 and allowed sufficient phasing for the location of the light atoms by Fourier maps. The oxygen atom was chosen from the shortest uranium to light atom bond-length, and fourteen other peaks assigned as fluorine. Three cycles of refinement with all atoms included and isotropic temperature factors gave an R factor of 0.095. An absorption correction with maximum and minimum transmission factors 0.359 and 0.211 respectively, was performed on the data set. Further cycles of refinement using anisotropic thermal parameters for all atoms reduced R to 0.046. The final cycles employed a weighting parameter $\underline{g}$ (0.00063) $[\omega \alpha \frac{1}{\sigma^2}(F) + gF^2]$ and an isotropic extinction parameter $\underline{x}$(0.0001) $[F_c = F(1-xF^2/\mathrm{Sin}\theta)]$. The final difference Fourier map revealed no significant features and an analysis of the weighting scheme over $|F_o|$ and $\mathrm{Sin}\theta/\lambda$ was satisfactory. Final atomic positional parameters are in Table 2, the anisotropic thermal parameters are in Table 3. The interatomic distances and angles are in Tables 4 and 5 respectively, and the observed and calculated structure factors are found in Appendix 1.

Final residual indices for 1170 reflexions:-

$$R = \sum(|F_o| - |F_c|)/\sum|F_o| = 0.0456$$

$$R_w = [\sum w(|F_o| - |F_c|)^2/\sum w|F_o|^2]^{\frac{1}{2}} = 0.0431$$

3.7 Discussion

The structure of the $UF_4O.2SbF_5$ adduct is related to that of α-UF_4O[21] itself, the uranium oxide tetrafluoride having a pentagonal-bipyramidal array of light atoms about the uranium with four bridging and three terminal atoms (Figure 5). Two types of antimony atom exist in the structure, in which ring units of two uranium, two Sb(1) and 4F atoms are linked through the uranium atoms into endless zig-zag chains to Sb(2) atoms by F atoms.

The fluorine bridge angles of 150 and 156° in the $(U\text{-}F\text{-}Sb(1)\text{-}F)_2$ ring are approximately the average of the fluorine bridge bond angles in SbF_5 (141 and 170°). The fluorine bridges with the Sb(2) atoms in the chain are equal, within experimental error, their average value being 162°. The overall structure may, therefore, be thought of as a fluorine bridged network (Figure 6) in which the features of two of the three structure types commonly found for transition metal and actinide metal pentafluorides and oxide tetrafluorides exist together. The two structure types represented are the distorted tetrameric ring arrangement typified by RhF_5,[70] and the VF_5 type,[71] where octahedra are joined in polymeric zig-zag chains.

In molecular structures determined by X-ray diffraction methods,

Figure 5

The $UF_4O.2SbF_5$ asymmetric unit.

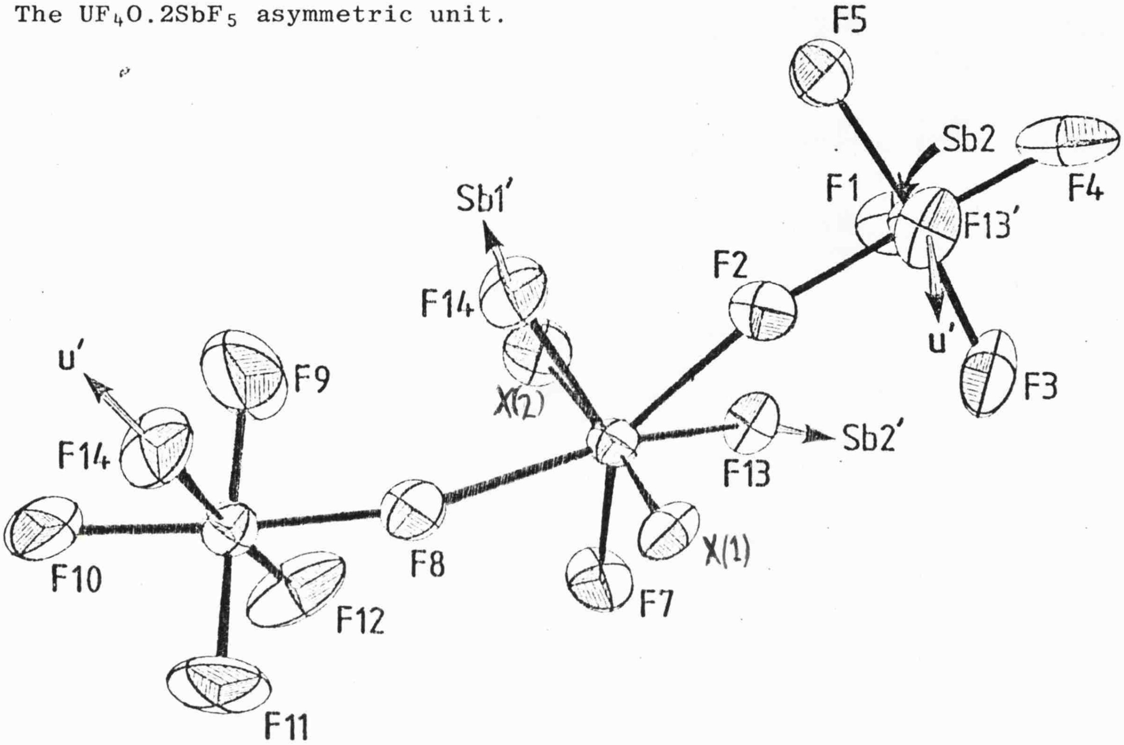

Figure 6

Stereoscopic view of the unit cell contents of $UF_4O.2SbF_5$.

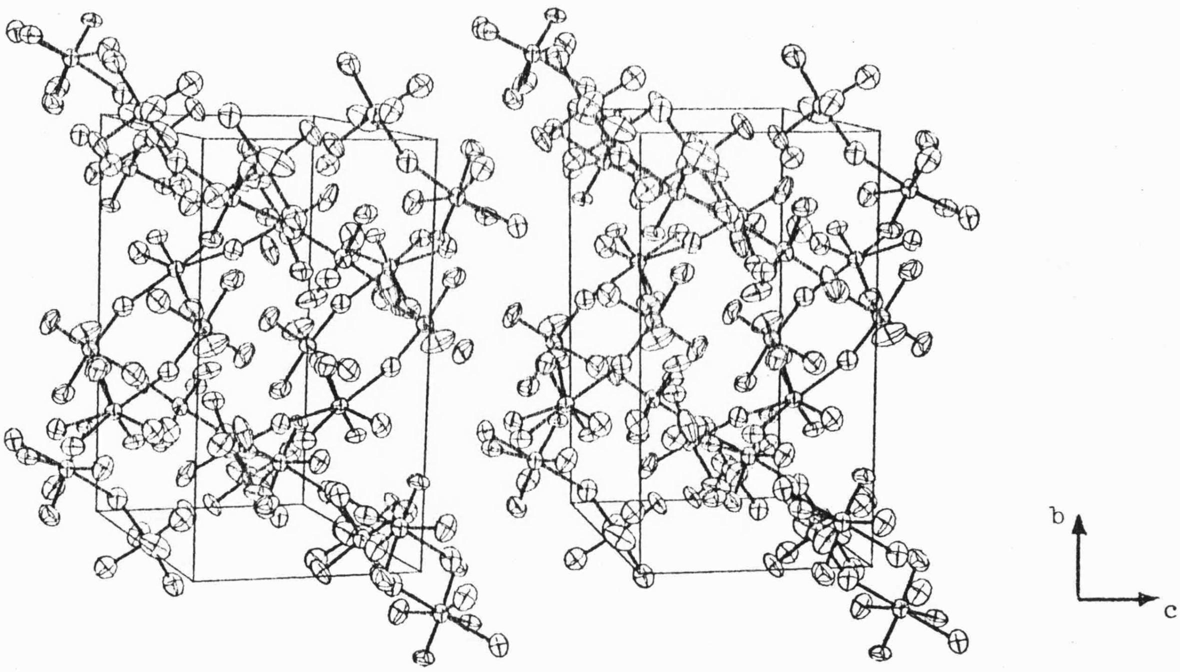

there is usually ambiguity in the placement of an oxygen atom with respect to fluorine atom positions. In most cases a final assignment has to be made with the help of supporting characterisation data. In the case of $UF_4O.2SbF_5$ it was concluded from the vibrational spectra of the adduct (Table 1), that the oxygen is non-bridging. The terminal atom in the equatorial plane is at a distance of 1.98 Å from the uranium, is comparable with the U-F bond distance found in UF_6,[72] and can clearly be assigned to a fluorine atom. Therefore, one of the two short terminal bonds axial to the pentagonal belt belongs to the U-O bond, as in the case of α-UF_4O. The axial bond distances, U-X(1) 1.820(15) Å and U-X(2) 1.825(15) Å are, within error limits, equivalent and cannot be uniquely assigned to U-O or U-F. It can be assumed that these axial positions are occupied in a disordered way by F and O atoms, and the bond distances an average of the expected U-O and U-F distances. The average U-X bond length of 1.822 Å is between those found for the disordered axial atoms of α-UF_4O by Paine et al. (1.77 and 1.79 Å)[21] and Levy et al. (1.87 and 1.88 Å).[23]

Vibrational data, prior to the structure determination, indicated an ionic contribution to the bonding within the adduct. The shift of the band associated with ν(U=O) in the Raman spectra from 875 cm^{-1} in UF_4O, to 910 cm^{-1}, suggested the ionic formulation $[UF_3O]^+[Sb_2F_{11}]^-$. However, it is clear from the structure determination that in the absence of adjacent Sb atoms the $[Sb_2F_{11}]^-$ unit does not occur in the structure. Further evidence of an ionic contribution to the bonding is provided by the volume per light atom of 19 $Å^3$, which is close to the volume expected for the close packed fluorine atoms of an ionic lattice (18 $Å^3$).

A comparison of the U and Sb bridging fluorine distances with those observed in the parent compounds suggests a slight tendency towards the ionic formulation $[UF_2O]^{2+}[SbF_6]_2^-$. The average U-F bridging distance of 2.34(2) Å is significantly longer than the 2.27(1) Å distance found for the equivalent bonds in UF_4O.[21] The average Sb-F bridging distance is slightly shorter at 1.951(17) Å compared with 2.02(3) Å found in the solid state structure of SbF_5.[73] The terminal Sb-F bond lengths are of the expected order, but less symmetric about Sb(1) (1.789 - 1.871(15) Å) than Sb(2) (1.818 - 1.849(15) Å).

The $[M]^{2+}[SbF_6]_2^-$ formulation is unique amongst known structures, and a bond length comparison with closely related adducts is, thus, impossible. Despite the 1:2 composition of the adduct, a comparison of ionicity with $[M]^+[SbF_6]^-$ adducts is of greater validity than with those containing the $[Sb_2F_{11}]^-$ ion. The adduct $NbF_5.SbF_5$ is reported as having a contribution to the structure from the ionic form $[NbF_4]^+[SbF_6]^-$,[64] and like UF_4O, NbF_5 is both a good fluoride ion acceptor, and has a tetrameric structure.[74] The Sb-F bridge distance in SbF_5 (2.02(5) Å) is shortened by the same amount in both adducts to 1.95(2) Å. However, the bond distance is still 0.13 Å greater than the Sb-F distance required for a regular wholly ionic octahedron. A corresponding increase in the fluorine bridge distance is observed for both the U-F and Nb-F bonds of the two adducts. The U-F bridging distance of 2.34(2) Å is 0.07 Å longer than found in UF_4O, whereas the Nb-F bridging distance (2.17(2) Å) is 0.11 Å longer than the equivalent bond of NbF_5.

It is difficult to estimate a value for a non-bridged contact distance between the U and F atoms, and no quantitative assessment of the degree of ionic character, indicated by the increased U-F bond length, can be made. If, for an Sb-F bond we assume the average bridging distance of the neutral SbF_5 tetramer, 2.025(30) Å, represents a neutral Sb-F bond length (D_n), and the Sb-F bond length of the recently determined $KSbF_6$ structure,[75] 1.845(10) Å, to be representative of a regular ionic octahedron (D_i) an estimation of ionic character may be made. The Sb-F bridging distance of the adduct (D_a), 1.95(2) Å, is closer to the expected covalent distance and, although the degree of ionic character is not expected to be linearly proportional, the following equation is an approximation:-

Ɨ $= (D_c - D_a/D_c - D_i) = (2.02 - 1.95/2.02 - 1.845) = 0.40(3).$

The value calculated for $UF_4O.2SbF_5$ can be compared only with other antimony pentafluoride adducts for which detailed structures have been reported, Table 6.

TABLE 6

Calculated ionicity values of some antimony pentafluoride compounds

	$Sb\text{-}F_{(B)}$ (Å)	Ɨ $= (D_c - D_a/D_c - D_i)$
$(SbF_5)_4$	2.02	0.00
$UF_4O.2SbF_5$	1.949*	0.40
$NbF_5.SbF_5$	1.945	0.43
$BrF_3.SbF_5$	1.91	0.63
$ClF_3.SbF_5$	1.905*	0.66
$KSbF_6$	1.845	1.00

* distances result from averaging of asymmetric bonds

The higher values obtained for the adducts of SbF_5 with BrF_3 and ClF_3 are as expected. However, the comparable values for $NbF_5.SbF_5$ and $UF_4O.2SbF_5$, also indicate considerable ionic contribution to the bonding within the adducts, contrary to the evidence of NMR and conductivity measurements for $NbF_5.SbF_5$.

Although the adduct samples obtained from the reactions of UF_4O and SbF_5 were microcrystalline, no single crystals were obtained either directly or from solution in anhydrous HF. Variation of the reaction conditions used in the method from which single crystals of $UF_4O.2SbF_5$ were obtained, might provide an alternative preparative method and single crystals. For example, the 1:1 adduct might be prepared from the reaction:-

$$XeF^+SbF_6^- + Cs^+ UF_5O^- \longrightarrow UF_3O^+ SbF_6^- + \text{mixed products } (CsSbF_6, CsF, Xe \text{ and } F_2)$$

Variation of the stoichiometry previously used with $XeF_2.2bF_5$ and $CsUF_5O$ may also yield adducts other than $UF_4O.2SbF_5$, as the $[Sb_2F_{11}]^-$ unit of the xenon adduct clearly breaks, to give $[SbF_6]^-$ ions during the reaction.

The structures of the 1:1 and 1:3 adducts are expected to exhibit a similar degree of ionic character, with a probable gradation of ionicity 1:1 > 1:2 > 1:3. It seems likely that the 1:3 adduct would be more closely related, structurally, to the 1:2 adduct than would the 1:1, as transition from 1:3 to 1:2 adduct is readily achieved by warming in dynamic vacuum, whereas the 1:2 to 1:1 conversion does not occur. The additional $[SbF_6]^-$ ion of the $UF_4O.3SbF_5$ may form an $[Sb_2F_{11}]^-$ ion in the zig-zag chain that links the tetrameric rings.

TABLE 2

Atomic positional parameters for $UF_4O.2SbF_5$, with estimated standard deviations in parentheses.

	x/a	y/b	z/c
U	0.22398(11)	0.14423(6)	0.20255(9)
Sb(1)	-0.15905(19)	-0.04818(11)	0.20172(17)
Sb(2)	0.61561(18)	0.26878(11)	0.02113(16)
X(1)	0.092(2)	0.2319(10)	0.1071(17)
F(1)	0.7436(19)	0.2334(12)	0.1857(14)
F(2)	0.4219(16)	0.2019(9)	0.0766(13)
F(3)	0.526(2)	0.3670(10)	0.0950(17)
F(4)	0.7842(18)	0.3353(12)	-0.0403(16)
F(5)	0.6589(19)	0.1625(9)	-0.0654(14)
X(2)	0.3288(19)	0.0393(10)	0.2707(18)
F(7)	0.1262(19)	0.1694(11)	0.3685(15)
F(8)	-0.0288(17)	0.0591(10)	0.1651(14)
F(9)	0.036(2)	-0.1103(12)	0.199(3)
F(10)	-0.2772(19)	-0.1574(10)	0.2150(17)
F(11)	-0.3538(20)	0.0219(11)	0.1737(19)
F(12)	-0.115(3)	-0.0253(12)	0.3828(17)
F(13)	0.4612(17)	0.2019(8)	0.3551(13)
F(14)	0.203(2)	0.0640(11)	-0.0044(15)

TABLE 3

Anisotropic thermal parameters, with estimated standard deviations in parentheses

The temperature factors are in the form $\exp[-2\pi^2(h^2U_{11}a^2 + ... 2hkU_{12}ab)]$

	U_{11}	U_{22}	U_{33}	U_{23}	U_{13}	U_{12}
U	0.0339(5)	0.0408(6)	0.0277(5)	0.0025(5)	0.0046(3)	0.0098(4)
Sb(1)	0.0411(9)	0.0409(10)	0.0386(10)	0.0072(9)	0.0086(8)	0.0109(8)
Sb(2)	0.0328(8)	0.0451(10)	0.0316(9)	0.0036(8)	0.0013(7)	0.0067(7)
X(1)	0.060(10)	0.029(9)	0.047(11)	0.007(8)	0.008(8)	0.000(8)
F(1)	0.067(10)	0.094(13)	0.035(9)	0.011(9)	0.006(8)	0.013(9)
F(2)	0.038(7)	0.065(9)	0.036(8)	0.004(8)	0.000(6)	0.016(7)
F(3)	0.115(14)	0.046(10)	0.072(12)	0.016(9)	0.023(11)	0.008(9)
F(4)	0.046(8)	0.118(14)	0.061(11)	0.018(10)	0.001(7)	0.051(9)
F(5)	0.077(9)	0.046(9)	0.042(8)	0.004(8)	0.024(7)	0.005(7)
X(2)	0.052(9)	0.057(10)	0.099(14)	0.008(10)	0.001(8)	0.002(8)
F(7)	0.070(10)	0.079(12)	0.043(9)	0.016(8)	0.021(8)	0.012(8)
F(8)	0.050(8)	0.060(9)	0.043(9)	0.010(8)	0.010(7)	0.024(7)
F(9)	0.068(11)	0.068(12)	0.19(2)	0.008(14)	0.029(13)	0.015(9)
F(10)	0.061(9)	0.063(10)	0.070(11)	0.001(10)	0.009(8)	0.030(8)
F(11)	0.052(9)	0.082(12)	0.109(16)	0.006(11)	0.018(9)	0.002(8)
F(12)	0.141(18)	0.096(13)	0.036(10)	0.008(10)	0.001(11)	0.043(12)
F(13)	0.054(8)	0.041(8)	0.039(8)	0.000(7)	0.012(6)	0.001(7)
F(14)	0.085(11)	0.075(11)	0.043(9)	0.028(9)	0.024(8)	0.039(9)

TABLE 4

Interatomic distances (Å), with estimated standard deviations in parentheses.

U-X(1)	1.820(15)
U-F(2)	2.322(14)
U-X(2)	1.825(15)
U-F(7)	1.976(16)
U-F(8)	2.325(13)
U-F(13)	2.356(12)
U-F(14)	2.360(15)
Sb(1)-F(8)	1.949(14)
Sb(1)-F(9)	1.789(19)
Sb(1)-F(10)	1.871(15)
Sb(1)-F(11)	1.828(16)
Sb(1)-F(12)	1.812(17)
Sb(1)-F(14)	1.954(15)
Sb(2)-F(1)	1.849(14)
Sb(2)-F(2)	1.970(13)
Sb(2)-F(3)	1.818(17)
Sb(2)-F(4)	1.835(17)
Sb(2)-F(5)	1.845(14)
Sb(2)-F(13)	1.929(12)

TABLE 5

Interatomic angles (°), with estimated standard deviations in parentheses

F(2)-U-X(1)	80.5(6)	F(12)-Sb(1)-F(9)	95.2(9)
X(2)-U-X(1)	167.2(7)	F(12)-Sb(1)-F(10)	95.8(8)
X(2)-U-F(2)	102.1(6)	F(12)-Sb(1)-F(11)	93.4(9)
F(7)-U-X(1)	92.1(7)	F(14)-Sb(1)-F(8)	85.1(7)
F(7)-U-F(2)	141.1(6)	F(14)-Sb(1)-F(9)	86.3(7)
F(7)-U-X(2)	93.5(7)	F(14)-Sb(1)-F(10)	87.9(7)
F(8)-U-X(1)	84.3(6)	F(14)-Sb(1)-F(11)	85.2(7)
F(8)-U-F(2)	138.0(5)	F(14)-Sb(1)-F(12)	176.2(7)
F(8)-U-X(2)	85.7(6)	F(2)-Sb(2)-F(1)	86.6(6)
F(8)-U-F(7)	78.0(6)	F(3)-Sb(2)-F(1)	93.1(7)
F(13)-U-X(1)	113.7(6)	F(3)-Sb(2)-F(2)	84.9(7)
F(13)-U-F(2)	71.8(5)	F(4)-Sb(2)-F(1)	97.6(7)
F(13)-U-X(2)	78.8(6)	F(4)-Sb(2)-F(2)	175.7(6)
F(13)-U-F(7)	76.7(5)	F(4)-Sb(2)-F(3)	93.7(8)
F(13)-U-F(8)	149.2(5)	F(5)-Sb(2)-F(1)	93.5(7)
F(14)-U-X(1)	86.9(6)	F(5)-Sb(2)-F(2)	85.5(6)
F(14)-U-F(2)	70.3(5)	F(5)-Sb(2)-F(3)	168.0(7)
F(14)-U-X(2)	82.2(7)	F(5)-Sb(2)-F(4)	95.4(7)
F(14)-U-F(7)	147.9(6)	F(13)-Sb(2)-F(1)	173.7(7)
F(14)-U-F(8)	70.0(5)	F(13)-Sb(2)-F(2)	87.1(7)
F(14)-U-F(13)	132.6(5)	F(13)-Sb(2)-F(3)	86.6(7)
F(9)-Sb(1)-F(8)	86.0(7)	F(13)-Sb(2)-F(4)	88.8(7)
F(10)-Sb(1)-F(8)	172.3(7)	F(13)-Sb(2)-F(5)	85.7(7)
F(10)-Sb(1)-F(9)	90.0(8)	Sb(2)-F(2)-U	163.0(7)
F(11)-Sb(1)-F(8)	88.2(7)	Sb(2)-F(13)-U	161.5(7)
F(11)-Sb(1)-F(9)	169.7(9)	Sb(1)-F(8)-U	150.2(7)
F(11)-Sb(1)-F(10)	94.7(7)	Sb(1)-F(14)-U	156.4(7)
F(12)-Sb(1)-F(8)	91.2(7)		

CHAPTER 4

The Preparation of Molybdenum and Tungsten Oxide Tetrafluoride-Antimony Pentafluoride Adducts and the Crystal Structure of $MoF_4O.SbF_5$

4.1 Introduction

The oxide tetrafluorides of molybdenum and tungsten were first prepared by the action of anhydrous hydrogen fluoride on the oxide tetrachlorides.[76,77] A variety of methods have since been reported for the preparation of both MoF_4O[78-80] and WF_4O.[79-85] The most convenient method for the preparation of large quantities of the materials, is the thermal reaction of the metals with an oxygen-fluorine mixture in a dynamic system.[86]

The physical and chemical properties of MoF_4O and WF_4O have been extensively studied. Both are colourless crystalline solids which are readily hydrolysed in the atmosphere. Vapour density measurements[87] and gas phase infrared data[80,88] have shown that both are essentially monomeric in the vapour phase. Further vapour phase infrared spectra of MoF_4O have been interpreted on the basis of C_{4v} molecular symmetry,[89] rather than the C_{2v} symmetry predicted by the valence-shell electron-pair repulsion theory.[90]

The crystal structure of MoF_4O[91] consist of polymeric zig-zag chains, with the molybdenum atoms linked by cis-fluorine bridges. A second form of MoF_4O has been described as trimeric,[92] and the existence of polymorphic forms is supported by Raman spectra for sublimed MoF_4O, and MoF_4O crystallised from a melt which indicate slightly different structures.[93]

The crystal structure of WF_4O[94] was originally interpreted as an oxygen-bridged tetrameric arrangement. Due to the difficulty in distinguishing oxygen and fluorine atoms by X-ray methods, in the presence of a heavy metal atom, the bridging atom was assumed to be oxygen on the basis of infrared data and symmetry considerations. Studies of the solid and liquid phases of WF_4O by vibrational spectroscopy[87,93,95] were found to be inconsistent with this model. The band at 1050 cm^{-1} attributed to a very short terminal tungsten-fluorine bond,[94] was reassigned to a terminal tungsten-oxygen bond. Further infrared studies on WF_4O, using labelled ^{18}O, resulted in a shift of the band attributed to the tungsten-terminal atom bond from 1050 cm^{-1} to 997 cm^{-1}.[96] The same study showed by ^{19}F n.m.r. that all the fluorine atoms are not terminal. The evidence clearly indicates that the crystallographic study was in error, and that the tetrameric units are fluorine bridged.

The acid properties of the oxytetrafluorides of molybdenum, tungsten and uranium towards some inorganic fluoride ion donors have been studied by Bougon et al.[29] In HF solutions, evidence was obtained for partial ionization to give $M_2O_2F_9^-$, and values of equilibrium constants show that WF_4O is the stronger Lewis-acid. The ionic structures found for the adducts formed with the strong bases FNO and $ClOF_3$ is further evidence for the Lewis-acid nature of the oxytetrafluorides. In the MF_4O-FNO-HF system, the anions $MO_2F_9^-$, MOF_5^- and MOF_6^{2-} (M = Mo or W) are formed in amounts dependent on the F^- ion concentration. Ionic complexes containing the anion MOF_5^- (M = Mo or W) result from reactions between alkali fluorides and the hexafluorides in the presence of moisture.[97,98]

The oxytetrafluorides are also capable of forming essentially covalent fluoride bridged adducts. Xenon difluoride and tungsten oxide tetrafluoride form the adducts $XeF_2.nWF_4O$ (n = 1 or 2).[99] ^{19}F n.m.r. of the solutions and vibrational spectroscopy of the solids are indicative of covalent structures with xenon-fluorine-tungsten bridges having no appreciable contribution to the bonding from the ionic formulations $[XeF]^+[WF_5O]^-$ or $[XeF]^+[W_2F_9O_2]^-$. An X-ray structural investigation on $XeF_2.WF_4O$ has confirmed this structure for solid $XeF_2.WF_4O$.[100]

Following work on the uranium oxide tetrafluoride-antimony pentafluoride system, and the successful preparation and characterisation of the adducts $UF_4O.nSbF_5$ (n = 1, 2 or 3), it was decided to attempt the analogous reactions with MoF_4O and WF_4O, in order to see whether similar structures were produced. The X-ray single crystal study of $UF_4O.2SbF_5$ indicated a basically fluorine bridged structure with a considerable contribution from the ionic formulation $[UF_2O]^{2+}[SbF_6]_2^-$. The chemistry of SbF_5 (discussed in section 3.1) and MoF_4O and WF_4O indicates that SbF_5 is a far stronger Lewis-acid than the oxide tetrafluorides, which should favour ionic formulations. It can be predicted from the relative Lewis acidities of MoF_4O and WF_4O[29] that the adducts with tungsten would have less ionic contribution to the bonding and would be expected to be less stable. The tetrameric nature of both SbF_5 and WF_4O structures might also be instrumental in determining the structure of adducts formed between them.

4.2 Preparation

Reactions between molybdenum oxide tetrafluoride and excess of antimony pentafluoride were performed in a preseasoned (ClF_3) and weighed Kel-F reactor. Finely ground MoF_4O was added in a dry-box, and the reactor evacuated before re-weighing. The manifold and reactor were pumped to good vacuum before SbF_5 was added in static vacuum. The 5:1 excess of SbF_5 required was approximated by volume and then the reactor re-weighed. Typically, 1.336 mMol of MoF_4O and 6.645 mMol of SbF_5 were used. The reaction mixture was warmed (40-50°) until all the MoF_4O was dissolved. The product remained homogeneous at room temperature and the free SbF_5 was removed in dynamic vacuum. The weight of the reactor was monitored at set intervals during a twenty hour period. A graph of SbF_5 weight loss vs time of pumping [Figure 7(a)] was plotted. Some stability for the adduct $MoF_4O.2SbF_5$ is indicated by the change of slope at 1:2 composition. The pump curve was halted, and, after 12 hr, well defined crystals formed, but after 4 days only 30% of the reaction mixture was crystalline and cooling did not promote further crystallisation. On the assumption that the crystals were of 1:1 adduct and not a 1:2 adduct of low melting point, pumping was resumed. After 20 hr the weight corresponded to 1:1 composition, and thereafter virtually zero rate of SbF_5 loss (<0.00001 g min^{-1}) occurred.

The mass spectrum of the solid revealed the species SbF_6^+, SbF_5^+, SbF_4^+, SbF_3^+, SbF_2^+, SbF^+, Sb^+ and MoF_2O^+, $MoFO_2^+$, $MoF_2O_2^+$ and MoF_3O^+. The dioxyfluoride species may be attributed to impurities in the sample but more likely arise from reaction with residual oxygen in the mass spectrometer. The Raman spectra of MoF_4O and a powdered sample of the adduct were recorded at the same time to eliminate marker zero errors, the results are listed in Table 7. The Raman shift of the metal-oxygen band from 1042 cm^{-1} to 1047 cm^{-1} may be taken as some indication of ionic character in the adduct. The upfield shift is expected for an increased positive charge on the metal atom, but the magnitude suggests a covalent compound with only slight contribution from the formulation $[MoF_3O]^+[SbF_6]^-$.

Upon close examination, crystals appeared to be of two forms. Examples of each were ground and the X-ray powder diffraction patterns recorded. The first crystal form (I), were block shaped crystals, and were suspected to be MoF_4O, but gave a diffraction pattern which could be indexed as primitive cubic, a = 5.03 Å. [It is suspected that these

Figure 7

Weight loss against time plots for
a) $MoF_4O.nSbF_5$

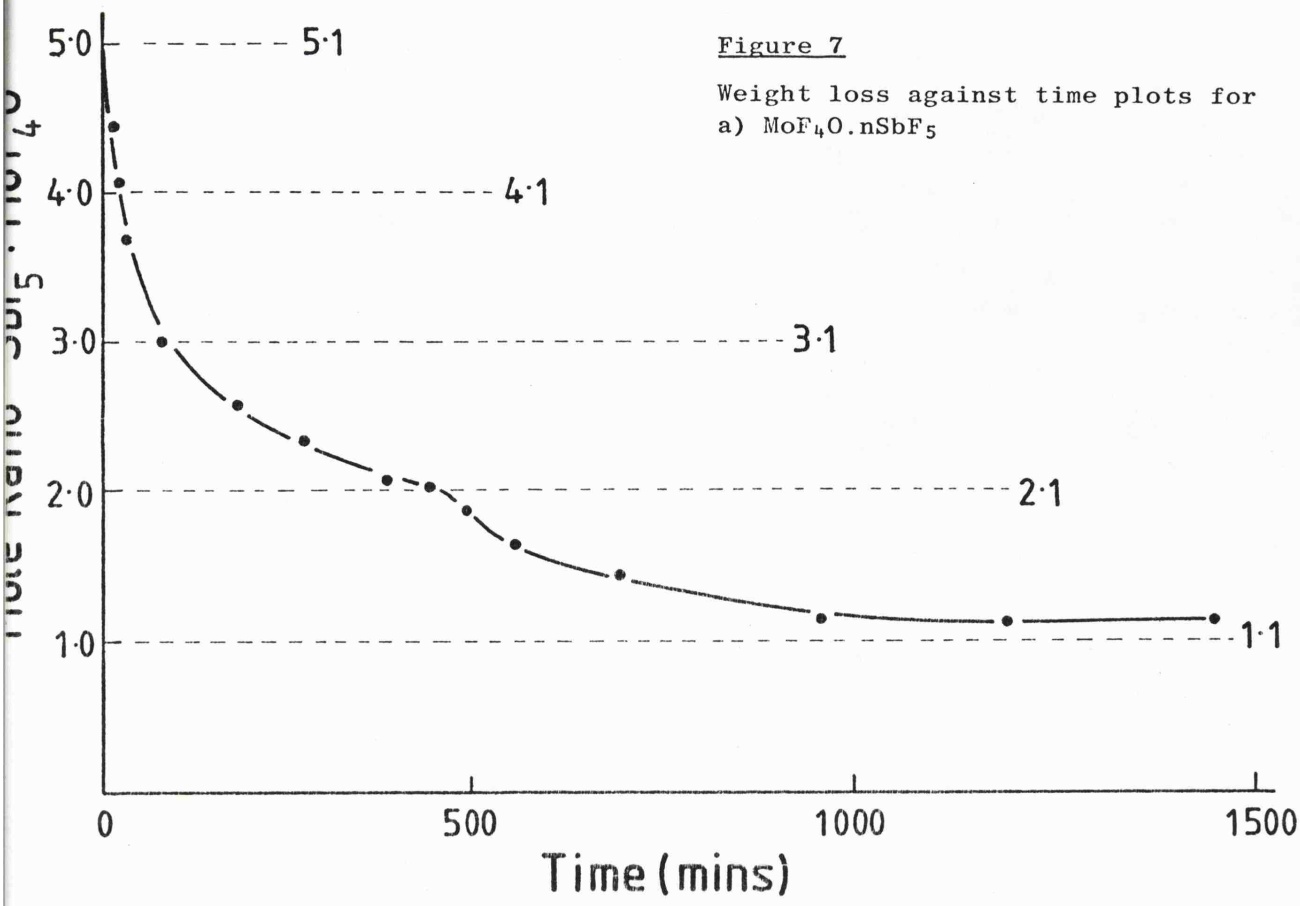

b) $WF_4O.nSbF_5$

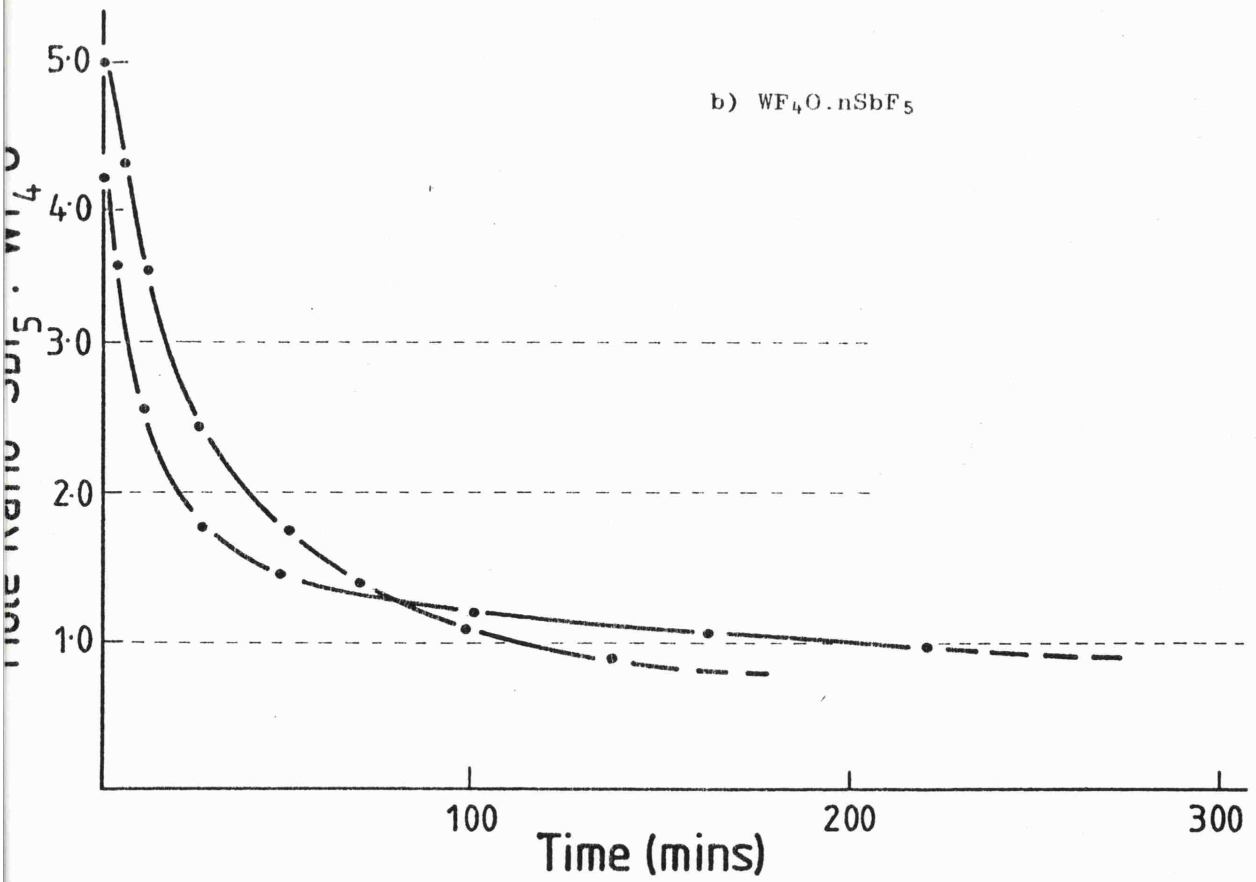

TABLE 7

The Raman spectrum (cm^{-1}) of the adduct $MoF_4O.SbF_5$ compared with those of pure MoF_4O and SbF_5

$MoF_4O.SbF_5$	MoF_4O	SbF_5
1047 cm^{-1} (s)	1042 cm^{-1} (s)	
766 (mw)	740 (m)	
704 (m)	721 (mw)	718 cm^{-1} (s)
675 (s)	688 (s)	670 (vs)
621 (w)		
578 (w)	571 (w)	
	529 (w)	
	506 (vw)	
338 (w)	333 (m)	349 (vw)
314 (w)	309 (ms)	
	275 (w)	268 (m)
233 (w)	222 (mw)	231 (mw)
		189 (mw)

crystals are an antimony adduct of the form $H_xO_y^+SbF_6^-$, see chapter 10.] The bulk of the crystals were of form II, and gave a diffraction pattern (Table 8), which could be indexed using the cell parameters found in the single crystal study.

The reaction conditions used for the tungsten oxide tetrafluoride-antimony pentafluoride system were identical, but the results were not consistent. Possibly this system is more strongly influenced by small changes in the amount of heating applied to obtain the initial solution. Three reactions each gave different points of apparent stability on the pump curve, but in all cases SbF_5 was still being lost when the 1:1 composition was reached [Figure 7(b)]. The bulk of the samples consisted of interfering crystals, all good single crystals separated gave cell parameters that were, within experimental error, indistinguishable from WF_4O.

The mass spectra of the product revealed only the species SbF_4^+, SbF_3^+, SbF_2^+, SbF^+, Sb^+ and WF_3O^+, WF_2O^+, WF_3^+, WFO^+ and WF_2^+. Despite careful pre-treatment of the mass spectrometer, parent ions of complex fluorides introduced to the spectrometer are rarely seen and the mass spectra obtained is as would be expected for $WF_4O.SbF_5$. The Raman spectra of the product (Table 9) indicates little or no ionic character. The ν_1 Sb-F band at 670 cm^{-1} is consistent with Sb-F frequency for SbF_5 rather than SbF_6^- (662 cm^{-1}). Similarly the metal-oxygen stretch at 1061 cm^{-1} is close to that found for WF_4O (1058 cm^{-1}). An X-ray powder diffraction pattern showed only differences in intensity for the reflections {130} and {040} from those of WF_4O, but was otherwise identical. There is no clear explanation of these observations, either the adduct is not crystalline and the powder pattern is due to WF_4O impurity, or SbF_5 fits into the WF_4O structure without significant

TABLE 8

X-ray powder diffraction pattern of $MoF_4O.SbF_5$

Line	intensity	$\sin^2\theta \times 10^4$	$\sin^2\theta \times 10^4$ (calc) based on single crystal study	Assignment
a	mw	182	-	-
b	vw	221	218	020
c	mw	239	246	111
d	m	263	264	002
e	mw	322	326	120
f	s	384	-	-
g	s	407	408	102
h	mw	443	435	200
i	w	489	482	022
j	m	537	520	$21\bar{1}$
k	vw	568	557	031
l	vw	603	591	211
m	w	651	649	013
n	mw	724	-	-
o	w	945	956	$23\bar{1}$
p	vw	1173	1190	213
q	m	1238	1236	104
r	w	1301	1307	240
s	mw	1454	1454	124

[Cu-K_α radiation]

TABLE 9

Raman spectra (cm^{-1}) of the adduct $WF_4O.SbF_5$ compared with that of pure WF_4O.

$WF_4O.SbF_5$	WF_4O
1061 (vs)	1058 (vs)
758 (mw)	744 (m)
710 (s)	728 (w)
	687 (vw)
670 (s)	669 (vw) (sh)
	663 (mw)
556 (vw)	563 (w)
	532 (vw)
	523 (w)
	388 (w)
	367 (vw)
334 (w)	330 (mw)
	318 (m) (sh)
312 (w)	314 (s)
279 (w)	265 (w)
242 (vw)	242 (mw)
	215 (mw)
	151 (mw)
133 (vw)	135 (w)

alteration of the cell parameters.

As no suitable single crystals were obtained by the removal of the excess of SbF_5, attempts were made to recrystallise the adduct from anhydrous HF, and CH_3CN containing a trace of HF. The latter method yielded no single crystals. From HF solution colourless crystals were formed. An X-ray single crystal study located only one type of heavy metal atom in a tetragonal cell (a = 7.17 Å, c = 5.05 Å). This was identified as antimony by the Raman spectrum. It was, therefore, suspected that the crystals were again of the composition $H_xO_y\ SbF_6$, and are discussed in chapter 10.

A further attempt to obtain single crystals of $WF_4O.SbF_5$ was made using the method employed for the preparation of $UF_4O.SbF_5$, whereby stoichiometric quantities of the reactants are mixed in solution. A Kel-F reactor was charged with 1.04 mMol of WF_4O, and SbF_5 (0.990 mMol) and the solvent, WF_6, were added in static vacuum. Complete solution was obtained by gentle warming of the mixture. A white solid product, consisting of interfering and single crystals, was obtained upon removing the solvent. The weight of the reactor and product was greater than expected from the weights of WF_4O and SbF_5 used. This is due to WF_6 either taking part in the reaction or becoming absorbed on the reactor walls. The Raman and infrared spectra are consistent with those of the previous samples of $WF_4O.SbF_5$, as is the X-ray powder diffraction pattern.

Unlike the UF_4O-SbF_5 system, it appears that both MoF_4O and WF_4O form only stable adducts of 1:1 composition with SbF_5.

4.3 Single Crystal X-ray Investigation of $MoF_4O.SbF_5$

The crystals grown from excess of SbF_5 were of suitable dimensions and appearance, several crystals were sealed in preseasoned Pyrex capillaries. The crystal used for the investigation had approximate dimensions 0.2 mm × 0.1 mm × 0.07 mm, and was wedged obliquely in the tube. This required that the capillary be fixed on the arcs at approximately 45°. Preliminary cell dimensions were obtained from Weissenberg photographs taken using Cu-K_α (Ni filtered) radiation and precession photographs, using Mo-K_α (Zr filtered) radiation. Final cell dimension were determined from an oscillation photograph for the rotation axis $\underline{b}$, and from optimised counter angles for zero and upper layer reflections on a Weissenberg diffractometer.

4.4 Crystal Data

F_9MoOSb ; $\underline{M}$ = 404.75

Monoclinic $\underline{a}$ = 7.470(8), $\underline{b}$ = 10.40(2), $\underline{c}$ = 9.606(9) Å

$\underline{\beta}$ = 93.13 ± 0.3°

$\underline{U}$ = 745.06 Å^3; $\underline{D_c}$ = 3.61 g cm^{-3}; $\underline{z}$ = 4

$\underline{F}$(000) = 727.82; Mo-K_α radiation; λ = 0.71069 Å

$\underline{\mu}$(Mo-K_α) = 50.12 cm^{-1}

Space group $\underline{P}2_1/\underline{n}$ (non-standard setting of $\underline{P}2_1/\underline{c}$, No. 14). Neutral scattering factors were used, with anomalous dispersion coefficients.

4.5 Collection of the Intensity Data

Data were collected from layers h01 to h101, using the Stadi-2 diffractometer, in the +h, +k, +l quadrant for the h0l layer, and in the two quadrants ±h, for the remaining layers. A total of 1123 unique reflections were obtained with $I/\sigma I \geqslant 3$. Data were collected using an ω-scan technique. Monitoring of check reflections throughout each layer indicated no significant deterioration of the crystal during the data collection. Lorentz, polarisation and absorption corrections were made to the data set.

4.6 Solution of the structure

The program system SHELX was used. A Patterson summation was used to locate the molybdenum and antimony atoms. Three cycles of least squares refinement gave an R factor of 0.20, and allowed sufficient phasing for the location of the light atoms by Fourier maps. The oxygen atom was chosen from the shortest molybdenum to light-atom bond length, three cycles of refinement with all atoms included and isotropic temperature factors gave an R factor of 0.11. An absorption correction, maximum and minimum transmission factors 0.524 and 0.359 respectively, was performed on the data set. Further cycles of refinement using anisotropic thermal parameters for all atoms reduced R to 0.043. Final cycles employed a weighting parameter g (0.00076) $[\omega \propto 1/\sigma^2(F) + g F^2]$ and an isotropic extinction parameter $\underline{x}$ (0.00045) $[F_c = F(1 - x F^2/\mathrm{Sin}\theta)]$. The final difference Fourier revealed no significant features and an analysis of the weighting scheme over $|F_o|$ and $\mathrm{Sin}\theta/\lambda$ was satisfactory. Final atomic positional parameters are given in Table 10, the anisotropic thermal parameters are in Table 11. The interatomic distances and angles are in Tables 12 and 13 respectively, and the observed and calculated structure factors are found in Appendix 2.

Final residual indices for 1123 reflections:-

$$R = \sum(|F_o| - |F_c|)/\sum|F_o| = 0.0413$$

$$R_w = [\sum w(|F_o| - |F_c|)^2/\sum w|F_o|^2]^{\frac{1}{2}} = 0.0408$$

TABLE 10

Atomic positional parameters for $MoF_4O.SbF_5$, with estimated standard deviations in parentheses.

	x/a	y/b	z/c
Sb	0.28909(9)	0.01861(6)	0.19183(7)
Mo	0.62617(12)	0.32094(9)	0.16927(9)
O	0.7902(11)	0.2514(8)	0.0828(8)
F(1)	0.4693(9)	0.1481(6)	0.1594(7)
F(2)	0.4555(10)	-0.1050(7)	0.1597(10)
F(3)	0.2241(12)	0.0160(8)	0.0060(8)
F(4)	0.1237(12)	0.1442(8)	0.2197(13)
F(5)	0.3529(15)	0.0199(11)	0.3744(8)
F(6)	0.4713(10)	0.3544(7)	0.0241(6)
F(7)	0.6703(10)	0.2574(7)	0.3393(6)
F(8)	0.3901(9)	0.3895(6)	0.2769(7)
F(9)	0.7085(10)	0.4752(7)	0.1925(8)

TABLE 11

Anisotropic thermal parameters, with estimated standard deviations in parentheses

The temperature factors are in the form $\exp[-2\pi^2(h^2U_{11}a^2 + \ldots\ldots 2hkU_{12}ab)]$

	U_{11}	U_{22}	U_{33}	U_{23}	U_{13}	U_{12}
Sb	0.0296(4)	0.0267(4)	0.0348(4)	-0.0024(3)	0.0081(2)	-0.0043(3)
Mo	0.0253(4)	0.0268(6)	0.0408(5)	-0.0021(3)	0.0029(3)	-0.0020(4)
O	0.039(5)	0.041(5)	0.069(5)	-0.007(4)	0.021(4)	0.003(4)
F(1)	0.048(4)	0.035(4)	0.070(4)	-0.015(3)	0.017(3)	-0.018(3)
F(2)	0.039(4)	0.041(4)	0.147(8)	-0.001(4)	0.022(5)	0.005(3)
F(3)	0.090(6)	0.084(6)	0.049(4)	0.019(4)	-0.010(4)	-0.035(5)
F(4)	0.058(5)	0.052(5)	0.202(11)	-0.039(6)	0.047(6)	0.008(4)
F(5)	0.119(8)	0.141(9)	0.047(4)	0.007(5)	-0.002(5)	-0.065(7)
F(6)	0.053(4)	0.063(5)	0.041(4)	0.002(3)	-0.013(3)	-0.006(4)
F(7)	0.059(5)	0.048(4)	0.053(4)	0.005(3)	-0.002(3)	0.006(4)
F(8)	0.040(4)	0.042(4)	0.061(4)	-0.001(3)	0.012(3)	0.009(3)
F(9)	0.046(4)	0.036(4)	0.086(5)	-0.002(3)	0.005(3)	-0.011(3)

TABLE 12

Interatomic distances (Å) with estimated standard deviations in parentheses

a) bond distances

Sb-F(1)	1.942(6)
Sb-F(2)	1.826(7)
Sb-F(3)	1.824(7)
Sb-F(4)	1.827(8)
Sb-F(5)	1.792(8)
Sb-F(8)	1.931(6)
Mo-O	1.681(7)
Mo-F(1)	2.145(6)
Mo-F(6)	1.797(6)
Mo-F(7)	1.776(6)
Mo-F(8)	2.210(6)
Mo-F(9)	1.728(7)

b) non-bond distances

Sb...Mo	4.041
Sb...Mo	4.010
Mo...F(3)	3.690
Mo...F(2)	3.535
O...F(1)	2.763
O...F(6)	2.645
O...F(7)	2.668
O...F(9)	2.641
O...F(3)	2.909
F(1)...F(2)	2.635
F(1)...F(3)	2.668
F(1)...F(4)	2.677
F(1)...F(5)	2.645
F(1)...F(6)	2.509
F(1)...F(7)	2.500
F(1)...F(8)	2.828
F(2)...F(3)	2.544
F(2)...F(5)	2.589
F(2)...F(8)	2.685
F(3)...F(4)	2.592
F(3)...F(7)	2.866
F(3)...F(8)	2.646
F(4)...F(5)	2.555
F(4)...F(8)	2.651
F(5)...F(8)	2.638
F(6)...F(8)	2.561
F(6)...F(9)	2.650
F(7)...F(8)	2.547
F(7)...F(9)	2.692
F(8)...F(9)	2.705

TABLE 13

Interatomic angles (°), with estimated standard deviations in parentheses

F(2)-Sb-F(1)	88.7(0.3)
F(3)-Sb-F(1)	90.2(0.3)
F(3)-Sb-F(2)	88.4(0.4)
F(4)-Sb-F(1)	90.5(0.4)
F(4)-Sb-F(2)	178.5(0.5)
F(4)-Sb-F(3)	90.5(0.5)
F(5)-Sb-F(1)	90.1(0.4)
F(5)-Sb-F(2)	91.4(0.5)
F(5)-Sb-F(3)	179.6(0.3)
F(5)-Sb-F(4)	89.8(0.6)
F(1)-Mo-O	91.6(0.3)
F(6)-Mo-O	98.9(0.4)
F(6)-Mo-F(1)	78.5(0.3)
F(7)-Mo-O	101.0(0.4)
F(7)-Mo-F(1)	78.6(0.3)
F(7)-Mo-F(6)	149.9(0.3)
F(8)-Mo-O	172.5(0.3)
F(8)-Mo-F(1)	81.0(0.2)
F(8)-Mo-F(6)	78.7(0.3)
F(8)-Mo-F(7)	78.6(0.3)
F(9)-Mo-O	101.5(0.4)
F(9)-Mo-F(1)	166.7(0.3)
F(9)-Mo-F(6)	97.5(0.3)
F(9)-Mo-F(7)	100.4(0.4)
F(9)-Mo-F(8)	85.8(0.3)
Mo-F(1)-Sb	163.0(0.4)
Mo-F(8)-Sb	161.6(0.4)

4.7 Discussion

The structure of $MoF_4O.SbF_5$ is related to that of MoF_4O,[91] with alternate antimony and molybdenum atoms linked through fluorine bridges into a polymeric zig-zag chain (Figure 8). Equivalent atoms of each chain are aligned in the ab plane. The arrangement of the pairs of bridging fluorine atoms about the molybdenum atom is cis, and trans for the antimony atom. The light atoms are approximately octahedrally arranged about the antimony atom, with angles of $90 \pm 1.6°$, but the octahedron is elongated in the direction of the trans fluorine bridges. The average antimony to fluorine bridge distance is 1.94(1) Å compared with the average antimony to terminal fluorine distance of 1.82(1) Å. The light atom array about molybdenum is less regular, due to the presence of the oxygen atom and the cis fluorine bridging arrangement. The molybdenum atom is effectively displaced away from the adjacent bridging fluorine atoms and towards the two light atoms in the same plane (Figure 9).

Unlike MoF_4O, which has asymmetric molybdenum to fluorine bridge bonds of 1.94(1) Å and 2.29(2) Å, the bridging distances to molybdenum in the SbF_5 adduct are approximately equal at 2.15(1) Å and 2.21(1) Å. The possibility that the bridging atoms could be alternately oxygen and fluorine was rejected on the evidence of vibrational spectroscopic data and the equivalence of the bridging bonds. The terminal atoms perpendicular to the bridging plane were assigned to fluorine, the bond distances to molybdenum of 1.78(1) Å and 1.80(1) Å being typical of metal to terminal fluorine atom bond lengths. The assignment of the oxygen atom to one of the two light atoms equatorial to the bridging atoms is not conclusive, but has been made on the basis of the shortest molybdenum to light atom bond length. In the structure of MoF_4O, the

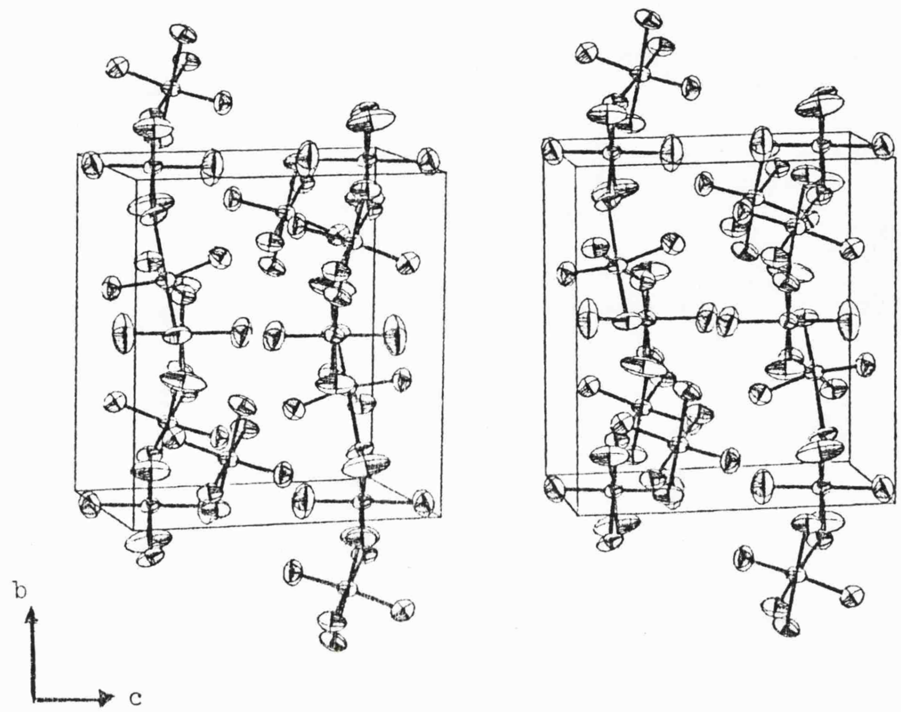

Figure 8

Stereoscopic view of the unit cell contents of $MoF_4O.SbF_5$.

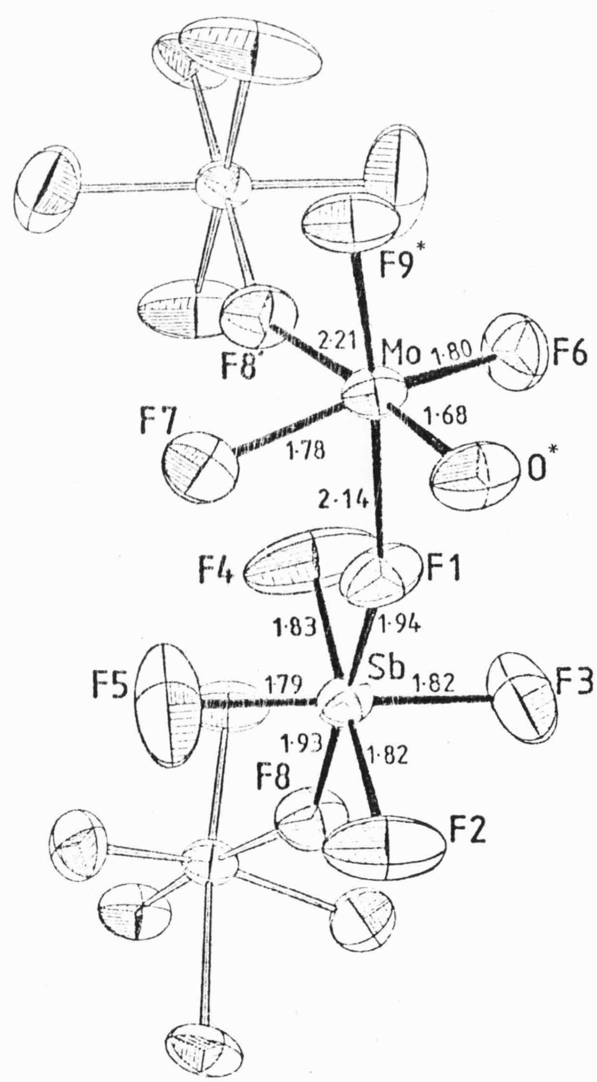

Figure 9

The asymmetric unit of $MoF_4O.SbF_5$.

light atom opposite the longer fluorine bridge has a bond distance of 1.65(1) Å, compared with 1.82(1) Å for the light atom trans to the short fluorine bridge and the oxygen atom was thus fixed unequivocally. However, the equivalent atoms of the SbF_5 adduct have bond lengths of 1.68(1) Å and 1.73(1) Å, and though this indicates a preference for placing the oxygen atom at the co-ordinates 1.68(1) Å from molybdenum, this distance is longer than expected for a metal to oxygen bond, and the 1.73(1) Å bond length is short for metal-fluorine, which suggests a degree of disorder between these positions.

The zig-zag chain structure of the adduct is in contrast with the tetrameric form of the antimony pentafluoride solid state structure.[73] The SbF_5 tetramer is a distorted fluorine bridged structure with antimony-fluorine-antimony angles of 141 and 170° and thus is between the regular tetrameric type of structure exhibited by NbF_5[74] and the highly distorted tetramers typified by RhF_5.[70]

From the closer association of the bridging fluorine atoms with the antimony atoms than the molybdenum atoms it can be argued that there is some contribution from the ionic formulation $[MoF_3O]^+[SbF_6]^-$. The average Sb-F fluorine bridge distance of the adduct, 1.94(1) Å, is less than the fluorine bridge distance of 2.02(5) Å found in the tetrameric SbF_5 structure.[73] The average Mo-F bridge distance of the adduct, 2.18(1) Å, is greater than the average of the equivalent but asymmetric bonds in the MoF_4O structure (2.12(1) Å).[91] This reflects the greater affinity of antimony for fluorine, but the Raman spectrum with almost insignificant shift to higher frequency of the ν_1 band for the Mo = O bond suggests an essentially covalent compound.

An estimate of the degree of ionic character of the adduct may be calculated using the method applied to the $UF_4O.2SbF_5$ structure (chapter 3). As with the uranium adduct, no estimate of the Mo-F distance representative of a donor fluorine atom in an ionic structure can be established. However, a comparison of Sb-F bridged bond distances for the adduct (D_a) with the average bridging distance of the neutral SbF_5 tetramer (D_n), and the Sb-F distance found in regular ionic octahedra (D_i), allows an estimation of ionic character to be made:-

$$\frac{D_c - D_a}{D_c - D_i} = \frac{2.02 - 1.94}{2.02 - 1.845} = 0.46\ (3)$$

The estimated ionic character of 46% is of the same order as the value obtained for the $UF_4O.2SbF_5$ adduct. This is contrary to the evidence of the Raman data. However, the natures of the two adducts $UF_4O.2SbF_5$ and $MoF_4O.SbF_5$ are significantly different. As ionic structures, the anticipated formulations would be $[UF_2O]^{2+}2[SbF_6]^-$ and $[MoF_3O]^+[SbF_6]^-$, and it can reasonably be argued that the contributions to bonding from the ionic form of the uranium compound, in which two positive charges are associated with the $[UF_2O]^{2+}$ cation, might give rise to a significantly greater Raman shift than in the case of the molybdenum cation $[MoF_3O]^+$. It appears that the calculations of ionic character in both structures are, at best, indications of a degree of ionicity in essentially covalent, fluorine bridged structures. The Raman shift is apparently not significant as a measure of ionicity in two compounds which differ so much in their basic structures.

The inability to grow crystals of the adduct $WF_4O.SbF_5$ may be attributable to the stronger Lewis acidity of WF_4O than MoF_4O.[29] With increased Lewis acid nature, less contribution from ionic bonding would be expected within the structure, with a lower resultant bond energy. The structure of the $WF_4O.SbF_5$ adduct may, thus, be too disordered at room temperature to obtain good single crystals.

CHAPTER 5

The Preparation and Crystal Structure of $ReF_4O.SbF_5$

5.1 Introduction

Rhenium oxide tetrafluoride was first reported as a blue crystalline solid, by Hargreaves and Peacock,[101] as a product of the reaction between tungsten hexacarbonyl and an excess of rhenium hexafluoride. However, under rigorously dry conditions it has been found[102] that the major product of this reaction is $Re(CO)_3F_3$. An earlier reported preparation of ReF_4O,[103] by the fluorination of rhenium metal in the presence of oxygen, was shown later to produce ReF_5O.[104] Several preparative methods have since been devised for ReF_4O; these include the slow hydrolysis of ReF_6 on Pyrex wool,[105] the action of ReF_6 on ReO_3[106] and the reaction of excess of ReF_6 with B_2O_3.[107] The method used here was the controlled hydrolysis of an excess of ReF_6 by H_2O in anhydrous HF. This method was reported by Paine[105] as producing only 10% yield, but was found to be efficient for the preparations of UF_4O,[20,26] NpF_4O[108] and PuF_4O,[109] and under the conditions used was found here to give a high yield of ReF_4O.

The physical properties of the oxide tetrafluorides of the third-row transition elements are remarkably similar.[86,105,110] The chemical reactivity is found to increase with the molecular weight.[86] The rhenium compound is considerably more reactive than MoF_4O or WF_4O, and more readily hydrolysed by traces of moisture to produce perrhenic acid, rhenium dioxide and hydrofluoric acid. Rhenium oxide tetrafluoride, like several of the transition metal and actinide metal oxide tetrafluorides exhibits polymorphic solid forms. The dark blue phase of ReF_4O[88,111] has the MoF_4O endless chain type of structure,[91,93] with the rhenium atoms linked through cis-fluorine bridges, with a Re-F-Re bridging angle of 139°. The pale blue metastable form of ReF_4O has a trimeric unit,[112] similar to those of the metastable forms of MoF_4O[92,93]

and TcF_4O,[113] with similar bond lengths and angles found around rhenium, to those in the normal chain structure. The rhenium atoms lie at the corners of a triangle, with the bridging fluorine atoms cis- to each other as in the other form.

Following the preparation of antimony pentafluoride adducts with uranium, molybdenum and tungsten oxide tetrafluorides, and the single crystal studies on $UF_4O.2SbF_5$ and $MoF_4O.SbF_5$, it was decided to investigate the ReF_4O-SbF_5 system. It was concluded that the inability to produce single crystals of the adduct $WF_4O.SbF_5$ was due to the greater Lewis acidity of WF_4O over MoF_4O and a corresponding reduction in the contribution to the bonding within the adduct from an ionic form. Since ReF_4O is expected to be a stronger Lewis acid than WF_4O a similar argument would suggest even less stability for the adducts $ReF_4O.nSbF_5$, and an identical preparative method was used to test this.

5.2 Reaction between Rhenium Oxide Tetrafluoride and Antimony Pentafluoride

The reaction between rhenium oxide tetrafluoride and excess of antimony pentafluoride was performed in a preseasoned (ClF_3) and weighed Kel-F reactor. ReF_4O, from the controlled hydrolysis of ReF_6, was added to the reactor in a dry-box, and the reactor evacuated and reweighed. The manifold was then pumped to a good vacuum and SbF_5 added to the reactor in static vacuum. The approximate 12:1 excess of SbF_5 required was estimated by volume, and the reactor reweighed after addition. The ReF_4O, 0.0870 g (0.315 mMol) was dissolved in the excess of SbF_5, 0.8007 g (3.694 mMol) by gently warming the reactor until a dark blue solution was obtained. The rate of weight loss against pumping time was observed as for the adducts of SbF_5 with uranium,

Figure 10

The mass spectrum of $ReF_4O.SbF_5$.

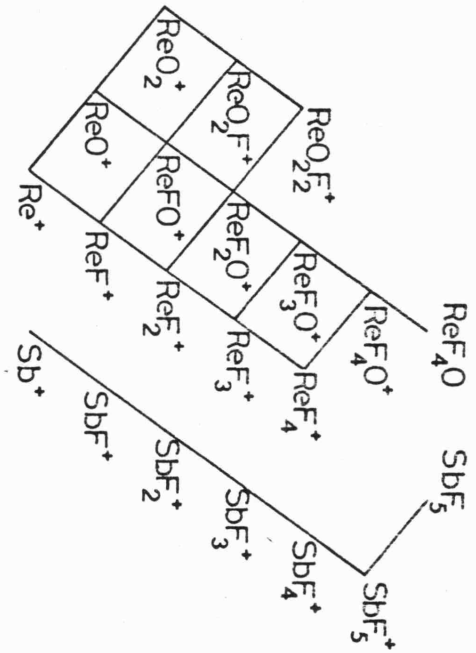

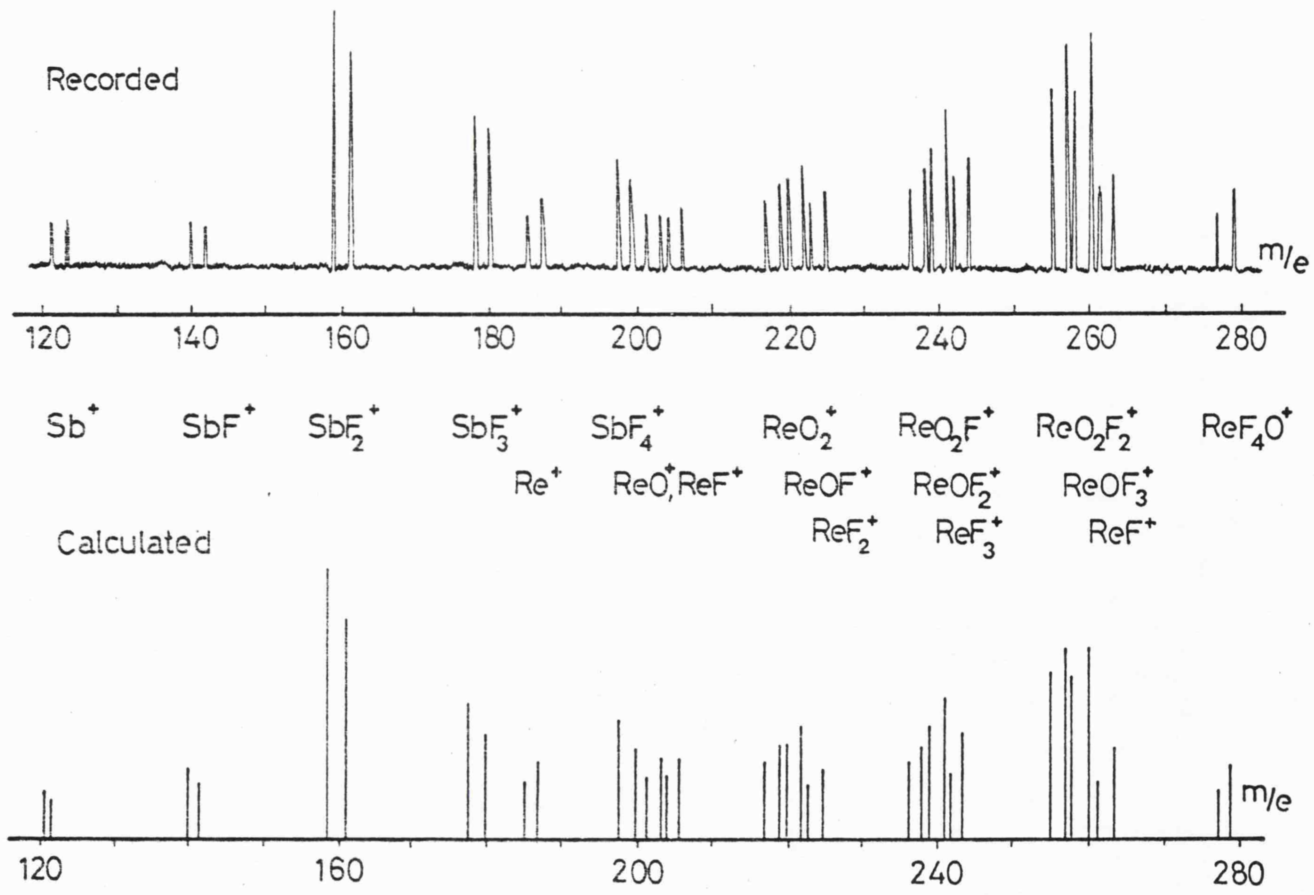

molybdenum and tungsten. The pump curve was similar to that observed with the WF_4O-SbF_5 system, SbF_5 continuing to be lost quite rapidly at 2:1 composition. At this composition pale blue crystals appeared in the liquid, and the reaction mixture was allowed to stand at room temperature for 24 hours, during which time all the material crystallised.

Examples of the single crystals were transferred in a dry-box to a preseasoned Pyrex capillary apparatus. A sample of the material was ground for X-ray powder diffraction, mass spectrometry and Raman studies but decomposed in the process and no X-ray powder pattern or Raman spectrum were obtained. However, several of the single crystals which were isolated for the X-ray study, although giving sufficiently good photographs to determine that the unit cell was identical to the crystal eventually used for data collection, were twinned and accordingly were used for mass spectrometry. The mass spectra were identical (Figure 10), showing the mass peaks ReF_4O^+, ReF_4^+, ReF_3O^+, ReF_3^+, ReF_2O^+, ReF_2^+, $ReFO^+$, ReF^+, ReO^+, Re^+ and SbF_4^+, SbF_3^+, SbF_2^+, SbF^+, Sb^+. From the mass spectra it seems certain that the crystals are of a $ReF_4O.nSbF_5$ adduct. The crystallisation occurring at a ReF_4O:SbF_5 ratio of 1:2 suggest that this would be the form of the single crystals.

5.3 Single crystal X-ray Investigation of $ReF_4O.nSbF_5$

The pale blue crystals grown from excess of SbF_5, were of suitable dimensions for a single crystal study and several were sealed into preseasoned Pyrex capillaries. The crystal chosen for the investigation had the approximate dimensions 0.26 mm x 0.11 mm x 0.11 mm and was a well-defined rectangular block. Approximate cell dimensions were obtained from Weissenberg photographs taken using Cu-$\underline{K}\alpha$ (Ni filtered) radiation and precession photographs using Mo-$\underline{K}\alpha$ (Zr filtered) radiation. The final cell dimensions were determined from an oscillation photograph for the rotation axis $\underline{a}$, and from optimised counter angles for zero and upper layer reflections on a Weissenberg diffractometer.

5.4 Crystal Data

F_9O Re Sb ; $\underline{M}$ = 494.93

Monoclinic $\underline{a}$ = 5.561(10), $\underline{b}$ = 10.198(8), $\underline{c}$ = 12.622(9) Å

$\underline{\beta}$ = 99.37 (20)°

$\underline{U}$ = 706.26 $Å^3$; $\underline{D_c}$ = 4.656 gcm^{-3}; $\underline{Z}$ = 4

$\underline{F}$(000) = 859.80; Mo-$\underline{K}\alpha$ radiation; λ = 0.71069 Å

μ(Mo-$\underline{K}\alpha$) = 200.95 cm^{-1}

Space group $\underline{P2_1/c}$ (C^5_{2h} No. 14). Neutral atomic scattering factors were used with anomalous dispersion coefficients.

5.5 Collection of Intensity Data

Data were collected from layers 0kl to 7kl using the Stadi-2 diffractometer, in the +h,+k,+l quadrant only for the 0kl layer and in the two quadrants +h,+k,±l for the upper layers. Data were collected using an $\underline{\omega}$-scan technique, with a count time of 0.3 second at 0.01° increments of $\underline{\omega}$. The intensities of reflections with $0.06 < \sin\theta/\lambda < 0.7$ $Å^{-1}$ were collected at 22 to 25°C. A total of 1075 unique reflections were obtained with $I/\sigma I \geqslant 3$. Monitoring of check reflections throughout the data collection for each layer showed no significant overall deterioration of the crystal during the data collection. However, the check reflection observed during the collection of 2kl data, consistently decreased in intensity during the data collection for that layer, with a total loss of approximately 4%. At this stage the check reflection used for the zero layer was re-measured and also found to be 4% low. The 0kl check reflection was thereafter re-measured after each layer, but showed no further loss of intensity, and no significant trend was observed in the weighting analysis. Layer scale factors were, therefore, not applied to the data. Lorentz, polarisation and absorption corrections were made to the data set.

5.6 Solution of the Structure

The program system SHELX was used. A Patterson summation was used to locate the rhenium and antimony atoms. The solution of the Patterson map was complicated by the approximate zero values for the fractional co-ordinates X/A and Z/C of the antimony atom and Y/B for the rhenium. The resultant vectors indicated a heavy atom on a special position, but three cycles of least-squares refinement indicated further heavy atoms which were ruled out by volume considerations. The final solution of the Patterson summation allowed 4 atoms of rhenium and antimony in general positions of the space group $\underline{P}2_1/\underline{c}$, with approximately 18 $\mathring{A}^3$ for each fluorine atom assuming a molecular formula of $ReF_4O.SbF_5$. Three cycles of least-squares refinement gave an R factor of 0.14 and allowed sufficient phasing for the location of the light atoms by difference Fourier maps. The oxygen atom was chosen to correspond with the shortest rhenium to light atom distance, and three cycles of refinement with all atoms included with isotropic thermal parameters gave an R factor of 0.071. An analysis of the weighting scheme over $|F_o|$ and $\sin\theta/\lambda$ with various values of fixed or refining weighting parameter, $g[\omega \propto 1/\sigma^2(F) + gF^2]$ proved unsatisfactory. Poor agreement between reflections h(n)l and h(n+1)l was obtained and several reflections with deviations greater than 2σ occurred for reflections with k = 1 and 3. Convergence was improved by repeating the absorption correction with a reduced value for the absorption coefficient (μ), which effectively decreased all measured crystal dimensions.

Final cycles, for which all atoms were refined anisotropically, employed a weighting parameter g(.001) and 13 deviant reflections were omitted. The final difference Fourier revealed no significant features and an analysis of the weighting scheme over $|F_o|$ and $\sin\theta/\lambda$ was now satisfactory.

Final atomic parameters are given in Table 14, the anisotropic thermal parameters are in Table 15. The interatomic distances and angles are in Tables 16 and 17 respectively and the observed and calculated structure factors are found in Appendix 3.

Final residual indices for 1062 reflections:-

$$R = \sum(|F_o|-|F_c|)/\sum|F_o| = 0.0576$$

$$R_w = [\sum w(|F_o|-|F_c|)^2/\sum w|F_o|^2]^{\frac{1}{2}} = 0.0612$$

5.7 Discussion

The structure of $ReF_4O.SbF_5$ contains dimers of the adduct, with two rhenium atoms and two antimony atoms, linked through fluorine bridges into distorted 'tetrameric' rings (Figure 11). The structure is, therefore, more closely related to that of the solid state tetrameric structure of SbF_5[73] than ReF_4O,[88,111] which forms endless chains. However, the bond angles about the fluorine bridge atoms, of 137.8(9) and 148.0(9)° show the dimer ring is less planar than that of SbF_5, and approximates to the distorted tetrameric ring arrangements of RhF_5[70]

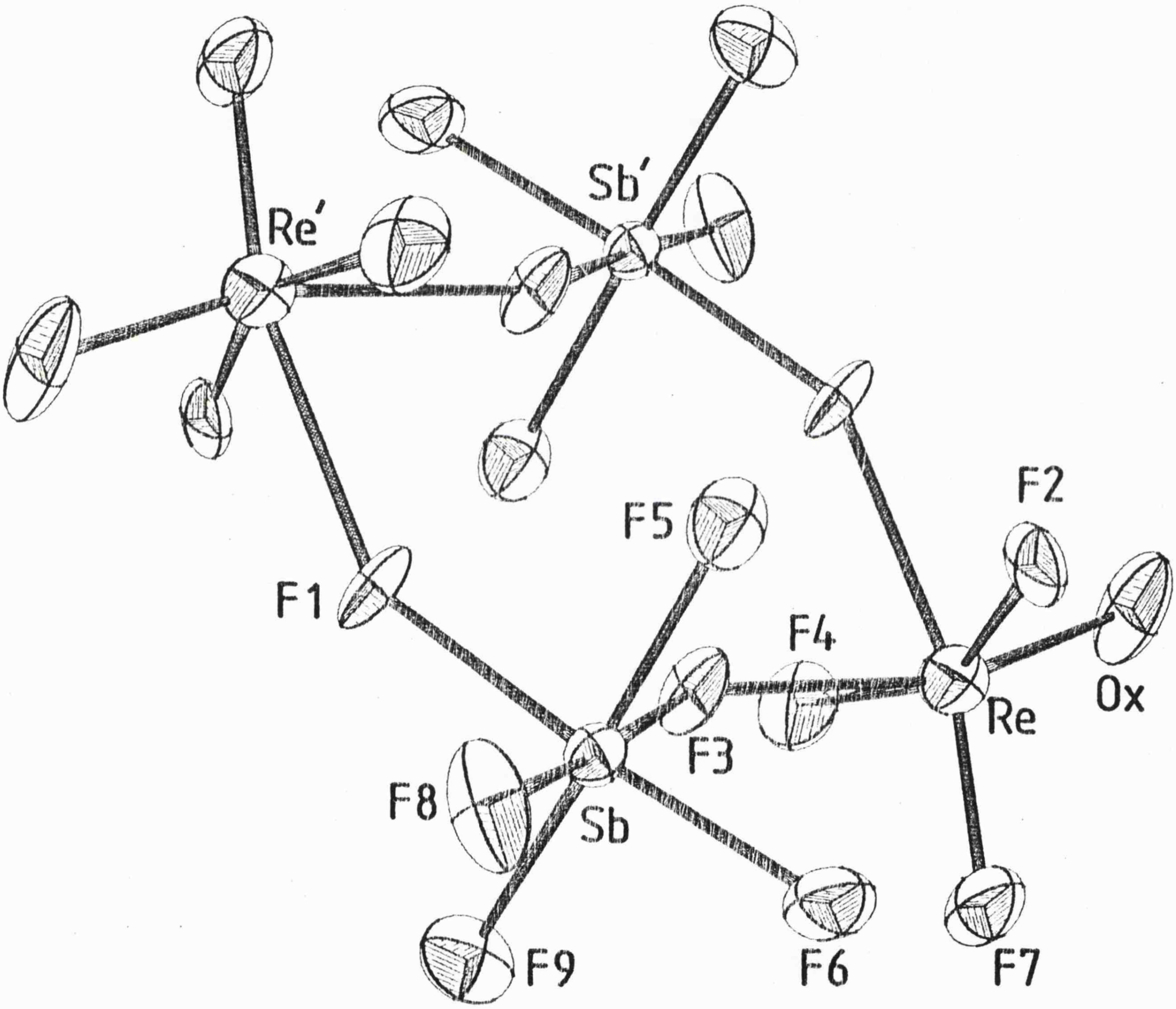

Figure 11

The dimer ring unit $2(ReF_4O.SbF_5)$.

and RuF_5,[68] which have average bridge bond angles of 135 and 132° respectively. With the chosen origin of the unit cell, no complete tetramer is contained within the cell and the stereoscopic view of the unit cell contents, Figure 12, is extended to show the tetramers lying across the {010} faces.

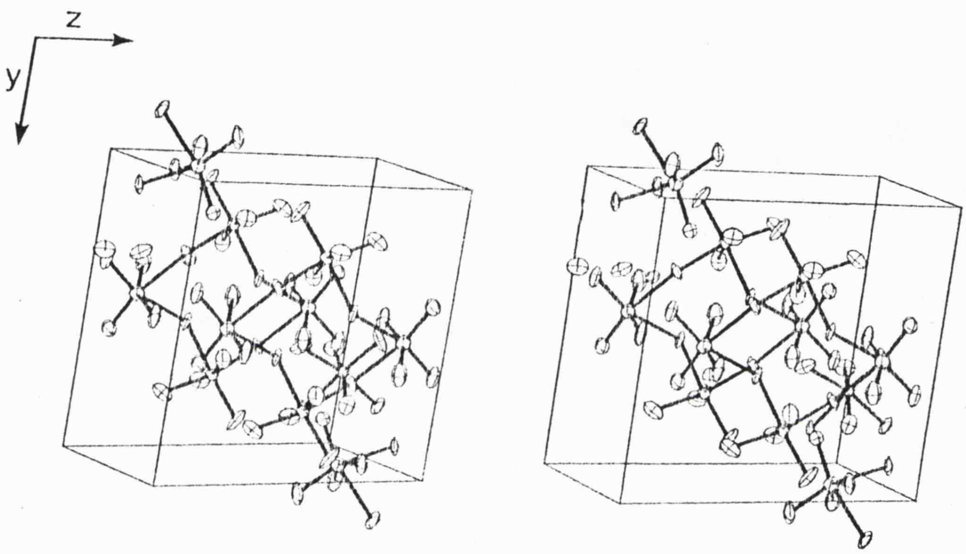

Figure 12

Stereoscopic view of the unit cell contents of $ReF_4O.SbF_5$.

The antimony and rhenium atoms are both displaced from the centre of the bonded light atom arrays, away from the cis- fluorine bridge atoms. The displacement is less apparent in the antimony environment where angles between adjacent fluorine atoms about the Sb atom are between 84.2(7)° and 97.1(8)°. The average Sb to terminal F atom distance of 1.84 Å is close to the distance (1.82 Å) found in the SbF_5 tetramer.

The average of the two Sb to fluorine bridge distances, 2.00 Å, is also much nearer to the distance found in SbF_5 (2.03 Å), than was found for the uranium and molybdenum adducts. The light atom array about rhenium is less regular, with angles between adjacent light atoms about the rhenium varying from 81.7(6)° to 106.5(9)°. The oxygen atom position, in the plane of the <u>cis</u>- bridges, was chosen entirely by bond length considerations. Vibrational spectra of the adduct were not obtained due to the instability of the material to grinding, and oxygen bridging could not, therefore, be ruled out as was possible for the uranium and molybdenum adducts. However, the light atom distance of 1.66(2)Å from Re and the distance 1.72(2)Å of the other terminal atom in the bridging plane are similar to the bond lengths in the molybdenum adduct and on this basis the oxygen position can be assigned for this adduct, with the same probability of disorder. The Re to oxygen bond distance compares with the distance, 1.63(4)Å, found in the monoclinic form of ReF_4O, and is less than the average terminal oxygen distance, 1.695 Å, found in the Re_2O_7 structure.[114] The remaining two terminal atoms, axial to the <u>cis</u>- bridging plane, have an average bond length to Re of 1.84 Å. The fluorine bridge distance of 2.08 and 2.23 Å are, within errors, equivalent to the distances found in ReF_4O.

The comparability of the Sb to F bridge bond lengths of the adduct and the solid state SbF_5 tetramer indicates a considerably smaller ionic contribution to the bridging fluorine atom than occurs in the uranium and molybdenum adducts. Using the equation established in chapter 3 for the derivation of approximate degrees of ionicity a value may be calculated for the $ReF_4O.SbF_5$ adduct.

$$I = (D_c-D_a)/(D_c-D_i) = (2.02-2.00)/(2.02-1.845) = 0.114$$

Thus, the estimated contribution from the formulation $[ReF_3O]^+[SbF_6]^-$

of 11% is much smaller than for the $[UF_2O]^{2+}[SbF_6]_2^-$ or $[MoF_3O]^+[SbF_6]^-$ contributions, and the rhenium adduct can thus be regarded as a covalent molecule with only a minor contribution from the ionic form. This is expected from the higher Lewis acidity of ReF_4O, than UF_4O and MoF_4O, approximating more closely with that of SbF_5. The determined ionicity indicates that considerable ionic contribution to the bonding is not a requirement for the formation of a stable and ordered adduct, and this raises the problem of why no single crystals of a tungsten adduct could be obtained.

It seems probable that an adduct with a ReF_4O to SbF_5 ratio of 1:2 could be formed, which would take the form of the $UF_4O.2SbF_5$ adduct, with the additional Sb units chain linking the dimers in a similar manner to the uranium adduct.

TABLE 14

Final atomic positional parameters for $ReF_4O.SbF_5$, with estimated standard deviations in parentheses.

	x/a	y/b	z/c
Re	0.3257(18)	0.0166(11)	0.2094(9)
Sb	-0.0159(3)	0.2554(16)	0.0017(14)
0	0.482(4)	0.154(2)	0.2421(17)
F(1)	0.188(3)	0.0970(16)	0.0605(13)
F(2)	0.021(3)	0.0594(18)	0.2359(12)
F(3)	-0.097(3)	0.1478(17)	-0.1277(12)
F(4)	0.535(2)	-0.0680(19)	0.1320(13)
F(5)	-0.263(3)	0.1709(18)	0.0561(13)
F(6)	-0.203(3)	0.3907(20)	-0.0527(14)
F(7)	0.386(3)	-0.0860(19)	0.3192(14)
F(8)	0.100(3)	0.3301(17)	0.1347(13)
F(9)	0.256(3)	0.3077(18)	-0.0523(13)

TABLE 15

Anisotropic thermal parameters, with estimated standard deviations in parentheses. The temperature factors are in the form - $\exp[-2\pi^2(h^2U_{11}a^2 + \ldots\ 2hkU_{12}ab)]$.

	U_{11}	U_{22}	U_{33}	U_{23}	U_{13}	U_{12}
Re	0.0293(5)	0.0274(6)	0.0314(6)	-0.0023(5)	0.0048(4)	0.0008(5)
Sb	0.0247(7)	0.0165(8)	0.0226(8)	-0.0005(7)	0.0054(6)	-0.0021(6)
O	0.052(11)	0.030(11)	0.035(12)	-0.015(9)	-0.007(10)	0.002(9)
F(1)	0.040(8)	0.030(9)	0.022(8)	0.004(7)	-0.004(6)	0.007(7)
F(2)	0.035(7)	0.055(11)	0.020(8)	-0.015(8)	-0.001(6)	0.012(7)
F(3)	0.040(7)	0.044(10)	0.017(8)	-0.005(7)	-0.001(6)	-0.015(8)
F(4)	0.028(7)	0.057(12)	0.032(9)	-0.003(8)	0.004(6)	0.009(7)
F(5)	0.027(6)	0.051(11)	0.036(9)	0.002(8)	0.012(6)	-0.000(7)
F(6)	0.045(8)	0.057(13)	0.036(10)	0.022(9)	0.016(8)	0.025(9)
F(7)	0.045(9)	0.056(12)	0.033(10)	0.016(9)	-0.004(8)	0.008(9)
F(8)	0.051(9)	0.032(9)	0.033(10)	-0.011(8)	0.008(7)	-0.008(8)
F(9)	0.038(7)	0.041(10)	0.040(10)	0.002(8)	0.013(7)	-0.007(8)

TABLE 16

Interatomic distances (Å), with estimated standard deviations in parentheses.

a) bond distances

Re-F(1)	2.079(15)
Re-F(2)	1.832(15)
Re-F(4)	1.850(15)
Re-F(7)	1.725(17)
Re-F(3)	2.231(15)
Re-0	1.660(20)
Sb-F(1)	2.043(15)
Sb-F(3)	1.959(15)
Sb-F(5)	1.845(14)
Sb-F(6)	1.797(16)
Sb-F(8)	1.860(16)
Sb-F(9)	1.835(15)

F(1)...F(2)	2.566
F(1)...F(3)	2.684
F(1)...F(4)	2.607
F(1)...F(5)	2.610
F(1)...F(8)	2.631
F(1)...F(9)	2.638
F(1)...0	2.654
F(1)...F(3)	2.710
F(2)...F(5)	2.787
F(2)...F(7)	2.593
F(2)...0	2.729
F(2)...F(3)	2.588
F(3)...F(5)	2.641
F(3)...F(6)	2.750
F(3)...F(9)	2.609
F(3)...F(4)	2.559
F(3)...F(7)	2.749
F(4)...F(7)	2.635
F(4)...0	2.693
F(4)...F(5)	2.803
F(5)...F(6)	2.677
F(5)...F(8)	2.652
F(6)...F(8)	2.742
F(6)...F(9)	2.689
F(6)...0	2.914
F(7)...0	2.715
F(7)...0	2.894
F(8)...F(9)	2.654

b) non-bond distances

Re...Sb	3.846
Re...F(5)	3.592
Re...F(8)	3.508
Re...Sb	4.033
Re...F(3)	2.250
Re...F(9)	3.577
Sb...F(2)	3.546
Sb...F(7)	3.671

TABLE 17

Interatomic bond angles (°), with estimated standard deviations in parentheses.

F(2)-Re-F(1)	81.7(0.6)
F(4)-Re-F(1)	82.9(0.7)
F(4)-Re-F(2)	152.5(0.7)
F(7)-Re-F(1)	163.8(0.7)
F(7)-Re-F(2)	93.6(0.8)
F(7)-Re-F(4)	94.9(0.8)
0-Re-F(1)	89.7(0.9)
0-Re-F(2)	102.6(0.9)
0-Re-F(4)	100.0(0.9)
0-Re-F(7)	106.5(0.9)
F(3)-Sb-F(1)	84.2(0.7)
F(5)-Sb-F(1)	84.2(0.7)
F(5)-Sb-F(3)	87.9(0.7)
F(6)-Sb-F(1)	177.9(0.7)
F(6)-Sb-F(3)	94.0(0.8)
F(6)-Sb-F(5)	94.6(0.8)
F(8)-Sb-F(1)	84.6(0.7)
F(8)-Sb-F(3)	168.8(0.7)
F(8)-Sb-F(5)	91.4(0.8)
F(8)-Sb-F(6)	97.1(0.8)
F(9)-Sb-F(1)	85.6(0.7)
F(9)-Sb-F(3)	86.9(0.7)
F(9)-Sb-F(5)	168.9(0.8)
F(9)-Sb-F(6)	95.5(0.7)
F(9)-Sb-F(8)	91.8(0.7)
Sb-F(1)-Re	137.8(0.9)
Sb-F(3)-Re	148.0(0.9)

CHAPTER 6

The Crystal Structures of $NaTaF_6$ and β-$CsNbF_6$

6.1 Introduction

Most of the known compounds having the formulation $A^IB^VX_6$, are fluorides. Compounds containing the heavier halogens are much less stable and only a few $A^IB^VCl_6$ salts are known. The fluorides, $A^IB^VF_6$, crystallise with structures which are, basically, of the NaCl or CsCl cubic types. Various modifications of the ideal cubic structures are required to give the A^+ ions suitable numbers of fluorine contacts.

The structures of known $A^IB^VF_6$ compounds were reviewed in detail by Kemmitt, Russell and Sharp[115] (1963). Little structural data has been reported for these compounds following this review, and accordingly, only a brief summary of the five recognised structure types is given here.

a) $LiSbF_6$ structure type: This structure may be regarded as a slightly distorted sodium chloride lattice, and is found only among complex fluorides of the smaller cations, Li^+ and Na^+. The rhombohedral structure, R_1 (space group $\underline{R}\bar{3}$), was characterised by the structure determination of $LiSbF_6$.[116] Discrete SbF_6^- ions exist in the lattice, which is the same as that of VF_3,[117] with lithium and antimony atoms occupying the positions of the vanadium atoms and, thus, the lithium ions are octahedrally co-ordinated by fluorines from six SbF_6^- groups.

b) $NaSbF_6$ structure type: The sodium hexafluoroantimonate structure[118,119] has a face centred cubic unit cell, C_1 (space group $\underline{Fm3m}$), with a sodium chloride lattice of Na^+ and SbF_6^- ions. As with $LiSbF_6$, the A^+ ion is regarded as having octahedral co-ordination by fluorine.

c) $CsPF_6$ structure: Like the $NaSbF_6$ structure, the $CsPF_6$ type[120] is also a cubic structure related to the sodium chloride lattice, but is based on a primitive cubic cell, C_2 (space group $\underline{P}\underline{a}3$). The A^+ cation of this structure is reported to have a co-ordination number of 12, but there is confusion in the literature as to the distinction between the C_1 and C_2 types of structure.

d) $KNbF_6$ structure: Most silver salts and some potassium salts have a tetragonal pseudo-cubic structure, T (space group $\underline{P}\bar{4}2\underline{m}$). A structure determination on $KNbF_6$,[121] and more recently that of $KSbF_6$,[75] show that the K^+ and MF_6^- ions are arranged in a CsCl lattice, but with slight distortion of the MF_6^- ions. Each potassium ion is co-ordinated to eight fluorine atoms as nearest neighbours, with a further four fluorine atoms as next nearest neighbours.

e) $KOsF_6$ structure: Complex fluorides containing the larger cations (Tl^+, Rb^+, Cs^+) are found to have this rhombohedral structure, R_2 (space group $\underline{R}\bar{3}\underline{m}$). The $KOsF_6$ structure,[122] is found to be related to the CsCl lattice, but has lower symmetry due to distortion of the OsF_6^- octahedron by contraction along a three-fold axis. The A^+ ion in this structure is co-ordinated to 12 fluorine atoms.

It appears that a major factor determining the structure type is the size of the A^+ ion, and that with increasing size the cation co-ordination number increases. Thus, the lithium salts having the smallest ionic radius have six co-ordinate (R_1) structures, whilst caesium salts with the exception of $CsPF_6$, have the twelve co-ordinate (R_2) structure. Kemmitt et al.[115] tabulate the $A^I B^V F_6$ structures with unit cell parameters and only the distribution of structure types is given here (Table 18).

Different phases have been reported for several of the $A^I B^V F_6$ compounds. Bode and Clausen[120] first reported that potassium hexafluoro-

TABLE 18

The distribution of $A^{I}B^{V}F_6$ structure types

B	A: Li	Na	Ag	K	Tl	Rb	Cs
P	a	b	b/c	c/e	c	c	c
As	a	a	b/c	e	e	e	e
V, Ru, Ir, Os	a	a	d	e	e	e	e
Re, Mo, W Sb, Nb, Ta	a	b	d	d	e	e	e

where, a = $LiSbF_6$ structure type, b = $NaSbF_6$, c = $CsPF_6$, d = $KNbF_6/KSbF_6$, e = $KOsF_6$.

phosphate crystallised in both the cubic (C_2) and rhombohedral (R_2) structures. Heyns and Pistorius[123] confirmed the existence of these phases, finding that they were dependent upon temperature and reversible upon heating and cooling; the cubic (Fm3m) form becomes rhombohedral below 0°C. They reported a further phase change at approximately -15°C to an undetermined space group. The phase changes were found also to be dependent upon variations of pressure and also impurity, and it is possible that the R_2 form investigated by Bode and Clausen[120] was stabilised by small quantities of impurity. Potassium and silver hexafluorantimonate, commonly found to crystallise in the tetragonal, $KNbF_6$, structure have been reported as cubic (C_2),[124,125] and this may be due to the investigation of alternate phases. The tetragonal form of $KSbF_6$ has recently been determined by a single crystal study,[75] but the alternate (C_2) structure remains in doubt.

It seems likely that many of the $A^IB^VF_6$ compounds may give rise to alternate phases when subject to changes in temperature or pressure, and the presence of impurities may well be a significant factor. Such phases may be reversible upon the application of temperature and pressure changes as for KPF_6, or be caused by the conditions of crystallisation and be irreversible.

Calculation of lattice energies by co-workers, requiring accurate atomic parameters resulted in an investigation of the structures of sodium hexafluorotantalate and tungstate. With this study it was hoped to clarify the cubic (C_1) structure. No single crystals of $NaWF_6$, suitable for X-ray study, could be obtained and the structure was investigated by neutron diffraction of the micro-crystalline powder (Chapter 7). Crystals of $CsNbF_6$ obtained from the preparation and attempted crystallisations of $CsNb_2F_{11}$ were investigated as a new phase.

6.2 Preparation of Sodium Hexafluorotantalate(V)

Sodium hexafluorotantalate(V) was prepared by the reaction of stoichiometric quantities of sodium fluoride and tantalum metal with an excess of bromine trifluoride.

$$NaF + Ta \xrightarrow{\text{xs } BrF_3} (NaBrF_4 + BrF_2^+TaF_6^- \longrightarrow) NaTaF_6 + 2BrF_3$$

The apparatus (Figure 13) was carefully preseasoned before the addition of the starting materials. Bromine trifluoride was transferred in dynamic vacuum into trap (A), which was cooled by liquid nitrogen, the apparatus was then sealed at point (B). The BrF_3 was warmed to room temperature and Br_2 and BrF impurities removed by pumping the

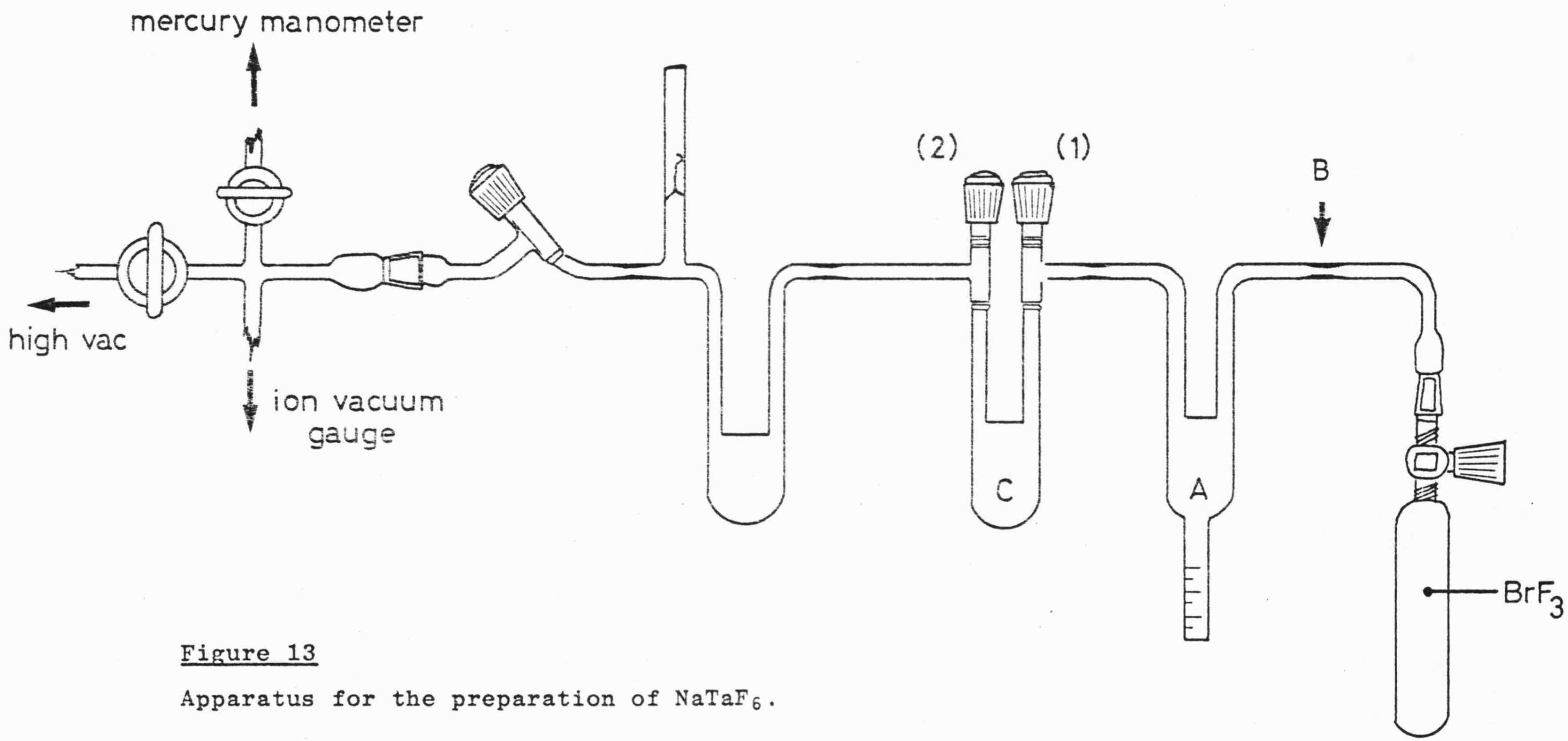

Figure 13

Apparatus for the preparation of $NaTaF_6$.

liquid. With valve (1) closed, dry nitrogen was admitted and valve (2) removed to allow the addition of 0.1019g (2.426 mMol) of NaF and 0.4382g (2.421 mMol) of Ta metal, the apparatus was then re-evacuated. A small quantity of BrF_3 was transferred in dynamic vacuum to trap (C) which was cooled to -196°. The valves were then closed and the reaction allowed to warm slowly to room temperature. Extremely vigorous reaction occurred. Further small portions of BrF_3 were added until the reaction became less vigorous, and at this stage the total excess of BrF_3 was added and the reaction allowed to warm to room temperature and stand for two hours. Valve (2) was opened regularly to release the Br_2 evolved. The excess of BrF_3 was then removed, and the product evacuated for several days, until Br_2 was no longer released. The product was an off-white powder.

The X-ray powder diffraction pattern of the product (Table 19), was consistent with the previously reported pattern of Kemmitt _et al._,[115] and similarly could be indexed as a face-centred cubic cell (a = 8.28 Å). The microcrystalline product was, therefore, of the same phase as has previously been reported.

Single crystals were grown by two methods. A small amount of solid was dissolved in HF in an F.E.P. tube. Slow removal of the HF yielded brittle crystals, of cubic appearance, suitable for X-ray single crystal study. A further sample of the product was transferred to a pre-seasoned crystal growing apparatus (Figure 14). SO_2 dried over P_2O_5, was added in static vacuum at -80°, and warmed to obtain a solution. Insoluble material was trapped in the side arm by rotation of the apparatus. The solution was then cooled to -30°. After several days fine needle crystals were observed, but attempts to isolate them were unsuccessful.

TABLE 19

X-ray powder diffraction pattern of $NaTaF_6$

Line	Intensity	$\mathrm{Sin}^2\theta \times 10^4$	Assignment
a	v.s	263	{111}
b	v.s	350	{200}
c	s	694	{220}
d	s	957	{311}
e	w	1044	{222}
f	w	1088	
g	s	1393	{400}
h	m	1657	{331}
i	s	1746	{420}
j	ms	2094	{422}
k	ms	2358	{311}{333}
l	m	2785	{440}
m	m	3054	{531}
n	m	3133	{442}{600}
o	v.w	3260	
p	m.w	3469	{620}

(Cu-$\underline{K}\alpha$ radiation, $\lambda = 1.5418$ Å)

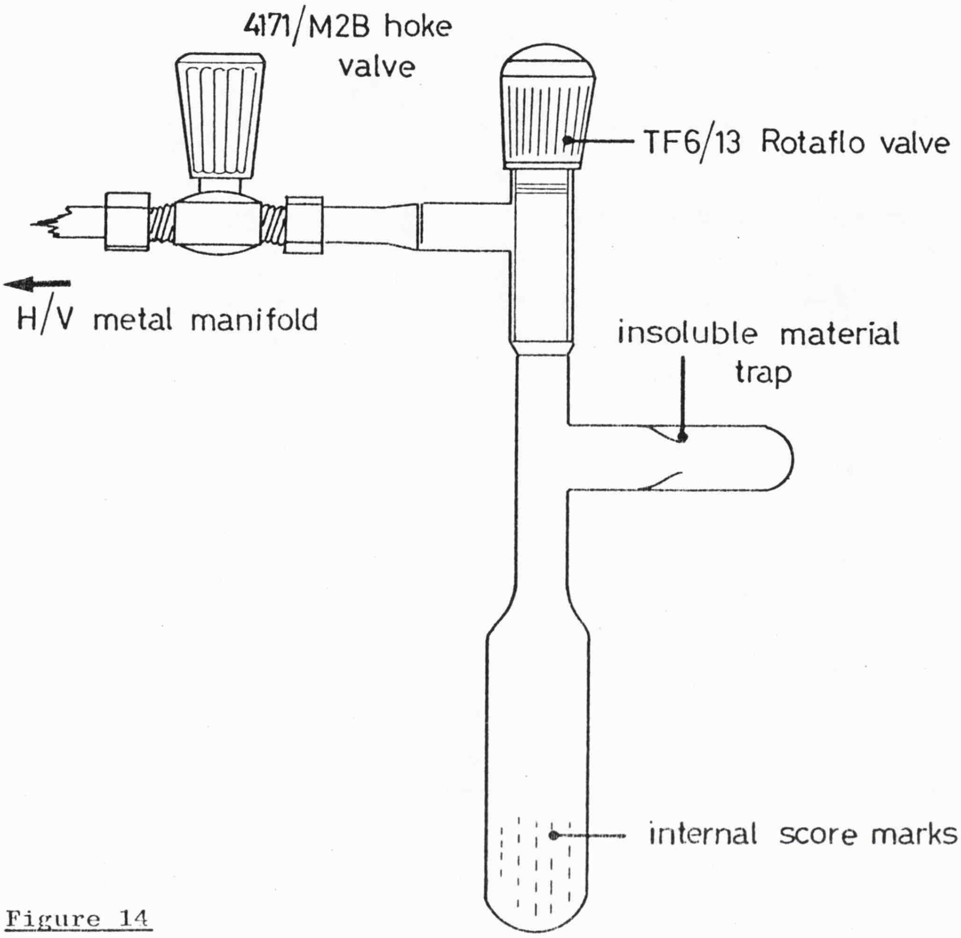

<u>Figure 14</u>

Crystal growing apparatus.

<u>6.3 Single crystal X-ray Investigation of Sodium Hexafluorotantalate(V)</u>

The crystals grown from HF were of suitable dimensions for single crystal study. Several crystals were wedged and sealed in preseasoned Pyrex capillaries, by manipulation within a crystal sorting apparatus (Figure 2). The crystal used for the investigation had approximate dimensions 0.26 mm × 0.25 mm × 0.07 mm, with clearly defined faces, and was mounted about the $\underline{c}$ axis. Upon close examination under high magnification, all crystals grown from HF solution appeared to be "hopper faced" (Figure 15), but produced diffraction patterns without evidence of twinning. Preliminary values of cell dimension $\underline{a}$ were

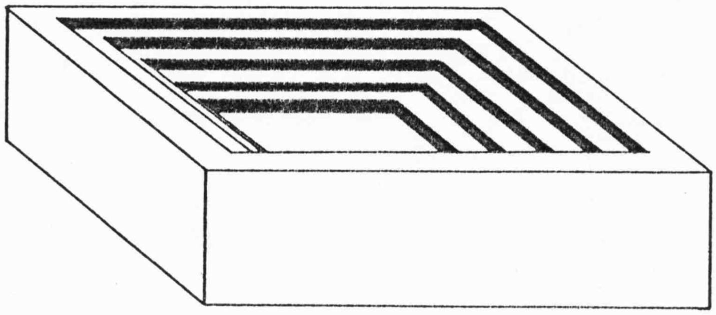

Figure 15

Typical 'Hopper' faced crystal of $NaTaF_6$.

obtained from Weissenberg photographs, using Cu-$K\alpha$ (Ni filtered) radiation, and precession photographs using Mo-$K\alpha$ (Zr filtered) radiation. The final value of a was determined from optimised counter angles for zero layer reflections on a Weissenberg diffractometer.

6.4 Crystal Data

F_6Na Ta ; M = 317.95

Cubic a = 8.264 (1) Å

U = 564.48 Å^3 ; D_c = 3.741 g cm^{-3} ; z = 4

F(000) = 547.81 ; Mo-$K\alpha$ radiation ; λ = 0.71069 Å

μ(Mo-$K\alpha$) = 187.25

Space group $Fm3m$ (O_h^5 No. 225). Neutral atomic scattering factors were used with anomalous dispersion coefficients.

6.5 Collection of the Intensity Data

Data were collected from layers hk0 to hk12, using the Stoe(stadi-2) diffractometer in the +h, +k, +1 quadrant for the hk0 layer, and in the two quadrants ±h, for the remaining layers. Data were collected using an ω-scan technique, the counter angle (2θ) remaining fixed at the calculated value for each reflection. Background count times of 20 secs either side of the reflection were taken, and an ω-scan rate of 1°/min was used. The ω-scan width was calculated for each reflection by the formula of Freeman *et al.*[5] The intensities of 465 reflections with $5° \leqslant 2\theta \leqslant 80°$ were collected at 22 to 25°. Monitoring of check reflections throughout each layer indicated no significant deterioration of the crystal during the data collection. Lorentz and polarisation corrections were made to the data set.

6.6 Solution of the Structure

Because of the plate-like nature of the crystal, the absorption correction for the data set was performed before refinement was attempted. The program ABSCR was used, and maximum and minimum transmission factors of 0.5274 and 0.2104 respectively were obtained. In the early stages of refinement, using the program system SHELX, $R\bar{3}$ symmetry was assumed for a face-centred cubic lattice. Three cycles of full matrix least-squares refinement, with Ta at 0,0,0 and Na at ½,½,½, gave an R factor of 0.15 for 174 unique reflections. The fluorine atom was located from the Fourier difference map, and further cycles of least-squares gave an R factor of 0.035. Final cycles using $R\bar{3}$ symmetry, with anisotropic temperature factors and a weighting parameter *g*, further reduced the R factor to 0.020. The X/A and Y/B co-ordinates of the fluorine atom were found to be, within estimated standard deviations, equal to zero. This indicates higher symmetry than $\underline{R}\bar{3}$, and refinement was continued in the space group $\underline{F}\underline{m}3\underline{m}$ (data averaged to 121 unique reflections). Final cycles employed a weighting parameter $\underline{g}(.00036)[\underline{\omega} \; \alpha \; {}^{1}/\sigma^2(F) + g \; F^2]$ and gave an R factor of 0.0217. An analysis of the weighting scheme over $|F_o|$ and $\mathrm{Sin}\theta/\lambda$ was satisfactory. However, the final difference Fourier map reveals unidentified peaks of ±6 electrons compared with <0.5 electron found using $\underline{R}\bar{3}$ symmetry. Since the negative peaks are equally large it is assumed they result from residual systematic error, and that the marginally lower $\underline{R}$ factor obtained in the $\underline{R}\bar{3}$ space group is due to relaxation of the constraints on the atomic thermal parameters. The space group $\underline{F}\underline{m}3\underline{m}$ was chosen as appropriate, and the final atomic and thermal parameters are listed in Table 20. The observed and calculated structure factors are found in Appendix 4.

Final residual indices for 121 unique reflections:-

$$R = \sum(|F_o| - |F_c|/\sum|F_o| = 0.0217$$

$$R_w = [\sum\omega(|F_o| - |F_c|)^2/\sum\omega|F_o|^2]^{\frac{1}{2}} = 0.022$$

TABLE 20

Final atomic and thermal parameters for sodium hexafluorotantalate with estimated standard deviations in parentheses

Atom	X/A	Y/B	Z/C	U_{11}	U_{22}	U_{33}
Ta	0.00	0.00	0.00	0.0216(2)		
Na	0.50	0.50	0.50	0.0265(11)		
F	0.00	0.00	0.2261(6)	0.094(4)	0.094(4)	0.0139(17)

The bond length, Ta — F = 1.868(1) Å

The non-bond contact, Na---F = 2.264(1) Å

F....F = 2.642(3) Å

6.7 Preparation of caesium hexafluoroniobate(V)

The crystals of caesium hexafluoroniobate(V) used in this study resulted from the reaction of a 2:1 excess of niobium pentafluoride with caesium fluoride in SO_2 solvent. The apparatus, a combination reactor and crystal growing apparatus (Figure 14), was pumped to high vacuum and seasoned with fluorine. CsF (1.394 mMol) and NbF_5 (2.790 mMol) were added to the reactor in the dry-box, and the reactor re-evacuated for several hours at high vacuum. SO_2, dried over P_2O_5, was transferred to the reactor which was then sealed at the Rotaflo valve, and a solid CO_2 cooling collar was attached just below the valve. The SO_2 was allowed to reflux for 2 hours, before the solution was tipped through the solid trap into the scored bulb, and the apparatus cooled to -25°C. After 20 days crystals were observed, and the solution was returned to the reaction bulb and the SO_2 removed from the bulk product in static and finally dynamic vacuum. A batch of single crystals was transferred in the dry-box to a preseasoned capillary apparatus for sorting, and samples of the bulk product and ground single crystals were transferred to capillaries for Raman investigation.

The Raman spectra of the single crystals and microcrystalline product clearly indicated different compounds (Table 21). The microcrystalline product gave a Raman spectrum essentially equivalent to the spectrum found by Gillespie <u>et</u> <u>al</u>.[126] for $CsNb_2F_{11}$. The only significant difference was the reduced intensity of the band at 684 cm^{-1} which is in the expected region of V_1 (Nb-F) for NbF_6^-. Raman spectra of the sample from single crystals were found to be equivalent with the spectra reported for $CsNbF_6$.[127]

TABLE 21

Raman spectra of the products of $CsNb_2F_{11}$ preparation

Microcrystalline sample	$CsNb_2F_{11}$[126] assignment		Single crystals	$CsNbF_6$[127] assignment	
211 cm^{-1} (21)	211 (cm^{-1})(36)				
251 (29)	251 (48)				
293 (27)	289 (37)		283 (cm^{-1})(18)	280 (cm^{-1})(m)	$\nu_5(NbF_6)^-$
590 (16)	588 (12)		564 (7)	562 (w)	$\nu_2(NbF_6)^-$
598 (4)(sh)					
668 (54)	666 (44)	$\nu(Nb_2F_{11})^-$			
683 (4)	685 (31)		686 (100)	683 (s)	$\nu_1(NbF_6)^-$
726 (100)	726 (100)	$\nu(Nb_2F_{11})^-$			
			804 (4)		

6.8 Single Crystal X-ray Investigation of Caesium Hexafluoroniobate(V)

The crystals grown from solution in SO_2 were of approximately cubic appearance. The crystal chosen for the investigation had approximate dimensions 0.21 mm × 0.16 mm × 0.15 mm and was bounded by the faces {001}, {110} and {$\bar{1}$10}. Preliminary cell dimensions were obtained from Weissenberg photographs taken using Cu-K_α (Ni filtered) radiation, and precession photographs using Mo-K_α (Zr filtered) radiation. The photographs indicated that the structure was triclinic, as opposed to the rhombohedral structure previously reported for $CsNbF_6$.[128] Final cell dimensions were obtained from the optimised counter angles for zero and upper layer reflections on a Weissenberg diffractometer. The use of ω-scan methods to maximise reflections for determination of the cell parameters, showed that the reflections were double peaks, indicating some twinning of the crystal, and care was needed to observe corresponding peaks from the same crystal component during maximisation of each reflection.

6.9 Crystal Data

$Cs\,F_6\,Nb$; $\quad M = 339.81$

Triclinic $\quad a = 7.077\ (2)$ Å ; $\quad b = 7.924\ (3)$ Å ; $\quad c = 5.274\ (4)$ Å

$\alpha = 89.47\ (15)°$; $\quad \beta = 81.61\ (12)°$; $\quad \gamma = 90.08\ (12)°$

$U = 292.6$ Å^3 ; $\quad D_c = 3.856\ \mathrm{g\ cm^{-3}}$; $\quad z = 2$

μ (Mo-K_α) $= 76.58\ \mathrm{cm^{-1}}$; $\quad F(000) = 297.93$

Mo-K_α radiation ; $\quad \lambda = 0.71069$ Å

Space group C$\bar{1}$ C-centred version of P$\bar{1}$, No. 2.

Neutral atomic scattering factors were used with anomalous dispersion coefficients.

6.10 Collection of Intensity Data

Data were collected from layers hk0 to hk7 using the (Stoe stadi-2) diffractometer in the ±h, ±k, +l quadrants for all layers. Data were collected using an *ω*-scan technique, with the counter angle (2θ) fixed at the calculated value for each reflection. The *ω*-scan width was calculated for each reflection using the Freeman-Guss equation, to include both maxima of the *ω*-scan. The initial value chosen for the mosaicity term, ϕm, in the calculation, resulted in a truncation of the peaks on the hk4 layer and was, therefore, increased from 3.5 to 4.5 for layers hk5 to hk7.

The intensities of reflections having $\sin\theta/\lambda$ values of $\geqslant 0.122$ and $\leqslant 0.704$ Å^{-1} were collected, and a total of 753 reflections were obtained with $I/\sigma I \geqslant 3$. Check reflections, monitored during the data collection for each layer, indicated no deterioration of the crystal. Lorentz, polarisation and absorption corrections were made to the data set.

6.11 Solution of the Structure

The program system SHELX was used. Refinement was attempted initially in the monoclinic space group *C*2/*m*, as the cell parameters α and γ approximate to 90°. However, data averaged to 346 unique reflections gave a high R_{av} factor for the data averaging, indicating that the assumed space group symmetry *C*2/*m* was incorrect. This was supported by the refinement, for which final cycles gave an R factor of 0.11, with high values for the thermal parameters of the fluorine atoms, and significant residual peaks in the difference Fourier map. The refinement was continued in space group $C\bar{1}$ (*C*-centred version of $P\bar{1}$ No. 2), and the R_{av} for the 601 unique reflections averaged was reduced to 0.025. Three cycles of least-squares with Cs and Nb on the same special positions as for the space group $\underline{C}2/\underline{m}$, gave an R factor of 0.17 and the fluorine atoms were located from the difference Fourier map. Further cycles with the fluorine atoms included reduced R to 0.09. The isotropic thermal parameters of the fluorine atoms were all high, indicating that they were either in the wrong positions or highly anisotropic. Peaks in the Fourier difference map of 3 electrons at bond distances from niobium, suggested possible alternate positions for the fluorine atoms. Three cycles of refinement with all atoms having anisotropic temperature factors reduced the R factor to 0.056. However, the thermal parameters of the fluorine atoms were still high, and the possibility of a disordered structure was investigated. Because of the interdependence of the parameters involved, it was necessary to refine the site occupation factors of the alternate fluorine atoms first, and then to fix the values for final cycles of least-squares involving refinement of thermal parameters.

The largest peaks in the final Fourier difference map of the ordered structure, formed an alternative octahedron about the niobium atom, slightly displaced from the established fluorine atoms. The first disordered structure (model 2) included both sets of fluorine atoms, with the site occupation factors refined as x and 1-x. Final cycles gave an R factor of 0.058, with reduced isotropic thermal parameters and residual peaks in the Fourier map. However, the three strongest peaks of 1.5 electrons appeared to represent a further alternate octahedron of fluorine atoms and a second disordered structure (model 3) with three sites for each fluorine was investigated. Final cycles for this model gave an R factor of 0.056 and all isotropic thermal parameters were reduced to satisfactory values. A weighting parameter $\underline{g}$ (.00044) [$\underline{\omega} \propto {}^{1}/\sigma^2 (F) + g F^2$] was used and an analysis of the weighting scheme over $|F_o|$ and $\sin\theta/\lambda$ was satisfactory.

A further disordered structure (model 4), with the octahedra disordered only in two dimensions, and free to rock about an ordered fluorine pair, gave less satisfactory convergence and was rejected. Similarly, attempts to restrain the positional parameters of the fluorine atoms in order to attain a regular octahedron were unsuccessful.

The disordered structure (model 3) was considered to be the most satisfactory representation. The final atomic positional parameters are given in Table 23; the thermal parameters are in Table 24. The interatomic distances are in Table 22, and the observed and calculated structure factors are found in Appendix 5.

Final residual indices for 601 unique reflections:-

$$R = \sum(|F_o| - |F_c|)/\sum|F_o| = 0.056$$

$$R_w = [\sum w(|F_o| - |F_c|)^2/\sum\omega|F_o|^2]^{\frac{1}{2}} = 0.066$$

TABLE 22

Interatomic distances (Å) with estimated standard deviations in parentheses

Nb-F1	1.732(19)
Nb-F2	2.008(21)
Nb-F3	2.026(24)
Nb-F4	1.756(28)
Nb-F5	1.961(27)
Nb-F6	2.011(34)
Nb-F7	1.852(40)
Nb-F8	2.156(29)
Nb-F9	1.908(42)

TABLE 23

Final atomic positional parameters for $CsNbF_6$ (model 3) including isotropic thermal parameters and site occupation factors for the fluorine atoms [estimated standard deviations in parentheses]

	x/a		y/b		z/c		s.o.f.	U_{11}
Cs	0.0	(00)	0.0	(00)	0.0	(00)		
Nb	0.0	(00)	0.5	(00)	0.5	(00)		
F1	0.2333(28)		0.4449(25)		0.3944(37)		0.453	0.0476(46)
F2	0.4061(33)		0.8044(27)		0.3130(42)		0.453	0.0559(54)
F3	0.4182(39)		0.1313(35)		0.2029(53)		0.453	0.0627(76)
F4	0.2417(36)		0.5504(35)		0.4034(29)		0.311	0.0442(53)
F5	-0.0472(51)		0.3649(39)		0.2067(59)		0.311	0.0561(76)
F6	0.4019(51)		0.1920(40)		0.3091(60)		0.311	0.0602(72)
F7	0.2657(53)		0.4771(51)		0.4734(70)		0.236	0.0448(83)
F8	-0.1287(62)		0.3404(58)		0.2456(89)		0.236	0.0480(95)
F9	-0.0271(60)		0.6495(52)		0.2201(85)		0.236	0.0437(98)

TABLE 24

Anisotropic thermal parameters for Cs and Nb atoms, with estimated standard deviations in parentheses. The temperature factors are in the form exp $[-2\pi^2(h^2U_{11}a^2 + \ldots\ldots 2hkU_{12}ab)]$.

	U_{11}	U_{22}	U_{33}	U_{23}	U_{13}	U_{12}
Cs	0.0400(7)	0.0301(6)	0.0383(6)	-.0030(4)	0.0171(4)	-.0015(4)
Nb	0.0346(8)	0.0284(7)	0.0333(7)	-.0034(5)	0.0143(6)	-.0019(5)

6.12 Discussion of the Sodium Hexafluorotantalate(V) and Caesium Hexafluoroniobate(V) Structures

The face centred cubic (C_1) structure was found to be appropriate for sodium hexafluorotantalate(V), as previously established by X-ray powder diffraction.[115] There is no distortion of the unit cell or TaF_6^- ion which would justify the choice of a lower symmetry space group than $\underline{Fm3m}$ (Figure 16). Of the $A^IB^VF_6$ structures, only six have been found to have the C_1 structure. These are all complex fluorides of sodium (B = P,[129] Mo,[130] W,[130] Sb,[118,119] Nb,[115] Ta[128]), and fluorine atom co-ordinates have been given for only two of these structures. Bode and Teufer,[129] placed the F atoms of the $NaPF_6$ structure, on 24 of the 192 general x, y, z positions of the space group $\underline{Fm3m}$, with the Y/B

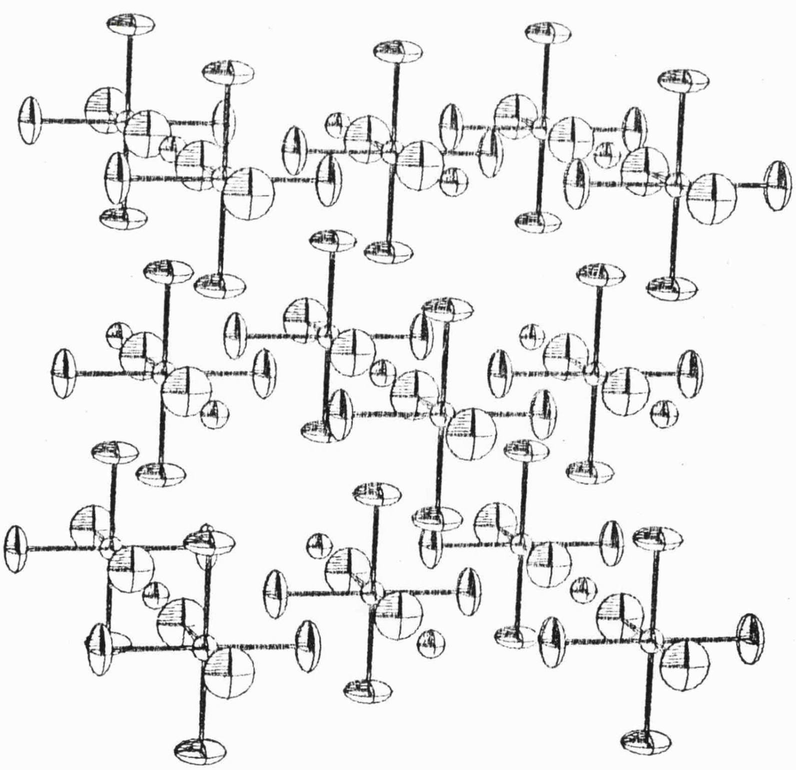

Figure 16

The unit cell contents of $NaTaF_6$.

and Z/C fractional co-ordinates close to zero. The resulting co-ordination of the Na^+ cation by F atoms is, thus, six as as would be found for the special position x,o,o. Schrewelius,[118] similarly placed the F atoms in the $NaSbF_6$ structure in the general x,y,z, positions, with a resulting bond distance of 1.95 Å. Teufer[119] disputed the F atom position, suggesting fluorine should be placed on a special site x,o,o, (x = 0.217), resulting in a bond distance of 1.78 Å. Teufer substantiates the F atom position by comparison of the bond length with that of $KSbF_6$[75] (1.77 Å). The bond distance of Schrewelius does seem to be too long, as it is comparable with the Sb-F bridge distances in the predominately covalent $MF_4O.nSbF_5$ adducts (M = U, Mo and Re) reported in chapters 3 to 5 of this thesis.

The structure of sodium hexafluorotantalate(V) is found to be in agreement with the Teufer structure for $NaSbF_6$. The F atoms about the Ta occupy the special positions x,o,o, (x = 0.226), and despite the larger ionic radius of Ta, the Ta-F bond length, 1.868(5) Å, is still less than the bond length proposed by Schrewelius for Sb-F. However, it may be that the C_1 structures all belong to the space group Fm3m, but show a trend for the F atoms to move from the special position x,o,o, as the ionic radius, $R_{B^{5+}}$, decreases. The effect of such a trend would thus be least, or non-existent, with $NaTaF_6$ as Ta^{5+} has the largest ionic radius of the series.

The previously reported rhombohedral structure for caesium hexafluoroniobate(V),[116] is that expected from consideration of the common structure types for the $A^IB^VF_6$ compounds, and in particular the structures with large cations. The triclinic cell found in this determination represents not only a new phase for $CsNbF_6$, but the first reported $A^IB^VF_6$ structure which does not conform to one of the five structure types described in the introduction. The unit cell volume of the more usual rhombohedral ($\underline{R}\bar{3}m$) structure is almost exactly half the triclinic unit cell ($\underline{C}\bar{1}$) determined.

$CsNbF_6$, $R\bar{3}m$ and $C\bar{1}$ unit cell parameters:-

	a(Å)	b(Å)	c(Å)	α(°)	β(°)	γ(°)	U(Å³)	Z	U/Z
$\underline{R}\bar{3}\underline{m}$	5.32			96.84	90.0	90.0	148	1	148
$\underline{C}\bar{1}$	7.077	7.924	5.274	90.53	98.39	90.08	292	2	146

The very high thermal parameters resulting from the refinement of an ordered NbF_6^- environment within the structure (Figure 17), indicate that this phase has low thermal stability. The arrangement of the fluorine atoms about the niobium is that of a highly distorted octahedron. The bond distances of the three pairs of fluorine atoms to niobium being 2.000(12), 1.966(12) and 1.723(10) Å with F-Nb-F angles of 103, 101, and 81°.

The disordered structure, model 3, resulted in the best convergence of data, with the lowest thermal parameters for the fluorine atoms (Figure 18). From the data it is impossible to decide upon the exact nature of disorder. The fluorine atoms may oscillate between the alternate, approximately octahedral positions, as a unit, or the disorder may be distributed throughout the lattice with only one orientation found at each site. Model 2, where only two orientations of the fluorine atoms was considered, allows refinement of the site occupation factors of the two alternate positions individually for the three fluorine atoms. The site occupation factors obtained were significantly different (Figure 19, Table 25), and this indicates that the distorted octahedron found in the ordered structure (model 1) does not only oscillate between alternate sites but further deforms.

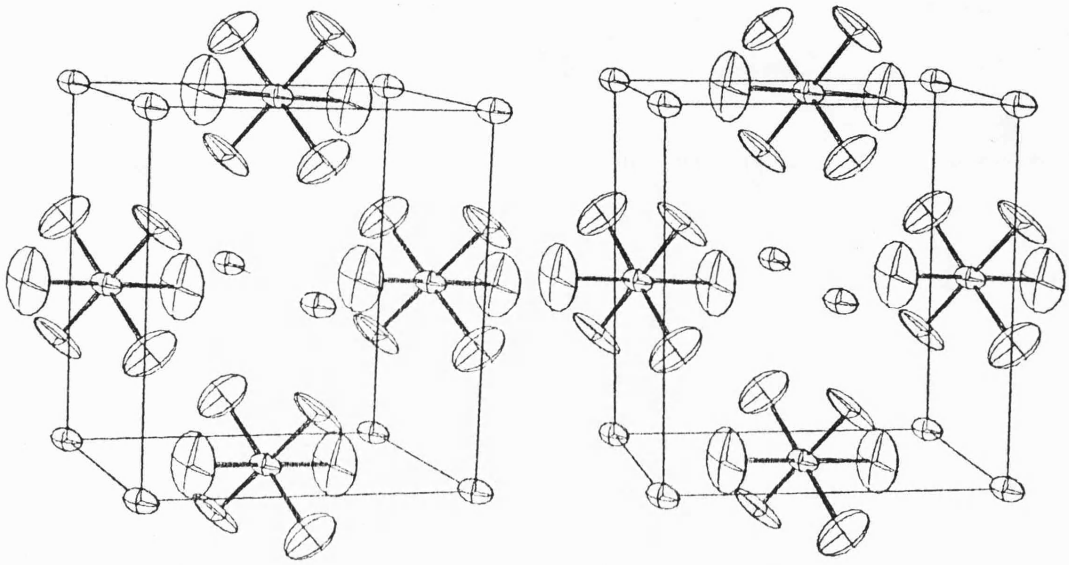

Figure 17

Stereoscopic view of the unit cell contents of $CsNbF_6$ (ordered model 1).

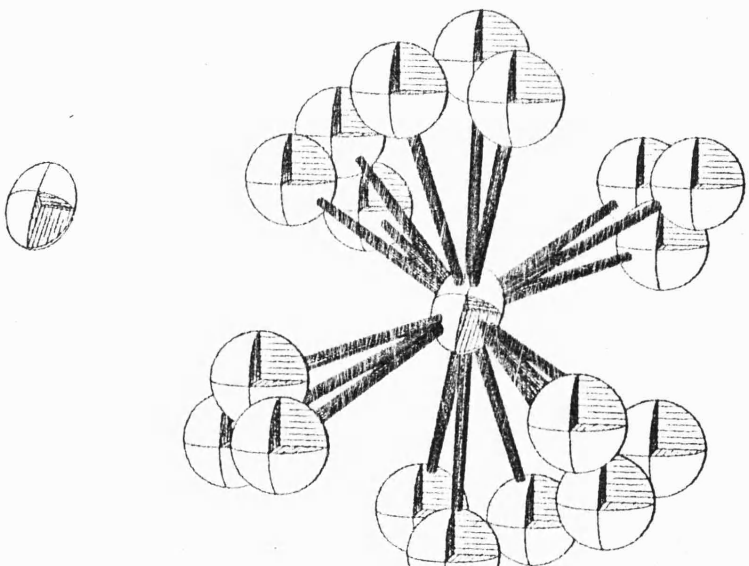

Figure 18

The fluorine atom environment about Nb in the disordered structure (model 3).

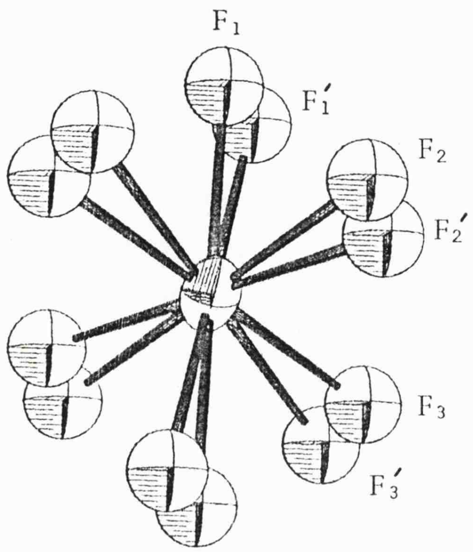

atom	S.O.F
F_1	0.5997
(F_1'	0.4003)
F_2	0.6134
(F_2'	0.3866)
F_3	0.6667
(F_3'	0.3333)

Figure 19

Disordered model (2), niobium environment.

TABLE 25

Site occupation factors for the fluorine atoms in $CsNbF_6$ model (2).

The possibility that the disorder is distributed throughout the lattice with only one orientation at each site cannot be discounted however. A likely cause of such disorder would be impurities within the lattice and it seems probable that this, rather than the low temperature of crystallisation, is the cause of the new phase determined. A further possible cause of disorder throughout the lattice is crystal twinning, which was indicated by the doubled diffraction peaks observed during data collection. However, the $\underline{C}\bar{1}$ structure represents a low temperature phase determined at room temperature, and the disorder may be about each niobium atom as a result of the freedom for the NbF_6^- octahedron to "rattle" in a cell which will have expanded from its low temperature volume.

The disordered model chosen from those investigated may, therefore, be representative of the fluorine environment expected about the niobium or merely represent positions found throughout the lattice.

CHAPTER 7

A Study of the $NaWF_6$ Structure by Neutron Diffraction

7.1 Introduction

The determination of all but the simplest structures by profile refinement of powder diffraction patterns appears, at first sight, to be uncompetitive with the more usual single crystal methods. However, recent developments in the techniques of profile refinement of powder data have made the method a realistic alternative for the refinement of moderately complex structures. Though simple structures may be solved by profile refinement, the method is designed primarily for the refinement of atomic parameters of structures solved approximately by other methods.

Due to the overlap of adjacent Bragg peaks in all but the simplest powder diffraction patterns the intensity of the structure factor for each reflection cannot be derived simply by integrating under the peaks[131] and a new approach is needed to interpret the structural information contained in complex powder patterns. Rietveld originated and developed[132,133] a method to directly use the profile intensities to decide between structural models, rather than separate individual Bragg reflections. The measured profile of a single powder diffraction peak is dependent on the neutron wavelength distribution, the monochromator mosaic distribution, transmission functions of the slits and the sample shape and crystallinity. Despite these contributions the product is almost exactly a Gaussian peak, for which the contribution to the profile at any position of 2θ can be calculated [$y_{i(calc)}$]. For each 2θ point of a pattern the contributions from all the Bragg reflections in the region are calculated and the total $y_{i(calc)}$ from all contributing reflections is compared with the observed value $y_{i(obs)}$. The unconstrained structure parameters determining $y_{i(calc)}$ are then adjusted to minimize the quantity.

$$\chi^2 = \sum_i w_i \, [y_i(\text{obs}) - \frac{1}{c} y_i(\text{calc})]^2$$

The summation is over all the 2θ points measured (i), $w_i \alpha\ 1/\sigma_i^2 \simeq 1/y_i(\text{obs})$ is the weight allotted to the count $y_i(\text{obs})$, and c is a scale factor. Corrections for peak asymmetry at very low scattering angles[134] and the angular dependence of the half-widths of the diffraction peaks[135] are used. The least-squares parameters are described in section 7.5, but may be divided into two groups. The first group are profile parameters which describe the positions, half-widths and possible asymmetry of the diffraction peaks. The second group are structure parameters that define the contents of the asymmetric unit cell.

An updated version[136] of Rietveld's original method was used in the solution of the $NaWF_6$ structure. This allowed the inclusion of anisotropic temperature factors for the atoms.

The use of neutron rather than X-ray diffraction techniques has both advantages and disadvantages. Single crystal investigations by neutron diffraction are often impractical due to the large size of crystals required and the errors incurred through extinction. However, for the study of some structural problems profile refinement of neutron diffraction patterns by powder samples has considerable advantages. Neutrons are always scattered by atomic nuclei; scattering by electrons is negligible except for atoms possessing a magnetic moment. As the nucleus of an atom is negligibly small in comparison with the wavelength of the scattered radiation, diffracted waves from the opposite sides of the atom do not interfere destructively, and neutron scattering factors are angularly independent instead of falling with increasing θ angles as with X-ray scattering. Similarly, neutron scattering factors are not proportional to atomic numbers, as are X-ray scattering factors, and vary relatively little for all elements. The principle advantage of neutron diffraction is a direct result of this approximate equivalence of scattering factors, as it allows accurate determination of light atom positions in the presence of heavy atoms. Studies of the orthorhombic form of PbO by X-ray[137] and neutron diffraction[138,139] demonstrate the insensitivity of the positional parameters of the oxygen atom derived from the X-ray data because of the overwhelming contribution to the diffraction pattern of the lead atoms. The neutron diffraction data allows accurate location of both atoms but is relatively insensitive to placement of lead or oxygen on incorrect sites, and it is often essential to locate heavy atoms initially by X-ray methods. The extreme example of a light atom is hydrogen. In compounds containing no heavy atom it is possible, with extremely good data, to obtain approximate hydrogen atom positions with X-ray data. Usually in the presence of heavy atoms, or with an average quality data set, the positions of hydrogen atoms can only be inferred from packing considerations and probable bonding schemes, but with neutron diffraction data, hydrogen atoms can be located directly and accurately even in the presence of heavy atoms.

The location of atoms within the unit cells of the $A^{I}B^{V}F_6$ compounds may satisfactorily be refined using neutron diffraction powder data. Preliminary X-ray single crystal studies are not required as the locations of the heavy atoms have been determined by X-ray powder diffraction and a few single crystal studies to be on known special positions of the relevant space groups. Similarly, unit cell dimensions can accurately be measured by X-ray powder diffraction and the number and type of atoms in the unit cell can simply be determined by volume considerations. The positional parameters of the fluorine atom may then accurately be determined and the effect of applying constraints with different space groups observed. This method is particularly sensitive to incorrect application of constraints placing light atoms, such as the fluorine atom octahedra on special positions of a space group when, in fact, the atoms are orientated slightly away from the axes and are in general positions.

Since no preliminary single crystal study was required, the location of fluorine atoms within $A^{I}B^{V}F_6$ compounds by refinement of powder data seems an appropriate method as it is frequently easier to obtain a powder specimen than a single crystal of sufficient quality to allow data collection. The reduced time required for data collection is a further advantage of this method; there being no sorting and aligning of crystals, data may be collected in as little as twenty-four hours. Finally, it is comparatively easy to collect data over large ranges of temperature and pressure to examine lattice changes, or by the use of reduced temperature, simplify disordered structures.

7.2 Preparation of Sodium hexafluorotungstate(V)

The sample was prepared using the method of Hargreaves and Peacock,[130] involving the reaction between sodium iodide and tungsten hexafluoride in sulphur dioxide solvent. For neutron diffraction samples are required in large quantities and the required amount, approximately 25 g, was prepared in three batches. Typically, 24.7 mMol of sodium iodide was added to the preseasoned apparatus (Figure 20), through the stopper and the apparatus was re-evacuated and sealed at the constriction (A). The WF_6 ampoule was cooled before opening the break-seal and the slight excess of WF_6, 28.2 mMol, was transferred to

<u>Figure 20</u>

Apparatus for the preparation of $NaWF_6$.

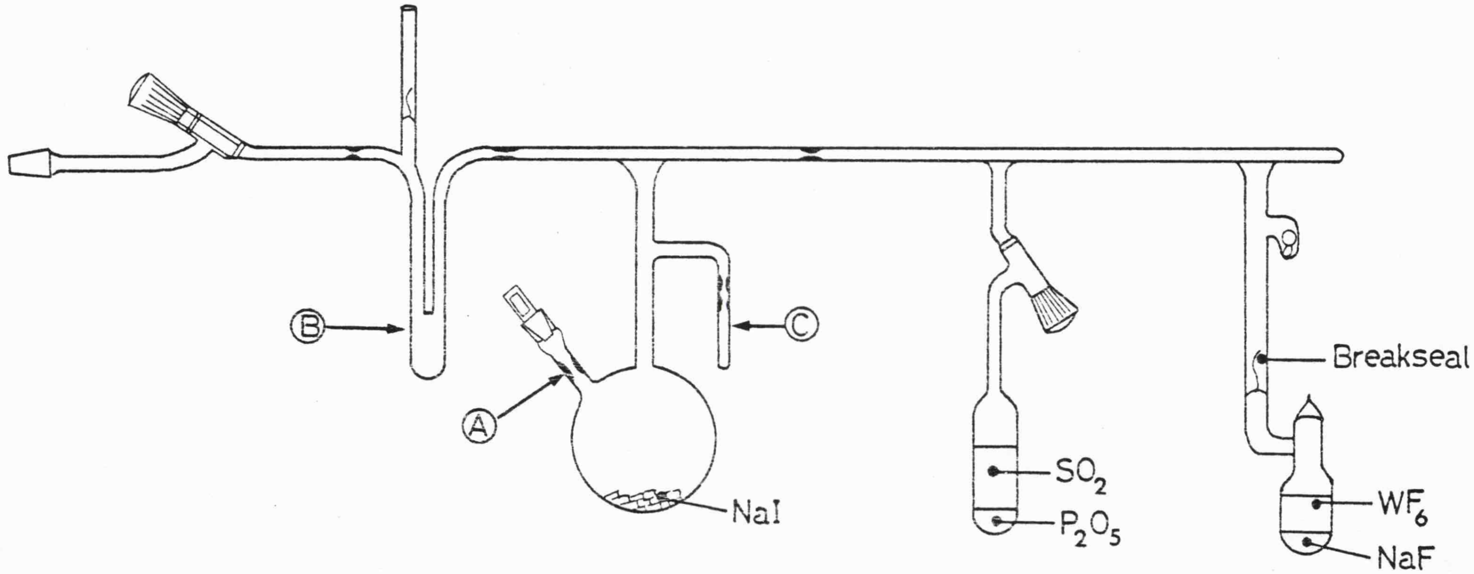

the reactor in static vacuum, the reactor being cooled to -78°C. Approximately 80 cm^3 of SO_2 was then transferred to the cooled reactor causing an immediate colour change in the reactants from white, through yellow, brown and orange to red. The SO_2 was allowed to reflux to a solid CO_2 collar around the reactor neck for 2 hours. After the removal of SO_2 and excess of WF_6, trap B was cooled to -196°C causing the rapid sublimation of the iodine side-product. This was hastened by warming the reactor at 100°C, until the product became pink/buff in colour and no further iodine was liberated. Approximately 0.1 g of yellow crystals were observed to have sublimed out of the reactor during the heating stage of two of the three reactions. The crystals were identified by mass spectroscopy to be sulphur (S_8), which suggest oxygen impurity is to be found in the sample.

The reactor was sealed from the manifold, and a small quantity of the product was sealed into the side arm (C) for purity checks by X-ray powder patterns and mass spectroscopy. The mass spectra of the three samples were all very similar, with WF^+, $WF_4{}^+$, $WF_3{}^+$, $WF_2{}^+$, WF^+ and W^+ abundance patterns, but in each sample the major peaks were $WOF_3{}^+$, $WOF_2{}^+$ and WOF^+ with traces of $WO_2F_2{}^+$. Despite the size of the $WOF_3{}^+$ peak it seems likely that most of the oxygen is from contamination upon admitting the sample to the mass spectrometer.

The X-ray powder patterns of all three samples were identical, Table 26. The pattern was measured and the $\sin^2\theta$ values calculated. The pattern was found to be identical with that obtained by Hargreaves and Peacock[130] at low 2θ angles ($2\theta < 60°$), and could accordingly be indexed as face-centred cubic, with a = 8.157 Å compared with the previously reported value of 8.18 Å. However, above 2θ of 60°, two weak lines could only be indexed assuming a primitive cubic cell. As no extra

TABLE 26

X-ray powder diffraction pattern of $NaWF_6$

line	intensity	$Sin^2\theta \times 10^4$	Assignment (fcc)	pc
a	v.s	266	{111}	
b	v.s	355	{200}	
c	s	718	{220}	
d	s	984	{311}	
e	m.w	1075	{222}	
f	m.s	1431	{400}	
g	m	1696	{331}	
h	s	1787	{420}	
i	m	2144	{422}	
j	s	2418	{511}	
k	m	2858	{440}	
l	m.s	3121	{531}	
m	w	3393		{611}
n	m.w	3569	{620}	
o	v.w	3669		{621}
p	w	3829	{533}	
q	w	3929	{622}	

Cu-$\underline{K}\alpha$ radiation, λ = 1.5418 Å

lines were found at lower 2θ angles, it seems unlikely that the peaks which are not in agreement above 60° are due to impurity. The powder pattern will be dominated by the tungsten atoms and it seems probable that whereas the tungsten and sodium atoms are in face-centred positions, the orientation of the fluorine atoms do not conform, making the face-centred tungsten atoms unequivalent.

The samples of $NaWF_6$ were transferred to a standard neutron diffraction can, Figure 21, which had been preseasoned with ClF_3 after careful evacuation.

Figure 21

A standard neutron diffraction sample can.

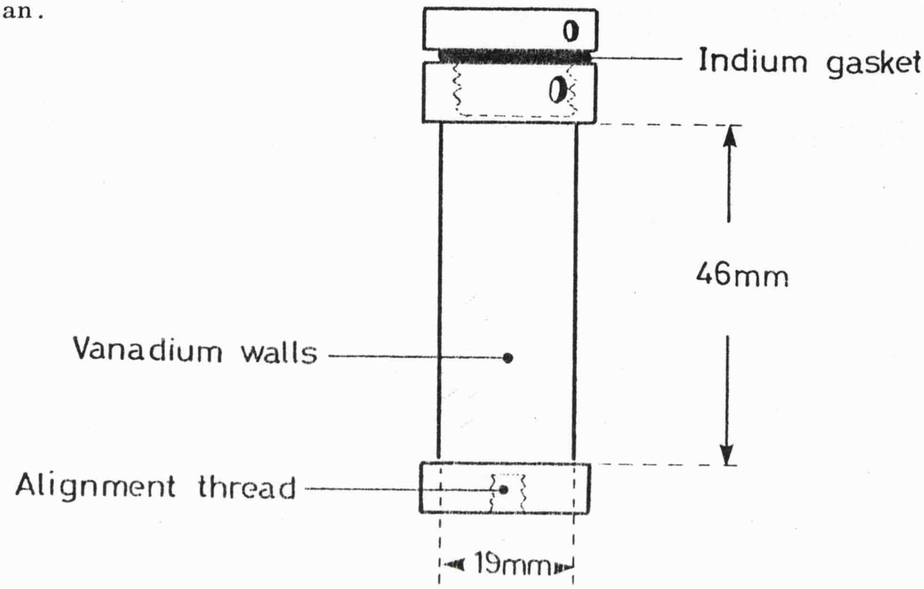

7.3 Data Collection

Neutron diffraction data for $NaWF_6$ was collected at A.E.R.E. Harwell. Data was first collected using the High Resolution Powder Diffractometer (H.R.P.D), but the results were unsatisfactory. This was partly due to the fact that one of the detectors was not functioning, but may also be due to a relatively low degree of crystallinity in the sample. The ratio of background to peak height for the strongest reflections was only 1:2. The data was later re-collected using P.A.N.D.A., and a more satisfactory data set was obtained, with a 1:7 ratio of background to peak height.

The P.A.N.D.A. instrument has nine detectors, which move in a horizontal 2θ arc about the sample, in the plane of the incident and diffracted neutron beams. The detectors are arranged in banks of three (one above and below the equatorial counter) at the same 2θ, with 5° of 2θ between each set. The sample can has a screw thread in the base, by which it is accurately located in the neutron beam, on the axis about which the counters rotate. The diffractometers used for powder work at Harwell, including P.A.N.D.A., have been fully described by Wedgewood.[140]

Two test scans were set to scan through 5° of 2θ at the highest and lowest 2θ values of the proposed range, to ensure that peaks were present. The arrangement of the detectors at 5° intervals means a 5° scan observes 15° in 2θ without overlap. The test scan at low 2θ was used to compare the observed and calculated peak positions as a check for sample decomposition prior to data collection. The calculated peak positions were based on the measured radiation wavelength of 1.2492 Å.

The data collection 2θ scan range for the low angle counters was chosen to be 14.00° to 95.50°, and the middle and high angle counters, therefore, scanned 19° to 100.5° and 24° to 105.5° respectively. This resulted in the two Bragg peaks for the {111} and {200} planes, being measured only by the two low angle sets of detectors. A 2θ step increment of 0.1° was chosen and the time of count/step could then be calculated in order to make maximum use of allocated machine time, with allowance for dead time during angle reset and print-out times.

7.4 Preliminary treatment of the diffraction data

The collected intensity data was first read from the paper tape and listed, using a preliminary program, as a check for spurious high bursts of background radiation which would register on all counters during the same count time. The program Collat was then used to sort the data from the three sets of counters, according to the machine used, counters in use and the angle between them, and the step increment. Initially the data from the equatorial and two non-equatorial counters of each set is summed. The program then sums counts from each set of counters at the appropriate 2θ value to give a total count. As the data is collated, scale factors between the first and subsequent counters are calculated on the basis of the points where all of the counters record a value. These scale factors are then applied in calculating the total counts at points where not all of the counters contribute, thus bringing these values onto the same scale. The series of collated total counts give the observed profile against which it is attempted to fit a calculated profile by refinement of the least-squares parameters.

7.5 Refinement of the structure

The structure refinement program is used in two stages. A pre-profile stage determines which reflections may contribute to each of the observed points in the powder diffraction profile. This stage should also be repeated at any point in the refinement where significant alterations have been made to the unit cell or profile parameters. The unit cell dimension, $\underline{a}$, was calculated from an X-ray powder pattern and the remaining pre-profile parameters determined during data collection.

Parameters used in the determination of the calculated pre-profile were:-

Space group, cubic $\underline{P}\ \underline{a}\ 3$ (T_h^6 No. 205)

Unit cell, $\underline{a}$ = 8.157 Å

Half-width parameters, $\underline{U}$ = 13772.0; $\underline{V}$ = -8119.0; $\underline{W}$ = 2284.0

Zero point error, 0.00°

Neutron wavelength, $\underline{\lambda}$ = 1.2492 Å

Abscissa increment, $\delta 2\theta = 0.10°$.

The half-width parameters, $\underline{U}$, $\underline{V}$ and $\underline{W}$ are found approximately by measuring the half-width, H_k, of selected peaks and finding a least-squares fit to these observed quantities using the equation:-

$$H_k^2 = U \tan^2\theta_k + V \tan\theta_k + W$$

The equation is simplified from the formula of Caglioti et al.[135] and adequately takes account of the angular dependence of the half-widths.

The second stage of the refinement program determines the calculated intensity at each point in the observed powder diffraction profile. The zero point error, unit cell dimensions and half-width parameters can be refined or constrained at this stage, as may the other least-squares parameters which determine the calculated intensity. The other allowed least-squares parameters are the position in the unit cell of each of the atoms in the asymmetric unit, the nature and magnitude of the thermal vibrations of these atoms and a scale factor relating the ordinates of the calculated and observed profiles. In addition to the least-squares parameters it is necessary to know the number and types of atom in the asymmetric unit, and the contribution at any abscissa value which arises from background rather than Bragg reflections.

For the first cycles of least-squares refinement the unit cell dimension, $\underline{a}$, the half-width parameters and overall scale factor were refined. In addition an overall temperature factor, rather than individual isotropic or anisotropic thermal parameters, and the X/A co-ordinate of the fluorine atom were refined. The W atom was fixed at the origin, Na at $\frac{1}{2},\frac{1}{2},\frac{1}{2}$, and the Y/B and Z/C co-ordinates of the F atom were initially constrained at zero, thus attempting to refine the structure in the space group $\underline{Fm3m}$. Three cycles of least-squares refinement gave an R factor of 0.27. Further cycles used the refined value for the unit cell dimension as a constrained parameter, and individual isotropic temperature factors for the atoms were refined, as was the zero point error. The Y/B and Z/C co-ordinates of the F atom were also allowed to refine, thus changing the space group to $\underline{Pa}3$, and the resulting R factor was 0.18. Final cycles with the Z/C co-ordinate of the F atom given a positive value further reduced R to 0.16 . The final atomic parameters for $NaWF_6$ are given in Table 27, and the final observed and calculated profiles are shown in Figure 22, and listed in Appendix 6.

The final residual indices for 111 reflections are:-

$$R = 100 \sum |I(obs) - \frac{1}{c} I(calc)| / \sum I(obs) = 0.167$$

$$R_w = 100[\sum_w (y\{obs\} - \frac{1}{c} y\{calc\}^2 / \sum_w (y\{obs\})^2]^{-2} = 0.168$$

TABLE 27

Final atomic parameters for $NaWF_6$ with estimated standard deviations in parentheses where the values were refined

F_6NaW ; $\underline{M}$ = 320.83

Cubic ; $\underline{a}$ = 8.168(1) Å

$\underline{U}$ = 545.0 Å^3; $\underline{D_c}$ = 3.91 g cm^{-3}; $\underline{Z}$ = 4

	x/a	y/b	z/c	$B = 8\pi^2 U$
Na	0.5	0.5	0.5	3.689(327)
W	0.0	0.0	0.0	0.073(120)
F	0.2187(4)	0.0101(14)	0.0126(13)	5.244(131)

Interatomic distances: W — F = 1.791(4) Å
Na•—•F = 2.299(4) Å
F •—•F = 2.533 Å

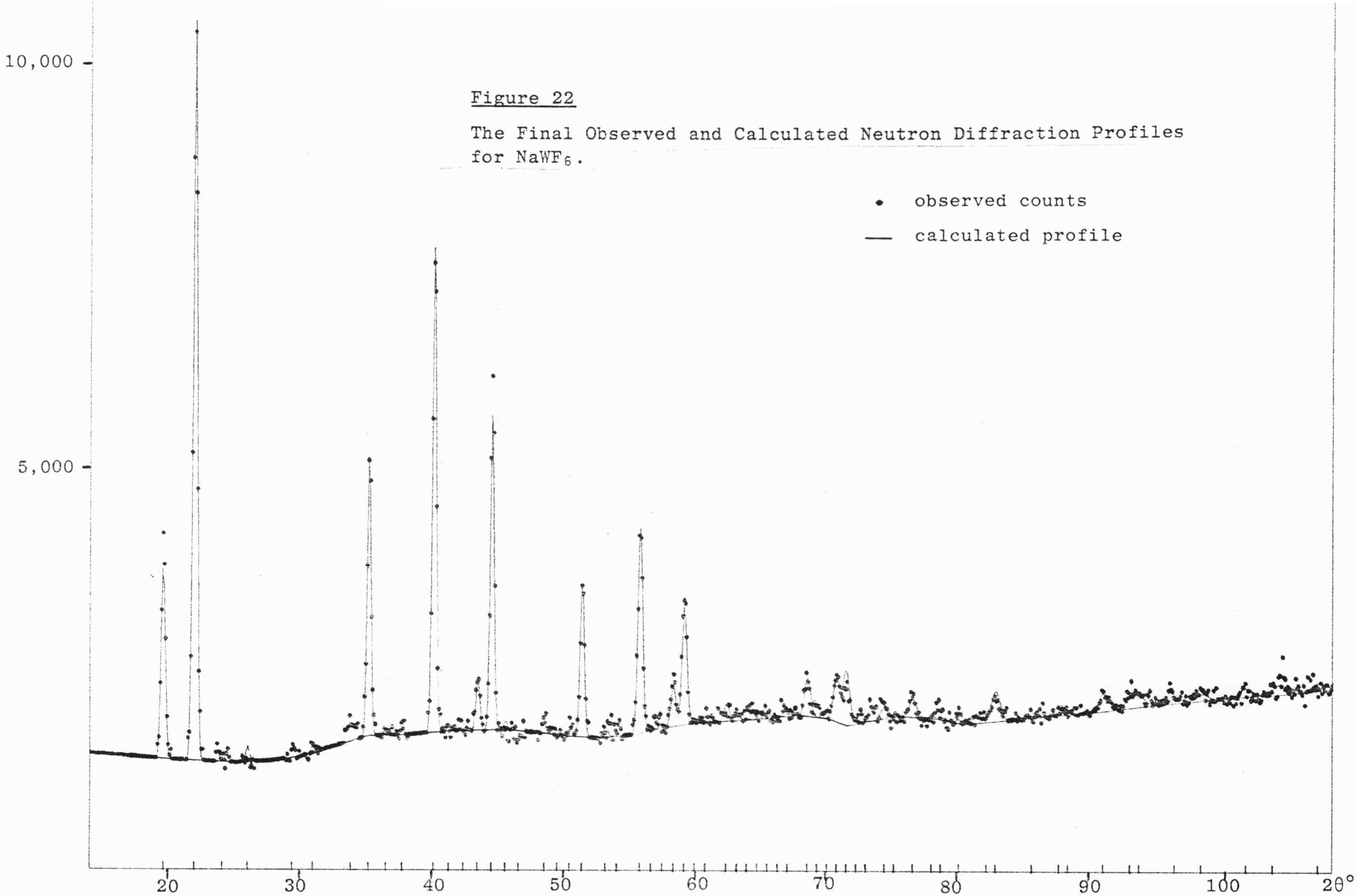

Figure 22

The Final Observed and Calculated Neutron Diffraction Profiles for $NaWF_6$.

7.6 Discussion

The primitive cubic structure, space group Pa3, was found to appropriate for sodium hexafluorotungstate(V). This is contrary to the previously reported face-centred cubic cell reported by Hargreaves and Peacock.[130] However, as noted in the preparative section of this chapter, the X-ray diffraction powder pattern obtained on the sample used for neutron diffraction was in complete agreement with that of Hargreaves and Peacock below a 2θ value of 60°, and only two weak reflections above 60° indicated that the structure might be other than face-centred. Despite the fact that the intensities of equivalent reflections from neutron and X-ray diffraction are not related, the non-face-centred cubic reflections are also weak in the neutron data.

The primitive cubic (Pa3) structure requires that the octahedra of fluorine atoms about tungsten at the origin and face-centred positions are rotated in opposite directions from the special (x,o,o) positions (Figure 23). Thus the structure is also different to those proposed for $NaPF_6$[129] and $NaSbF_6$[118] where the octahedra are rotated equally in the same directions, to be on 24 of the 192 general (x,y,z) positions of the space group Fm3m. The y/b and z/c co-ordinates of the F atom in the $NaWF_6$ structure are close to zero (.0101(14) and .0126(13) respectively) and the X-ray powder pattern would be expected, through the overwhelming contribution of the face-centred heavy atoms, to indicate the space group Fm3m. The $NaTaF_6$ structure (chapter 6) was found to be face-centred cubic Fm3m, and it was considered that the compounds exhibiting the cubic structure, designated C_1, might show a trend for the F atoms to move from the special position x,o,o, as the ionic radius of $R_{B_5^+}$ decreases. The compounds attributed this structure $NaMF_6$ (M = Mo, W, Sb, Nb, Ta) have only a small range of ionic radii,

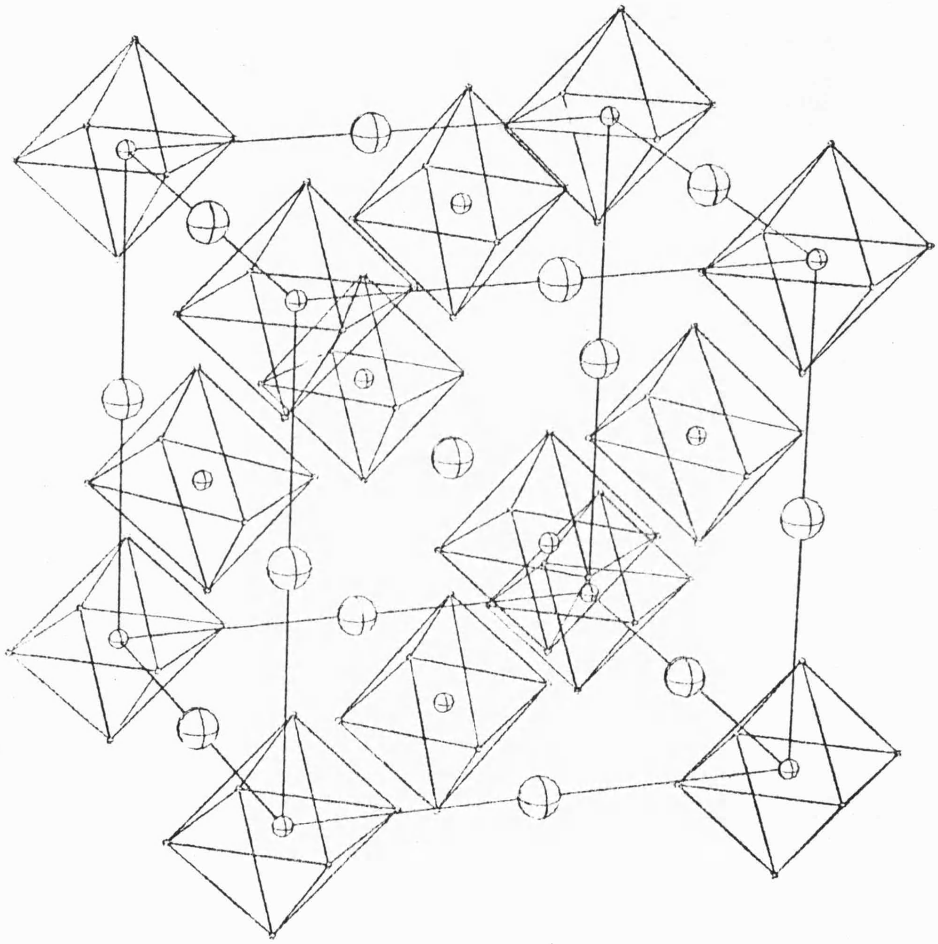

Figure 23

The Unit Cell packing in $NaWF_6$.

of which Ta and W are representative of the extremes. Therefore, if the F atoms of $NaWF_6$ are shifted furthest, in this series, from the special position, the $\underline{Fm3m}$ structure is a close approximation of this structure type. The W-F bond length is of the expected order for this type of compound (1.791 Å), and the Na atom retains, in $\underline{Pa3}$ symmetry, six F atoms as nearest neighbours at 2.299 Å.

The final R factor obtained, 0.167, is not directly comparable with R factors resulting from the refinement of single crystal data sets. The value could probably be reduced further with greater familiarity with the program. In particular the operation of the low 2θ angle asymmetry parameter, a correction which appeared desirable for this data set, was not satisfactorily applied to the calculated profile. However, the estimated standard deviation of all the refined parameters is acceptably low, and the isotropic temperature factors are of the expected orders for this type of structure on the Na and F atoms, and for the W atom virtually no thermal motion is indicated.

Though the intensity of X-ray diffraction peaks are not directly related to those found by neutron diffraction, they both depend upon a basic minimum degree of crystallinity. Neutron diffraction data were collected for the three compounds $NaWF_6$, $CsWF_6$ and $CsIF_6$; of these $NaWF_6$ gave the only data set which was considered probable to yield a satisfactory structure refinement, and all three samples gave comparably poor X-ray powder diffraction patterns, despite the heavy atom contributions. It seems probable that for neutron diffraction data to produce acceptable structure refinements the sample should be capable of producing sharp X-ray diffraction patterns, except where no heavy atom is present in the compound.

CHAPTER 8

The Crystal Structures of $(NH_4)_2PtF_6$ and K_2OsF_6

8.1 Introduction

As with the $A^{I}B^{V}F_6$ compounds discussed in chapters 6 and 7 of this thesis, the complex fluorides of the general formula $A_2^{I}B^{IV}F_6$ may be classified by a few known structure types, with only minor deviations from these types. For the $A_2^{I}B^{IV}F_6$ compounds having the larger cations (A = K, Cs, Rb, Tl and NH_4) there are three basic types of structure, with many of the compounds known to exhibit two and even all three polymorphic forms. The hexafluoride, K_2SiF_6,[141] is representative of the cubic structure, space group $\underline{Fm3m}$. A trigonal type, space group $\underline{P\bar{3}m1}$, is typified by K_2GeF_6,[142] but has been recently more accurately determined for K_2ReF_6.[143] The compound K_2MnF_6[144] is taken as representative of the third structure type which is hexagonal, space group $P6_3mc$. The structures of known $A_2^{I}B^{IV}F_6$ compounds are summarised in Table 28.

The K_2SiF_6 structure, which is more commonly referred to as the well known K_2PtCl_6 (antifluorite) structure,[145] has four molecules in the unit cell. There is octahedral arrangement of the F atoms about the Si atom, and the octahedra and K atoms are arranged as are the Ca and F atoms of the CaF_2 structure, with cubic close-packed layers (layer sequence ABC, ABC). The cations, A^+, are coordinated by twelve F atoms, three from each of the equidistant $BF_6{}^{2-}$ octahedra. This type of structure is found in many of the hexafluorides, and is almost exclusively adopted by the other hexahalides. The trigonal, K_2ReF_6, structure type has one molecule in the unit cell and the atoms have a similar arrangement to that found in the CdI_2 structure, the layers are arranged in hexagonal close-packing (sequence AB, AB). In the ideal structure the cations, A^+, would have 12 equidistant F neighbours, but most of the compounds deviate slightly from the perfect structure, with

TABLE 28

The Structures of $A_2{}^{I}B^{IV}F_6$ Compounds

A^+	Structure Type	Li	Na	Structure Type	K	NH_4	Rb	Cs
r_{A^+}		0.68	0.97		1.33	1.43	1.48	1.6[illegible]
B^{IV} $r_{B^{4+}}$								
Si 0.42	Hex	a=8.22, c=4.56[150]	a=8.86, c=5.04[146]	Hex		a=5.78, c=4.79[178,179]		
				Cub	a=8.13[141,161]	a=8.395[179,180]	a=8.45[161]	a=8.87[141,161]
Ge 0.53				Trig	a=5.62, c=4.65[142]	a=5.85, c=4.77[142]	a=5.82, c=4.79[172]	
	Hex		a=8.99, c=5.12[156]	Hex	a=5.71, c=9.27[162]		a=5.94, c=9.63[162]	
				Cub		a=8.46[181]		a=8.99[177]
Mn 0.60				Trig	a=5.71, c=4.65[144]			
	Hex	a=8.42, c=4.59[152]	a=9.03, c=5.13[150]	Hex	a=5.67, c=9.35[144]	a=5.91, c=9.55[182]	a=5.85, c=9.50[144,173]	
				Cub	a=8.28[144,163]		a=8.43[144,173]	a=8.92[144]
Cr 0.60	Hex		a=9.14, c=5.15[157]	Hex	a=5.70, c=9.35[163,164]		a=5.95, c=9.69[164]	
	Mono	4.58, 4.58, 9.99, β 117.2[153]		Cub	a=8.16[163,164]		a=8.52[164]	a=9.02[164]
Pd 0.65				Trig	a=5.72, c=4.67[165]			
	Hex		a=9.23, c=5.25[158]	Hex	a=5.74, c=9.51[166]		a=5.98, c=9.70[141]	
	Mono	10.1, 4.64, 4.63, β 117[154]		Cub			a=8.57[166]	a=9.00[166,168]
Pt 0.65	Hex		a=9.41, c=5.16[150,159]	Trig	a=5.76, c=4.64[167,168]		a=5.96, c=4.83[168]	a=6.22, c=5.01[168]
	Mono	10.23, 4.68, 4.65, β 117[154]		Cub		a=8.455†		
Ti 0.68				Trig	a=5.71, c=4.65[141,171]	a=5.96, c=4.82[141]	a=5.88, c=4.78[141]	a=6.15, c=4.96[141]
	Hex		a=9.21, c=5.15[150]	Hex	a=5.75, c=9.46[171]		a=5.91, c=9.81[141]	
				Cub	c=8.32[171]		a=8.49[141]	a=8.96[141]
Re 0.72	Ortho		5.81, 4.49, 10.10[157]	Trig	a=5.88, c=4.61[143]	a=6.06, c=4.77[174,175]	a=6.01, c=4.77[159,174,175]	a=6.30, c=4.99[174,175]
Hf 0.78				Trig			a=6.13, c=4.81[176]	a=6.39, c=5.00[176]
				Ortho	a=6.51, b=11.4, c=6.69[169]			
Zr 0.79	Trig	a=4.98, c=4.66[147,155]		Trig			a=6.16, c=4.82[176]	a=6.41, c=5.01[176]
	Mono		5.56, 5.41, 16.1, β 959[160]	Ortho	a=6.85, b=11.4, c=6.94[169,170]			
Os 0.88	Hex		a=9.36, c=5.11[157]	Trig	a=5.82, c=4.62†[159]			a=6.26, c=5.00[159]
	Ortho		5.80, 4.50, 10.14[157]					

† present work

resulting coordinations of (9 + 3) or (3 + 6 + 3). In the K_2ReF_6 structure determination, the ReF_6^{2-} octahedron was found to be slightly compressed giving F-Re-F angles for adjacent F atoms of 93.8(2) and 86.2(2)°, and the K^+ ions were not found to be coplanar with hexagonal close-packed layers of F atoms. As a result the 12 F neighbours to each K^+ are in the 3 + 6 + 3 arrangement, respectively 2.789, 2.957 and 2.998(4) Å from K^+. The hexagonal, K_2MnF_6, structure type is related in the case of polymorphic forms, to the K_2GeF_6 structure by a doubling of the c axis and, therefore, has two molecules in the unit cell. The layers appear to have a double hexagonal close-packing arrangement (layer sequence ABAC, ABAC).

Until recently there were few reported structures for the $A_2^IB^{IV}F_6$ compounds containing the smaller alkali ions of Li and Na. The most common structure found with Li and Na is a trimolecular hexagonal structure, space group P321, typified by Na_2SiF_6.[146] The other structures types are a second unimolecular trigonal form, represented by Li_2ZrF_6,[147] and a monoclinic form of which Na_2SnF_6[148] is considered to be representative.

The three structure types all exhibit close-packing of the A^+ and BF_6^{2-} ions, and there is less connection between the relative sizes of the cations (A = K, Cs, Rb, Tl and NH_4) and the BF_6^{2-} ions and the structures than for the $A^IB^VF_6$ compounds. It has been suggested by Cox[149] that for the complex fluorides A_2BF_6, the two structure types, cubic and trigonal, are of nearly equal energy and that their distribution is approximately random. Certainly the irregular distribution of the cubic, trigonal and hexagonal structures, and the existence of complex fluorides in three modifications suggest the structures are similar energetically.

There is doubt concerning the nature of the bonds within the $A^{I}_{2}B^{IV}F_6$ compounds. For some of these compounds, the $BF_6{}^{2-}$ ion appears stable in aqueous solution and, in these cases, it is reasonable to consider the structures as true ionic aggregates. However, this is not the case for most of the fluorides and the nature of the bond between the atoms B and F in such cases is not clear. From consideration of interatomic distances the A to F contacts of such compounds have been described as ionic, covalent and transitional. This problem is particularly true of the ammonium compounds where hydrogen bonding may have significance in determining the structures. A consideration of the unit cell size and interatomic distances in the $(NH_4)_2PtF_6$ structure compared with those of other hexafluoroplatinates may help to clarify this problem.

8.2 Preparation of ammonium hexafluoroplatinate(IV)

Crystals of ammonium hexafluoroplatinate(IV) were provided by D. C. Puddick. Potassium hexafluoroplatinate(IV) was prepared by the direct fluorination of potassium hexachloroplatinate(IV) at 300°C.[151]

$$K_2PtCl_6 + 3F_2 \xrightarrow{300^\circ} K_2PtF_6 + 3Cl_2$$

The purity of the K_2PtF_6 was checked by its X-ray powder diffraction pattern. The K_2PtF_6 was converted to the ammonium salt by passing an aqueous solution through a column containing a cation exchange resin (Zeocarb 225 SRC 10), which had previously been charged by ammonium chloride solution.

$$K_2PtF_6 + 2(NH_4)^+ \longrightarrow (NH_4)_2PtF_6 + 2K^+$$

Upon evaporating the effluent the ammonium hexafluoroplatinate(IV) was obtained as yellow-orange crystals. Infrared spectra of the product, taken over the ranges 5000 cm^{-1} to 650 cm^{-1} (NH_4^+ bands) using NaCl plates and HCB mull, and 800 cm^{-1} to 200 cm^{-1} (Pt-F bands) using polythene plates and nujol mull, showed no evidence of impurity. However, upon close examination two distinct crystal types were found. Both types were of hexagonal plate form, but approximately 10% were orange whilst the remainder were yellow-green in colour. A batch of crystals were separated into the two visible forms by a needle under a microscope. The best examples of each were mounted on glass filaments for single crystal studies and the remainder ground for a preliminary X-ray powder diffraction study. For both crystal forms the diffraction patterns indicated basically face-centred cubic cells.

TABLE 29

X-ray powder diffraction pattern of $(NH_4)_2PtF_6$

line	intensity	$Sin^2\theta \times 10^4$	$(h^2 + k^2 + l^2)$ assignment (fcc)
a	10	250	3
b	9	335	4
c	9	672	8
d	10	923	11
e	8	1342	16
f	7	1597	19
g	7	1674	20
h	7	2009	24
i	8	2260	27
j	6	2679	32
k	7	2928	35
l	6	3011	36
m	5	3344	40
n	4	3598	42.8?

However, the pattern obtained from the yellow-green crystals (Table 29) contained one very weak line which could not be indexed on this assumption, and the cubic indexing may over-simplify a rhombohedral cell. The cubic cell parameters obtained were 9.861 Å for the orange crystals and 8.424 Å for the yellow-green crystals.

The orange crystals were identified by a single crystal study as $(NH_4)_2PtCl_6$, the structure of which has been reported by Wyckoff and Posnjak.[183] Details of the data collection and structure refinement, therefore, are not reported but the atomic parameters found in this study are expected to be more accurate than those previously reported, where data was collected by intensity measurements from Weissenberg photographs and are thus given in Tables 32 to 33. It is uncertain whether the $(NH_4)_2PtCl_6$ impurity resulted from incomplete fluorination of the K_2PtCl_6.

8.3 Single Crystal X-ray Investigation

Ammonium hexafluoroplatinate(IV) crystals are not air sensitive and crystals were mounted on thin pyrex filaments with small quantities of adhesive (Araldite). The crystal selected for the investigation was of hexagonal plate appearance, with dimensions 0.28 mm × 0.28 mm × 0.30 mm across the hexagonal faces and 0.125 mm depth. The crystal was mounted about the $\underline{c}$ axis of the hexagonal cell, the axis being the body-centred diagonal of the face-centred cubic unit cell finally chosen as appropriate. Preliminary cell dimensions were obtained from Weissenberg photographs, taken using Cu-$\underline{K}_\alpha$ (Ni filtered) radiation and precession photographs using Mo-$\underline{K}_\alpha$ (Zr filtered) radiation. The final values for the cell parameters were determined from the optimised counter angles for zero and upper layer reflections on a Stoe Weissenberg diffractometer.

8.4 Crystal Data for ammonium hexafluoroplatinate(IV)

$F_6H_8N_2Pt$; $\underline{M}$ = 345.1

Cubic $\underline{a}$ = 8.455(8) Å

$\underline{U}$ = 603.6 $Å^3$; $\underline{D_c}$ = 3.792 g cm^{-3} ; $\underline{Z}$ = 4

$\underline{F}$(000) = 616 ; M_o-$\underline{K}_\alpha$ radiation ; λ = 0.71069 Å

μ(M_o-$\underline{K}_\alpha$) = 224.0 cm^{-1}

Space group $\underline{Fm3m}$ (O_h^5 No. 225). Neutral atomic scattering factors were used with anomalous dispersion coefficients.

8.5 Collection of the Intensity Data

Data were collected from layers hk0 to hk15 of the hexagonal cell (a = 5.976 Å, c = 14.648 Å), using the Stoe (Stadi-2) diffractometer in the four quadrants ±h, ±k, +l. The data were collected using an ω-scan technique, with 2θ constant at the calculated value for each reflection. The intensities of reflections with $0.122 \leqslant \sin\theta/\lambda \leqslant 0.904$ $Å^{-1}$ were collected, and 906 reflections were obtained with $I/\sigma I \geqslant 3$. Check reflections were monitored during the data collection for each layer, and indicated no deterioration of the crystal. Lorentz and polarisation corrections were made to the data set. The data was corrected for absorption by the program ABSCR.[8]

8.6 Solution of the ammonium hexafluoroplatinate(IV) structure

The program system SHELX was used. In the early stages of refinement, symmetry of the space group $\underline{R}\bar{3}$ was assumed, and the data averaged to 274 unique reflections, with an R_{AV} factor of 0.0287. Platinum was located on the origin, special position, 1a (Wyckoff notation), of the space group. The fluorine and nitrogen atom positions were located from a difference Fourier map. The hydrogen atoms were not located. Two cycles of full matrix least-squares refinement gave an R factor of 0.052 with isotropic thermal parameters, and this was reduced to 0.0265 when the atoms were allowed to refine anisotropically. Correlation between the anisotropic thermal parameters for the fluorine atom (where $U_{22} = 2U_{21}$, and $U_{23} = 2U_{13}$) suggested the space group symmetry was higher than $\underline{R}\bar{3}$. Refinement was, therefore, attempted in the space groups $\underline{R}3\underline{m}$ and $\underline{F}\underline{m}3\underline{m}$. For $\underline{R}3\underline{m}$ the data averaged to 171 unique reflections with an R_{AV} factor of 0.0274. The number of parameters refined was decreased from 15 to 12 by restraints imposed on the anisotropic thermal parameters. Refinement in the space group $\underline{F}\underline{m}3\underline{m}$ further decreased the degrees of freedom, with only the fluorine atom refining anisotropically. The data averaged to 71 unique reflections (R_{AV} 0.0278) and 6 parameters were refined.

Final cycles of least-squares in each space group employed a weighting parameter, g, and the final R factors for the space groups $\underline{R}\bar{3}$, $\underline{R}3\underline{m}$ and $\underline{F}\underline{m}3\underline{m}$ were respectively 0.0265, 0.0272 and 0.0278. An analysis of the weighting scheme over $|F_o|$ and $\sin\theta/\lambda$ was satisfactory in each case, however, the final Fourier difference map for the space group $\underline{F}\underline{m}3\underline{m}$ showed a 7 electron residual peak on a special position, x,x,x.

Statistical significance tests were performed on the R factors for the three space groups, using the method of Hamilton.[184] The hypothesis that the restrained model of $\underline{F}\underline{m}3\underline{m}$ symmetry was appropriate was tested. The ratio of the generalised R factors for $\underline{F}\underline{m}3\underline{m}$ (R_G') and $\underline{R}\bar{3}$ (R_G'') was compared with values, in the significance level tables, determined by the number of data refined and the number of variable parameters. The ratio R_G'/R_G'' (1.034) was found to be approximately equivalent to the value determined from the 0.05 significance level table. Therefore, the *Fm3m* structure cannot be rejected at the 5% probability level. Although this indicates the space group $R\bar{3}$ produces a better refinement, this was thought to be entirely due to the reduction of residual systematic errors in the absorption correction. Accordingly the results from the *Fm3m* refinement are considered to be appropriate, and the parameters listed are for this space group.

The final atomic positional and thermal parameters are in Table 30, and the interatomic distances (bond and non-bond) are given in Table 31. The observed and calculated structure factors are found in Appendix 7.

Final residual indices for the 71 unique reflections are:-

$$R = \sum(|F_o| - |F_c|)/\sum|F_o| = 0.0278$$

$$R_w = [\sum w(|F_o| - |F_c|)^2/\sum w|F_o|^2]^{\frac{1}{2}} = 0.0243$$

The final atomic positional and thermal parameters for the ammonium hexachloroplatinate(IV) structure are in Table 32, and the interatomic distances are given in Table 33.

Final residual indices for 99 unique reflections are:-

$$R = \sum(|F_o| - |F_c|)/\sum|F_o| = 0.0165$$

$$R_w = [\sum w(|F_o| - |F_c|)^2/\sum w|F_o|^2]^{\frac{1}{2}} = 0.0165$$

8.7 Preparation of potassium hexafluoroosmate(IV)

Potassium hexafluoroosmate(IV) was prepared by the method of Hepworth *et al.*[122] Osmium tetroxide was formed by heating osmium metal in a current of oxygen, the volatile material collected in a cooled trap. The osmium tetroxide (1.86 g) was then refluxed, with an excess of 48% HBr (25 cm^3) and absolute alcohol (1.5 cm^3), for eight hours.

$(NH_4)_2PtF_6$

TABLE 30

Final atomic positions and thermal parameters with standard deviations derived from the least-squares refinement. The temperature factors are in the form $\exp[-2\pi^2(h^2U_{11}a^{*2} + \ldots. + 2hkU_{12}a^*b^*)]$ and are given $\times 10^4$.

	x/a	y/b	z/c	U_{11}	U_{22}	U_{33}
Pt	0.0	0.0	0.0	156(4)		
N	0.25	0.25	0.25	287(41)		
F	0.0	0.0	0.2298(10)	356(26)	356(26)	150(32)

TABLE 31

The interatomic distances (Å), with estimated standard deviations in parentheses.

Pt —— F	1.935(10)
N ····· F	2.993(12)
Pt ···· N	3.66 (12)

$(NH_4)_2PtCl_6$

TABLE 32

Final atomic positions and thermal parameters with standard deviations in parentheses. The temperature factors are in the form $\exp[-2\pi^2(h^2U_{11}a^2 + ... + 2hkU_{12}ab)]$ and are given $\times 10^4$.

	x/a	y/b	z/c	U_{11}	U_{22}	U_{33}
Pt	0.00	0.00	0.00	.0145(1)		
N	0.25	0.25	0.25	.0302(5)	.0302(5)	.0275(5)
Cl	0.00	0.00	0.2356(9)	.0316(14)		

TABLE 33

The interatomic distances (Å), with estimated standard deviations in parentheses.

Pt——Cl	2.323(2)
N ····· Cl	3.488(4)
Pt ···· N	4.264(4)

$$Os + 2O_2 \xrightarrow{heat} OsO_4$$

$$OsO_4 + 4HBr \longrightarrow OsBr_4$$

The excess of HBr was then removed by heating in a silica crucible, and the heating continued for two hours, to produce a black friable solid.

Potassium hexafluoroosmate(V) was prepared by the reaction of stoichiometric quantities of osmium tetrabromide (1.3999 g, 2.746 mMol) and potassium bromide (0.3270 g, 2.748 mMol), with an excess of bromine trifluoride.

$$OsBr_4 + KBr + 2BrF_3 \longrightarrow KOsF_6 + 3\tfrac{1}{2}\ Br_2$$

The apparatus used was as for the preparation of sodium hexafluoro-tantalate(V) (Figure 13), and the experimental procedure was identical. After the removal of the excess of BrF_3 in dynamic vacuum, the product was pumped for 1 hour at 190°C, until an off-white powder remained. The purity of the $KOs^{V}F_6$ was ascertained by an X-ray powder diffraction pattern.

Potassium hexafluoroosmate(IV) was prepared by the alkaline hydrolysis of potassium hexafluoroosmate(V). To a solution of $KOs^{V}F_6$ in deionised water was added a solution of KOH and the crystallisation of $K_2Os^{IV}F_6$ was induced by the "common ion effect" of a small quantity of KF. The microcrystalline product was washed with cold water and then absolute alcohol. Crystals suitable for X-ray study were obtained by allowing a saturated solution to evaporate.

8.8 Single Crystal X-ray Investigation

Potassium hexafluoroosmate(IV) is moderately stable in the atmosphere, and the crystals were, therefore, sorted open to the air, but sealed in

Pyrex capillaries to prevent deterioration during single crystal study. The crystal chosen for the investigation had the appearance of a hexagonal plate with the approximate dimensions 0.023 mm × 0.031 mm × 0.030 mm across the hexagonal faces and 0.0093 mm in depth. The crystal was mounted about the a axis of the hexagonal cell of a rhombohedral lattice. Preliminary cell dimensions were obtained from Weissenberg photographs taken using Cu-K_α (Ni filtered) radiation and precession photographs using M_o-K_α (Zr filtered) radiation. The final values for the cell parameters were determined from the optimised counter angles for zero and upper layer reflections.

8.9 Crystal Data for potassium hexafluoroosmate(IV)

F_6K_2Os ; $M = 382.4$

Trigonal $a = 5.821$ Å ; $c = 4.623(8)$ Å ; $\gamma = 120.0°$

$U = 135.67$ Å^3 ; $D_c = 4.68$ g cm^{-3} ; $Z = 1$

$\mu(M_o\text{-}K_\alpha) = 240.92$ cm^{-1} ; $F(000) = 165.96$

M_o-K_α radiation ; $\lambda = 0.71069$ Å

Space group $P\bar{3}m1$ (D^3_{3d} No. 164). Neutral atomic scattering factors were used with anomalous dispersion coefficients.

8.10 Collection of Intensity Data

Data were collected from the layers h01 to h101, using the Stoe Stadi-2 diffractometer in the quadrants ±h, k, ±1. The data were collected using an ω-scan technique, the width of the scan was determined for each reflection and counts taken every 0.01° for 0.3 seconds. A pre-scan of each reflection was used to determine whether attenuation was required for count rates > 10000 counts s^{-1} to prevent flooding of the counter. The intensities of reflections with $6° \leqslant 2\theta \leqslant 80°$ were collected, and 1802 reflections with $I/\sigma I \geqslant 3$ were obtained. Check reflections were monitored during the data collection for each layer and indicated no deterioration of the crystal. Lorentz, polarisation and absorption corrections were made to the data set.

8.11 Solution of the potassium hexafluoroosmate(IV) structure

The program system SHELX was used. The refinement of the structure was based on the space group ($\underline{P}\bar{3}\underline{m}1$) and atomic parameters found for the K_2ReF_6[143] structure. Three cycles of least-squares refinement with osmium on the origin, potassium at $^1/_3$, $^2/_3$, 0.3 and fluorine at 0.162, -0.162, 0.228 gave an R factor of 0.076. The positional parameters refined for the fluorine atom, x/a (= -y/b) and z/c, remained within error limits the same as for the K_2ReF_6 structure, and the z/c parameter of the potassium atom showed only a small shift. Further cycles of least-squares refinement using allowed anisotropic thermal parameters for all atoms reduced the R factor to 0.055. The residual difference Fourier map at this stage showed several large unexplained electron density peaks along the ooz axis, including 4.6 electrons on the osmium site (0,0,0). The residual peaks were considered to be a result of an inadequate absorption correction. The averaging of the 1802 reflections collected, by the symmetry operations of the space group $\underline{P}\bar{3}\underline{m}1$, to 576 reflections produced an internal R_{AV} of 0.099. Further attempts were made to improve the absorption correction, however, accurate measurements of the crystal dimensions were difficult due to distortion produced by the capillary walls and the lowest R_{AV} value obtained was 0.0916. Final cycles of least-squares, using this data, employed a weighting parameter g(0.00735) $[\omega \alpha\ ^1/\sigma^2\ (F) + g\ F^2]$ and an isotropic extinction parameter x(.0341) $[F_c = F(1 - xF^2/\mathrm{Sin}\theta)]$.

The final difference Fourier was, however, only marginally improved and residual peaks were present on the ooz axis. The analysis of the weighting scheme over $|F_o|$ and $\sin\theta/\lambda$ was satisfactory. The absence of any significant trends in the data or high thermal parameters support the conclusion that the residual peaks in the Fourier map result from absorption correction errors.

Final atomic positional parameters are given in Table 34, the anisotropic thermal parameters are in Table 35, and the interatomic distances and angles are in Table 36. The observed and calculated structure factors are found in Appendix 8.

Final residual indices for 576 unique reflections:-

$$R = \sum(|F_o|-|F_c|)/\sum|F_o| = 0.0493$$

$$R_w = [\sum w(|F_o|-|F_c|)^2/\sum w|F_o|^2]^{\frac{1}{2}} = 0.0447$$

TABLE 34

Final atomic positional parameters for potassium hexafluoroosmiate(IV) with estimated standard deviations in parentheses

	x/a	y/b	z/c
Os	0.0	0.0	0.0
K	0.3333	0.6667	0.2979(6)
F	0.1612(5)	-0.1612(5)	-0.2286(10)

TABLE 35

Thermal parameters of the form exp $[-2\pi^2(h^2U_{11}a^2 + \ldots\ldots 2hkU_{12}ab)]$ with estimated standard deviations in parentheses

	U_{11}	U_{22}	U_{33}	U_{23}	U_{13}	U_{12}
Os	.0109(2)	.0109(2)	.0155(2)			.0055(1)
K	.0200(5)	.0200(5)	.0249(8)			.0100(2)
F	.0330(18)	.0330(18)	.0278(17)	-.0039(7)	.0039(7)	.0234(21)

TABLE 36

a) Interatomic distances (Å) with estimated standard deviations in parentheses

Os —— F	1.936(5)
K------3F	2.798(5)
K------6F	2.929(5)
K------3F	2.987(5)
K-----Os	3.632(5)

b) Interatomic angles

F — Os — F	86.8(2)
F — Os — F	93.2(2)

8.12 Discussion of the ammonium hexafluoroplatinate(IV) and potassium hexafluoroosmate (IV) structures

The structure of ammonium hexafluoroplatinate(IV) was found to be isostructural with the cubic K_2PtCl_6, or K_2SiF_6 structure. The $BF_6{}^{2-}$ anions of the $A_2^{1}B^{IV}F_6$ compounds commonly show distortion from $\underline{Fm3m}$ symmetry by compression along a three-fold axis.[143] The $PtF_6{}^{2-}$ ion showed no distortion from the $\underline{m3m}$ symmetry required by the space group, and refinement in lower symmetry space groups did not lead to any significant departure from this geometry. The $NH_4{}^+$ ion has, therefore, twelve equidistant F atom neighbours at 2.99 Å (Figure 24). The unit

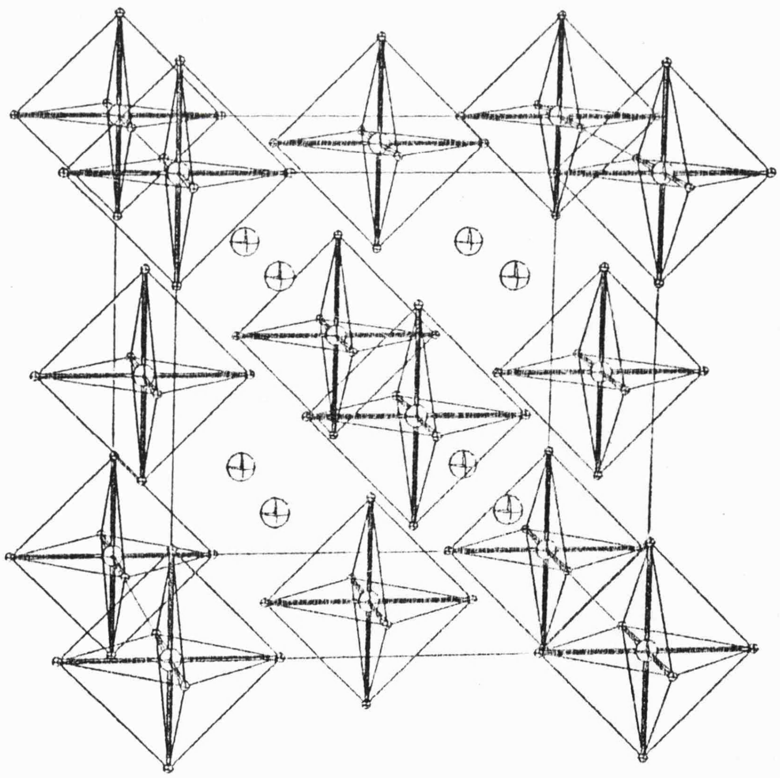

Figure 24

Unit cell packing of the $(NH_4)_2PtF_6$ structure.

cell size of ammonium hexafluoroplatinate is almost equal to those of the other $(NH_4)_2BF_6$ compounds (B = Ge, Si) that are known to have cubic modifications. The unit cell size is thus not related to the size of the $r_{B^{4+}}$ ion. However the unit cell size is determined, for any given BF_6^{2-} series, by the size of the alkali ion, A^+, involved. This is clearly illustrated from the cell parameters for the cubic structures in Table 28, with the unit cell volumes increasing with the ionic radius A^+, such that Cs > Rb > NH_4 > K. The ionic radii of the ammonium and rubidium ions are approximately equal, respectively 1.43 and 1.48 Å, and the comparability of the unit cell volumes for the known compounds suggest hydrogen bonding has little effect upon the ammonium structures. A comparison of the Pt-F bond distance is not possible with Rb_2PtF_6 as the z/c value is not quoted in the literature. However, the Pt-F bond length, found for $(NH_4)_2PtF_6$ 1.936 Å, is comparable with that found in the trigonal K_2PtF_6 structure (1.91 Å).

The potassium hexafluoroosmate (IV) structure (Figure 25) is as expected isostructural with the K_2ReF_6 structure,[143] although polymorphic forms may be discovered for both compounds. The OsF_6^{2-} ions are not perfectly regular, despite the Os-F distance (1.932 Å) being equal by space group symmetry. The ions are compressed along a three-fold axis, and the resulting angles between the fluorine atoms about the osmium are 86.8(2), 93.2(2) and 180°. The distortion is similar to that found in the ReF_6^{2-} ion of the K_2ReF_6 structure where the angles found were 86.2, 93.8 and 180°. The K^+ ions are not coplanar with the ABAB... layers of F atoms and the 12 F neighbours of each K^+ are in a 3 + 6 + 3 arrangement with K-F distances of 2.798(5), 2.929(5) and 2.987(5) Å. The distortion of the OsF_6^{2-} ion, is also similar to that found in the OsF_6^- ion of the $KOsF_6$ structure,[122] but in this compound

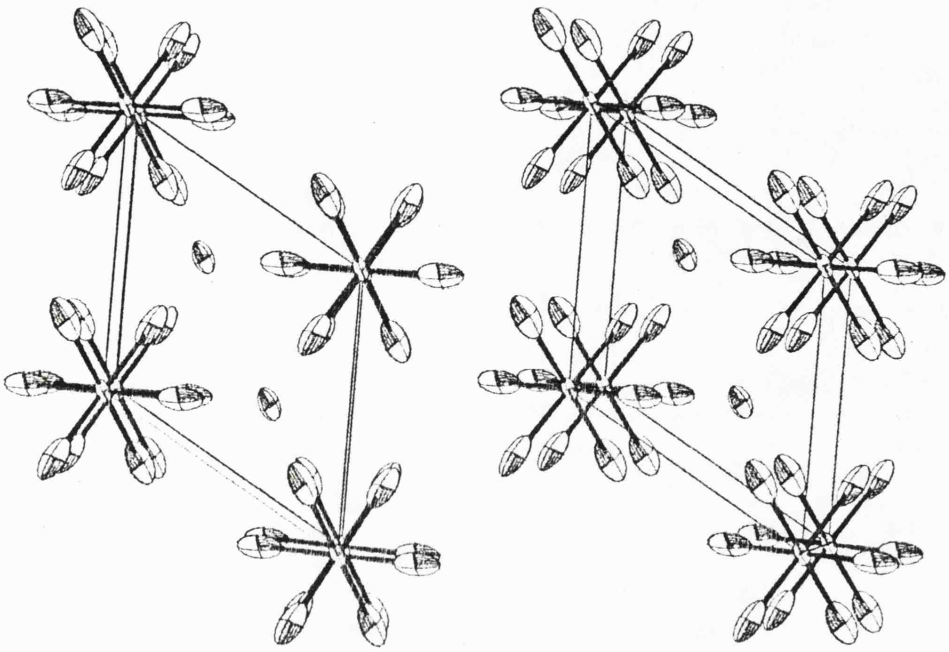

Figure 25

Stereoscopic view of the unit cell contents of K_2OsF_6.

the K^+ ion has a 6 + 6 arrangement of nearest F atom neighbours. The average K^+ to F contact distance is shorter, 2.911 Å in the K_2OsF_6, compared with 3.005 Å in $KOsF_6$, whilst the Os-F bond length is greater, respectively 1.94 and 1.82 Å. This suggests a contribution to the K_2OsF_6 structure from a covalent bonding model, although the increasing Os-F bond distance may be due entirely to the larger radius of Os(IV) than that of Os(V).

CHAPTER 9

The Crystal Structure of $NF_4.SbF_6$

9.1 Introduction

Recent interest has developed in compounds containing the tetrafluoronitrogen(V) cation, NF_4^+, due to their potential as oxidisers for solid propellant gas generators. The applications of solid propellant gas generators in space vehicle fuel systems and HF-DF chemical lasers, required the development of new materials for gas generator systems with radically new properties. The new materials were required, for safety in rocket propulsion, to yield combustion products which are oxidiser compatible, to minimise the risk of accidents. Materials were also required that would act as a fluorine atom gas generator for continuous wave HF-DF chemical laser. Pilipovich[185] sought to solve these problems by the use of a fluorocarbon as the binder and primary fuel source, and an oxidiser, where the oxidising ability was contained principally in the cation. Salts derived from Lewis acids and NO_2F were found to be useful as oxidisers, however it is preferable to employ the lower molecular weight Lewis acids in order to assure volatility of the combustion products and the most satisfactory oxidiser was found to be $NF_4^+BF_4^-$.

The synthesis and characterisation of the tetrafluoronitrogen(V) compounds, and the subsequent applications that have been developed are a recent occurrence. Prior to 1965 theoretical calculations[186,187] indicated that compounds containing the NF_4^+ cation should be thermodynamically unstable and unlikely to produce stable crystalline solids. However, in 1966 compounds containing the NF_4^+ cation were simultaneously reported by Christe *et al.*[188,189] and Tolberg *et al.*[190,191] The non-existence of a stable NF_5 parent molecule was overcome by reacting NF_3 and F_2 with a strong Lewis acid in the presence of a suitable activation energy source. Christe *et al.* used a low-temperature glow discharge method for the synthesis of NF_4AsF_6. Tolberg et al. used high pressure and thermal activation to prepare NF_4SbF_6 and NF_4AsF_6. Various synthetic methods have since been established. The compound NF_4BF_4 was first prepared by the low-temperature glow discharge method,[192,193] but may also be synthesised by using γ-irradiation at low-temperature.[194] The synthesis of NF_4BF_4, NF_4AsF_6 and $NF_4SbF_6.nSbF_5$ using u.v. photolysis was originally reported as giving very low yields,[195] however, the method has been developed[196] and at temperatures approaching -196°C, results in a simple and high-yield preparation which may also be used for the compounds NF_4PF_6 and NF_4GeF_5. A further method involves displacement reactions[196-198] from the NF_4^+ salts, particularly NF_4BF_4 and NF_4SbF_6, which may be most easily prepared in a pure state.

The properties of the $NF_4^+MF_6^-$ compounds have been extensively studied by Christe and co-workers. The X-ray powder patterns of all the NF_4^+ compounds that have been recorded have been indexed in the tetragonal system. From consideration of the unit cell volumes the compounds NF_4MF_6 (M = P, As, Sb and Bi), have been described as having two molecules in the unit cell, and on the lack of characteristic absences tentatively placed in the space group $P4/m$.[189,196,198] It is suggested that the structures are similar to that of $PCl_4^+PCl_6^-$,[199] where each ion (PCl_4^+ or PCl_6^+) has eight neighbouring ions of opposite charge. The average volume per fluorine atom, based on the X-ray powder data, gives a very low value for the $NF_4^+PF_6^-$ salt (16.23 $\mathring{A}^3$). The value is dependent only on unit cell volume and, therefore, increases in the order $PF_6^- < AsF_6^- < SbF_6^- < BiF_6^-$. The ionic nature of the adducts is confirmed by the vibrational spectra of the compounds,[196,198] where the bands attributable to the M-F bonds are as expected in the

MF_6^- anions[61,66,67] rather than the MF_5 molecule.[200] Similarly, the four fundamentals expected for the tetrahedral NF_4^+ cation are established.[194,201,202]

In view of the interest in the NF_4^+ salts and the applications under development, a full crystal structure study of chosen compounds is important. A study of the $NF_4^+BF_4^-$ structure is being undertaken by Professor Bau[203] using crystals supplied by K. Christe and co-workers. However, difficulty is being found in distinguishing the tetrahedral ions and a single crystal study of an $NF_4^+MF_6^-$ compound may help to fix the NF_4^+ ion in the structure. Crystals of $NF_4^+AsF_6^-$ and $NF_4^+SbF_6^-$ supplied by K. Christe were investigated, however, the $NF_4^+AsF_6^-$ crystals were of poor quality and gave diffraction patterns which showed they were powders.

9.2 Single crystal X-ray investigation

Crystals of $NF_4.SbF_6$ were supplied by K. Christe sealed in quartz capillaries. Samples of crystals grown from both HF and BrF_5 solutions were investigated. Those from HF gave powder diffraction patterns comparable with the NF_4AsF_6 samples which were also investigated. The crystals from BrF_5 solution all had a slight orange colouration, indicating the presence of trace quantities of bromine, but gave better diffraction patterns. The crystals were generally large for X-ray single crystal study, and the crystal chosen for the investigation was brick-shaped with the approximate dimensions, 0.64 mm × 0.50 mm × 0.26 mm. The crystal was mounted about a {110} axis of the tetragonal cell. The preliminary cell dimensions were obtained from Weissenberg photographs, taken using Cu-$\underline{K}\alpha$ (Ni filtered) radiation and precession photographs using Mo-$\underline{K}\alpha$ (Zr filtered) radiation. The final values for the unit cell parameters were determined from the optimised counter angles for zero and upper layer reflections on a Stoe Weissenberg diffractometer. Although the crystal used for the structure study was the one which gave the simplest diffraction pattern, the reflections at low 2θ values were very broad, up to 10° in ω, and this was attributed to disorder. Problems later encountered in the solution of the structure confirmed that the structure was partially disordered at room temperature. In an attempt to obtain an ordered structure, data was recollected at low temperature by Dr. N. W. Alcock using the four-circle diffractometer, at the University of Warwick. However, the compound was found to exhibit a phase transition between the two temperatures of data collection, with a doubled c-axis at the low temperature (-120°C), and the data was not, therefore, expected to allow elucidation of the room temperature structure. In fact the Patterson map obtained from the low temperature data set (Table 37) appeared representative of a still further disordered structure, and has not been conclusively solved.

9.3 (a) Crystal Data for tetrafluoronitrogen(V) hexafluoroantimonate(V)

$F_{10}NSb$; $\underline{M}$ = 325.74

Tetragonal $\underline{a}$ = 7.956(5) Å ; $\underline{c}$ = 5.840(4) Å

$\underline{U}$ = 369.63 Å^3 ; $D_{\underline{c}}$ = 2.928 g cm^{-3} ; Z = 2

$\underline{F}$(000) = 296.0 ; Mo-$\underline{K}\alpha$ radiation ; λ = 0.71069 Å

μ(Mo-$\underline{K}\alpha$) = 35.77 cm^{-1}

Space group $\underline{P}4/\underline{nmm}$ (D_{4h}^7 № 129). Neutral atomic scattering factors were used with anomalous dispersion corrections.

9.3 (b) Crystal Data - low temperature form

Tetragonal $\underline{a}$ = 7.979(4) Å ; $\underline{c}$ = 11.428(4) Å

$\underline{U}$ = 727.56 Å^3 ; $\underline{D_c}$ = 2.975 g cm^{-3} ; Z = 4

Space group: not resolved, $\underline{P4_2/n}$ appeared to be most applicable.

TABLE 37

Patterson map of the low temperature data set

height	x/a	y/b	z/c
999	.000	.000	.000
969	.500	.500	.500
445	.500	.500	.061
188	.061	.069	.500
79	.079	.086	.933
69	.440	-.002	.285

9.4 (a) Collection of the Room Temperature Intensity Data

The crystal was mounted about the {110} axis of the tetragonal cell and data were collected for layers 0kl to 8kl of the larger cell (a = 11.251 Å, c = 5.840 Å), using the Stoe Stadi-2 diffractometer in the quadrants h, ±k, ±l for all layers. The data were collected using an ω-scan technique with 2θ constant at the calculated value for each reflection. The intensities of reflections with 0.171 ⩽ Sinθ/λ ⩽ 1.166 Å^{-1} were collected, and 1177 reflections with I/σI ⩾ 3 were obtained. As observed from Weissenberg photographs (section 9.2), low 2θ angle reflections are asymmetric and broad (ω ⩽ 11°), and high background counts resulted on one side of several high intensity peaks. Due to the asymmetry of the peaks, the high background values are on opposite sides of the maxima, calculated from cell dimensions, for the quadrants ±k, and an ω-scan range of 15° would be required to collect the broadest peaks. The affected reflections were, therefore, collected with high background and the worst examples omitted after the early stages of refinement. Check reflections were monitored during the data collection of each layer and no deterioration of the crystal was indicated. Lorentz, polarisation and absorption corrections were made to the data set.

9.4 (b) Collection of the Low-Temperature Intensity Data

The data were collected at -120°C by Dr. N. W. Alcock using the Syntex $P2_1$ four-circle diffractometer at Warwick University. For a four-circle instrument, the crystal is mounted in arbitrary orientation and the control computer requires only the accurate location and indices of a few reflections, in this case 11, in order to collect a data set. The reflections are located photographically, and at this stage it was observed that weak reflections required a doubling of the c-axis. The intensities of reflections in the h, k, 1 quadrant were recorded for layers 0kl to 9kl, in the range $0 \leqslant 2\theta \leqslant 50°$, and a total of 767 reflections were obtained. Lorentz, polarisation and absorption corrections were applied to the data set.

9.5 Solution of the room-temperature structure

The program system SHELX was used. A Patterson summation was used to locate the antimony atom. Antimony was found to be on $\frac{1}{4}$, $\frac{1}{4}$, Z and, therefore, the refinement was undertaken in the space group $\underline{P}4/\underline{nmm}$. Three cycles of least-squares refinement gave an R factor of 0.19 and allowed sufficient phasing for the location of the nitrogen atom and the fluorine atoms about the nitrogen on respectively positions 2b ($\frac{3}{4},\frac{1}{4},\frac{1}{2}$) and 8i ($\frac{3}{4}$,x,x) of the space group. However, several possible sites for the fluorine atoms about the antimony were indicated with a maximum peak height of 2 electrons. From the bond distances the most likely set of F atoms was chosen. Further cycles of refinement with all atoms included and isotropic temperature factors gave an R factor of 0.108, but the two axial ($\frac{1}{4},\frac{1}{4}$,z) F atoms were moved to position approximately 1 Å from Sb and the temperature factors of all the F atoms about Sb were high, ($U_{11} > 0.25$). Allowing all atoms to refine anisotropically further reduced R to 0.083 without improving the temperature factors of the F atoms about Sb. The refinement was continued without symmetry operations, except for the centre of symmetry, thus requiring all the atoms of one molecule to be given individual coordinates. The environment of F atoms about Sb was made disordered, by using all Fourier peaks between 1.74 and 1.90 Å from the Sb atom as partial F atoms, refining site occupation factors. Three cycles of least-squares with 18 F atoms refining isotropically about the Sb atom and the remaining atoms with anisotropic temperature factors, gave an R factor of 0.088. Six of the F atoms were shifted to distances greater than 2.0 Å, and were thus rejected for further cycles. However, with further cycles of refinement several more partial fluorine atoms were moved to positions >2.0 Å from Sb, and new possible sites appeared in the Fourier difference map. Although the residual peaks in the Fourier difference map were $\leqslant 1.2$ electrons, the temperature factors of the refined atoms were not significantly lower than for those chosen in the ordered structure refinement of the space group P4/nmm. Accordingly, the ordered structure was chosen as most appropriate, although representing an incomplete solution to the structure. Final cycles of refinement used only the variables of atomic coordinates and thermal parameters of the Sb, N and F atoms of the NF_4 group. The reported atomic positional parameters for the F atoms about Sb are those which were dominant in the Fourier difference map and are included as the most likely fluorine positions in an apparently disordered environment. The final cycles of least-squares refinement employed a weighting parameter, g(.001) [$\omega \alpha\ 1/\sigma^2(F) + g\ F^2$]. An analysis of the weighting scheme over $|F_o|$ and $\sin\theta/\lambda$ was satisfactory. The final atomic positional parameters are given in Table 38, the thermal parameters are in Table 39, and the interatomic distances are in Table 40. The observed and calculated structure factors are found in Appendix 9.

The final R factors refer to the space group $\underline{P}4/\underline{mmm}$ refinement, with parameters refined only for the antimony, nitrogen and four fluorines of the NF_4 group.

Final residual indices for 240 unique reflections:-

$$R = \sum(|F_o| - |F_c|)/\sum|F_o| = 0.1073$$

$$R_w = [\sum\omega(|F_o| - |F_c|)^2/\sum\omega|F_o|^2]^{\frac{1}{2}} = 0.0836$$

TABLE 38

Final atomic positional parameters of the $NF_4.SbF_6$ room temperature structure, with estimated standard deviations in parentheses where refined.

	x/a	y/b	z/c	site occupancy
Sb	0.25	0.25	0.0997(4)	0.25
N	0.75	0.25	0.500	0.25
F1	0.75	0.3772(36)	0.3747(30)	1.00

Unrefined fluorine atoms about Sb, taken from a difference Fourier map.

	x/a	y/b	z/c	site occupancy
F2	0.25	0.0206	0.0425	1.00
F3	0.25	0.25	0.8026	0.25
F4	0.25	0.25	0.4669	0.25

TABLE 39

Anisotropic thermal parameters, with estimated standard deviations in parentheses. The temperature factors are given in the form $\exp[-2\pi^2(hU_{11}a^2 + \ldots\ldots 2hkU_{12}ab)]$

	U_{11}	U_{22}	U_{33}	U_{23}
Sb	.061(1)	.061(1)	0.0663(14)	
N	.088(11)	.088(11)	.077(17)	
F1	.136(16)	.123(16)	.139(10)	.036(10)

TABLE 40

Interatomic distances (Å)

$N-F_1$	1.250(19)	N.....Sb	4.614
$Sb-F_2$	1.86	N.....Sb	5.302
$Sb-F_3$	1.73		
$Sb-F_4$	2.14		

9.6 Discussion of the $NF_4.SbF_6$ structure

The tetragonal structure, space group $\underline{P}4/\underline{nmm}$, was considered to best represent the room temperature structure of $NF_4.SbF_6$. However, the refinement represents an incomplete solution to the structure due to apparent disorder. The positional parameters of the antimony, nitrogen and four fluorine atoms bonded to the nitrogen refined satisfactorily, and the resultant N-F bond distance, 1.25 Å, is of the expected order. Even when refinement was attempted without symmetry operations, the fluorine atoms bonded to the nitrogen retained the expected tetrahedral symmetry, although the thermal parameters indicate considerable motion. In the case of the fluorine atoms about antimony, however, the positional parameters reported are those of the dominant peaks in the Fourier map (also consistent with the special positions of the space group), but appear to be representative of a disordered sphere of partial atoms.

The arrangement of the ions in the unit cell (Figures 26, 27) suggest the reason for the apparent distortion of the F atoms about Sb from an octahedral array. Considering the antimony and nitrogen atom positions only, it might be expected that the Sb atom would have a z/c coordinate of zero. However, the fluorines of the NF_4 cation, which is a well-defined tetrahedron, require the axial F(Sb) atoms to be shifted along the $\frac{1}{4}$, $\frac{1}{4}$, z axis to equalise the F(N)····F(Sb) interaction. The antimony atom is displaced along the $\frac{1}{4}$, $\frac{1}{4}$, z axis in the expected direction, though less than is required to give equal bond distances to the two reported F atoms (F3, 1.73 and F4, 2.14 Å). The four F atoms in the ab plane (F1) are still less displaced from $z = 0$. The result is that each Sb atom has four nearest N neighbours (4.61 Å) in the +c direction, and four more at 5.30 Å, in the -c direction.

Figure 26

Stereoscopic views of the unit cell of NF_4SbF_6

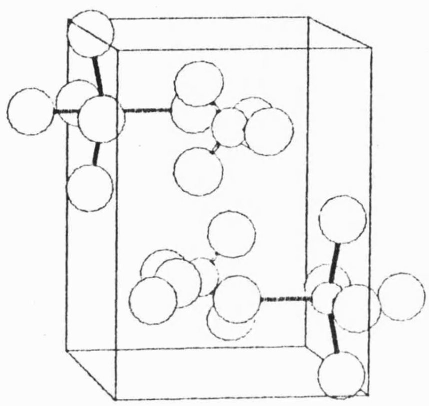

a) down the $\underline{a}$ axis

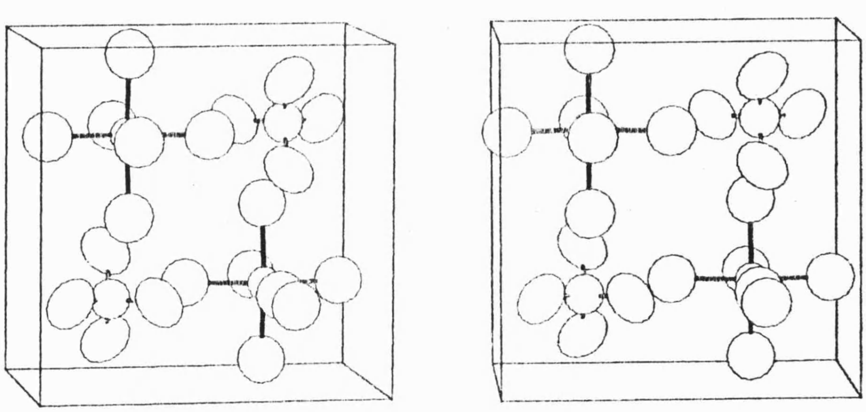

b) down the $\underline{c}$ axis

However, this does not explain the disorder of the F environment about the Sb atom. When two F atoms are positioned on the $\frac{1}{4}$, $\frac{1}{4}$, z four-fold axis, a close non-bond contact between the two atoms in adjacent cells is caused as a result of the short $\underline{c}$ cell parameter (5.840 Å). With the two atoms on the positions given in Table 38, the distance between atoms of adjacent cells is obviously too short, 1.97 Å (cf. Van der Waal's radii, F = 1.35 Å). However, the Sb-F bond lengths could acceptably be <1.80 Å, producing a contact distance of 0.46 Å less than the sum of Van der Waal's radii. The problem is comparable with that encountered in the $PCl_4^+PCl_6^-$ structure,[199] where the chlorine atoms on the four-fold axis are located with a contact distance 0.45 Å less than the sum of Van der Waal's radii. The disorder apparent in the arrangement of the F atoms about Sb may possibly result from problems of locating the F atoms about a four-fold axis, or the structure may exhibit a phase change near room temperature, since the data collected at -100°C was of a separate phase.

CHAPTER 10

The Crystal Structures of $H_3O.SbF_6$ and $H_3O.TaF_6$

10.1 Introduction

The concept of a hydrogen ion occurring as a hydrated species in aqueous solution is some 70 years old,[204,205] however, it is extremely difficult to characterise the various hydrated proton complexes in solution. Recent crystal structure determinations, including neutron diffraction studies, of the hydrates of several strong acids have been reviewed in detail by Lundgren and Olovsson[206] with particular emphasis on the local bonding within the hydrated proton species. A clearly unsymmetric monohydrated proton, $H^+\cdots OH_2$, has not been identified and neutron diffraction studies of two monohydrates of strong acids[207,208] indicate equivalence of the three protons. The complex may therefore be regarded as a distinct chemical entity, H_3O^+, termed an oxonium ion. The $H_5O_2{}^+$ ion may be considered, according to bond lengths and symmetry, as aquaoxonium ion, $H_3O^+.H_2O$, or diaqua-hydrogen ion, $[H_2O\cdots H\cdots OH_2]^+$. The small size of the proton does not permit symmetric ions of the higher hydrates, thus, ions with $H \geqslant 7$ may be regarded as hydrates, $H_3O^+.nH_2O$ or $H_5O_2{}^+.nH_2O$. Williams[209] has recently reviewed the vibrational spectroscopic data for the hydrated proton complexes. In general spectroscopic techniques are widely used to characterise H-bonds, however, because of the complexity of the solid state spectra produced by these species it is difficult to differentiate between them. The frequencies of the ν_1-ν_4 modes for the species H^+nH_2O ($n = 1, 2, 3, 4$) overlap. Similarly, the assignment of the ν_1, symmetric stretch, and ν_3, asymmetric stretch bands is questionable. Early studies of the oxonium compounds indicated clearly defined frequency regions for the ν_1 and ν_3 modes of H_3O^+. However, the most recent i.r. studies of the oxonium ion[210,211] indicate that the frequencies are a function of donor-acceptor distances in the hydrogen bonds formed. The range of spectral frequencies for the ν_1 and ν_3 bands, respectively 3380-3150 and 3800-2400 cm^{-1}, introduces the possibility of frequency reversal. Though the ν_2 and ν_4 bands of the hydrated proton complexes may be unequivocally assigned, these bands also are not definitive of the separate hydrates.

The first reported isolation and characterisation of an $(H_xO_y)^+$ salt with a metal hexafluoro anion was by Bonnet et al.[212] for the antimony salt, $H_5O_2^+.SbF_6^-$. From differential thermal analysis studies of solutions of SbF_5 in H_2O and HF, the thermal conditions required to obtain stable crystalline phases of the hydrates $SbF_5.2H_2O$, $4SbF_5.5H_2O$, $SbF_5.H_2O$, $3SbF_5.2H_2O$ and the compound $SbF_5.HF.2H_2O$ were determined. The vibrational spectra of $SbF_5.2H_2O$ and $SbF_5.HF.2H_2O$ were found to be consistent with the ionic formulations $H_3O^+.SbF_5OH^-$ and $H_5O_2.SbF_6^-$, the bands associated with the Sb-F bond occurring at the lower frequencies (663 cm^{-1}) established for SbF_6^-,[43,61,66] rather than that expected for SbF_5.[200] The hydroxonium salt $H_5O_2^+SbF_6^-$ has also been isolated as a side product from the reaction system UF_4O-HF-SbF_5,[213] when reactions were performed in thin wall F.E.P. tubing. The H_2O involved in the reactions was presumed to result from inadequate drying of the HF or diffusion through the reactor walls. The composition $H_5O_2^+SbF_6^-$ was indicated by Sb and F analyses, and the i.r. spectrum showed peaks at the expected frequency for $H_5O_2^+$ or H_3O^+. The X-ray powder pattern was found to be closely related to $KSbF_6$, which was first reported as cubic[124] ($a = 10.15$ Å, $U = 1039.5$ Å^3), and more recently been determined as tetragonal[75] ($a = 5.16$ Å, $c = 10.67$ Å, $U = 268.12$ Å^3).

The oxonium compounds $H_3O^+.SbF_6^-$ and $H_3O^+.AsF_6^-$ have been isolated as white stable crystalline solids by Christie and co-workers from the H_2O-HF-MF_5 system,[214] following the discovery of the antimony salt as a product of the controlled hydrolysis of $BrF_4^+Sb_2F_{11}^-$ in HF. Differential scanning calorimetry measurements show that both are thermally very stable with decomposition not occurring until 357 and 193° for the Sb and As compounds respectively. The thermal stability is very much greater than for previously reported $H_3O^+X^-$ salts ($X = CF_3SO_3$, ClO_4, $CH_3C_6H_4SO_3$). From X-ray powder diffraction patterns, the $H_3O^+ AsF_6^-$ salt was found to be cubic ($a = 8.015$ Å) with $Z = 4$. The $H_3O^+ SbF_6^-$ salt was indexed as tetragonal ($a = 11.48$, $c = 8.78$) with $Z = 8$, and was described in terms of a distorted cubic $KSbF_6$ structure. The compound $H_3O^+UF_6^-$ has been prepared[215] but is thermally less stable than the Sb and As salts, decomposing at about 68°. Three bands assigned to the ν_5(U-F) bond frequency were considered to be the result of distortion of the anion. X-ray powder diffraction patterns were indexed assuming a cubic unit cell, $a = 5.223$ Å.

More recently, Selig et al.[216] have studied the hydrolysis reactions of MF_6 (M = Os, Ir, Pt, Ru and Rh) in hydrogen fluoride, with the intention of preparing the uncharacterised and largely unknown oxide-fluorides of Ir, Pt, Ru and Rh. The OsF_6 was used principally as a standard, being known to readily yield OsF_4O. However, the hydrolysis of IrF_6, PtF_6 and RuF_6 were found to yield the oxonium salts $H_3O^+ MF_6^-$, and in the case of platinum with an excess of water, $(H_3O)_2^+PtF_6^{2-}$. The hydrolysis of RhF_6 was inconclusive, but was considered to have produced an unstable oxonium salt. The X-ray powder patterns of the three compounds (Ir, Pt and Ru) are isostructural, with only small differences in the unit cell dimensions, and have been indexed as rhombohedral.

All the oxonium salts of hexafluorometallates described, were first observed either as impurities or unexpected products of reactions. Similarly the oxonium salts reported here, of hexafluoroantimonate(V) and tantalate(V), were isolated as minor impurities resulting from side reactions. The hexafluoroantimonate(V) salt was briefly mentioned in chapter 4, occurring as inconsistent block-shaped crystals in the preparation of $MoF_4O.SbF_5$, and has subsequently been observed as a minor product in the reaction systems UF_4O and WF_4O-HF-SbF_5. Crystals of the hexafluorotantalate(V) compound were formed during the attempted recrystallisation of $CsTaF_6$ from SO_2.

In the presence of heavy anions, determination of the cations to be H_3O^+ or $H_5O_2^+$ requires precise analysis. The H_3O^+ SbF_6^- and $H_5O_2^+$ SbF_6^- salts have been described respectively as tetragonal[214] and cubic,[213] however the unit cell dimensions measured for the two salts give calculated volumes / fluorine and oxygen atoms of 20.7 Å^3 and 15.8 Å^3, and it seems more likely that the compound Christie et al. studied was the $H_5O_2^+$ salt and that noted by Bougon and co-workers was the H_3O^+ salt. The resulting calculated volumes of the fluorine and oxygen atoms then becomes 18.1 Å^3 in each case. In view of the uncertainty concerning the composition and structure of these compounds, the isolation of single crystals of antimonate and tantalate salts presented the opportunity of clarifying this type of compound. Although these structure determinations proved not to be entirely satisfactory, they are believed to be consistent with the formulation $(H_3O)^+MF_6^-$, M = Sb or Ta.

10.2 Characterisation of Oxonium hexafluoroantimonate(V)

Single crystals of oxonium hexafluoroantimonate(V) were isolated from the reaction between MoF_4O and SbF_5 in thin walled F.E.P. tubing. The rectangular block-shaped crystals of $H_3O^+.SbF_6^-$ were inconsistent with the major product ($\sim$1:100, $H_3O^+.SbF_6^-$: $MoF_4O.SbF_5$) and could, thus, be separated in a crystal sorting apparatus (Figure 2). Similar side-products have been observed in the reaction systems, MF_4O-HF-SbF_5 (where M = W or U). Though the formation of hydrated proton compounds in the latter systems may be explained by incomplete drying of the HF, in the reaction between MoF_4O and SbF_5, the H_2O appears to result from diffusion through thin-walled F.E.P. reactors.

Insufficient crystals of the H_3O^+ SbF_6^- compound were obtained from the $MoF_4O.SbF_5$ preparation to allow the i.r. spectrum to be taken, however, the i.r. spectrum of crystals from the UF_4O-HF-SbF_5 system, which gave the same unit cell parameters, was taken in the range 4000-400 cm^{-1}, (Table 41). The hydrated proton nature of the cation is confirmed by the bands at 3600 and 3520 cm^{-1} which are in the expected region for the H^+nH_2O ν_1 and ν_3 bands, and the peaks at 1606 and 905 cm^{-1}, respectively ν_4 and ν_2 of H^+nH_2O. The ν_1, Sb-F band, is also present in the i.r. spectrum at the expected frequency for SbF_6^-, 661 cm^{-1}. The Raman spectrum of the single crystal used for data collection was also obtained (Table 41), and clearly characterised the SbF_6^- anion, peaks occurring at 666 (ν_1), 590 (ν_2) and 283 (ν_4) cm^{-1}. The spectra are in excellent agreement with those obtained by Christie et al. for the compound described as $H_3O^+.SbF_6^-$, the only discrepancy appearing in the lower frequency of the ν_1 and ν_3 hydrated proton bands of the spectrum obtained by Christie and co-workers.

TABLE 41

$H_3O^+ SbF_6^-$ Present work i.r.	$H_3O^+ SbF_6^-$ Present work Raman	$H_3O^+ SbF_6^-$ Christie *et al.*[214] i.r.	$H_3O^+ SbF_6^-$ Christie *et al.*[214] Raman	H_3O^+ Williams[209]	Assignments (H^+nH_2O)	Assignments $(SbF_6)^-$
3600 (w)		3330 (vs)		3500-	ν_1, ν_3	
3520 (m)		3150 (vs)		2500		
1606 (w)		1615 (s)		1665	ν_4	
930 (w)						
905 (m)		900 (s)		1125	ν_2	
661 (vs)	666 (vs)	670 (vs)	663			ν_1
	590 (w)	588 (sh)	590			ν_2
			490			
			450			
			287			ν_4
	283 (m)		280			ν_5
			265			

Vibrational Spectra of $H_3O^+ SbF_6^-$ (cm^{-1})

10.3 Single Crystal X-ray Investigation of $H_3O^+.SbF_6^-$

The crystal used for the investigation was sealed in a preseasoned Pyrex capillary, and had the approximate dimensions 0.46 mm × 0.35 mm × 0.22 mm. The crystal was mounted about the 110 axis of the cubic cell. Preliminary cell dimensions were obtained from Weissenberg photographs, taken using Cu-K_α (Ni filtered) radiation and precession photographs using Mo-K_α (Zr filtered) radiation. The final value for the unit cell parameter was determined from the optimised counter angles for zero layer reflections on a Stoe Weissenberg diffractometer.

10.4 Crystal Data for $H_3O^+.SbF_6^-$

F_6H_3O Sb ; $\underline{M}$ = 254.75

Cubic $\underline{a}$ = 10.130(8) Å

$\underline{U}$ = 1039.51 Å^3; $\underline{D_c}$ = 3.255 g cm^{-3} ; Z = 8

$\underline{F}(000)$ = 927.98 ; Mo-K_α radiation ; λ = 0.71069 Å

μ(Mo-K_α) = 49.69 cm^{-1}

Space group Ia3 (T_h^7 № 206). Neutral scattering factors were used, with anomalous dispersion coefficients.

10.5 Data Collection

The crystal was mounted about the 110 axis of the cubic cell, and data were collected for layers 0kl to 6kl of the aligned pseudo-tetragonal cell, using the Stoe Stadi-2 diffractometer, in the four quadrants h ±k ±l. The data were collected using an ω-scan technique, with 2θ at the calculated value for each reflection. The intensities of reflections with $0.171 \leqslant \mathrm{Sin}\theta/\lambda \leqslant 1.22$ Å^{-1} were collected, and a total of 719 reflections obtained with $I/\sigma I \geqslant 3$. Check reflections were monitored during the data collection of each layer and no deterioration of the crystal was indicated. Lorentz and polarisation corrections were made to the data set.

10.6 Solution of the $H_3O^+.SbF_6^-$ structure

The program system SHELX was used. Three cycles of least squares refinement with antimony on the Wyckoff position, 8a $(\frac{1}{2},\frac{1}{2},\frac{1}{2})$ of the space group $\underline{\underline{I}}\underline{a}3$ gave an R factor of 0.27. The Fourier difference map located a 9 electron peak, assumed to be oxygen, on the 8b position $(\frac{1}{4},\frac{1}{4},\frac{1}{4})$ with two sets of possible fluorine octahedra each at 1.90 Å from Sb. Three cycles of refinement with the oxygen atom included reduced the R factor to 0.22. The inclusion of either of the peaks on the general positions about Sb, as F atoms, with all atoms refining isotropically resulted in a reduced R factor of 0.13, however, the refinement cycles moved the F atoms to >2.0 Å from Sb. The inclusion of fluorine atoms also resulted in a more complex difference Fourier map, with several peaks $\leqslant 3$ electrons appearing. The problem was treated in the same manner as the other apparently disordered structures ($CsNbF_6$ chapter 6, and NF_4SbF_6 chapter 9) encountered in this study. The alternate fluorine atom positions indicated were refined as disordered, initially refining the site occupation factors and then the temperature factors. The resultant R factor of 0.12 was not significantly less than with an ordered structure; one of the fluorine atoms refined to a position 2.2 Å from Sb, and further possible fluorine sites appeared in the Fourier map. Refinement of various models with either ordered fluorine atoms or disordered atoms constrained to be 1.86(3) Å from antimony, did not improve the R factor or the residual Fourier map. For final cycles of least-squares refinement, the atomic positional and thermal parameters of that fluorine atom which remained at the expected distance from antimony in the disordered model, were refined. As in the case of NF_4SbF_6, this represents an incomplete solution, as the fluorine atom parameters reported appear representative of disorder. This is reflected in the structure factor table (Appendix 10), where agreement between $|F_o|$ and $|F_c|$ is good for even, even, even reflections with dominant contribution by the antimony and oxygen atoms but poor agreement is obtained for odd, odd, even reflections which are dependent only upon the fluorine (and hydrogen) atom parameters. The final atomic positional and thermal parameters are in Table 42. The observed and calculated structure factors are in appendix 10.

Final residual indices for 155 unique reflections:-

$$R = \sum(|F_o| - |F_c|)/\sum|F_o| = 0.119$$

TABLE 42

Final atomic positional and thermal parameters for $H_3O.SbF_6$, with estimated standard deviations in parentheses.

	x/a	y/b	z/c	U_{11}	U_{22}	U_{33}
Sb	0.5	0.5	0.5	0.0205(18)		
Ox	0.25	0.25	0.25	0.043(17)		
F	0.4334(33)	0.6444(34)	0.6021(22)	0.059(20)	0.158(35)	.003(12)
H	not located					

Sb——F	1.891(19) Å	F—Sb—F	180.0 °
Sb.....Ox	4.386	F—Sb—F	89.5(1.0)
Ox.....F	2.63	F—Sb—F	90.5(1.0)
F .....F	2.68		
F .....F	2.71		

10.7 Characterisation of oxonium hexafluorotantalate(V)

The crystal of oxonium hexafluorotantalate(V) used for the diffraction study also occurred as a trace impurity, in this case from the recrystallisation of caesium hexafluorotantalate(V). Data was collected on the assumption that the crystal was $CsTaF_6$. Preliminary determination of the unit cell parameters suggested a new phase of $CsTaF_6$, as found for $CsNbF_6$ (chapter 6), however, during the subsequent structure refinement the temperature factor of the atom designated as Cs gave an impossibly high value. This suggested that the crystal under investigation must have a cation of lower atomic number at this site.

A detailed inspection of the bulk material from the recrystallisation by X-ray powder diffraction and mass spectroscopy showed the material was predominately $CsTaF_6$ and, accordingly, an attempt was made to characterise the single crystal used for data collection. The Raman spectrum of the single crystal (Table 43), is more complex than that obtained for $Cs^+TaF_6^-$ by Keller et al.,[127] in which only the ν_1 (692 cm^{-1}), ν_2 (580) and ν_5 (270) bands expected for O_h symmetry were observed. The spectrum can be assigned in terms of a T_h^7 symmetry TaF_6^- ion, where the ν_1 (714 cm^{-1}) and ν_2 (618) bands are shifted to higher frequency than in $CsTaF_6$, as expected for a smaller cation, and the three bands in the ν_5 region (295, 291 and 273 cm^{-1}) can be attributed to factor group splitting of the ν_5 band expected in T_h^7 symmetry. The remaining bands have been tentatively assigned to rotatory modes, ν_R for H_3O^+ (704 and 669 cm^{-1}) and ν_R for TaF_6^- (225 cm^{-1}).

A further indication of the crystal composition was provided by the determination of the density. If the crystal was $CsTaF_6$ the calculated

TABLE 43

The Raman spectrum of $H_3O^+\ TaF_6^-$

$H_3O^+\ TaF_6^-$ Raman			$Cs^+TaF_6^-$ Raman	
714 (100)	ν_1	(TaF_6)		
704 (40)	νR	$(H_3O)^+$		
			692 (100)	ν_1
669 (38)	νR	$(H_3O)^+$		
618 (10)	ν_2	(TaF_6)		
			580 (10)	ν_2
295 (20)				
291 (40)	ν_5	(TaF_6)		
273 (38)				
			270 (7)	ν_5
225 (15)	νR	(TaF_6)		

density for a unit cell of 10.20 $\mathring{A}^3$ with Z = 8 would be 5.36 g cm^{-3}, however, if as was supposed the crystal is the hydroxonium salt, $H_3O^+\ TaF_6^-$, the density would be 3.00 g cm^{-3}. The crystal was measured in the Pyrex capillary used for data collection, using a vernier microscope eyepiece, routinely used for absorption correction measurements. The measured dimensions of the crystal (.0775 cm × .0667 cm × .0462 cm) gave a volume of .000238 cm^3. The capillary was then broken and the crystal placed on the pan of a zeroed Cahn Electrobalance (model G, range 1.0 ± .001 mg). Weighings at one minute intervals from the time of exposure to the atmosphere allowed extrapolation of the crystal weight (0.881 mg). The resulting calculated density 3.71 g

cm^{-3} is in good agreement with the expected density of the salt $H_3O^+ TaF_6^-$.

10.8 Crystal Data for $H_3O^+ TaF_6^-$

Preliminary cell dimensions were obtained from Weissenberg photographs, taken using Cu-K_α (Ni filtered) radiation, and the cell parameter, a (final value), was determined from the optimised counter angles for zero and upper layer reflections on a Stoe Weissenberg diffractometer. The crystal was mounted about the a axis of the cubic cell.

F_6H_3O Ta ; $M = 313.95$

Cubic $a = 10.225(6)$ Å

$U = 1069.0$ Å^3 ; $D_c = 3.901$ g cm^{-3} ; $Z = 8$

$F(000) = 1103.6$; Mo-K_α radiation ; $\lambda = 0.71069$ Å

μ(Mo-K_α) = 197.2 cm^{-1}

Space group $Ia3$ (T_h^7 № 206). Neutral scattering factors were used, with anomalous dispersion coefficients.

10.9 Data Collection

Data were collected from the layers 0kl to 6kl, using the Stoe Stadi-2 diffractometer, in the +h, +k, +l quadrant only. The intensities of reflections with $0.147 \leqslant \sin 2\theta/\lambda \leqslant 1.22$ Å^{-1} were collected, and a total of 218 reflections obtained with $I/\sigma I \geqslant 3$. The data were collected using an ω-scan technique, with 2θ constant at the calculated value for each reflection. Check reflections were monitored during the data collection of each layer and no deterioration of the crystal was indicated. Lorentz and polarisation corrections were made to the data set.

10.10 Solution of the $H_3O^+ TaF_6^-$ structure

The program system SHELX was used. The crystal was initially supposed to be a new phase of $CsTaF_6$, resulting from the recrystallisation of $CsTaF_6$ from SO_2. Three cycles of least-squares refinement with tantalum on the 8a position $(\frac{1}{2},\frac{1}{2},\frac{1}{2})$ and caesium on the 8b $(\frac{1}{4},\frac{1}{4},\frac{1}{4})$ position of the space group Ia3 resulted in an R factor of 0.19. However, the isotropic temperature factor of the atom designated as Cs gave an impossibly high value indicating a lighter atom on this site. The Raman spectrum and density measurements (section 10.7) together with the unit cell indicated the probability that the crystal was an aqua-hydrogen compound, and three cycles of least-squares refinement with oxygen replacing the caesium atom gave an R factor of 0.15 and an acceptable isotropic temperature factor for oxygen. As with the $H_3O.SbF_6$ structure, alternate fluorine sites were indicated in the residual Fourier map, however, in this case one of the positions for fluorine refined without either displacement of the atom away from tantalum or unacceptable thermal parameters. An R factor of 0.11 was obtained for the final cycles which employed a weighting parameter, g(.0001) $[\omega \alpha\ ^1/\sigma^2(F) + gF]$ and an analysis of the weighting scheme over $|F_o|$ and Sin θ/λ was satisfactory. The final Fourier difference map contained +3 and -2.5 electron peaks but these were not at tantalum-fluorine distances and agreement between the observed and calculated structure factors for the odd, odd, even reflections was generally good.

The final atomic positional and thermal parameters are in Table 44 and the observed and calculated structure factors are found in Appendix 11.

Final residual indices for 130 unique reflections:-

$$R = \sum(|F_o|-|F_c|)/\sum|F_o| = 0.109$$

$$R_w = [\omega(|F_o|-|F_c|)^2/\sum\omega|F_o|^2]^{\frac{1}{2}} = 0.102$$

TABLE 44

Final atomic positional and thermal parameters for $H_3O.TaF_6$, with estimated standard deviations in parentheses.

	x/a	y/b	z/c	U_{11}	U_{22}	U_{33}
Ta	0.5	0.5	0.5	0.0238(11)	-	-
Ox	0.25	0.25	0.25	0.046(16)	-	-
F	0.4355(35)	0.6475(26)	0.4053(24)	0.107(25)	0.019(11)	0.017(11)
H	not located					

Ta——F	1.910(15) Å	F—Ta—F	180.0 °
Ta.....Ox	4.43	F—Ta—F	92.7(1.0)
Ox.....F	2.69	F—Ta—F	87.3(1.0)
F .....F	2.64		
F .....F	2.76		

10.11 <u>Discussion of the $H_3O.MF_6$ structures</u>

The body-centred cubic structure, space group Ia3 was found to be appropriate for the structures of both $H_3O.SbF_6$ and $H_3O.TaF_6$. The final R factors for both structures are high, the small R factor for the tantalate resulting predominately from the greater overall contribution of tantalum than antimony. The high values for the R factor may be explained by the apparent disorder of the fluorine atoms, though as in the case of $NF_4.SbF_6$ the cause is not obvious, particularly for the $H_3O.TaF_6$ structure where no obvious alternate fluorine sites were indicated in the final difference Fourier map, and the thermal parameters of the fluorine atom included are not excessively high. For this structure a lower final R factor should be possible.

The unit cell packing of both compounds is essentially the same, and only one figure is used to describe both $H_3O.MF_6$ structures (Figure 27). In the $H_3O.SbF_6$ structure the eight nearest oxygen-antimony neighbours are at 4.39 Å and each oxygen atom has six nearest F atoms at 2.66 Å. In the $H_3O.TaF_6$ structure the eight nearest oxygen-tantalum distances are 4.43 Å and each oxygen atom has six nearest fluorine atoms at 2.69 Å. The angles between the fluorine atoms about Ta indicates a slight compression of the fluorine octahedron along a three-fold axis but in the antimonate structure the angles are within error limits of 90°.

Despite the unsatisfactory results of the structure refinement, the identity of the compounds as hydroxonium compounds, $H_3O.MF_6$ seems to

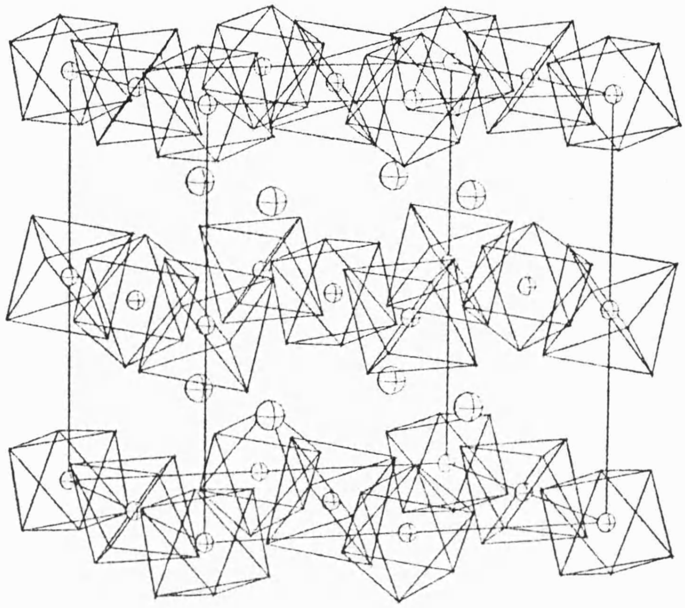

Figure 27

The $H_3O.MF_6$ (M = Sb or Ta) unit cell contents.

be unequivocally established. No other possible sites for oxygen atoms are indicated in the Fourier maps and the temperature factors of the oxygen atoms in both structures are of similar and expected values. This supports the conclusion reached in the introduction (section 10.1), based upon volume considerations that the compounds described by Christie et al. ($H_3O.SbF_6$) and Bougon and co-workers ($H_5O_2.SbF_6$) should, in fact, be reversed. This results in volumes per light atom of 18.1 $\mathring{A}^3$ in the case of each of the antimonate structures against the values of 15.8 $\mathring{A}^3$ ($H_3O.SbF_6$) and 20.7 $\mathring{A}^3$ ($H_5O_2.SbF_6$) proposed. The volumes per light atom found in this study are 18.5 $\mathring{A}^3$ and 19.1 $\mathring{A}^3$ for the antimony and tantalum compounds respectively.

A complete solution to these structures would best be obtained through neutron diffraction studies, which with the accurate location of hydrogen atoms, would not only provide the complete crystal structure but remove any doubt about the nature of the cation. However, the problem of obtaining samples of either $H_3O^+.MF_6^-$ or $H_5O_2^+.MF_6^-$ compounds in sufficiently large samples, for neutron diffraction without the other, or higher aqua-hydrogen compounds, as impurity probably requires a novel preparative method rather than precise reaction stoichiometry.

CHAPTER 11

The Preparation and Crystal Structure of WF_5N_3

11.1 Introduction

Several azido compounds derived from transition metal chlorides or oxide chlorides have been reported by Dehnicke and Strähle. The reactions, replacement and addition, were all performed with chlorine azide. The compounds VCl_4N_3,[217] CrO_2ClN_3, $MoCl_4(N_3)_2$,[218] $TiCl_3N_3$ and $VOCl_3N_3$[219] were isolated as unstable explosive solids, and characterised by i.r. spectroscopy. In each case the spectra showed absorption bands in regions expected for azido groups, 2180-2050 (ν_{as}, N_3), 1250-1225 (ν_s, N_3) and 700-660 cm^{-1} (δ, N_3), in addition to the bands associated with M-Cl or M=O. The monoazides $MoCl_5N_3$ and WCl_5N_3 were reported[218] as intermediates, which could not be isolated without the loss of N_2 and Cl_2 to give the chloronitride compounds MCl_3N. No azide derivatives of transition metal fluoro compounds have previously been reported.

Reactions in which one or more of the fluorine atoms of hexafluorotungsten(VI) may be replaced by chlorine,[220,221] alkoxy,[222] aroxy[222,223] or diethylamine[224,225] have been reported. Although various preparative routes to the compounds WF_5X are known, the reactions between WF_6 and the compounds Me_3SiX represent a general method. As a result of experiments to prepare novel transition metal fluoro compounds, or establish improved preparative routes for known compounds, by reactions of MF_6 (M = W, Mo, Re) with Me_3SiX, the first transition metal fluoro azide, WF_5N_3, has been isolated and characterised. Crystals of the compound, obtained from Genetron 113 solution, proved to be sufficiently stable to permit a single crystal X-ray study of the structure. In addition, evidence for the compounds MoF_5N_3 and $WF_{6-n}(N_3)_n$, ($n \geqslant 2$) has been obtained, however, the compounds are less stable than WF_5N_3 and have not been successfully isolated.

11.2 Preparation and Characterisation of WF_5N_3

CAUTION - This reaction is likely to EXPLODE

Azido pentafluoro tungsten(VI) was prepared by the reaction between trimethyl silyl azide and an excess of tungsten hexafluoride in Genetron 113 solvent. In a typical reaction 0.1362 g (1.184 mMol) of silyl azide was distilled in static vacuum, at -196°C, into a pre-seasoned Pyrex reaction vessel, (~10 cm^3 volume) fitted with a Rotaflo valve. Approximately 1 cm^3 of Genetron, pre-dried over P_2O_5 and stored over molecular sieve was then distilled into the reactor at -196°C, and the reactor allowed to warm to room temperature. This allowed the Genetron, collected at the top of the reactor, to wash the trimethylsilyl azide off the reactor walls. In reactions where this was not done, or the order of the addition of compounds was changed, a dark brown solid product resulted. This was presumed to result from reaction between small quantities of reagents on the walls of the vessel, which then initiated decomposition of the product in the diluant. An approximate 5 : 1 excess of tungsten hexafluoride, 1.805 g (6.06 mMol), was then added to the reactor which was allowed to warm slowly to room temperature. A yellow solid and solution resulted. The reactor was then warmed to 45°C for two hours to complete the reaction, by reflux to a solid CO_2 collar.

$$(CH_3)_3SiN_3 + WF_6\ (XS) \xrightarrow{\text{Genetron, } 45^\circ} WF_5N_3 + (CH_3)_3SiF$$

After cooling the reactor to room temperature, the $(CH_3)_3SiF$, excess of WF_6 and most of the solvent were removed in a static vacuum. If the product was dried under vacuum an explosion resulted, however, if the moist product was allowed to dry by evaporation in a dry-box it was found to be stable to grinding.

The azido pentafluoro tungsten(VI) was characterised by mass spectroscopy, infra-red and Raman spectroscopy and ^{19}F n.m.r. A sample was ground and sealed in preseasoned Pyrex capillaries, one such capillary was then heated in melting point apparatus and decomposition was found to occur at 63°C. The mass spectrum was, therefore, run with the probe at 58°C. The resultant spectrum surprisingly showed the parent ion $WF_5N_3^+$ and the fragmentation pattern shown in Table 45.

The vibrational spectra of the compound show absorption bands attributable to the azido-group. The infra-red at 2140 and 640 cm^{-1} and the Raman, obtained on the solution in Genetron, at 2157 cm^{-1}. The ^{19}F n.m.r. spectrum in Genetron shows the expected doublet and a poorly resolved quintet, respectively -144.8 and -136.5 ppm from CF_3Cl standard. The WF_6 (-163 ppm) and $(CH_3)_3SiF$ (+76.3 ppm) ^{19}F shifts are observed in the ^{19}F n.m.r. spectrum.

Reactions between WF_6 and an excess of trimethyl-silyl azide were performed in Genetron in attempts to obtain the azides $WF_{6-n}(N_3)_n$ ($n \geq 2$). All such reactions resulted in orange-red solutions which detonated at, or below, 25°C. Reactions between an excess of MoF_6 and $(CH_3)_3SiN_3$ yielded a yellow solid, assumed to be MoF_5N_3, which decomposed or detonated at approximately -10°C. Prior to the definitive mass spectroscopic and single crystal characterisations of WF_5N_3 an attempt was made to establish the identity of the compound from its reaction with CH_3CN, with the expected product being $WF_5N_4C.CH_3$, a nitrogen-carbon ring compound:-

TABLE 45

The mass spectrum fragmentation pattern of WF_5N_3, with approximate intensities in parentheses.

$$
\begin{tikzcd}
WF_5N_3^{+}\,(13) \arrow[r, "-F"] \arrow[dd, "-N_3"] & WF_4N_3^{+}\,(67) \arrow[d, "-N_2"] & & & & \\
 & WF_4N^{+}\,(22) \arrow[r] \arrow[d, "-N"] & WF_3N^{+}\,(7) \arrow[r] \arrow[d] & WF_2N^{+}\,(5) \arrow[r] \arrow[d] & WFN^{+}\,(3) \arrow[r] \arrow[d] & WN^{+}\,(2) \arrow[d] \\
WF_5^{+}\,(100) \arrow[r, "-F"] & WF_4^{+}\,(63) \arrow[r] & WF_3^{+}\,(31) \arrow[r] & WF_2^{+}\,(21) \arrow[r] & WF^{+}\,(8) \arrow[r] & W^{+}\,(4)
\end{tikzcd}
$$

However, the ^{19}F n.m.r. spectrum produced was extremely complex and has not been solved.

11.3 Single crystal X-ray Investigation of WF_5N_3

Yellow crystals were obtained upon standing the product of the reaction between an excess of WF_6 and $(CH_3)_3SiN_3$ in Genetron for several days. The crystals which formed on the reactor walls just above the solution were of suitable dimensions for a single crystal study and several were sealed into preseasoned Pyrex capillaries. The crystal chosen for the investigation was a rectangular block with approximate dimensions 0.279 mm × 0.111 mm × 0.033 mm. Approximate cell dimensions were obtained from Weissenberg photographs taken using Cu-K_{α} (Ni filtered) radiation and final cell dimensions were determined from an oscillation photograph for the rotation axis, $\underline{b}$, and from optimised counter angles for zero and upper layer reflections on a Weissenberg diffractometer.

11.4 Crystal Data

F_5N_3W ; $\underline{M}$ = 320.85

Monoclinic $\underline{a}$ = 5.240(8) Å ; $\underline{b}$ = 9.662(12) Å ; $\underline{c}$ = 10.835(8) Å

$\underline{\beta}$ = 102.4(1)°

$\underline{U}$ = 535.77 Å^3 ; $\underline{D_c}$ = 3.976 g cm^{-3} ; Z = 4

F(000) = 559.81 ; Mo-K_{α} radiation ; λ = 0.71069 Å

μ(Mo-K_{α}) = 206.96 cm^{-1}

Space group $P2_1/c$ (C_{2h}^5 № 14). Neutral atomic scattering factors were used with anomalous dispersion coefficients.

11.5 Collection of the Intensity Data

Data were collected from layers h 0 l to h 10 l, using the Stadi-2 diffractometer, in the two quadrants $\pm h, k, l$ for all layers. Data were collected using an $\underline{\omega}$-scan technique. The intensities of reflections with $0.086 < \mathrm{Sin}\theta/\lambda < 0.7$ Å^{-1} were collected, and a total of 1122 reflections were obtained with $I/\sigma I \geqslant 3$. Monitoring of check reflections throughout the data collection for each layer indicated that the crystal was slowly decomposing. Therefore, at the end of the data collection, each of the check reflections was re-determined with four scans in order to enable scale factors to be calculated for each layer - in such a way as to give increased weight to the reflections collected last. The calculated scales for each layer were used as a check against layer scale factors refined by the program SHELX. Lorentz and polarisation corrections were made to the data set.

11.6 Solution of the Structure

The program system SHELX was used. A Patterson summation was used to locate the tungsten atom, which was found to be in the general position ($Z = 4$), 0.151, 0.036, 0.288 of the space group $P2_1/c$. Three cycles of least-squares refinement with the variable parameters, overall scale factor and the atomic positional and isotropic temperature factor of the tungsten atom refining gave an R factor of 0.29 and allowed sufficient phasing for the location of the fluorine and nitrogen atoms by difference Fourier maps. Further cycles of least-squares, with all atoms included and refining isotropic temperature factors reduced the R factor to only 0.25. The temperature factors of all atoms were moderately low and the high R value can be attributed to absorption and layer scale factors. An absorption correction was performed on the data, maximum and minimum transmission values 0.3198 and 0.0454 respectively, and further cycles of refinement reduced the R factor to 0.19. Layer scale factors were then refined, and found to be in good agreement with the calculated values from the redetermined check reflections of data collection. Three cycles of least-squares refinement still with isotropic temperature factors for all atoms further reduced the R factor to 0.15, and upon allowing anisotropic refinement the R factor became 0.0757. For final cycles of refinement a weighting parameter, g (.008) $[\omega \propto 1/\sigma^2(F) + g F^2]$ was employed. An analysis of the weighting scheme over $|F_o|$ and $\sin\theta/\lambda$ was satisfactory.

Final atomic parameters are given in Table 46, the anisotropic thermal parameters are in Table 47. The interatomic distances and angles are in Tables 48 and 49 respectively and the observed and calculated structure factors are found in Appendix 12.

Final residual indices for 1056 unique reflections.

$$R = \sum(|F_o| - |F_c|)/\sum|F_o| = 0.0757$$

$$R_w = [\sum\omega(|F_o| - |F_c|)^2/\sum\omega|F_o|^2]^{\frac{1}{2}} = 0.0799$$

11.7 Discussion

The molecular structure of azido pentafluoro tungsten(VI) exhibits two unexpected, but related features. Firstly, the angle at N1 (W-N1-N2), is found to be 157°, compared with the more usual angles (114 to 120°) found in organic covalent azides.[226-228] Secondly, the N1-N2 bond lies in a plane with three fluorine atoms of the same molecule and, thus, the atom N2 is oriented towards one of the fluorine atoms (F5), rather than between two equidistant intramolecular contacts. The direction of the N1-N2 bond is considered to result from the arrangement of the molecules within the unit cell (Figure 28),

TABLE 46

Final atomic positional parameters for WF_5N_3, with estimated standard deviations in parentheses.

	x/a	y/b	z/c
W	.1510(2)	.0359(1)	.2879(1)
F1	-.0535(33)	-.0783(25)	.163(2)
F2	-.1530(25)	.1290(17)	.294(2)
F3	.4238(29)	-.0777(21)	.277(2)
F4	.0805(39)	-.0834(22)	.4084(16)
F5	.2073(34)	.1352(16)	.1573(17)
N1	.3519(38)	.1511(26)	.4073(25)
N2	.4829(38)	.2561(26)	.4493(19)
N3	.6045(48)	.3428(36)	.4944(27)

TABLE 47

Anisotropic thermal parameters, with estimated standard deviations in parentheses. The temperature factors are in the form $\exp[-2\Pi^2(h^2U_{11}a^2 + \ldots. 2hkU_{12}ab)]$

	U_{11}	U_{22}	U_{33}	U_{23}	U_{13}	U_{12}
W	.0317(5)	.0419(7)	.0518(6)	-.0026(5)	-.0030(3)	-.0001(4)
F1	.0565(87)	.0746(125)	.0865(121)	-.0202(109)	-.0043(87)	-.0272(87)
F2	.0386(67)	.0571(110)	.0819(113)	.0075(92)	.0016(68)	.0047(63)
F3	.0394(69)	.0576(97)	.1044(140)	-.0227(110)	-.0090(82)	.0026(70)
F4	.0785(109)	.0661(113)	.0601(95)	-.0055(98)	-.0041(85)	-.0116(101)
F5	.0725(101)	.0508(106)	.0661(89)	.0092(83)	.0093(80)	-.0096(78)
N1	.0333(78)	.0459(132)	.0927(168)	-.0171(124)	-.0051(98)	-.0100(82)
N2	.0443(89)	.0401(115)	.0448(102)	-.0043(94)	-.0101(75)	-.0017(92)
N3	.0533(135)	.0768(179)	.0908(175)	.0196(161)	-.0075(124)	-.0147(129)

TABLE 48

Interatomic distances (Å), with estimated standard deviations in parentheses.

W - F_1	1.890	(18)
W - F_2	1.843	(14)
W - F_3	1.826	(17)
W - F_4	1.838	(20)
W - F_5	1.785	(16)
W - N_1	1.854	(21)
N_1 - N_2	1.254	(31)
N_2 - N_3	1.102	(36)

TABLE 49

Interatomic angles (°), with estimated standard deviations in parentheses.

W -N_1-N_2	157.4	(23)	F_1-W-F_3	86.2	(9)
N_1-N_2-N_3	174.6	(29)	F_1-W-F_4	88.4	(9)
N_1-W -F_1	178.6	(11)	F_1-W-F_5	84.9	(9)
N_1-W -F_2	92.8	(9)	F_2-W-F_3	172.1	(7)
N_1-W -F_3	94.1	(9)	F_2-W-F_4	88.5	(8)
N_1-W -F_4	92.9	(10)	F_2-W-F_5	93.2	(8)
N_1-W -F_5	93.7	(10)	F_3-W-F_4	87.1	(10)
F_1-W -F_2	87.1	(8)	F_3-W-F_5	90.4	(9)
			F_4-W-F_5	173.1	(8)

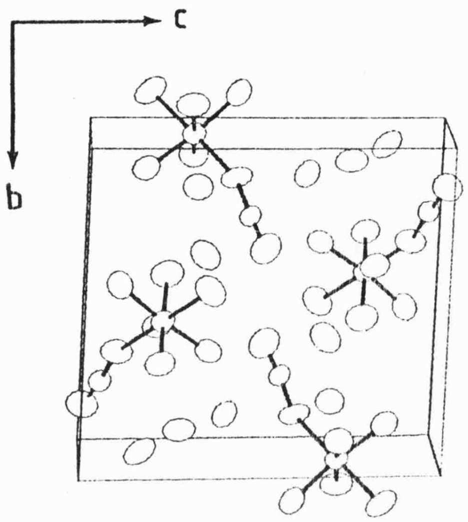

Figure 28

Stereoscopic view of the unit cell contents of WF_5N_3.

with the barrier to rotation of the N2 atom about the W-N1 axis, which is expected to be low, being overcome to allow a more favourable packing configuration. The angle of 157° found about N1, though not comparable with other azides is similar to the angle found about the nitrogen atom in the isothiocyanates, for example $(CH_3)_3SiNCS$ (154°).[229] The four fluorine atoms equatorial to the azide group are all distorted away from N1 with N1-W-F angles all >90° (92.8 to 94.1), and towards the fluorine atom (F1) trans to the azide group (F1-W-F, 84.9 to 88.4°).

Bond distances within the molecular unit (Figure 29) are of the expected order. The fluorine atom, F5, with the closest intramolecular contact to the azide group has the shortest bond length (1.78 Å), and the fluorine atom, F1, trans to the azide group, has the longest

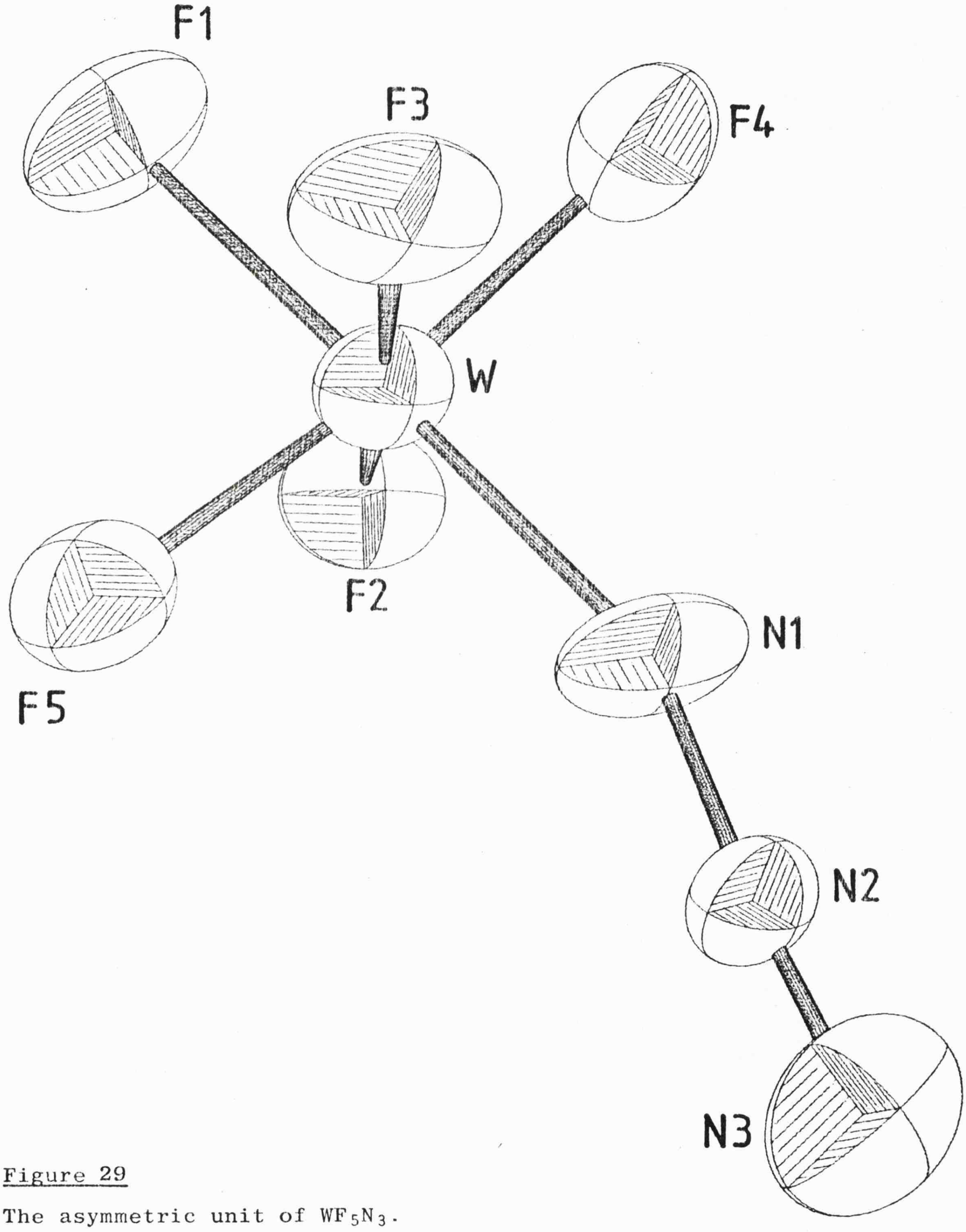

Figure 29

The asymmetric unit of WF_5N_3.

bond length (1.89 Å), the three remaining W-F distances are 1.82 to 1.84 Å. There are no reported transition metal to nitrogen of azide bond distances for comparison of the W-N1 bond (1.85 Å). However, the N1-N2 and N2-N3 bond distances, respectively 1.25 and 1.10 Å, are comparable to those of reported azides, with the terminal 1.10 Å bond distance a close approximation to an N≡N bond.

Each tungsten atom has six approximately equidistant neighbours (5.10 to 5.27 Å). The nitrogen atom N1 has four intramolecular contacts at 2.66 to 2.69 Å but, like N3, has no intermolecular contacts of <3.0 Å. The nitrogen atom N2 has two nearest fluorine atom neighbours at 2.82 and 2.98 Å, and the fluorine atom F4 has a close contact (2.82 Å) with its symmetry equivalent. The N1 and N3 atoms are in approximate planes of fluorine atoms in the {101} plane.

APPENDIX 1

Structure factor tables for $UF_4O.2SbF_5$

OBSERVED AND CALCULATED STRUCTURE FACTORS PAGE 1

FOR UF40.2S3F5

H	K	L	FO	FC
6	0	0	40	-35
7	0	0	79	-97
8	0	0	54	60
5	1	0	111	-110
6	1	0	28	31
7	1	0	31	-30
8	1	0	81	75
3	2	0	102	-105
5	2	0	83	-85
6	2	0	135	132
7	2	0	78	72
8	2	0	54	-50
1	3	0	369	-361
3	3	0	57	55
4	3	0	145	140
5	3	0	95	89
6	3	0	86	-86
7	3	0	49	57
0	4	0	34	-33
1	4	0	114	-114
2	4	0	176	177
3	4	0	123	119
4	4	0	280	-281
6	4	0	68	65
7	4	0	71	70
1	5	0	168	165
2	5	0	162	-162
3	5	0	134	-130
4	5	0	44	-39
5	5	0	150	149
6	5	0	176	167
7	5	0	116	-118
8	5	0	85	-83
0	6	0	72	71
2	6	0	164	-164
3	6	0	98	-96
4	6	0	155	155
7	6	0	54	-56
1	7	0	185	-188
2	7	0	33	-32
3	7	0	63	-65
4	7	0	88	86
5	7	0	73	70
8	7	0	40	-35
0	8	0	63	64
1	8	0	76	-80
2	8	0	65	-62
3	8	0	81	78
4	8	0	59	67
5	8	0	56	51
6	8	0	83	-88
7	8	0	82	-80
8	8	0	51	47
1	9	0	154	-156
2	9	0	147	-152
3	9	0	165	164
4	9	0	66	66
5	9	0	66	-64
6	9	0	53	-51
8	9	0	44	45
0	10	0	290	-294
1	10	0	62	-63
2	10	0	184	189
3	10	0	93	95
5	10	0	92	-95
7	10	0	46	49
1	11	0	66	61
2	11	0	68	80
3	11	0	57	-62
4	11	0	48	-41
0	12	0	76	-74
3	12	0	57	53

H	K	L	FO	FC
1	13	0	113	117
3	13	0	52	-53
4	13	0	47	-45
0	14	0	67	71
2	14	0	56	-60
4	14	0	63	65
5	14	0	45	40
3	15	0	50	62
5	15	0	48	-55
1	1	1	31	37
3	1	1	106	103
5	1	1	107	-109
6	1	1	61	-62
7	1	1	48	51
8	1	1	79	82
-8	2	1	35	-35
-4	2	1	271	-280
-2	2	1	219	219
-1	2	1	158	156
1	2	1	146	-140
2	2	1	190	179
3	2	1	110	104
4	2	1	75	-75
5	2	1	132	-128
6	2	1	46	54
7	2	1	142	139
-8	3	1	57	61
-5	3	1	31	-30
-4	3	1	103	108
-3	3	1	65	64
-2	3	1	101	-102
-1	3	1	392	-378
0	3	1	40	37
1	3	1	307	294
2	3	1	223	217
3	3	1	96	-91
4	3	1	234	-230
5	3	1	45	51
6	3	1	118	116
-7	4	1	36	38
-6	4	1	40	-43
-5	4	1	36	36
-3	4	1	282	-277
-2	4	1	43	-37
-1	4	1	79	78
0	4	1	264	255
1	4	1	157	156
2	4	1	206	-208
3	4	1	193	-190
5	4	1	100	102
6	4	1	83	78
7	4	1	43	-45
-5	5	1	79	-73
-4	5	1	39	43
-3	5	1	65	64
-1	5	1	37	-38
0	5	1	92	-92
1	5	1	72	67
2	5	1	34	32
3	5	1	83	-81
4	5	1	33	35
6	5	1	38	39
8	5	1	39	-33
-8	6	1	67	66
-7	6	1	34	-44
-3	6	1	84	-84
-2	6	1	271	-270
-1	6	1	148	148
0	6	1	188	183
1	6	1	65	65
2	6	1	160	-161
3	6	1	280	-278

H	K	L	FO	FC
4	6	1	49	51
5	6	1	169	161
6	6	1	40	-32
-7	7	1	59	-59
-6	7	1	36	43
-5	7	1	121	122
-4	7	1	135	-136
-3	7	1	95	-92
-2	7	1	102	103
-1	7	1	133	134
0	7	1	78	80
1	7	1	302	-303
2	7	1	180	-176
3	7	1	201	200
4	7	1	85	86
6	7	1	105	-105
8	7	1	82	72
-8	8	1	39	-47
-7	8	1	129	124
-6	8	1	47	42
-4	8	1	123	-121
-3	8	1	144	-142
-2	8	1	205	208
0	8	1	79	-78
3	8	1	101	106
4	8	1	57	-59
5	8	1	119	-119
6	8	1	75	74
7	8	1	47	45
-6	9	1	37	-38
-5	9	1	106	-107
-4	9	1	43	47
-3	9	1	43	49
-2	9	1	67	66
-1	9	1	92	90
0	9	1	127	-128
2	9	1	39	-40
3	9	1	73	-74
4	9	1	66	67
-5	10	1	78	76
-4	10	1	50	-54
-3	10	1	49	50
-1	10	1	71	73
0	10	1	42	-40
1	10	1	53	-57
2	10	1	131	135
3	10	1	61	-63
7	10	1	44	52
-7	11	1	52	52
-6	11	1	73	-75
-5	11	1	74	-73
-4	11	1	62	-55
-3	11	1	149	152
-2	11	1	96	100
-1	11	1	138	-142
4	11	1	65	-67
5	11	1	104	109
6	11	1	43	49
7	11	1	60	-54
-6	12	1	94	-96
-5	12	1	70	65
-4	12	1	130	133
-3	12	1	46	-50
-2	12	1	63	-56
-1	12	1	58	-60
0	12	1	73	76
1	12	1	119	123
2	12	1	115	-119
4	12	1	63	66
-6	13	1	45	47
-5	13	1	43	-38
-3	13	1	67	-67

OBSERVED AND CALCULATED STRUCTURE FACTORS PAGE 2

FOR UF40.2SBF5

H	K	L	FO	FC
-1	13	1	129	136
1	13	1	57	-56
2	13	1	73	-78
4	13	1	120	123
6	13	1	46	-44
-5	14	1	46	-18
-3	14	1	89	86
0	14	1	45	-43
1	14	1	58	-57
2	14	1	66	67
-5	15	1	61	62
-4	15	1	55	-50
1	15	1	61	-63
3	15	1	45	65
-2	16	1	80	86
0	16	1	93	-97
2	16	1	47	44
3	16	1	84	87
-1	17	1	46	-37
0	17	1	45	-33
1	17	1	71	78
2	17	1	54	42
-3	0	2	62	64
-2	0	2	306	313
-1	0	2	231	-235
0	0	2	236	-244
1	0	2	279	-279
2	0	2	210	220
3	0	2	304	322
4	0	2	168	-178
5	0	2	115	-120
6	0	2	86	-90
7	0	2	55	55
8	0	2	91	94
-7	1	2	125	134
-4	1	2	61	66
-3	1	2	51	51
-2	1	2	143	152
-1	1	2	302	-320
0	1	2	160	-147
1	1	2	378	364
3	1	2	36	-39
4	1	2	170	-167
5	1	2	76	-78
6	1	2	188	193
9	1	2	48	-46
-8	2	2	35	-32
-6	2	2	62	-61
-5	2	2	48	-48
-4	2	2	249	251
-3	2	2	27	-30
-2	2	2	124	-126
0	2	2	277	-255
1	2	2	168	158
3	2	2	76	-73
4	2	2	170	167
5	2	2	100	-98
-6	3	2	93	93
-4	3	2	48	-50
-3	3	2	162	159
-2	3	2	212	-211
-1	3	2	73	-73
0	3	2	65	53
1	3	2	113	106
2	3	2	195	188
3	3	2	166	-160
4	3	2	152	-147
5	3	2	43	30
7	3	2	78	74
-8	4	2	88	87
-7	4	2	66	-68
-6	4	2	192	-189

H	K	L	FO	FC
-5	4	2	110	110
-4	4	2	107	107
-3	4	2	135	131
-2	4	2	86	-85
-1	4	2	228	-224
0	4	2	254	243
1	4	2	130	123
2	4	2	124	-120
3	4	2	80	-73
5	4	2	160	156
7	4	2	104	-101
-8	5	2	129	-118
-7	5	2	43	-48
-6	5	2	58	63
-5	5	2	262	259
-4	5	2	59	58
-3	5	2	427	-419
-2	5	2	62	-60
-1	5	2	112	114
0	5	2	80	80
1	5	2	67	-63
2	5	2	205	-197
3	5	2	96	97
4	5	2	87	85
5	5	2	126	-126
6	5	2	50	-43
8	5	2	94	91
-8	6	2	49	-49
-7	6	2	61	62
-6	6	2	114	108
-5	6	2	88	-89
-4	6	2	65	-66
-3	6	2	64	-68
-2	6	2	106	107
-1	6	2	180	181
0	6	2	175	-176
1	6	2	47	-45
2	6	2	87	87
3	6	2	48	48
4	6	2	43	45
5	6	2	117	-118
7	6	2	85	82
-7	7	2	51	-51
-6	7	2	57	53
-2	7	2	183	-187
-1	7	2	66	-66
0	7	2	96	96
1	7	2	61	57
2	7	2	110	107
3	7	2	98	-101
4	7	2	72	-70
7	7	2	72	72
8	7	2	44	13
-7	8	2	50	42
-6	8	2	65	65
-4	8	2	172	-170
-2	8	2	174	175
-1	8	2	64	63
1	8	2	103	-102
3	8	2	46	40
4	8	2	101	-102
6	8	2	50	51
7	8	2	46	38
-7	9	2	79	78
-6	9	2	44	-44
-5	9	2	63	-58
-3	9	2	99	98
-2	9	2	40	41
-1	9	2	186	-187
0	9	2	103	-109
1	9	2	202	203
2	9	2	63	62

H	K	L	FO	FC
4	9	2	126	-129
5	9	2	115	116
-4	10	2	66	68
-3	10	2	57	-49
-2	10	2	114	-119
-1	10	2	55	48
0	10	2	154	155
1	10	2	94	100
2	10	2	137	-135
3	10	2	174	-177
5	10	2	102	108
-1	11	2	97	96
1	11	2	73	-74
4	11	2	62	65
6	11	2	47	-39
-4	12	2	50	-46
0	12	2	80	77
2	12	2	57	-58
-1	13	2	71	72
0	13	2	39	29
1	13	2	83	-82
2	13	2	66	-67
3	13	2	43	43
4	13	2	85	80
-4	14	2	82	-88
-2	14	2	75	84
-1	14	2	55	52
0	14	2	43	-44
1	14	2	62	-64
2	14	2	43	30
3	14	2	52	57
-5	15	2	70	-79
-3	15	2	73	79
-2	15	2	55	59
-1	15	2	51	-47
0	15	2	60	-64
-8	1	3	42	46
-7	1	3	52	54
-6	1	3	70	-77
-5	1	3	174	-193
-4	1	3	47	-46
-3	1	3	165	180
-2	1	3	141	146
-1	1	3	108	-113
0	1	3	282	-271
1	1	3	56	-58
2	1	3	116	117
8	1	3	57	-64
-8	2	3	67	68
-7	2	3	66	-73
-6	2	3	100	-100
-4	2	3	193	205
-3	2	3	172	182
-2	2	3	200	-215
-1	2	3	222	-235
0	2	3	110	103
1	2	3	129	122
3	2	3	171	-164
5	2	3	93	96
7	2	3	88	-85
-7	3	3	105	-98
-6	3	3	41	-38
-5	3	3	141	142
-3	3	3	158	-155
-1	3	3	88	90
0	3	3	156	145
1	3	3	115	-109
2	3	3	297	-292
3	3	3	141	142
4	3	3	200	199
5	3	3	58	55
6	3	3	149	-151

OBSERVED AND CALCULATED STRUCTURE FACTORS

FOR UF40.2SBF5

H	K	L	FO	FC	H	K	L	FO	FC	H	K	L	FO	FC
7	3	3	69	-80	0	10	3	78	72	8	2	4	54	-51
8	3	3	62	58	2	10	3	63	65	-7	3	4	111	-109
-8	4	3	74	-76	3	10	3	73	-76	-5	3	4	42	36
-5	4	3	46	42	5	10	3	65	57	-3	3	4	151	150
-4	4	3	73	71	-7	11	3	49	-41	-2	3	4	62	-70
-3	4	3	51	-53	-5	11	3	152	152	-1	3	4	93	92
-2	4	3	78	77	-3	11	3	124	-130	0	3	4	59	58
-1	4	3	55	-52	-2	11	3	93	-90	1	3	4	266	-250
0	4	3	107	-101	0	11	3	210	206	2	3	4	60	56
2	4	3	79	78	2	11	3	75	-82	4	3	4	88	85
3	4	3	178	172	-4	12	3	83	-82	5	3	4	92	87
5	4	3	144	-143	-3	12	3	80	-83	6	3	4	126	-127
6	4	3	62	-59	-2	12	3	137	139	-6	4	4	75	76
-4	5	3	59	56	-1	12	3	93	96	-5	4	4	110	110
-1	5	3	126	123	0	12	3	74	-69	-4	4	4	213	-219
2	5	3	46	49	3	12	3	83	86	-3	4	4	89	-92
3	5	3	57	-48	5	12	3	91	-87	-2	4	4	212	214
4	5	3	85	85	-5	13	3	64	-60	-1	4	4	91	93
5	5	3	57	-65	-4	13	3	44	40	1	4	4	298	-282
-8	6	3	61	-57	0	13	3	78	-78	2	4	4	60	-61
-7	6	3	73	-65	1	13	3	67	76	3	4	4	210	207
-6	6	3	96	98	2	13	3	70	76	5	4	4	50	-51
-5	6	3	56	54	3	13	3	68	-65	-7	5	4	137	128
-4	6	3	70	-71	4	13	3	46	-54	-6	5	4	61	-64
-3	6	3	103	97	-4	14	3	51	-47	-5	5	4	183	-180
-2	6	3	49	-47	-1	14	3	51	42	-3	5	4	143	141
-1	6	3	93	90	0	14	3	47	47	-2	5	4	308	318
0	6	3	158	-150	3	14	3	50	-52	-1	5	4	121	-122
1	6	3	175	-168	5	14	3	54	59	0	5	4	343	-324
2	6	3	205	202	-3	15	3	46	29	1	5	4	40	30
3	6	3	172	169	-1	15	3	68	-68	2	5	4	119	114
5	6	3	127	-127	1	16	3	69	70	3	5	4	148	146
6	6	3	83	-80	2	16	3	80	-76	5	5	4	95	-91
7	6	3	75	76	-8	0	4	135	139	6	5	4	79	77
8	6	3	59	48	-7	0	4	54	55	-6	6	4	42	-42
-8	7	3	46	35	-6	0	4	170	-174	-5	6	4	81	-73
-7	7	3	108	111	-4	0	4	35	33	-4	6	4	173	172
-5	7	3	67	-65	-3	0	4	146	149	-3	6	4	80	82
-4	7	3	88	-82	-2	0	4	108	-112	-2	6	4	162	-165
-3	7	3	114	114	-1	0	4	103	-105	0	6	4	60	-59
-2	7	3	93	94	0	0	4	201	203	1	6	4	137	131
-1	7	3	190	-191	2	0	4	204	-220	2	6	4	65	67
0	7	3	53	-44	3	0	4	104	-103	3	6	4	123	-122
1	7	3	139	136	4	0	4	78	-82	4	6	4	51	38
2	7	3	185	181	5	0	4	220	233	-7	7	4	72	-61
4	7	3	246	-242	6	0	4	109	110	-3	7	4	121	120
6	7	3	98	97	7	0	4	106	-123	1	7	4	116	-113
7	7	3	40	29	-7	1	4	45	-44	2	7	4	88	84
-6	8	3	124	-118	-6	1	4	63	-70	3	7	4	55	49
-4	8	3	180	182	-5	1	4	92	105	5	7	4	59	57
-3	8	3	40	28	-4	1	4	164	172	6	7	4	62	-57
-2	8	3	47	-46	-3	1	4	223	-234	-6	8	4	75	-74
-1	8	3	192	-193	-2	1	4	93	-96	-4	8	4	79	81
0	8	3	56	54	-1	1	4	70	69	-3	8	4	75	72
1	8	3	209	201	0	1	4	62	60	-2	8	4	51	-52
2	8	3	46	-39	1	1	4	97	95	-1	8	4	203	-203
3	8	3	51	-42	2	1	4	305	-307	0	8	4	56	50
6	8	3	51	49	3	1	4	101	102	1	8	4	110	107
7	8	3	73	-64	4	1	4	164	168	4	8	4	68	-60
-8	9	3	70	-57	7	1	4	97	-102	-7	9	4	43	-47
-6	9	3	97	94	-7	2	4	36	42	-6	9	4	75	-71
-4	9	3	53	41	-6	2	4	93	97	-5	9	4	86	86
-3	9	3	109	-109	-5	2	4	157	-162	-4	9	4	78	76
-2	9	3	113	-112	-4	2	4	38	-31	-3	9	4	94	-91
-1	9	3	91	91	-3	2	4	66	-68	-2	9	4	69	-75
1	9	3	91	90	-2	2	4	34	40	0	9	4	90	87
3	9	3	104	-105	-1	2	4	221	230	2	9	4	120	-119
4	9	3	51	49	0	2	4	63	-60	4	9	4	127	126
7	9	3	41	32	1	2	4	70	-67	6	9	4	50	-58
-7	10	3	46	-35	2	2	4	50	-44	-6	10	4	78	77
-3	10	3	72	76	3	2	4	112	-110	-4	10	4	44	-40
-2	10	3	119	-122	4	2	4	113	115	-3	10	4	51	-51

OBSERVED AND CALCULATED STRUCTURE FACTORS

FOR UF40.2SBF5

H	K	L	FO	FC	H	K	L	FO	FC	H	K	L	FO	FC
-1	10	4	56	63	0	4	5	44	-40	-2	14	5	59	-62
0	10	4	111	-108	1	4	5	75	73	2	14	5	46	46
1	10	4	48	-39	2	4	5	104	-101	0	15	5	56	57
2	10	4	92	89	3	4	5	64	-68	-3	16	5	58	-67
3	10	4	99	97	5	4	5	69	71	0	17	5	52	-51
4	10	4	43	36	6	4	5	78	74	-8	0	6	97	-92
5	10	4	117	-114	-6	5	5	51	55	-7	0	6	61	-56
6	10	4	63	-62	-5	5	5	59	-62	-6	0	6	68	64
-5	11	4	71	-64	-2	5	5	58	-55	-5	0	6	272	270
-3	11	4	55	45	-1	5	5	71	71	-4	0	6	56	-61
0	11	4	75	-65	0	5	5	90	-85	-3	0	6	203	-207
2	11	4	72	68	2	5	5	56	47	-1	0	6	45	41
4	11	4	66	-66	3	5	5	48	-46	0	0	6	151	150
-4	12	4	53	40	-8	6	5	114	109	1	0	6	49	-49
-1	12	4	52	-49	-6	6	5	65	-59	2	0	6	78	-82
2	12	4	55	57	-5	6	5	102	-105	3	0	6	164	175
4	12	4	46	-36	-3	6	5	156	160	5	0	6	70	-77
-4	13	4	58	-54	-1	6	5	56	-52	6	0	6	55	-61
-1	13	4	56	-52	0	6	5	66	62	-8	1	6	69	-72
2	13	4	68	69	3	6	5	126	-126	-7	1	6	120	117
4	13	4	70	-74	5	6	5	138	140	-6	1	6	56	55
-4	14	4	73	73	6	6	5	43	25	-5	1	6	87	-95
-3	14	4	55	49	-7	7	5	73	-70	-4	1	6	61	-60
-2	14	4	60	-60	-6	7	5	115	-113	-3	1	6	64	-69
-1	14	4	82	-85	-5	7	5	105	99	-2	1	6	177	185
1	14	4	93	98	-4	7	5	75	80	0	1	6	180	-179
3	14	4	71	-69	-2	7	5	55	-66	1	1	6	82	81
-3	15	4	75	-81	-1	7	5	56	-62	3	1	6	83	79
-2	15	4	62	-66	0	7	5	188	178	5	1	6	115	-118
0	15	4	91	85	2	7	5	139	-141	6	1	6	83	86
2	15	4	60	-62	4	7	5	75	72	-7	2	6	39	-36
-6	1	5	41	43	5	7	5	82	82	-6	2	6	57	59
-5	1	5	76	81	6	7	5	64	-54	-4	2	6	98	102
-4	1	5	57	63	-7	8	5	42	33	-2	2	6	149	-153
-3	1	5	151	-158	-6	8	5	53	50	1	2	6	142	137
-2	1	5	193	-198	-4	8	5	70	-68	2	2	6	141	143
-1	1	5	142	145	-3	8	5	125	-126	3	2	6	93	-88
0	1	5	300	295	-2	8	5	143	152	7	2	6	57	64
1	1	5	85	83	-1	8	5	177	183	-6	3	6	91	95
2	1	5	120	-121	0	8	5	64	-54	-4	3	6	179	-181
3	1	5	151	-157	1	8	5	123	-120	-1	3	6	60	62
5	1	5	57	64	2	8	5	137	-134	0	3	6	109	104
-6	2	5	103	106	3	8	5	114	112	1	3	6	119	-114
-4	2	5	167	-176	4	8	5	88	88	2	3	6	83	80
-3	2	5	134	-141	5	8	5	55	-63	4	3	6	80	-77
-2	2	5	138	147	-5	9	5	92	-85	7	3	6	65	64
-1	2	5	272	285	-4	9	5	46	35	-8	4	6	69	62
0	2	5	43	43	-3	9	5	89	91	-7	4	6	58	55
1	2	5	300	-292	0	9	5	168	-163	-6	4	6	95	-95
2	2	5	79	-76	1	9	5	55	-58	-3	4	6	98	105
3	2	5	146	152	2	9	5	73	71	-1	4	6	298	-309
4	2	5	91	94	4	9	5	72	69	0	4	6	60	58
5	2	5	47	-42	-4	10	5	64	-57	1	4	6	171	167
6	2	5	62	-69	1	10	5	101	-98	4	4	6	134	-132
-7	3	5	106	108	-4	11	5	63	-67	5	4	6	54	49
-6	3	5	62	65	-3	11	5	89	90	6	4	6	89	93
-5	3	5	50	-43	-2	11	5	137	141	-6	5	6	50	-47
-4	3	5	169	-181	-1	11	5	106	-105	-5	5	6	53	51
-2	3	5	180	190	0	11	5	115	-110	-4	5	6	68	67
0	3	5	82	-78	2	11	5	80	78	-3	5	6	212	-214
2	3	5	93	97	3	11	5	115	113	-2	5	6	94	-94
3	3	5	48	41	4	11	5	76	-81	-1	5	6	72	69
4	3	5	160	-167	-6	12	5	70	-66	0	5	6	188	180
5	3	5	56	-43	-4	12	5	98	102	1	5	6	198	195
6	3	5	79	83	-1	12	5	119	-125	2	5	6	211	-213
7	3	5	49	58	1	12	5	157	148	3	5	6	129	-133
-8	4	5	60	49	3	12	5	53	-56	4	5	6	67	70
-7	4	5	57	54	4	12	5	46	-34	5	5	6	60	55
-6	4	5	83	-79	-4	13	5	69	72	6	5	6	47	46
-5	4	5	73	-73	-2	13	5	78	-78	-8	6	6	56	-48
-3	4	5	45	37	4	13	5	74	74	-7	6	6	43	-36
-2	4	5	106	108	-3	14	5	48	32	-6	6	6	74	71

OBSERVED AND CALCULATED STRUCTURE FACTORS

FOR UF40.2SBF5

H	K	L	FO	FC	H	K	L	FO	FC	H	K	L	FO	FC
-3	6	6	73	-76	-5	4	7	104	99	4	2	8	94	98
-1	5	6	200	203	-3	4	7	150	-149	-7	3	8	62	-61
0	6	6	42	-47	-2	4	7	83	-85	-3	3	8	98	100
1	6	6	124	-118	-1	4	7	56	51	-2	3	8	103	-107
4	6	6	104	104	5	4	7	54	-56	-1	3	8	103	-112
6	6	6	53	-58	-2	5	7	68	-73	2	3	8	63	46
-6	7	6	53	50	0	5	7	46	-36	5	3	8	50	56
-4	7	6	75	-74	-7	6	7	69	-74	-7	4	8	53	-46
-2	7	6	60	-50	-6	6	7	56	58	-5	4	8	105	103
0	7	6	102	98	-5	6	7	129	131	-3	4	8	104	-110
1	7	6	61	-55	-3	6	7	119	-123	0	4	8	97	98
5	7	6	46	41	-2	6	7	102	-103	1	4	8	66	-58
-5	8	6	48	44	0	6	7	119	117	2	4	8	126	-133
-4	8	6	75	-73	1	6	7	74	-72	3	4	8	93	95
-2	8	6	59	68	-7	7	7	76	78	4	4	8	63	56
-1	8	6	56	50	-6	7	7	54	52	-6	5	8	53	54
1	8	6	116	-118	-4	7	7	142	-140	-3	5	8	58	-56
2	8	6	98	-96	-3	7	7	55	-52	-2	5	8	104	106
3	8	6	98	98	-2	7	7	185	193	0	5	8	186	-180
-7	9	6	75	75	-1	7	7	47	15	1	5	8	49	-38
-6	9	6	51	56	0	7	7	53	-56	2	5	8	45	54
-4	9	6	91	-93	1	7	7	83	-85	3	5	8	116	126
-2	9	6	129	136	3	7	7	86	90	5	5	8	144	-143
0	9	6	93	-92	4	7	7	78	-77	-5	6	8	87	-80
2	9	6	61	58	5	7	7	57	-60	-3	6	8	63	63
5	9	6	72	-73	-7	8	7	66	61	0	6	8	75	-77
-6	10	6	55	-57	-5	8	7	55	-62	2	6	8	111	106
-5	10	6	123	-124	-4	8	7	67	64	3	6	8	53	-50
-3	10	6	106	112	-3	8	7	47	34	-1	7	8	54	-55
-1	10	6	47	-46	-1	8	7	93	-97	2	7	8	57	66
0	10	6	62	-55	0	8	7	73	-77	4	7	8	46	-40
2	10	6	44	28	1	8	7	148	147	-1	8	8	86	-84
3	10	6	77	-78	2	8	7	62	58	1	8	8	73	75
5	10	6	48	40	3	8	7	52	-56	2	8	8	49	44
-2	11	6	47	-48	4	8	7	60	-64	4	8	8	75	-79
0	11	6	44	36	-2	9	7	67	-69	-6	9	8	73	-78
-5	12	6	51	-42	-1	9	7	68	78	-4	9	8	116	117
-4	13	6	65	67	3	9	7	97	-103	-2	9	8	76	-76
0	13	6	50	30	-3	10	7	65	70	-1	9	8	57	-58
-3	14	6	54	-57	4	10	7	51	-49	1	9	8	105	104
-1	14	6	65	74	0	11	7	121	120	3	9	8	68	-66
1	14	6	69	-74	2	11	7	108	-111	-5	10	8	76	72
-2	15	6	52	51	-3	12	7	90	-94	-3	10	8	93	-97
0	15	6	82	-80	-1	12	7	85	85	-2	10	8	83	-83
-3	1	7	62	60	2	12	7	88	-91	-1	10	8	66	64
-2	1	7	81	84	-1	13	7	71	72	0	10	8	78	78
0	1	7	167	-167	-3	14	7	61	55	2	10	8	60	-49
2	1	7	111	114	-7	0	8	98	93	1	11	8	51	-38
3	1	7	108	112	-6	0	8	110	-108	0	12	8	45	32
5	1	7	78	-80	-5	0	8	126	-119	-1	13	8	54	54
-8	2	7	47	34	-4	0	8	46	-48	-6	1	9	50	-50
-7	2	7	77	65	-3	0	8	100	98	-5	1	9	52	-54
-5	2	7	85	-87	-2	0	8	197	201	2	1	9	58	-57
-3	2	7	125	124	-1	0	8	156	-161	3	1	9	93	-90
-1	2	7	174	-178	0	0	8	118	-120	5	1	9	66	70
0	2	7	46	-48	2	0	8	45	53	-7	2	9	73	-74
1	2	7	143	147	3	0	8	78	72	-5	2	9	86	87
2	2	7	137	140	4	0	8	93	-102	-4	2	9	56	45
3	2	7	66	-66	-6	1	8	93	-90	-3	2	9	47	-49
4	2	7	146	-150	-4	1	8	179	179	-2	2	9	51	-66
6	2	7	67	62	-3	1	8	45	-42	-1	2	9	70	67
-7	3	7	63	-63	-2	1	8	59	-55	0	2	9	78	77
-6	3	7	128	-125	-1	1	8	50	-47	1	2	9	85	-77
-5	3	7	61	64	1	1	8	134	133	2	2	9	96	-93
-4	3	7	134	135	2	1	8	55	-62	4	2	9	83	82
-2	3	7	96	-102	3	1	8	83	-89	-6	3	9	68	71
-1	3	7	121	-126	-7	2	8	45	-47	-4	3	9	114	-119
0	3	7	154	146	-5	2	8	49	-51	-3	3	9	90	-82
1	3	7	63	65	-3	2	8	65	55	-2	3	9	111	108
2	3	7	83	-84	-1	2	8	106	101	-1	3	9	98	97
5	3	7	51	58	0	2	8	46	-38	0	3	9	45	-34
-8	4	7	69	-70	1	2	8	88	-97	1	3	9	119	-117

OBSERVED AND CALCULATED STRUCTURE FACTORS

FOR UF40.2SBF5

H	K	L	FO	FC	H	K	L	FO	FC	H	K	L	FO	FC
3	3	9	84	89	-5	0	10	120	116	-2	9	10	49	47
-5	4	9	83	-82	-4	0	10	56	45	-1	9	10	83	80
-3	4	9	61	63	-3	0	10	152	-151	-3	10	10	72	69
-2	4	9	83	85	-2	0	10	68	-61	0	10	10	96	-97
0	4	9	114	-109	0	0	10	164	164	-5	1	11	65	69
-1	5	9	57	50	1	0	10	56	58	-3	1	11	64	-59
4	5	9	47	18	2	0	10	152	-162	-4	2	11	87	-88
-4	6	9	57	-48	-6	1	10	51	54	-3	2	11	50	17
-3	6	9	127	125	-3	1	10	108	-107	-2	2	11	75	84
-2	6	9	88	89	-2	1	10	58	59	0	2	11	51	-48
-1	6	9	76	-71	-1	1	10	125	123	2	2	11	49	61
0	6	9	69	-71	0	1	10	53	-46	-3	3	11	50	54
1	6	9	53	-44	-6	2	10	77	68	-1	3	11	96	-99
2	6	9	69	76	-2	2	10	48	-51	1	3	11	101	94
4	6	9	51	-48	2	2	10	55	55	2	3	11	61	37
-6	7	9	91	-93	-4	3	10	96	-94	-3	4	11	69	-60
-4	7	9	103	103	1	3	10	106	-105	-2	4	11	48	-47
-3	7	9	59	52	-4	4	10	69	-61	-1	4	11	50	49
-2	7	9	47	-42	-2	4	10	109	110	0	4	11	66	54
-1	7	9	130	-133	0	4	10	63	-52	0	6	11	121	115
1	7	9	111	108	-5	5	10	84	-86	-3	7	11	67	-75
-4	8	9	77	68	-4	5	10	68	61	-2	7	11	57	50
-3	8	9	61	-60	-3	5	10	63	60	0	8	11	57	-62
-1	8	9	49	51	1	5	10	91	85	-2	0	12	113	116
2	8	9	50	-57	-2	6	10	67	-67	0	0	12	91	-89
2	9	9	64	65	-1	6	10	50	39	0	1	12	69	-66
0	10	9	49	53	-4	7	10	56	-54	-2	2	12	52	-57
1	10	9	47	-38	1	7	10	54	-58	0	3	12	57	37
-2	11	9	62	53	-3	9	10	59	-56	0	10	12	56	53
0	12	9	78	-72										

APPENDIX 2

Structure factor tables for $MoF_4O.SbF_5$

OBSERVED AND CALCULATED STRUCTURE FACTORS PAGE 1

FOR MOF40.SBF5.

H	K	L	FO	FC
2	0	0	173	-165
4	0	0	21	-17
8	0	0	25	23
10	0	0	28	22
2	1	0	127	-120
3	1	0	22	22
4	1	0	17	8
5	1	0	119	-116
6	1	0	82	79
7	1	0	73	75
1	2	0	146	-136
2	2	0	163	-157
4	2	0	132	128
5	2	0	50	49
7	2	0	29	28
8	2	0	42	-43
10	2	0	28	24
1	3	0	157	-145
2	3	0	61	60
3	3	0	178	173
4	3	0	34	-31
9	3	0	47	-50
1	4	0	12	7
2	4	0	224	-215
3	4	0	144	138
4	4	0	81	77
5	4	0	64	-65
7	4	0	33	-31
8	4	0	31	-32
9	4	0	28	32
10	4	0	25	21
1	5	0	30	30
2	5	0	80	78
3	5	0	24	23
4	5	0	52	-47
5	5	0	78	-74
7	5	0	65	65
8	5	0	29	-28
1	6	0	142	-138
2	6	0	69	-66
3	6	0	31	28
8	6	0	22	20
1	7	0	17	-12
2	7	0	47	-47
3	7	0	37	35
4	7	0	33	-29
5	7	0	46	-45
6	7	0	86	85
7	7	0	30	28
1	8	0	119	-115
2	8	0	46	-45
3	8	0	22	22
4	8	0	70	67
8	8	0	33	-35
1	9	0	43	-42
2	9	0	59	58
3	9	0	46	45
4	9	0	33	-34
-9	0	1	54	-56
-7	0	1	38	37
-5	0	1	83	82
-3	0	1	89	-85
3	0	1	75	76
5	0	1	100	-96
7	0	1	34	-35
-8	1	1	25	24
-7	1	1	51	48
-6	1	1	86	-88
-4	1	1	162	159
-3	1	1	96	-96
-2	1	1	190	-187
-1	1	1	59	62

H	K	L	FO	FC
1	1	1	135	146
2	1	1	67	67
3	1	1	62	-59
4	1	1	49	-46
5	1	1	56	-54
6	1	1	64	61
8	1	1	53	-52
9	1	1	28	29
10	1	1	34	34
-8	2	1	34	35
-7	2	1	28	31
-6	2	1	21	22
-5	2	1	72	-68
-4	2	1	70	-63
-3	2	1	21	-21
-1	2	1	247	251
1	2	1	188	-204
2	2	1	67	65
3	2	1	64	63
4	2	1	98	-92
5	2	1	45	-41
6	2	1	28	-28
7	2	1	43	44
8	2	1	21	22
-8	3	1	62	62
-7	3	1	37	-36
-6	3	1	111	-110
-5	3	1	43	42
-4	3	1	104	100
-3	3	1	38	-36
-2	3	1	55	-55
-1	3	1	22	23
1	3	1	40	-39
2	3	1	46	-46
4	3	1	106	-99
5	3	1	34	30
6	3	1	105	101
7	3	1	25	-25
8	3	1	30	-30
-9	4	1	23	-24
-8	4	1	21	-18
-6	4	1	36	-35
-4	4	1	61	56
-3	4	1	65	-62
-2	4	1	112	107
-1	4	1	109	110
1	4	1	17	-17
2	4	1	19	20
3	4	1	103	100
4	4	1	36	34
5	4	1	24	-22
6	4	1	34	33
7	4	1	24	22
8	4	1	38	-36
-8	5	1	20	16
-7	5	1	58	-58
-5	5	1	46	44
-4	5	1	134	128
-3	5	1	40	-40
-2	5	1	185	-184
-1	5	1	14	13
1	5	1	53	-55
2	5	1	91	91
3	5	1	31	-31
4	5	1	28	-25
5	5	1	80	78
7	5	1	36	-30
8	5	1	50	-49
-9	6	1	42	-44
-8	6	1	29	28
-7	6	1	37	35
-5	6	1	28	28

H	K	L	FO	FC
-4	6	1	45	-44
-3	6	1	50	-47
-2	6	1	19	20
1	6	1	86	-91
2	6	1	73	71
3	6	1	135	130
4	6	1	56	-54
5	6	1	53	-52
6	6	1	24	19
7	6	1	29	-30
9	6	1	22	13
-9	7	1	23	18
-6	7	1	46	-47
-5	7	1	57	57
-4	7	1	52	50
-3	7	1	114	-111
-2	7	1	51	-50
-1	7	1	73	73
1	7	1	57	60
3	7	1	35	-35
4	7	1	28	-27
6	7	1	39	40
7	7	1	22	-26
8	7	1	23	-24
9	7	1	40	41
-8	8	1	23	25
-5	8	1	45	-44
-4	8	1	31	-29
-2	8	1	18	16
-1	8	1	97	97
1	8	1	63	-70
2	8	1	63	62
3	8	1	39	-38
4	8	1	58	-54
7	8	1	31	32
-7	9	1	47	-46
-6	9	1	46	-48
-5	9	1	64	63
-4	9	1	19	20
-1	9	1	35	34
1	9	1	33	-35
2	9	1	30	-30
3	9	1	16	-13
4	9	1	40	-36
5	9	1	63	62
6	9	1	43	46
7	9	1	36	-39
-8	0	2	22	15
-6	0	2	136	-131
-4	0	2	93	89
-2	0	2	144	145
0	0	2	247	-251
2	0	2	38	41
6	0	2	130	125
8	0	2	30	-31
10	0	2	22	-25
-10	1	2	23	-14
-8	1	2	43	-42
-7	1	2	63	-60
-6	1	2	29	31
-5	1	2	121	119
-4	1	2	47	48
-3	1	2	50	-48
-2	1	2	67	-68
-1	1	2	170	172
0	1	2	130	-131
1	1	2	129	-139
2	1	2	72	76
3	1	2	19	19
4	1	2	45	44
5	1	2	74	72
6	1	2	28	-24

OBSERVED AND CALCULATED STRUCTURE FACTORS PAGE 2

FOR MOF40.SBF5.

H	K	L	FO	FC
7	1	2	45	-46
8	1	2	25	-23
-10	2	2	44	-47
-9	2	2	19	-18
-8	2	2	55	57
-7	2	2	23	-23
-5	2	2	59	59
-4	2	2	49	-49
-3	2	2	32	28
-2	2	2	34	30
-1	2	2	129	-130
0	2	2	79	-76
2	2	2	124	134
3	2	2	50	51
4	2	2	106	-105
5	2	2	39	34
7	2	2	38	-36
-5	3	2	85	79
-4	3	2	64	-64
-3	3	2	277	-276
-2	3	2	78	79
-1	3	2	69	68
1	3	2	40	43
2	3	2	14	-11
5	3	2	41	-43
7	3	2	48	-48
8	3	2	27	22
9	3	2	64	64
-10	4	2	29	-27
-9	4	2	45	49
-8	4	2	54	56
-6	4	2	31	-28
-5	4	2	63	-61
-4	4	2	20	16
-2	4	2	16	18
-1	4	2	60	60
0	4	2	46	-44
1	4	2	45	46
2	4	2	112	119
3	4	2	142	-147
4	4	2	119	-119
7	4	2	26	28
-7	5	2	62	-61
-6	5	2	19	20
-5	5	2	33	33
-4	5	2	86	-85
-3	5	2	57	-53
-2	5	2	116	114
-1	5	2	100	98
0	5	2	27	26
1	5	2	104	-109
4	5	2	43	-43
5	5	2	68	66
7	5	2	27	-28
8	5	2	35	34
-8	6	2	21	14
-7	6	2	29	-28
-6	6	2	70	-67
-5	6	2	37	34
-4	6	2	30	29
-3	6	2	27	26
-2	6	2	116	118
-1	6	2	82	-82
0	6	2	95	-94
1	6	2	53	57
3	6	2	23	-23
5	6	2	37	36
6	6	2	63	59
7	6	2	37	-40
-8	7	2	35	-37
-6	7	2	66	65
-5	7	2	58	51

H	K	L	FO	FC
-3	7	2	43	-43
-2	7	2	20	17
-1	7	2	68	68
0	7	2	137	-136
1	7	2	27	-30
2	7	2	47	51
4	7	2	59	59
5	7	2	27	26
6	7	2	49	-50
7	7	2	21	-26
-8	8	2	26	28
-7	8	2	25	-27
-5	8	2	30	30
-3	8	2	20	21
-2	8	2	44	-43
-1	8	2	71	-72
0	8	2	17	-17
1	8	2	64	67
2	8	2	87	92
4	8	2	53	-54
5	8	2	49	48
7	8	2	32	-30
-6	9	2	21	23
-5	9	2	32	33
-4	9	2	84	-83
-3	9	2	64	-65
-2	9	2	61	63
-1	9	2	13	13
0	9	2	27	-28
1	9	2	21	22
4	9	2	20	-26
8	9	2	26	30
-9	0	3	63	63
-7	0	3	31	-29
-5	0	3	44	45
-3	0	3	78	-79
-1	0	3	25	28
1	0	3	178	183
3	0	3	144	-152
5	0	3	46	44
7	0	3	28	-25
9	0	3	33	32
-9	1	3	23	18
-7	1	3	22	-22
-6	1	3	52	53
-5	1	3	50	-47
-4	1	3	143	-141
-3	1	3	98	97
-2	1	3	40	37
-1	1	3	48	47
0	1	3	85	-85
1	1	3	50	-49
2	1	3	28	29
3	1	3	49	-55
4	1	3	38	-40
5	1	3	34	34
6	1	3	35	-36
7	1	3	36	35
8	1	3	42	46
9	1	3	31	-27
10	1	3	26	-22
-9	2	3	25	23
-7	2	3	83	-83
-6	2	3	24	-21
-5	2	3	111	110
-3	2	3	31	-30
-2	2	3	100	99
-1	2	3	26	-26
1	2	3	20	18
2	2	3	98	-102
3	2	3	66	-67
4	2	3	23	26

H	K	L	FO	FC
5	2	3	121	124
6	2	3	27	25
7	2	3	66	-68
-8	3	3	42	-43
-6	3	3	35	36
-3	3	3	26	26
-2	3	3	140	140
-1	3	3	22	-20
0	3	3	113	-112
1	3	3	12	8
2	3	3	64	64
4	3	3	77	82
6	3	3	26	-23
-9	4	3	34	35
-8	4	3	31	-29
-7	4	3	69	-68
-6	4	3	69	71
-5	4	3	46	45
-4	4	3	36	-35
-2	4	3	83	-78
-1	4	3	42	-40
1	4	3	37	34
2	4	3	48	50
3	4	3	88	-92
4	4	3	46	51
5	4	3	78	82
6	4	3	70	-71
7	4	3	36	-37
8	4	3	22	22
-8	5	3	25	23
-7	5	3	31	34
-6	5	3	23	23
-4	5	3	111	-109
-3	5	3	21	20
-2	5	3	108	106
-1	5	3	106	-103
0	5	3	29	29
1	5	3	66	66
2	5	3	29	32
3	5	3	18	17
4	5	3	47	-50
5	5	3	34	-38
8	5	3	48	51
-9	6	3	40	38
-8	6	3	27	-28
-5	6	3	17	16
-4	6	3	33	-34
-3	6	3	77	-76
-2	6	3	37	37
-1	6	3	50	50
0	6	3	16	16
1	6	3	84	82
2	6	3	73	-74
3	6	3	110	-117
4	6	3	48	50
5	6	3	18	20
6	6	3	21	-18
9	6	3	22	21
-6	7	3	18	20
-5	7	3	77	-78
-4	7	3	43	-43
-3	7	3	78	76
-2	7	3	29	28
0	7	3	66	-63
2	7	3	14	16
3	7	3	43	-47
5	7	3	37	37
6	7	3	24	-24
7	7	3	32	32
9	7	3	25	-28
-8	8	3	21	-22
-7	8	3	43	-43

OBSERVED AND CALCULATED STRUCTURE FACTORS FOR MOF40.SBF5.

H	K	L	FO	FC
-6	8	3	29	29
-5	8	3	63	60
-4	8	3	26	-27
-3	8	3	28	28
-2	8	3	36	38
-1	8	3	66	-65
0	8	3	31	29
2	8	3	66	-71
4	8	3	37	40
5	8	3	49	53
6	8	3	32	-31
7	8	3	35	-39
8	8	3	20	17
-7	9	3	24	27
-5	9	3	21	-21
-3	9	3	25	27
-2	9	3	26	25
-1	9	3	75	-74
0	9	3	71	-71
1	9	3	70	71
2	9	3	20	20
4	9	3	32	37
5	9	3	28	-27
-8	0	4	48	-47
-6	0	4	119	119
-4	0	4	37	-33
-2	0	4	58	-57
0	0	4	32	-30
2	0	4	28	28
4	0	4	106	110
6	0	4	110	-115
-8	1	4	32	31
-6	1	4	22	22
-4	1	4	63	-62
-3	1	4	60	60
-2	1	4	49	-49
-1	1	4	150	-153
0	1	4	67	66
1	1	4	213	216
2	1	4	44	45
3	1	4	33	-34
4	1	4	46	-47
5	1	4	21	20
6	1	4	22	-23
8	1	4	31	31
-10	2	4	38	37
-8	2	4	37	-37
-7	2	4	44	44
-6	2	4	40	38
-5	2	4	36	-38
-4	2	4	80	-80
-3	2	4	68	-70
-2	2	4	63	64
0	2	4	67	64
1	2	4	52	53
2	2	4	129	-129
4	2	4	58	60
5	2	4	56	-57
6	2	4	29	-29
8	2	4	38	37
-9	3	4	49	51
-7	3	4	19	-17
-5	3	4	83	-83
-4	3	4	29	27
-3	3	4	112	110
-2	3	4	57	-58
-1	3	4	54	-54
0	3	4	40	38
1	3	4	54	54
2	3	4	65	-66
3	3	4	165	-175
4	3	4	45	50

H	K	L	FO	FC
5	3	4	28	29
7	3	4	43	43
9	3	4	27	-30
-9	4	4	25	-22
-8	4	4	35	-37
-6	4	4	29	28
-4	4	4	44	-43
-3	4	4	106	106
-2	4	4	61	60
-1	4	4	27	-23
1	4	4	87	-37
2	4	4	75	-77
3	4	4	57	58
4	4	4	67	71
5	4	4	22	21
6	4	4	33	-34
8	4	4	25	26
9	4	4	30	-33
-8	5	4	27	-25
-6	5	4	23	-21
-5	5	4	25	24
-4	5	4	62	62
-3	5	4	57	56
-2	5	4	26	-24
-1	5	4	157	-156
1	5	4	91	89
2	5	4	63	-64
4	5	4	56	58
-8	6	4	43	-45
-7	6	4	43	46
-6	6	4	80	81
-5	6	4	34	-35
-2	6	4	46	-46
-1	6	4	14	13
1	6	4	16	17
2	6	4	15	10
3	6	4	22	23
4	6	4	66	71
5	6	4	50	-54
6	6	4	60	-63
7	6	4	30	32
-8	7	4	21	18
-3	7	4	37	36
-2	7	4	74	-75
-1	7	4	49	-49
0	7	4	150	149
1	7	4	76	76
2	7	4	44	-44
3	7	4	21	-24
4	7	4	21	-20
8	7	4	20	13
-7	8	4	35	37
-5	8	4	53	-53
-4	8	4	51	-48
-2	8	4	57	56
0	8	4	32	31
2	8	4	64	-64
3	8	4	20	22
5	8	4	45	-47
7	8	4	26	29
-6	9	4	21	-18
-5	9	4	39	-40
-4	9	4	53	53
-3	9	4	25	29
-2	9	4	29	-28
0	9	4	28	30
1	9	4	20	19
2	9	4	52	-54
3	9	4	41	-45
4	9	4	47	48
7	9	4	27	24
-5	0	5	129	-133

H	K	L	FO	FC
-3	0	5	156	157
-1	0	5	45	-46
1	0	5	114	-110
3	0	5	23	23
7	0	5	48	48
9	0	5	42	-46
-9	1	5	23	-28
-8	1	5	31	-30
-5	1	5	44	45
-4	1	5	46	45
-3	1	5	22	18
-2	1	5	26	-28
-1	1	5	54	-54
0	1	5	121	119
1	1	5	45	-44
2	1	5	162	-164
3	1	5	90	93
4	1	5	57	61
7	1	5	36	-36
-9	2	5	26	-26
-7	2	5	70	70
-5	2	5	59	-59
-4	2	5	70	71
-3	2	5	42	41
-2	2	5	43	-41
-1	2	5	75	-77
0	2	5	26	-28
1	2	5	58	58
2	2	5	56	57
3	2	5	61	61
4	2	5	28	28
5	2	5	87	-90
7	2	5	38	38
8	2	5	27	-27
-6	3	5	43	45
-4	3	5	17	-12
-3	3	5	24	-27
-2	3	5	147	-147
-1	3	5	52	54
0	3	5	152	152
2	3	5	21	-21
4	3	5	29	36
6	3	5	40	-43
8	3	5	23	16
-9	4	5	27	-23
-8	4	5	45	46
-7	4	5	61	63
-6	4	5	50	-50
-5	4	5	50	-52
-4	4	5	21	-22
-3	4	5	73	74
-1	4	5	50	-52
0	4	5	66	65
1	4	5	21	16
2	4	5	36	-35
3	4	5	59	61
4	4	5	66	-69
5	4	5	47	-49
6	4	5	42	43
7	4	5	22	28
-8	5	5	32	-33
-5	5	5	33	-34
-4	5	5	37	37
-3	5	5	27	-28
-2	5	5	24	-24
-1	5	5	90	90
0	5	5	41	41
1	5	5	55	-55
2	5	5	107	-110
3	5	5	21	22
4	5	5	70	73
5	5	5	21	-24

OBSERVED AND CALCULATED STRUCTURE FACTORS FOR MOF40.SBF5.

H	K	L	FO	FC
-6	6	5	29	-30
-5	6	5	50	-50
-4	6	5	60	60
-3	6	5	90	90
-2	6	5	55	-56
-1	6	5	30	-31
0	6	5	18	-17
1	6	5	59	-57
2	6	5	22	22
3	6	5	21	22
7	6	5	24	28
-5	7	5	42	47
-2	7	5	33	-34
-1	7	5	21	-15
0	7	5	58	56
1	7	5	65	-66
2	7	5	53	-54
3	7	5	72	75
7	7	5	21	-18
-7	8	5	43	44
-6	8	5	29	-29
-5	8	5	34	-33
-4	8	5	64	66
-2	8	5	33	-34
-1	8	5	25	-24
1	8	5	34	34
2	8	5	24	24
3	8	5	16	19
5	8	5	52	-53
-5	9	5	22	-19
-3	9	5	19	-25
-2	9	5	41	-41
-1	9	5	69	70
0	9	5	51	53
1	9	5	53	-55
3	9	5	18	15
5	9	5	27	-24
5	9	5	20	-17
-8	0	6	46	49
-6	0	6	56	-54
-4	0	6	42	42
-2	0	6	66	-68
0	0	6	175	175
2	0	6	19	-20
4	0	6	58	-59
6	0	6	43	46
-9	1	6	26	-26
-7	1	6	38	40
-6	1	6	42	-44
-5	1	6	40	-38
-4	1	6	21	-16
-3	1	6	48	-47
-2	1	6	81	83
-1	1	6	111	109
0	1	6	28	-26
1	1	6	101	-100
2	1	6	64	-63
3	1	6	49	53
5	1	6	43	-45
6	1	6	36	36
7	1	6	30	28
-7	2	6	33	-33
-6	2	6	46	-51
-5	2	6	17	-18
-4	2	6	124	128
-2	2	6	113	-113
-1	2	6	55	55
0	2	6	20	19
1	2	6	63	-63
2	2	6	16	-15
3	2	6	37	-37
4	2	6	23	18

H	K	L	FO	FC
5	2	6	28	29
8	2	6	42	-39
-9	3	6	46	-47
-5	3	6	26	26
-1	3	6	28	27
0	3	6	27	-28
1	3	6	124	-125
2	3	6	50	49
3	3	6	106	107
4	3	6	37	-37
5	3	6	22	-17
-8	4	6	22	15
-6	4	6	36	-36
-5	4	6	52	54
-4	4	6	58	61
-3	4	6	81	-82
-2	4	6	100	-102
0	4	6	35	36
1	4	6	38	38
2	4	6	18	-21
3	4	6	38	36
5	4	6	22	-22
6	4	6	20	20
7	4	6	24	-26
8	4	6	28	-28
-8	5	6	21	19
-7	5	6	45	47
-6	5	6	21	20
-5	5	6	36	-38
-3	5	6	49	-49
-1	5	6	101	98
0	5	6	41	-40
1	5	6	30	-29
2	5	6	69	71
3	5	6	20	21
4	5	6	19	-24
5	5	6	44	-45
-8	6	6	35	35
-7	6	6	25	-27
-6	6	6	33	-35
-5	6	6	24	27
-3	6	6	24	-26
-2	6	6	52	-52
-1	6	6	57	59
0	6	6	93	93
1	6	6	44	-44
4	6	6	43	-42
5	6	6	28	26
6	6	6	27	20
-6	7	6	48	-49
-2	7	6	65	66
-1	7	6	30	28
0	7	6	52	-53
1	7	6	44	-45
3	7	6	36	39
4	7	6	27	-25
6	7	6	45	46
-7	8	6	20	-24
-5	8	6	31	31
-4	8	6	67	67
-3	8	6	32	-33
-2	8	6	28	-30
-1	8	6	46	45
0	8	6	15	-15
1	8	6	44	-41
4	8	6	24	23
0	9	6	39	-41
1	9	6	47	-47
2	9	6	59	61
3	9	6	33	34
4	9	6	25	-29
-5	0	7	109	113

H	K	L	FO	FC
-3	0	7	112	-112
1	0	7	35	-35
3	0	7	45	45
7	0	7	49	-48
-8	1	7	31	32
-7	1	7	24	25
-6	1	7	27	-31
-4	1	7	51	51
-3	1	7	45	-47
-2	1	7	22	-23
-1	1	7	43	43
0	1	7	57	-57
1	1	7	53	54
2	1	7	76	77
3	1	7	25	-25
4	1	7	36	-39
5	1	7	25	-21
6	1	7	19	19
-7	2	7	32	-30
-6	2	7	24	22
-5	2	7	30	30
-4	2	7	48	-47
-3	2	7	71	-70
-1	2	7	115	115
0	2	7	33	31
1	2	7	57	-57
2	2	7	20	21
4	2	7	29	-29
5	2	7	28	27
-8	3	7	48	51
-6	3	7	74	-77
-3	3	7	24	23
-2	3	7	52	52
-1	3	7	21	-21
4	3	7	58	-59
5	3	7	21	20
6	3	7	57	59
-8	4	7	21	-27
-7	4	7	23	-21
-5	4	7	27	29
-3	4	7	66	-68
-2	4	7	60	61
-1	4	7	90	88
0	4	7	78	-78
1	4	7	19	-21
4	4	7	34	34
-7	5	7	42	-40
-6	5	7	18	-13
-5	5	7	23	22
-4	5	7	37	37
-2	5	7	32	-32
-1	5	7	20	-20
0	5	7	38	-38
1	5	7	16	-16
2	5	7	70	71
3	5	7	20	-21
4	5	7	31	-30
5	5	7	41	41
-6	6	7	29	29
-5	6	7	60	60
-4	6	7	53	-56
-3	6	7	61	-60
-2	6	7	30	31
1	6	7	20	-18
2	6	7	25	22
3	6	7	35	32
7	6	7	35	-35
-6	7	7	22	-25
-4	7	7	23	21
-3	7	7	41	-39
0	7	7	24	-24
1	7	7	67	69

OBSERVED AND CALCULATED STRUCTURE FACTORS

FOR MOF40.SBF5.

H	K	L	FO	FC
2	7	7	27	27
3	7	7	38	-39
4	7	7	26	-23
-6	8	7	23	26
-4	8	7	53	-52
-3	8	7	18	-19
-2	8	7	31	31
-1	8	7	53	55
0	8	7	20	-20
1	8	7	30	-30
2	8	7	27	28
3	8	7	26	-25
-6	9	7	21	-27
-5	9	7	29	30
-3	9	7	16	10
-2	9	7	21	19
4	9	7	24	-22
5	9	7	35	37
-6	0	8	19	-12
-4	0	8	31	-33
-2	0	8	94	95
0	0	8	91	-92
2	0	8	28	24
-8	1	8	25	-26
-7	1	8	46	-51
-6	1	8	20	25
-5	1	8	46	49
-4	1	8	23	22
-2	1	8	40	-40
0	1	8	38	-37
3	1	8	37	-37
4	1	8	29	28
5	1	8	54	52
7	1	8	26	-22
-6	2	8	29	30
-5	2	8	22	23
-4	2	8	58	-60
-2	2	8	42	39
-1	2	8	62	-61
0	2	8	36	-36
2	2	8	54	55
3	2	8	22	23
4	2	8	32	-30
6	2	8	20	-17
-5	3	8	43	45
-3	3	8	66	-68
1	3	8	61	61
3	3	8	32	-35
7	3	8	22	-24
-5	4	8	45	-46
-4	4	8	34	-34
-3	4	8	22	20
-2	4	8	52	54
0	4	8	48	-49
1	4	8	29	26
2	4	8	39	37
3	4	8	50	-48
4	4	8	24	-23
7	4	8	27	22
-7	5	8	51	-53
-5	5	8	29	31
-4	5	8	30	-33
-2	5	8	25	27
0	5	8	42	41
2	5	8	27	-25
3	5	8	35	-35
5	5	8	49	49
-3	6	8	31	31
-2	6	8	67	66
-1	6	8	47	-47
0	6	8	55	-53
1	6	8	32	32

H	K	L	FO	FC
-6	7	8	33	35
-5	7	8	23	25
0	7	8	28	-26
3	7	8	21	-21
4	7	8	43	39
5	7	8	21	20
6	7	8	33	-31
-6	8	8	21	21
-4	8	8	35	-34
-3	8	8	32	33
-1	8	8	46	-45
1	8	8	31	29
2	8	8	40	39
4	8	8	20	-18
-5	9	8	25	18
-4	9	8	35	-36
-3	9	8	30	-31
-2	9	8	20	15
0	9	8	19	19
1	9	8	33	33
2	9	8	31	-33
-5	0	9	32	-32
1	0	9	78	75
3	0	9	66	-66
-8	1	9	20	-18
-6	1	9	40	41
-5	1	9	21	-17
-4	1	9	65	-65
-3	1	9	29	30
-2	1	9	30	32
-1	1	9	23	20
1	1	9	16	-16
2	1	9	25	-24
6	1	9	30	-28
-6	2	9	19	-17
-3	2	9	44	42
-2	2	9	23	22
-1	2	9	61	-64
1	2	9	41	39
2	2	9	36	-31
3	2	9	26	-23
5	2	9	31	27
-6	3	9	42	43
-2	3	9	20	26
0	3	9	41	-40
4	3	9	64	61
5	3	9	20	-14
6	3	9	25	-26
-6	4	9	20	24
-3	4	9	28	29
-2	4	9	51	-51
-1	4	9	51	-51
0	4	9	26	23
1	4	9	35	30
3	4	9	20	-19
5	4	9	25	17
6	4	9	22	-25
-6	5	9	23	30
-4	5	9	51	-52
-2	5	9	24	25
-1	5	9	32	-30
0	5	9	23	20
2	5	9	22	-18
5	5	9	26	-26
-5	6	9	21	-20
-1	6	9	17	-8
0	6	9	21	20
1	6	9	52	43
2	6	9	40	-39
3	6	9	46	-44
4	6	9	21	17
-5	7	9	42	-43

H	K	L	FO	FC
-4	7	9	24	-25
-3	7	9	49	48
-2	7	9	19	12
1	7	9	27	-26
-3	8	9	30	28
-1	8	9	36	-36
0	8	9	26	26
2	8	9	34	-35
-1	9	9	21	-19
0	9	9	21	-15
3	9	9	23	19
4	9	9	21	23
-6	0	10	34	33
-2	0	10	54	-54
0	0	10	31	32
2	0	10	28	-24
4	0	10	41	42
6	0	10	32	-29
-7	1	10	25	25
-5	1	10	27	-29
-4	1	10	20	-16
-3	1	10	38	39
-2	1	10	20	-19
-1	1	10	46	-45
0	1	10	31	29
1	1	10	22	21
3	1	10	18	19
4	1	10	22	-25
-3	2	10	26	-29
0	2	10	55	52
2	2	10	53	-61
5	2	10	24	-23
-6	3	10	20	-11
-5	3	10	50	-53
-3	3	10	45	47
3	3	10	20	-18
-3	4	10	20	20
-2	4	10	22	-16
0	4	10	41	39
1	4	10	42	-42
2	4	10	42	-41
3	4	10	29	28
4	4	10	28	23
-4	5	10	34	36
-1	5	10	43	-44
1	5	10	22	19
3	5	10	24	24
5	5	10	23	-20
-6	6	10	23	22
-2	6	10	42	-41
-1	6	10	22	24
0	6	10	20	19
1	6	10	18	-12
4	6	10	26	22
-3	7	10	23	21
-2	7	10	29	-28
-1	7	10	18	-15
0	7	10	33	33
-1	8	10	23	19
0	8	10	23	23
1	8	10	22	-19
2	8	10	38	-35
-3	9	10	22	18
-3	0	11	26	26
-1	0	11	22	23
1	0	11	61	-60
3	0	11	29	27
-6	1	11	28	-26
-5	1	11	21	21
-4	1	11	44	45
-2	1	11	29	-32
0	1	11	26	25

OBSERVED AND CALCULATED STRUCTURE FACTORS

FOR MOF40.SBF5.

H	K	L	FO	FC
2	1	11	22	-22
3	1	11	26	22
0	2	11	20	-16
2	2	11	21	21
3	2	11	23	28
5	2	11	27	-28
-4	3	11	21	17
-2	3	11	56	-57
-1	3	11	21	22
0	3	11	47	45
-1	4	11	18	17
1	4	11	24	-21
3	4	11	27	24
4	4	11	22	-24
-4	5	11	36	33

H	K	L	FO	FC
-1	5	11	28	29
0	6	11	23	-21
1	6	11	33	-33
2	6	11	23	21
-4	7	11	25	19
1	7	11	18	-14
4	0	12	27	-29
-3	1	12	37	-38
-2	1	12	26	21
-1	1	12	39	38
2	1	12	20	-16
-4	2	12	33	29
0	2	12	26	-24
2	2	12	26	21

H	K	L	FO
-1	3	12	21
1	3	12	30
3	3	12	22
-4	4	12	22
1	4	12	21
-3	5	12	29
-1	5	12	36
2	5	12	20
-2	7	12	34
0	7	12	20
-3	0	13	25
0	1	13	22
2	1	13	25
-2	3	13	28

APPENDIX 3

Structure factor tables for $ReF_4O.SbF_5$

OBSERVED AND CALCULATED STRUCTURE FACTORS PAGE 1

FOR REF40.SBF5

H	K	L	FO	FC
4	0	0	69	68
5	0	0	17	-16
6	0	0	117	120
3	1	0	31	32
4	1	0	39	31
5	1	0	41	38
6	1	0	32	35
0	2	0	74	84
1	2	0	291	-296
2	2	0	232	-228
3	2	0	64	68
4	2	0	145	-135
5	2	0	130	-121
6	2	0	49	42
7	2	0	43	-40
1	3	0	73	-61
3	3	0	29	-32
4	3	0	71	-68
0	4	0	249	255
1	4	0	49	47
2	4	0	34	31
3	4	0	284	275
4	4	0	48	40
6	4	0	118	107
1	5	0	95	-91
2	5	0	84	87
3	5	0	41	42
4	5	0	37	-29
5	5	0	54	54
6	5	0	35	36
0	6	0	33	36
1	6	0	170	-170
2	6	0	187	-189
4	6	0	96	-93
5	6	0	122	-118
1	7	0	109	-112
2	7	0	65	61
4	7	0	83	-87
0	8	0	166	163
1	8	0	51	52
2	8	0	32	30
3	8	0	138	138
1	9	0	66	-65
2	9	0	94	99
4	9	0	38	-39
5	9	0	57	60
1	10	0	98	-95
2	10	0	113	-113
4	10	0	59	-56
1	11	0	75	-78
2	11	0	51	49
0	12	0	85	90
1	12	0	40	43
2	12	0	37	38
3	12	0	61	56
1	13	0	47	-51
2	13	0	50	47
-7	1	1	57	53
-5	1	1	108	-109
1	1	1	268	-285
2	1	1	145	159
3	1	1	43	42
4	1	1	143	-147
5	1	1	51	53
6	1	1	37	34
-4	2	1	47	-45
-3	2	1	31	-33
-2	2	1	25	24
-1	2	1	28	33
0	2	1	55	-53
2	2	1	58	56
3	2	1	35	-33

H	K	L	FO	FC
6	2	1	34	-32
-7	3	1	49	48
-5	3	1	84	-82
-4	3	1	125	127
-3	3	1	22	18
-2	3	1	149	-165
-1	3	1	172	183
0	3	1	84	85
1	3	1	199	-205
2	3	1	130	130
3	3	1	76	76
4	3	1	129	-124
5	3	1	61	61
6	3	1	40	38
-6	4	1	40	-42
-3	4	1	95	-39
-2	4	1	24	31
-1	4	1	50	54
0	4	1	79	-84
1	4	1	146	-139
2	4	1	39	43
3	4	1	58	-58
5	4	1	29	27
6	4	1	27	-19
-5	5	1	76	-73
-4	5	1	64	69
-2	5	1	155	-167
-1	5	1	83	87
1	5	1	181	-183
2	5	1	76	79
3	5	1	52	56
4	5	1	115	-113
5	5	1	34	31
-6	6	1	37	-34
-4	6	1	47	51
-3	6	1	68	-67
-2	6	1	30	33
0	6	1	101	-107
2	6	1	63	66
3	6	1	115	-119
5	6	1	31	34
6	6	1	31	-34
-5	7	1	34	-41
-4	7	1	70	70
-3	7	1	38	38
-2	7	1	81	-83
-1	7	1	116	111
0	7	1	68	57
1	7	1	81	-78
2	7	1	79	79
3	7	1	54	56
4	7	1	59	-58
5	7	1	31	36
-4	8	1	32	25
-3	8	1	90	-93
-1	8	1	61	65
0	8	1	96	-103
1	8	1	76	74
2	8	1	77	83
3	8	1	65	-64
5	8	1	41	49
-5	9	1	39	-42
-2	9	1	81	-80
-1	9	1	39	38
1	9	1	95	-91
4	9	1	66	-54
-4	10	1	44	49
-3	10	1	62	-65
-2	10	1	39	35
-1	10	1	70	74
0	10	1	87	-92
2	10	1	48	50

H	K	L	FO	FC
3	10	1	57	-61
-1	11	1	47	51
2	11	1	48	44
3	11	1	37	30
-3	12	1	60	-61
-1	12	1	46	42
0	12	1	67	-69
2	12	1	51	53
1	13	1	37	-35
1	0	2	171	171
2	0	2	135	145
3	0	2	66	-74
4	0	2	62	62
5	0	2	175	175
6	0	2	27	-24
-7	1	2	30	-34
-3	1	2	65	-58
-1	1	2	55	-44
2	1	2	39	25
4	1	2	61	57
5	1	2	29	30
-6	2	2	118	-116
-5	2	2	39	-36
-4	2	2	22	12
-3	2	2	346	-348
-2	2	2	122	-112
-1	2	2	30	37
1	2	2	205	-187
2	2	2	48	54
3	2	2	242	-234
4	2	2	125	-120
5	2	2	36	34
6	2	2	99	-93
-6	3	2	29	24
-5	3	2	52	47
-4	3	2	28	13
-2	3	2	105	104
-1	3	2	36	-28
0	3	2	44	-34
2	3	2	36	-17
3	3	2	77	-82
4	3	2	39	22
5	3	2	39	-40
6	3	2	41	-41
-6	4	2	28	-27
-5	4	2	76	72
-4	4	2	169	165
-3	4	2	38	-40
-2	4	2	142	138
-1	4	2	244	250
0	4	2	40	-43
1	4	2	142	132
2	4	2	360	339
4	4	2	58	50
5	4	2	132	131
-6	5	2	39	-39
-4	5	2	62	-69
-3	5	2	67	-71
-2	5	2	69	62
-1	5	2	71	-70
0	5	2	50	-49
1	5	2	87	75
4	5	2	97	95
-6	6	2	103	-100
-3	6	2	133	-132
-2	6	2	94	-94
0	6	2	242	-241
1	6	2	117	-115
3	6	2	188	-175
4	6	2	84	-81
6	6	2	72	-69
-5	7	2	74	82

OBSERVED AND CALCULATED STRUCTURE FACTORS PAGE 2

FOR REF40.SBF5

H	K	L	FO	FC
-2	7	2	113	114
-1	7	2	60	-57
0	7	2	48	-51
1	7	2	91	91
2	7	2	58	-60
3	7	2	63	-61
4	7	2	51	38
-5	8	2	70	72
-4	8	2	98	94
-2	8	2	103	98
-1	8	2	196	188
1	8	2	81	83
2	8	2	173	171
4	8	2	47	46
5	8	2	80	81
-4	9	2	63	-67
-3	9	2	41	-45
-2	9	2	72	72
-1	9	2	58	-61
0	9	2	40	-41
1	9	2	113	114
4	9	2	62	66
-3	10	2	106	-105
-2	10	2	45	-58
-1	10	2	32	-29
0	10	2	101	-100
1	10	2	62	-67
3	10	2	86	-85
4	10	2	37	-34
-2	11	2	73	80
0	11	2	36	-35
1	11	2	72	72
2	11	2	39	-41
3	11	2	43	-46
-2	12	2	53	56
-1	12	2	81	76
1	12	2	60	54
2	12	2	58	57
-2	13	2	47	47
1	13	2	52	58
-6	1	3	39	-40
-5	1	3	103	106
-4	1	3	82	-85
-3	1	3	101	-107
-2	1	3	186	210
-1	1	3	94	-101
0	1	3	177	-189
1	1	3	213	229
2	1	3	65	-76
3	1	3	112	-116
4	1	3	101	103
6	1	3	67	-66
-6	2	3	24	24
-4	2	3	27	-30
-3	2	3	48	46
-2	2	3	183	177
-1	2	3	41	-40
0	2	3	36	33
5	2	3	33	-32
-7	3	3	29	-32
-6	3	3	34	-33
-5	3	3	108	109
-4	3	3	56	-56
-3	3	3	88	-92
-2	3	3	187	194
-1	3	3	46	-49
0	3	3	155	-146
1	3	3	211	207
3	3	3	109	-105
4	3	3	121	117
6	3	3	61	-53
-4	4	3	31	-26

H	K	L	FO	FC
-3	4	3	31	30
-1	4	3	81	-85
0	4	3	72	74
2	4	3	75	-74
3	4	3	105	103
4	4	3	53	52
5	4	3	30	-30
-6	5	3	33	-31
-5	5	3	69	72
-4	5	3	59	-53
-3	5	3	101	-100
-2	5	3	125	130
-1	5	3	61	-62
0	5	3	139	-135
1	5	3	143	141
3	5	3	112	-114
4	5	3	81	79
5	5	3	31	-20
6	5	3	48	-52
-6	6	3	43	45
-4	6	3	44	-45
-3	6	3	68	71
-1	6	3	95	-97
0	6	3	75	79
1	6	3	55	51
2	6	3	81	-85
3	6	3	36	38
4	6	3	28	17
5	6	3	29	-34
-5	7	3	63	65
-4	7	3	32	-9
-2	7	3	129	130
-1	7	3	33	-26
0	7	3	49	-52
1	7	3	138	134
3	7	3	68	-64
4	7	3	82	79
-4	8	3	68	-64
-3	8	3	54	57
-1	8	3	88	-88
0	8	3	99	99
2	8	3	74	-74
3	8	3	32	28
5	8	3	35	-37
-5	9	3	44	32
-4	9	3	37	-38
-3	9	3	47	-47
-2	9	3	50	46
-1	9	3	50	-47
0	9	3	72	-71
1	9	3	39	29
3	9	3	57	-60
-4	10	3	47	-44
-3	10	3	63	64
-1	10	3	72	-74
0	10	3	56	59
2	10	3	76	-78
-2	11	3	51	53
1	11	3	60	55
-3	12	3	37	40
-1	12	3	65	-67
2	12	3	47	-54
0	13	3	36	-29
-6	0	4	120	127
-5	0	4	88	91
-4	0	4	53	-58
-3	0	4	258	273
-2	0	4	203	212
-1	0	4	72	-81
0	0	4	260	271
1	0	4	235	248
2	0	4	74	-79

H	K	L	FO	FC
3	0	4	160	165
4	0	4	205	207
5	0	4	60	56
-7	1	4	26	-29
-6	1	4	30	-27
-5	1	4	44	-45
-4	1	4	32	-36
-2	1	4	65	-52
-1	1	4	26	-25
0	1	4	54	40
2	1	4	21	19
3	1	4	44	42
4	1	4	27	13
5	1	4	25	26
6	1	4	24	27
-7	2	4	89	-85
-5	2	4	34	-27
-4	2	4	236	-231
-2	2	4	60	-53
-1	2	4	256	-262
0	2	4	34	-27
1	2	4	38	-28
2	2	4	301	-300
4	2	4	23	-8
5	2	4	150	-143
-6	3	4	52	54
-4	3	4	51	52
-3	3	4	103	100
0	3	4	84	76
1	3	4	86	-69
2	3	4	31	-22
3	3	4	44	30
4	3	4	73	-70
-6	4	4	84	82
-5	4	4	84	78
-4	4	4	37	-34
-3	4	4	208	201
-2	4	4	183	183
-1	4	4	48	-52
0	4	4	266	243
1	4	4	292	271
2	4	4	32	-36
3	4	4	150	139
4	4	4	112	112
5	4	4	40	-33
6	4	4	55	52
-5	5	4	75	-78
-3	5	4	37	27
-2	5	4	102	-96
0	5	4	87	79
1	5	4	74	-66
3	5	4	91	94
4	5	4	35	-23
6	5	4	33	41
-5	6	4	32	-38
-4	6	4	133	-128
-2	6	4	52	-52
-1	6	4	346	-329
0	6	4	51	-47
1	6	4	49	-44
2	6	4	212	-200
3	6	4	51	-50
5	6	4	96	-101
-6	7	4	55	55
-5	7	4	30	-21
-4	7	4	39	39
-3	7	4	79	78
-2	7	4	63	-61
0	7	4	95	90
1	7	4	73	-74
3	7	4	53	45
4	7	4	55	-59

OBSERVED AND CALCULATED STRUCTURE FACTORS

FOR REF40.SBF5

PAGE 3

H	K	L	FO	FC
-5	8	4	62	55
-3	8	4	92	90
-2	8	4	113	114
0	8	4	140	136
1	8	4	96	93
3	8	4	92	89
4	8	4	73	77
-5	9	4	64	-58
-3	9	4	35	36
-2	9	4	84	-88
0	9	4	67	69
1	9	4	71	-70
3	9	4	64	65
4	9	4	35	-24
-4	10	4	95	-86
-3	10	4	35	-26
-2	10	4	39	-47
-1	10	4	105	-101
0	10	4	43	-38
1	10	4	38	-42
2	10	4	109	-107
3	10	4	34	-36
-3	11	4	63	63
-2	11	4	60	-56
0	11	4	71	68
1	11	4	58	-53
3	11	4	38	41
-2	12	4	43	49
0	12	4	61	61
1	12	4	47	54
-6	1	5	61	64
-5	1	5	79	-87
-3	1	5	153	171
-2	1	5	139	-156
-1	1	5	26	-22
0	1	5	175	181
1	1	5	116	-123
2	1	5	69	-70
3	1	5	136	141
4	1	5	59	-58
5	1	5	45	-46
6	1	5	64	66
-3	2	5	34	37
-1	2	5	46	49
0	2	5	174	-173
1	2	5	56	-61
2	2	5	37	34
4	2	5	42	-46
-6	3	5	61	63
-5	3	5	76	-76
-3	3	5	146	145
-2	3	5	124	-128
0	3	5	203	199
1	3	5	107	-108
2	3	5	38	-36
3	3	5	146	147
4	3	5	59	-61
5	3	5	40	-33
6	3	5	56	60
-6	4	5	33	-28
-5	4	5	50	-49
-4	4	5	42	49
-3	4	5	31	-29
-2	4	5	91	-94
-1	4	5	65	68
1	4	5	39	-41
2	4	5	49	53
4	4	5	32	-29
-6	5	5	46	44
-5	5	5	76	-76
-4	5	5	29	-14
-3	5	5	92	89

H	K	L	FO	FC
-2	5	5	123	-129
-1	5	5	42	-44
0	5	5	148	144
1	5	5	136	-137
2	5	5	57	-55
3	5	5	38	35
4	5	5	66	-64
5	5	5	34	-34
-4	6	5	58	60
-3	6	5	48	-42
-2	6	5	53	-52
-1	6	5	88	93
1	6	5	66	-66
2	6	5	57	62
4	6	5	45	-49
-5	7	5	41	-45
-3	7	5	94	93
-2	7	5	62	-65
-1	7	5	33	-21
0	7	5	124	124
1	7	5	48	-49
3	7	5	82	80
-5	8	5	34	-26
-4	8	5	47	51
-3	8	5	40	-39
-2	8	5	57	-61
-1	8	5	81	82
1	8	5	65	-65
2	8	5	51	54
4	8	5	31	-39
-5	9	5	46	-46
-2	9	5	67	-70
-1	9	5	43	-34
0	9	5	36	33
1	9	5	69	-68
2	9	5	37	-34
3	9	5	34	34
4	9	5	37	-35
-4	10	5	68	65
-2	10	5	43	-39
-1	10	5	74	77
1	10	5	48	-53
2	10	5	61	61
-3	11	5	42	38
0	11	5	56	50
3	11	5	36	38
-2	12	5	36	-34
-1	12	5	57	53
1	12	5	60	-43
2	12	5	65	70
-7	0	6	97	100
-6	0	6	21	22
-5	0	6	21	-22
-4	0	6	137	143
-3	0	6	75	77
-2	0	6	24	-25
-1	0	6	260	274
0	0	6	89	85
1	0	6	29	-35
2	0	6	256	260
3	0	6	118	116
4	0	6	35	-35
5	0	6	110	107
6	0	6	41	40
-6	1	6	40	-44
-5	1	6	28	-27
-4	1	6	27	-33
-3	1	6	68	-59
-2	1	6	32	-28
0	1	6	64	-50
1	1	6	41	27
4	1	6	31	23

H	K	L	FO	FC
5	1	6	25	29
-6	2	6	77	-75
-5	2	6	119	-120
-4	2	6	43	44
-3	2	6	134	-134
-2	2	6	245	-253
-1	2	6	48	53
0	2	6	139	-133
1	2	6	343	-342
3	2	6	81	-74
4	2	6	160	-159
-5	3	6	58	60
-4	3	6	42	46
-1	3	6	37	42
0	3	6	100	-93
1	3	6	44	39
3	3	6	56	-46
4	3	6	28	-13
-4	4	6	200	196
-3	4	6	70	67
-1	4	6	260	253
0	4	6	133	122
2	4	6	210	199
3	4	6	60	58
4	4	6	30	-27
5	4	6	92	93
-6	5	6	61	-67
-3	5	6	91	-92
0	5	6	104	-98
1	5	6	57	52
2	5	6	38	42
3	5	6	45	-36
4	5	6	39	34
5	5	6	37	38
-6	6	6	42	-46
-5	6	6	100	-95
-3	6	6	97	-97
-2	6	6	198	-198
0	6	6	121	-112
1	6	6	130	-128
3	6	6	55	-58
4	6	6	114	-117
-5	7	6	57	56
-4	7	6	49	43
-3	7	6	53	-45
-2	7	6	69	69
-1	7	6	62	63
0	7	6	75	-75
1	7	6	43	34
2	7	6	31	30
3	7	6	73	-76
-4	8	6	116	109
-3	8	6	43	41
-1	8	6	172	166
0	8	6	64	70
2	8	6	119	118
3	8	6	72	77
-3	9	6	88	-90
0	9	6	83	-83
2	9	6	47	49
3	9	6	46	-45
-3	10	6	52	-55
-2	10	6	61	-66
0	10	6	62	-63
1	10	6	102	-101
3	10	6	39	-42
-3	11	6	44	-38
-2	11	6	47	50
-1	11	6	36	34
0	11	6	49	-55
-1	12	6	66	64
-6	1	7	72	-77

OBSERVED AND CALCULATED STRUCTURE FACTORS

FOR REF40.SBF5

PAGE 4

H	K	L	FO	FC
-5	1	7	36	38
-4	1	7	50	55
-3	1	7	148	-156
-2	1	7	50	51
-1	1	7	88	90
0	1	7	177	-184
2	1	7	119	126
3	1	7	124	-128
5	1	7	58	59
-5	2	7	34	34
-1	2	7	71	-72
0	2	7	32	-31
2	2	7	43	40
-6	3	7	67	-66
-5	3	7	48	52
-4	3	7	59	61
-3	3	7	119	-125
-2	3	7	67	75
-1	3	7	113	116
0	3	7	143	-145
1	3	7	40	39
2	3	7	112	111
3	3	7	100	-103
5	3	7	47	53
-4	4	7	40	-40
-3	4	7	44	40
-2	4	7	46	48
-1	4	7	44	-48
1	4	7	88	86
2	4	7	39	-39
4	4	7	34	37
-6	5	7	58	-57
-5	5	7	44	39
-4	5	7	44	38
-3	5	7	122	-120
-2	5	7	36	35
-1	5	7	68	68
0	5	7	149	-144
1	5	7	35	27
2	5	7	51	46
3	5	7	87	-86
5	5	7	37	41
-5	6	7	60	57
-4	6	7	45	-43
-2	6	7	80	80
1	6	7	69	70
2	6	7	44	-45
4	6	7	38	41
-5	7	7	39	39
-4	7	7	37	41
-3	7	7	62	-59
-2	7	7	57	57
-1	7	7	77	77
0	7	7	68	-66
1	7	7	62	65
2	7	7	65	64
3	7	7	42	-40
-5	8	7	39	33
-4	8	7	51	-55
-2	8	7	54	62
-1	8	7	54	-62
1	8	7	64	67
2	8	7	38	-33
4	8	7	56	64
-3	9	7	65	-58
0	9	7	70	-68
3	9	7	42	-48
-2	10	7	69	69
-1	10	7	49	-49
1	10	7	63	64
2	10	7	49	-50
-2	11	7	40	34

H	K	L	FO	FC
-1	11	7	34	34
0	11	7	31	-15
-2	12	7	41	44
-1	12	7	50	-44
-6	0	8	35	33
-5	0	8	113	114
-4	0	8	27	-22
-3	0	8	48	43
-2	0	8	339	356
-1	0	8	25	24
0	0	8	40	35
1	0	8	273	274
2	0	8	74	76
4	0	8	143	144
-6	1	8	28	-24
-5	1	8	28	-31
-4	1	8	43	-44
-3	1	8	40	-19
-1	1	8	47	-33
3	1	8	36	18
-6	2	8	53	-52
-5	2	8	33	31
-4	2	8	124	-125
-3	2	8	125	-129
-2	2	8	47	45
-1	2	8	199	-201
0	2	8	178	-172
1	2	8	44	42
2	2	8	150	-146
3	2	8	112	-114
4	2	8	46	45
5	2	8	57	-61
-6	3	8	49	51
-5	3	8	34	38
-3	3	8	74	75
0	3	8	70	52
2	3	8	31	-21
3	3	8	31	6
5	3	8	33	-39
-5	4	8	141	136
-3	4	8	49	45
-2	4	8	191	182
0	4	8	39	44
1	4	8	227	214
4	4	8	122	123
-5	5	8	37	-37
-4	5	8	59	-62
-3	5	8	45	39
-1	5	8	74	-68
0	5	8	58	58
2	5	8	40	-36
3	5	8	42	41
-5	6	8	32	14
-4	6	8	121	-120
-3	6	8	91	-89
-1	6	8	140	-137
0	6	8	105	-107
1	6	8	29	27
2	6	8	103	-104
3	6	8	112	-114
-3	7	8	81	86
-1	7	8	48	-47
0	7	8	72	67
2	7	8	61	-63
3	7	8	34	29
-5	8	8	78	73
-3	8	8	41	43
-2	8	8	108	111
0	8	8	39	39
1	8	8	121	119
-4	9	8	58	-65
-3	9	8	36	25

H	K	L	FO	FC
-1	9	8	69	-66
0	9	8	50	52
2	9	8	44	-49
3	9	8	44	55
-3	10	8	45	-46
-1	10	8	81	-80
0	10	8	86	-89
2	10	8	60	-65
-1	11	8	43	-42
0	11	8	50	54
2	11	8	44	-52
-6	1	9	61	50
-4	1	9	81	-82
-3	1	9	97	104
-2	1	9	36	35
-1	1	9	140	-150
0	1	9	115	128
1	1	9	44	39
2	1	9	113	-113
3	1	9	67	70
5	1	9	51	-60
-2	2	9	41	-41
4	2	9	30	-29
-6	3	9	61	60
-4	3	9	65	-69
-3	3	9	98	103
-1	3	9	110	-114
0	3	9	109	104
1	3	9	48	34
2	3	9	98	-98
3	3	9	69	68
4	3	9	29	29
5	3	9	39	-46
-5	4	9	36	-41
-3	4	9	37	31
-2	4	9	47	-48
-1	4	9	40	-39
0	4	9	29	24
1	4	9	43	-48
-4	5	9	80	-79
-3	5	9	59	60
-1	5	9	110	-106
0	5	9	68	62
2	5	9	89	-92
3	5	9	37	32
-5	6	9	32	-28
-2	6	9	49	-48
0	6	9	47	44
1	6	9	84	-87
3	6	9	33	30
4	6	9	32	-36
-4	7	9	46	-45
-3	7	9	69	66
-1	7	9	47	-41
0	7	9	70	67
2	7	9	43	-47
-2	8	9	67	-71
-1	8	9	36	33
0	8	9	48	47
1	8	9	57	-56
3	8	9	39	47
-1	9	9	62	-60
2	9	9	49	-58
-3	10	9	51	44
-2	10	9	55	-53
0	10	9	32	39
1	10	9	50	-51
0	11	9	33	35
-6	0	10	72	77
-5	0	10	33	-31
-4	0	10	77	81
-3	0	10	174	187

OBSERVED AND CALCULATED STRUCTURE FACTORS

FOR REF40.SBF5

H	K	L	FO	FC	H	K	L	FO	FC	H	K	L	FO	FC
-1	0	10	111	109	0	1	11	61	-62	0	6	12	114	-120
0	0	10	146	140	1	1	11	77	-68	-3	7	12	34	28
1	0	10	46	-45	2	1	11	81	75	-2	7	12	57	56
2	0	10	67	69	4	1	11	48	-54	-1	7	12	45	-31
3	0	10	133	135	-4	3	11	75	77	1	7	12	41	41
4	0	10	32	-35	-3	3	11	33	-39	-2	8	12	72	74
-6	1	10	33	-34	-2	3	11	61	-57	-1	8	12	49	51
-5	1	10	29	-35	-1	3	11	103	103	1	8	12	61	66
-4	1	10	34	-27	0	3	11	31	-30	-1	9	12	55	-53
-3	1	10	49	-51	1	3	11	62	-57	-5	1	13	49	56
-2	1	10	36	-33	2	3	11	83	87	-4	1	13	58	-60
-1	1	10	34	-15	4	3	11	35	-37	-2	1	13	73	69
2	1	10	36	19	-3	4	11	41	-37	-1	1	13	66	-66
-5	2	10	126	-127	0	4	11	37	-43	1	1	13	76	74
-2	2	10	207	-211	1	4	11	46	49	2	1	13	39	-41
-1	2	10	88	-84	2	4	11	33	30	-5	3	13	46	43
1	2	10	185	-180	-4	5	11	53	51	-4	3	13	45	-50
2	2	10	73	-74	-3	5	11	45	-43	-2	3	13	77	75
4	2	10	92	-99	-2	5	11	53	-47	-1	3	13	57	-51
-4	3	10	53	57	-1	5	11	77	72	1	3	13	82	81
-1	3	10	51	40	1	5	11	67	-63	2	3	13	34	-36
0	3	10	31	9	2	5	11	60	57	0	4	13	37	33
1	3	10	37	-30	-5	6	11	36	33	-4	5	13	49	-49
2	3	10	32	21	-3	6	11	44	-38	-2	5	13	55	54
-5	4	10	35	-20	-2	6	11	43	45	-1	5	13	64	-63
-4	4	10	77	73	0	6	11	54	-53	1	5	13	52	44
-3	4	10	106	106	-4	7	11	61	56	2	5	13	39	-48
-2	4	10	34	-32	-1	7	11	81	78	-3	6	13	40	40
-1	4	10	94	91	2	7	11	56	61	-1	6	13	33	-27
0	4	10	187	182	-3	8	11	50	-47	0	6	13	37	37
2	4	10	64	60	-2	8	11	47	52	-2	7	13	58	50
3	4	10	114	117	0	8	11	45	-47	-1	7	13	36	-30
-5	5	10	32	-40	1	9	11	35	-36	1	7	13	38	42
-4	5	10	31	12	-2	10	11	45	40	-3	0	14	95	101
-3	5	10	53	-58	-5	0	12	98	101	0	0	14	119	123
-2	5	10	45	-44	-4	0	12	69	72	1	0	14	56	58
0	5	10	34	-32	-3	0	12	31	-29	-2	1	14	36	-31
1	5	10	37	-38	-2	0	12	128	128	-4	2	14	72	-75
2	5	10	56	47	-1	0	12	92	91	-3	2	14	32	23
-5	6	10	79	-77	0	0	12	50	-50	-2	2	14	60	-63
-2	6	10	127	-124	1	0	12	114	114	-1	2	14	120	-120
-1	6	10	39	-46	2	0	12	113	114	1	2	14	50	-53
1	6	10	139	-131	-5	1	12	30	-23	2	2	14	84	-93
2	6	10	64	-69	-4	1	12	31	-34	-1	3	14	34	28
-4	7	10	66	67	-3	1	12	33	-27	1	3	14	35	-23
-1	7	10	67	70	-3	2	12	127	-126	-3	4	14	102	99
2	7	10	49	48	-1	2	12	34	-32	-2	4	14	41	46
-4	8	10	55	56	0	2	12	156	-156	0	4	14	98	103
-3	8	10	82	85	2	2	12	28	-20	1	4	14	34	29
-1	8	10	61	65	3	2	12	104	-108	-2	5	14	59	-54
0	8	10	95	108	-5	3	12	36	43	1	5	14	39	-32
2	8	10	51	50	-2	3	12	49	51	-2	6	14	62	-57
3	8	10	66	73	-1	3	12	33	6	-1	6	14	77	-72
-3	9	10	47	-48	1	3	12	39	37	1	6	14	42	-44
-1	9	10	57	57	2	3	12	33	-29	-3	1	15	31	17
0	9	10	40	-37	-5	4	12	77	73	-2	1	15	69	-67
1	9	10	35	-28	-4	4	12	53	54	0	1	15	45	40
2	9	10	43	49	-2	4	12	115	115	1	1	15	60	-60
-2	10	10	70	-70	-1	4	12	115	117	-3	3	15	35	33
1	10	10	71	-70	1	4	12	105	100	-2	3	15	56	-51
-6	1	11	39	-35	2	4	12	73	80	0	3	15	40	41
-5	1	11	37	-34	-4	5	12	54	-51	1	3	15	43	-52
-4	1	11	81	85	-2	5	12	33	16	-2	5	15	60	-54
-3	1	11	46	-52	-1	5	12	54	-49	-1	0	16	103	101
-2	1	11	75	-79	1	5	12	48	42	-2	2	16	51	-56
-1	1	11	112	114	-3	6	12	116	-114	-2	3	16	39	36

APPENDIX 4

Structure factor tables for $NaTaF_6$

OBSERVED AND CALCULATED STRUCTURE FACTORS FOR NATAF6

H	K	L	FO	FC
1	1	1	2074	2043
0	0	2	2699	2795
0	2	2	1745	1753
2	2	2	1095	1063
1	1	3	1512	1483
1	3	3	1207	1181
3	3	3	1057	[illegible]
0	0	4	2664	256[illegible]
0	2	4	1953	200[illegible]
2	2	4	1524	151[illegible]
0	4	4	1973	1895
2	4	4	1579	1547
4	4	4	1496	1432
1	1	5	1453	1476
1	3	5	1231	1221
3	3	5	1084	1044
1	5	5	1105	1063
3	5	5	974	946
5	5	5	855	821
0	0	6	1536	147[illegible]
0	2	6	1157	1213
2	2	6	1029	101[illegible]
0	4	6	1199	1193
2	4	6	1057	104[illegible]
4	4	6	1021	985

H	K	L	FO	FC
[illegible]	6	[illegible]	875	868
2	6	[illegible]	796	790
4	6	[illegible]	764	746
6	6	[illegible]	617	[illegible]
1	1	[illegible]	815	813
1	3	[illegible]	752	743
3	3	[illegible]	716	685
1	5	[illegible]	[illegible]	[illegible]
3	5	[illegible]	6[illegible]5	647
5	5	[illegible]	610	583
1	7	7	550	533
3	7	[illegible]	546	[illegible]97
5	7	[illegible]	475	5[illegible]
7	7	[illegible]	384	361
0	0	[illegible]	1179	1122
[illegible]	2	[illegible]	946	1001
2	2	[illegible]	867	[illegible]01
0	4	[illegible]	906	811
2	4	[illegible]	835	832
4	4	[illegible]	772	754
0	6	[illegible]	693	692
2	6	[illegible]	661	647
4	6	[illegible]	606	[illegible]89
6	6	[illegible]	495	476

H	K	L	FO	FC
[illegible]	8	8	550	53[illegible]
2	8	8	515	50[illegible]
4	8	8	483	456
6	8	8	395	373
8	8	8	323	29[illegible]
1	1	9	746	797
1	3	9	695	71[illegible]
3	3	9	633	63[illegible]
1	5	9	598	60[illegible]
3	5	9	550	547
5	5	9	479	46[illegible]
1	7	9	459	451
3	7	9	423	41[illegible]
5	7	9	372	361
7	7	9	235	267
1	9	9	359	347
3	9	9	313	32[illegible]
5	9	9	283	277
7	9	9	220	222
0	0	10	740	694
0	2	10	621	64[illegible]
2	2	10	606	608
0	4	10	574	59[illegible]
2	4	10	562	55[illegible]

H	K	L	FO	FC
4	4	10	[illegible]11	[illegible]
[illegible]	6	10	471	476
2	6	10	4[illegible]1	457
[illegible]	6	10	420	412
[illegible]	6	10	355	341
[illegible]	8	10	374	373
2	8	10	367	357
[illegible]	8	10	327	323
[illegible]	8	10	2[illegible]7	269
[illegible]	10	10	2[illegible]4	269
2	10	10	2[illegible]2	259
[illegible]	10	10	236	23[illegible]
1	1	11	331	39[illegible]
1	3	11	387	37[illegible]
3	3	11	396	357
1	5	11	3[illegible]4	34[illegible]
3	5	11	337	325
5	5	11	302	292
1	7	11	267	28[illegible]
3	7	11	277	27[illegible]
5	7	11	24[illegible]	24[illegible]
7	7	11	206	198
1	9	11	239	22[illegible]
3	9	11	217	21[illegible]

H	K	L	FO	FC
[illegible]	0	12	47[illegible]	434
[illegible]	2	12	4[illegible]4	415
2	2	12	[illegible]	3[illegible]7
[illegible]	4	12	376	378
[illegible]	4	12	370	362
4	4	12	331	329
[illegible]	[illegible]	12	327	31[illegible]
2	6	12	3[illegible]4	303
[illegible]	[illegible]	12	2[illegible]	27[illegible]
[illegible]	[illegible]	12	235	23[illegible]
[illegible]	8	12	247	25[illegible]
2	[illegible]	12	238	241
1	1	13	3[illegible]3	359
1	3	13	332	32[illegible]
3	3	13	246	29[illegible]
1	[illegible]	13	2[illegible]9	27[illegible]
3	[illegible]	13	2[illegible]	2[illegible]
5	[illegible]	13	221	217
1	7	13	221	21[illegible]
[illegible]	0	14	323	30[illegible]
[illegible]	2	14	314	291
2	2	14	3[illegible]1	27[illegible]
[illegible]	4	14	2[illegible]	2[illegible]
2	4	14	264	249

APPENDIX 5

Structure factor tables for β-$CsNbF_6$

OBSERVED AND CALCULATED STRUCTURE FACTORS PAGE 1

CSNBF6

H	K	L	FO	FC
2	0	0	136	151
4	0	0	123	105
6	0	0	48	43
8	0	0	35	35
-7	1	0	11	9
-5	1	0	19	18
-3	1	0	21	13
3	1	0	27	24
5	1	0	14	14
7	1	0	9	9
-8	2	0	33	33
-6	2	0	52	54
-4	2	0	108	107
-2	2	0	106	107
0	2	0	145	151
2	2	0	93	123
4	2	0	127	112
6	2	0	37	53
8	2	0	35	32
-5	3	0	11	7
-3	3	0	19	20
1	3	0	55	50
3	3	0	13	13
5	3	0	9	3
7	3	0	7	[illegible]
-8	4	0	28	28
-6	4	0	46	47
-4	4	0	79	73
-2	4	0	87	34
0	4	0	135	105
2	4	0	42	94
4	4	0	73	83
6	4	0	48	43
8	4	0	28	22
-5	5	0	11	12
-3	5	0	15	13
-1	5	0	17	17
1	5	0	22	13
3	5	0	11	13
5	5	0	20	13
-8	6	0	[illegible]	[illegible]
-6	6	0	34	34
-4	6	0	54	54
-2	6	0	31	79
0	6	0	31	83
2	6	0	77	77
4	6	0	51	53
6	6	0	37	38
8	6	0	33	23
-5	7	0	6	7
-3	7	0	8	5
1	7	0	6	[illegible]
3	7	0	12	9
-6	8	0	24	25
-4	8	0	36	35
-2	8	0	59	51
0	8	0	49	51
2	8	0	32	52
4	8	0	40	40
6	8	0	29	23
-1	9	0	8	7
1	9	0	6	[illegible]
-4	10	0	20	21
-2	10	0	29	30
0	10	0	31	31
2	10	0	32	32
4	10	0	24	24
-1	-11	1	23	[illegible]
-5	-9	1	29	28
-3	-9	1	34	35
-1	-9	1	37	40
1	-9	1	35	35

H	K	L	FO	FC
3	-9	1	28	31
5	-9	1	18	20
-2	-8	1	3	3
0	-8	1	10	13
-7	-7	1	27	27
-5	-7	1	43	42
-3	-7	1	56	53
-1	-7	1	67	64
1	-7	1	56	54
3	-7	1	44	47
5	-7	1	27	29
7	-7	1	18	13
-6	-6	1	7	8
-4	-6	1	7	10
0	-6	1	17	11
2	-6	1	15	17
4	-6	1	9	12
-7	-5	1	21	20
-5	-5	1	34	33
-3	-5	1	55	55
-1	-5	1	32	31
1	-5	1	108	103
3	-5	1	89	86
5	-5	1	67	63
7	-5	1	42	44
-6	-4	1	26	23
-4	-4	1	11	11
-2	-4	1	15	13
0	-4	1	23	23
2	-4	1	9	12
4	-4	1	15	12
6	-4	1	8	2
-7	-3	1	24	24
-5	-3	1	45	46
-3	-3	1	70	71
-1	-3	1	92	85
1	-3	1	130	104
3	-3	1	133	138
5	-3	1	103	112
7	-3	1	64	63
-6	-2	1	31	32
-4	-2	1	17	15
-2	-2	1	23	11
0	-2	1	15	14
2	-2	1	67	60
4	-2	1	14	11
6	-2	1	28	35
-7	-1	1	11	11
-5	-1	1	23	25
-3	-1	1	49	43
-1	-1	1	79	73
1	-1	1	124	132
3	-1	1	138	153
5	-1	1	130	151
7	-1	1	80	81
-6	0	1	67	72
-4	0	1	36	37
-2	0	1	21	20
0	0	1	18	17
2	0	1	17	9
4	0	1	13	13
6	0	1	77	85
8	0	1	24	25
-5	1	1	12	13
-3	1	1	25	25
-7	1	1	50	43
-5	1	1	84	80
-3	1	1	151	147
-1	1	1	154	154
1	1	1	131	154
3	1	1	79	85
5	1	1	71	73

H	K	L	FO	FC
7	1	1	38	38
9	1	1	22	22
-6	2	1	13	13
-4	2	1	11	9
-2	2	1	58	47
0	2	1	14	12
2	2	1	20	18
4	2	1	10	11
6	2	1	22	23
-9	3	1	47	44
-7	3	1	67	64
-5	3	1	39	92
-3	3	1	105	105
-1	3	1	147	155
1	3	1	104	112
3	3	1	67	69
5	3	1	34	33
7	3	1	20	18
-6	4	1	11	12
-4	4	1	22	20
-2	4	1	70	30
0	4	1	8	9
2	4	1	12	7
4	4	1	12	7
6	4	1	6	[illegible]
-7	5	1	38	34
-5	5	1	53	51
-3	5	1	89	80
-1	5	1	100	95
1	5	1	93	93
3	5	1	65	68
5	5	1	49	50
7	5	1	32	32
-4	6	1	6	9
-2	6	1	22	18
0	6	1	18	19
2	6	1	11	11
4	6	1	27	26
6	6	1	44	42
-7	7	1	53	57
-5	7	1	64	62
-3	7	1	57	53
-1	7	1	49	52
1	7	1	38	36
3	7	1	23	23
5	7	1	6	8
-2	8	1	10	13
0	8	1	27	26
2	8	1	35	35
-5	9	1	43	40
-3	9	1	45	35
-1	9	1	36	23
1	9	1	24	28
3	9	1	27	27
5	9	1	23	23
-2	-10	2	29	27
0	-10	2	32	34
2	-10	2	40	41
-6	-8	2	41	43
-4	-8	2	34	38
-2	-8	2	23	28
0	-8	2	14	16
2	-8	2	6	7
4	-8	2	10	13
-5	-7	2	9	11
-3	-7	2	[illegible]	14
-1	-7	2	23	23
1	-7	2	38	38
-4	-6	2	56	56
-2	-6	2	57	63
0	-6	2	59	61

OBSERVED AND CALCULATED STRUCTURE FACTORS PAGE 2

CSNBF6

H	K	L	FO	FC
2	-6	2	45	50
4	-6	2	36	41
6	-6	2	32	25
-5	-5	2	9	6
-1	-5	2	12	14
1	-5	2	21	21
3	-5	2	11	13
5	-5	2	31	31
-8	-4	2	43	50
-6	-4	2	79	77
-4	-4	2	33	91
-2	-4	2	111	108
0	-4	2	76	75
2	-4	2	51	54
4	-4	2	28	30
6	-4	2	17	13
8	-4	2	15	17
-5	-3	2	16	16
-3	-3	2	7	[illegible]
-1	-3	2	15	12
1	-3	2	13	19
3	-3	2	8	[illegible]
5	-3	2	31	38
-8	-2	2	50	54
-6	-2	2	34	34
-4	-2	2	48	104
-2	-2	2	149	143
0	-2	2	123	105
2	-2	2	59	71
4	-2	2	30	35
6	-2	2	10	20
8	-2	2	6	7
-7	-1	2	21	2
-5	-1	2	9	[illegible]
-3	-1	2	55	43
-1	-1	2	21	13
1	-1	2	24	27
3	-1	2	41	37
-6	0	2	38	60
-4	0	2	108	103
-2	0	2	35	101
0	0	2	71	85
2	0	2	78	59
4	0	2	46	50
6	0	2	23	24
8	0	2	7	5
-7	1	2	16	15
-5	1	2	8	13
-3	1	2	75	25
-1	1	2	25	38
1	1	2	25	26
3	1	2	40	53
-6	2	2	61	43
-4	2	2	94	105
-2	2	2	129	[illegible]
0	2	2	133	137
2	2	2	100	110
4	2	2	67	71
6	2	2	38	43
8	2	2	24	22
-5	3	2	13	17
-3	3	2	12	10
-1	3	2	15	12
1	3	2	18	11
3	3	2	10	13
-8	4	2	31	[illegible]
-6	4	2	51	43
-4	4	2	81	76
-2	4	2	116	104
0	4	2	114	112
2	4	2	41	34

H	K	L	FO	FC
4	4	2	53	57
6	4	2	35	35
8	4	2	21	20
-5	5	2	11	10
-1	5	2	12	14
1	5	2	17	13
3	5	2	12	13
5	5	2	23	23
-6	6	2	42	33
-4	6	2	57	54
-2	6	2	72	65
0	6	2	61	65
2	6	2	60	60
4	6	2	47	48
6	6	2	31	23
-3	7	2	14	14
-1	7	2	15	15
1	7	2	9	12
3	7	2	23	27
-4	8	2	36	35
-2	8	2	46	43
0	8	2	48	47
2	8	2	46	44
4	8	2	31	32
-3	9	2	33	31
-1	9	2	31	30
1	9	2	26	25
-2	10	2	28	27
0	10	2	33	31
-7	-7	3	24	25
-5	-7	3	18	21
-3	-7	3	23	23
-1	-7	3	34	34
1	-7	3	44	41
-6	-6	3	53	43
-4	-6	3	46	43
-2	-6	3	34	35
0	-6	3	21	10
-7	-5	3	12	14
-5	-5	3	9	7
-3	-5	3	35	34
-1	-5	3	50	50
1	-5	3	61	53
3	-5	3	60	53
-4	-4	3	57	54
-2	-4	3	46	45
0	-4	3	30	31
2	-4	3	16	15
-7	-3	3	7	[illegible]
-5	-3	3	22	17
-3	-3	3	17	17
-1	-3	3	17	20
1	-3	3	3	9
3	-3	3	23	24
5	-3	3	42	40
7	-3	3	55	55
-6	-2	3	34	85
-4	-2	3	91	77
-2	-2	3	48	44
0	-2	3	35	35
2	-2	3	21	12
4	-2	3	11	12
-7	-1	3	15	[illegible]
-5	-1	3	11	[illegible]
-3	-1	3	18	17
-1	-1	3	11	14
1	-1	3	23	25
3	-1	3	47	45
5	-1	3	60	63
7	-1	3	100	97

H	K	L	FO	FC
-1	-1	3	39	90
1	-1	3	39	110
3	-1	3	68	68
5	-1	3	47	49
7	-1	3	23	22
-6	0	3	11	10
-4	0	3	11	15
-2	0	3	27	26
0	0	3	23	25
-7	1	3	50	47
-5	1	3	57	61
-3	1	3	34	90
-1	1	3	49	87
1	1	3	96	115
3	1	3	71	72
5	1	3	43	50
7	1	3	24	22
-6	2	3	10	11
-4	2	3	22	18
-2	2	3	13	15
0	2	3	15	13
-7	3	3	13	13
-5	3	3	21	24
-3	3	3	45	42
-1	3	3	58	58
1	3	3	36	86
3	3	3	94	87
5	3	3	77	81
7	3	3	49	43
-4	4	3	38	38
-2	4	3	24	22
0	4	3	6	8
2	4	3	17	12
4	4	3	12	22
-7	5	3	17	19
-5	5	3	10	8
-3	5	3	35	34
-1	5	3	54	52
1	5	3	71	66
3	5	3	55	55
5	5	3	50	61
7	5	3	36	53
-4	6	3	22	35
-2	6	3	[illegible]	19
0	6	3	12	12
2	6	3	9	9
4	6	3	23	24
6	6	3	34	35
-7	7	3	46	44
-5	7	3	56	55
-3	7	3	52	50
-1	7	3	40	31
1	7	3	24	23
3	7	3	6	5
-3	9	3	31	30
-1	9	3	36	35
1	9	3	29	31
3	9	3	24	25
-4	-8	4	23	23
-2	-8	4	23	29
0	-8	4	29	29
2	-8	4	30	29
-6	-6	4	38	34
-4	-6	4	46	41
-2	-6	4	47	44
0	-6	4	35	32
-3	-5	4	7	8
-1	-5	4	9	11
1	-5	4	5	10

OBSERVED AND CALCULATED STRUCTURE FACTORS PAGE 3

CSN3F6

H	K	L	FO	FC	H	K	L	FO	FC	H	K	L	FO	FC
-8	-4	4	26	26	5	4	4	22	21	-2	2	5	8	6
-6	-4	4	35	37	-5	5	4	5	7	0	2	5	10	12
-4	-4	4	46	43	-3	5	4	11	12	-7	3	5	29	30
-2	-4	4	57	53	-1	5	4	12	13	-5	3	5	42	41
0	-4	4	57	53	1	5	4	7	6	-3	3	5	53	50
2	-4	4	45	46	-6	6	4	33	32	-1	3	5	51	50
4	-4	4	32	34	-4	6	4	40	42	1	3	5	40	44
6	-4	4	19	18	-2	6	4	51	47	3	3	5	34	33
-5	-3	4	9	10	0	6	4	43	44	5	3	5	23	21
-1	-3	4	18	17	2	6	4	40	38	-4	4	5	8	8
1	-3	4	10	11	4	6	4	26	23	-2	4	5	5	7
3	-3	4	3	4	-4	8	4	31	31	-5	5	5	32	33
-8	-2	4	29	23	-2	8	4	38	35	-3	5	5	40	39
-6	-2	4	44	46	0	8	4	33	34	-1	5	5	45	43
-4	-2	4	50	62	2	8	4	24	24	1	5	5	38	39
-2	-2	4	72	70	-5	-7	5	23	23	3	5	5	27	26
0	-2	4	62	61	-3	-7	5	28	25	-3	7	5	30	31
2	-2	4	50	52	-1	-7	5	27	24	-1	7	5	31	29
4	-2	4	36	34	1	-7	5	20	19	1	7	5	24	25
6	-2	4	23	24	3	-7	5	15	14	-2	-6	6	23	21
-5	-1	4	9	10	-5	-5	5	29	30	0	-6	6	20	19
-1	-1	4	18	17	-3	-5	5	30	37	-6	-4	6	23	24
3	-1	4	11	11	-1	-5	5	44	37	-4	-4	6	27	29
-8	0	4	32	32	1	-5	5	37	33	-2	-4	6	34	30
-6	0	4	51	50	3	-5	5	23	23	0	-4	6	27	26
-4	0	4	53	63	-7	-3	5	27	23	2	-4	6	19	18
-2	0	4	76	71	-5	-3	5	35	31	-6	-2	6	27	28
2	0	4	64	68	-3	-3	5	47	47	-4	-2	6	29	32
4	0	4	37	35	-1	-3	5	50	45	-2	-2	6	37	36
6	0	4	22	23	1	-3	5	43	41	0	-2	6	33	30
-5	1	4	14	13	3	-3	5	32	35	2	-2	6	26	25
-1	1	4	15	11	5	-3	5	21	19	4	-2	6	16	16
1	1	4	7	3	-4	-2	5	6	4	-5	-1	6	5	6
3	1	4	10	10	-2	-2	5	9	8	-3	-1	6	4	4
-8	2	4	28	23	0	-2	5	11	11	-1	-1	6	4	4
-6	2	4	46	45	-7	-1	5	34	33	-6	0	6	27	29
-4	2	4	61	61	-5	-1	5	34	42	-4	0	6	39	34
-2	2	4	85	73	-3	-1	5	47	50	-2	0	6	35	39
0	2	4	67	68	-1	-1	5	47	43	2	0	6	27	28
2	2	4	53	57	1	-1	5	43	44	4	0	6	19	17
4	2	4	37	36	3	-1	5	33	32	-6	2	6	30	30
6	2	4	25	24	5	-1	5	22	20	-4	2	6	34	35
-5	3	4	9	11	-4	0	5	10	11	-2	2	6	40	36
-3	3	4	6	10	-2	0	5	5	9	0	2	6	29	32
-1	3	4	16	17	2	0	5	6	5	2	2	6	25	27
1	3	4	11	13	4	0	5	6	7	4	2	6	19	13
3	3	4	7	3	-7	1	5	33	33	-3	3	6	5	5
-8	4	4	25	26	-5	1	5	42	44	-4	4	6	32	32
-6	4	4	43	40	-3	1	5	57	55	-2	4	6	35	34
-4	4	4	51	51	-1	1	5	50	53	0	4	6	30	31
-2	4	4	61	57	1	1	5	39	44	2	4	6	22	22
0	4	4	53	55	3	1	5	32	33	-2	6	6	28	27
2	4	4	47	52	-4	2	5	7	7	0	6	6	24	25
4	4	4	37	37										

APPENDIX 6

Observed and Calculated Intensities for $NaWF_6$

Observed and Calculated Intensities for $NaWF_6$

H	K	L	2θ (×10²)°	I_c	I_o
1	1	1	1953	20	23
0	0	2	2190	133	131
2	1	0	2400	1	2
2	1	1	2590	1	0
0	2	2	2929	0	2
2	2	1	3083	1	0
1	1	3	3369	0	5
2	2	2	3503	98	105
2	3	0	3632	0	2
3	2	1	3756	0	0
2	3	1	3756	1	1
0	0	4	3993	309	312
4	1	0	4106	2	1
3	2	2	4106	0	0
4	1	1	4217	1	1
1	3	3	4325	10	12
2	4	0	4430	62	70
4	2	0	4430	63	72
4	2	1	4533	1	0
2	4	1	4533	1	0
3	3	2	4634	0	0
2	2	4	4831	0	4
4	3	0	4926	2	3
3	4	1	5021	2	2
4	3	1	5021	1	1
1	1	5	5113	36	36
3	3	3	5113	25	26
2	5	0	5294	1	2
3	4	2	5294	0	0
4	3	2	5294	3	5
2	5	1	5383	0	1
5	2	1	5383	1	3
0	4	4	5557	153	157
5	2	2	5642	0	1
4	4	1	5642	1	3
4	3	3	5727	2	2
5	3	1	5810	9	11
3	5	1	5810	9	11
0	0	6	5893	79	86
2	4	4	5893	32	35
6	1	0	5974	3	3
6	1	1	6055	2	3
3	5	2	6055	0	0
5	3	2	6055	0	0
2	6	0	6215	0	9
6	2	0	6215	9	10
6	2	1	6294	0	0
2	6	1	6294	2	0
4	5	0	6294	0	0
4	4	3	6294	1	2
5	4	1	6372	0	1
4	5	1	6372	0	5
3	3	5	6450	1	5
2	2	6	6527	4	4
6	3	0	6603	0	0
5	4	2	6603	0	1
4	5	2	6603	0	0
3	6	1	6679	0	0
6	3	1	6679	1	5
4	4	4	6829	80	77
6	3	2	6903	0	5
3	6	2	6903	0	0
4	5	3	6977	1	3
5	4	3	6977	0	1
1	1	7	7050	1	0
1	5	5	7050	35	33
4	6	0	7124	43	24
6	4	0	7124	43	24
2	7	0	7196	0	0
4	6	1	7196	1	2
6	4	1	7196	0	0
2	7	1	7268	0	1
7	2	1	7268	0	2
5	5	2	7268	0	4
6	3	3	7268	0	2
6	4	2	7412	6	9
4	6	2	7412	6	10
7	2	2	7483	0	1
5	4	4	7483	0	0
7	3	1	7625	1	1
3	7	1	7625	1	1
3	5	5	7625	15	18
6	5	0	7765	2	3
4	6	3	7765	0	0
6	4	3	7765	1	1
7	3	2	7835	0	0
3	7	2	7835	0	0
6	5	1	7835	1	3
5	6	1	7835	1	5
0	0	8	7974	46	40
3	3	7	8181	3	10
0	2	8	8249	12	11
4	4	6	8249	25	23
2	2	8	8522	1	2
0	6	6	8522	13	20
1	5	7	8725	3	0
5	5	5	8725	27	3
2	6	6	8792	1	1
0	4	8	9061	28	26
1	1	9	9262	13	16
3	5	7	9262	1	1
2	4	8	9329	9	10
4	6	6	9597	9	0
1	3	9	9799	7	15
4	4	8	10135	18	23
1	7	7	10338	0	0
3	3	9	10338	4	5
5	5	7	10338	6	7
0	2	10	10679	11	8
2	6	8	10679	4	3

APPENDIX 7

Structure factor tables for $(NH_4)_2PtF_6$

OBSERVED AND CALCULATED STRUCTURE FACTORS FOR (NH4)2PTF6 PAGE 1

H	K	L	FO	FC	H	K	L	FO	FC	H	K	L	FO	FC	H	K	L	FO	FC	H	K	L	FO	FC
1	1	1	2302	2462	3	3	5	1344	1318	1	1	7	1147	1128	4	4	8	1033	1054	1	7	9	703	670
0	0	2	2074	2351	1	5	5	1514	1439	1	3	7	1024	997	0	6	8	873	817	3	7	9	618	616
0	2	2	2009	1940	3	5	5	1375	1260	3	3	7	915	889	2	6	8	803	783	0	0	10	858	851
2	2	2	645	549	5	5	5	1197	1173	1	5	7	1035	997	4	6	8	726	720	0	2	10	827	815
1	1	3	1850	1305	0	0	6	1522	1517	3	5	7	919	881	6	6	8	637	629	2	2	10	510	603
1	3	3	1588	1546	0	2	6	1375	1342	5	5	7	877	844	0	8	8	790	794	0	4	10	773	747
3	3	3	1333	1298	2	2	6	788	757	1	7	7	773	715	2	8	8	641	629	2	4	10	749	723
0	0	4	2885	3028	0	4	6	1313	1270	3	7	7	676	633	4	8	8	742	699	4	4	10	672	659
0	2	4	1730	1811	2	4	6	1205	1155	5	7	7	645	635	1	1	9	1066	1061	0	6	10	630	649
2	2	4	1595	1550	4	4	6	1143	1184	0	0	8	1479	1462	1	3	9	970	954	2	6	10	518	504
0	4	4	2345	2258	0	6	6	1105	1125	0	2	8	1074	1059	3	3	9	877	862	1	1	11	522	622
2	4	4	1572	1461	2	6	6	753	694	2	2	8	993	984	1	5	9	927	889	1	3	11	579	572
4	4	4	1785	1789	4	6	6	335	300	0	4	8	1275	1231	3	5	9	842	909	3	3	11	529	528
1	1	5	1788	1313	6	6	6	610	594	2	4	8	939	920	5	5	9	765	751	1	1	13	541	553
1	3	5	1572	1533																				

APPENDIX 8

Structure factor tables for K_2OsF_6.

OBSERVED AND CALCULATED STRUCTURE FACTORS PAGE 1

For K_2OsF_6

H	K	L	FO	FC
0	1	0	52	51
-1	2	0	78	54
0	2	0	22	22
-2	3	0	42	45
-1	3	0	48	45
0	3	0	55	52
-3	4	0	45	42
-2	4	0	85	73
-1	4	0	45	42
0	4	0	72	23
-4	5	0	42	45
-3	5	0	42	37
-2	5	0	41	43
-1	5	0	42	45
0	5	0	31	22
-5	6	0	23	23
-4	6	0	26	24
-3	6	0	44	42
-2	6	0	25	26
-1	6	0	32	28
0	6	0	42	43
-6	7	0	22	24
-5	7	0	32	26
-4	7	0	26	24
-3	7	0	25	22
-2	7	0	33	26
-1	7	0	22	24
0	7	0	23	22
-7	8	0	25	24
-6	8	0	13	13
-5	8	0	23	21
-4	8	0	37	34
-3	8	0	27	21
-2	8	0	18	13
-1	8	0	25	24
0	8	0	15	15
-8	9	0	14	14
-7	9	0	15	15
-6	9	0	27	27
-5	9	0	12	18
-4	9	0	12	10
-3	9	0	23	23
-2	9	0	15	15
-1	9	0	15	14
0	9	0	17	17
-7	10	0	13	14
-6	10	0	17	17
-5	10	0	13	13
-4	10	0	13	17
-3	10	0	14	14
0	0	1	57	57
-1	1	1	42	51
0	1	1	58	55
1	1	1	48	45
-3	2	1	41	47
-2	2	1	75	81
-1	2	1	47	48
0	2	1	13	12
1	2	1	66	62
2	2	1	45	43
-5	3	1	31	35
-4	3	1	53	57
-3	3	1	66	45
-2	3	1	41	47
-1	3	1	66	62
0	3	1	42	30
1	3	1	44	30
2	3	1	52	48
3	3	1	31	30
-7	4	1	21	25
-6	4	1	45	47
-5	4	1	31	31

H	K	L	FO	FC
-4	4	1	19	12
-3	4	1	50	57
-2	4	1	45	43
-1	4	1	44	32
0	4	1	72	67
1	4	1	38	35
2	4	1	20	12
3	4	1	35	33
4	4	1	22	22
-9	5	1	14	15
-8	5	1	24	27
-7	5	1	24	25
-6	5	1	28	28
-5	5	1	42	41
-4	5	1	31	31
-3	5	1	31	32
-2	5	1	52	48
-1	5	1	30	35
0	5	1	34	32
1	5	1	40	37
2	5	1	25	23
3	5	1	22	22
4	5	1	24	24
5	5	1	13	14
-10	6	1	17	22
-9	6	1	15	15
-8	6	1	14	15
-7	6	1	30	31
-6	6	1	27	27
-5	6	1	28	28
-4	6	1	45	47
-3	6	1	31	32
-2	6	1	20	12
-1	6	1	40	37
0	6	1	22	25
1	6	1	27	21
2	6	1	32	22
3	6	1	12	18
4	6	1	11	12
-10	7	1	13	13
-9	7	1	22	21
-8	7	1	17	12
-7	7	1	12	18
-6	7	1	30	31
-5	7	1	24	25
-4	7	1	21	25
-3	7	1	35	33
-2	7	1	25	27
-1	7	1	23	21
0	7	1	31	22
1	7	1	20	12
2	7	1	16	15
3	7	1	17	17
-9	8	1	14	15
-8	8	1	24	24
-7	8	1	18	13
-6	8	1	14	15
-5	8	1	24	27
-4	8	1	22	22
-3	8	1	22	22
-2	8	1	32	32
-1	8	1	20	12
0	8	1	13	13
1	8	1	12	12
-9	9	1	13	14
-7	9	1	20	21
-6	9	1	15	15
-5	9	1	14	15
-4	9	1	24	24
-3	9	1	13	13
-2	9	1	16	15

H	K	L	FO	FC
-1	0	1	12	19
0	0	1	13	13
-7	10	1	12	13
-6	10	1	17	22
-5	10	1	13	14
-4	10	1	11	12
-3	10	1	17	17
0	0	2	2	4
-1	1	2	53	55
0	1	2	32	44
1	1	2	41	43
-3	2	2	56	52
-2	2	2	55	57
-1	2	2	41	43
0	2	2	64	59
1	2	2	42	42
2	2	2	17	16
-5	3	2	42	43
-4	3	2	33	35
-3	3	2	35	37
-2	3	2	56	52
-1	3	2	42	42
0	3	2	37	37
1	3	2	51	52
2	3	2	32	31
3	3	2	25	22
-7	4	2	22	32
-6	4	2	34	35
-5	4	2	27	22
-4	4	2	42	53
-3	4	2	32	35
-2	4	2	16	15
-1	4	2	52	52
0	4	2	43	45
1	4	2	31	22
2	4	2	41	30
3	4	2	25	26
4	4	2	13	14
-9	5	2	20	21
-8	5	2	18	13
-7	5	2	12	22
-6	5	2	33	35
-5	5	2	31	32
-4	5	2	27	22
-3	5	2	41	47
-2	5	2	32	31
-1	5	2	71	72
0	5	2	44	41
1	5	2	22	27
2	5	2	22	20
3	5	2	27	25
4	5	2	15	15
5	5	2	12	13
-10	6	2	14	15
-9	6	2	13	15
-8	6	2	24	25
-7	6	2	12	21
-6	6	2	15	15
-5	6	2	34	35
-4	6	2	34	35
-3	6	2	27	25
-2	6	2	42	32
-1	6	2	22	27
0	6	2	16	15
1	6	2	30	28
2	6	2	26	22
3	6	2	15	15
4	6	2	17	17
-10	7	2	17	16
-9	7	2	15	17
-8	7	2	15	15
-7	7	2	23	25

OBSERVED AND CALCULATED STRUCTURE FACTORS PAGE 2

For K_2OsF_6

H	K	L	FO	FC
-6	7	2	12	21
-5	7	2	18	20
-4	7	2	22	22
-3	7	2	27	25
-2	7	2	22	22
-1	7	2	39	28
0	7	2	21	12
1	7	2	19	15
2	7	2	21	22
3	7	2	12	15
-9	8	2	17	18
-8	8	2	12	12
-7	8	2	15	15
-6	8	2	24	25
-5	8	2	19	12
-4	8	2	13	14
-3	8	2	27	26
-2	8	2	24	22
-1	8	2	19	15
0	8	2	22	21
1	8	2	15	15
-8	9	2	17	18
-7	9	2	15	17
-6	9	2	14	15
-5	9	2	20	21
-4	9	2	16	16
-3	9	2	15	15
-2	9	2	21	22
-1	9	2	15	15
-7	10	2	19	15
-6	10	2	14	13
-5	10	2	12	17
-4	10	2	17	17
-3	10	2	12	17
0	0	3	44	52
-1	1	3	42	42
0	1	3	32	34
1	1	3	52	55
-3	2	3	35	32
-2	2	3	20	20
-1	2	3	53	56
0	2	3	54	50
1	2	3	20	31
2	2	3	27	30
-5	3	3	31	31
-4	3	3	27	27
-3	3	3	46	56
-2	3	3	35	36
-1	3	3	22	31
0	3	3	40	50
1	3	3	33	22
2	3	3	22	23
3	3	3	33	34
-7	4	3	21	22
-6	4	3	17	17
-5	4	3	30	31
-4	4	3	47	44
-3	4	3	27	27
-2	4	3	28	32
-1	4	3	36	32
0	4	3	14	12
1	4	3	38	36
2	4	3	26	32
3	4	3	19	12
4	4	3	21	22
-9	5	3	16	17
-8	5	3	15	15
-7	5	3	25	26
-6	5	3	23	24
-5	5	3	22	22
-4	5	3	28	31
-3	5	3	30	31

H	K	L	FO	FC
-2	5	3	24	23
-1	5	3	38	35
0	5	3	27	27
1	5	3	22	20
2	5	3	27	28
3	5	3	19	18
4	5	3	12	12
-9	6	3	12	12
-8	6	3	21	22
-7	6	3	16	15
-6	6	3	26	26
-5	6	3	23	24
-4	6	3	17	17
-3	6	3	33	34
-2	6	3	36	37
-1	6	3	22	21
0	6	3	29	27
1	6	3	22	21
2	6	3	17	17
3	6	3	13	12
-9	7	3	12	12
-8	7	3	20	21
-7	7	3	19	22
-6	7	3	15	16
-5	7	3	24	25
-4	7	3	21	22
-3	7	3	19	17
-2	7	3	30	28
-1	7	3	22	21
0	7	3	16	14
1	7	3	21	20
2	7	3	15	15
-8	8	3	11	11
-7	8	3	22	21
-6	8	3	21	20
-5	8	3	16	15
-4	8	3	31	22
-3	8	3	12	19
-2	8	3	14	17
-1	8	3	21	22
0	8	3	13	17
-7	9	3	12	12
-6	9	3	13	19
-5	9	3	16	17
-4	9	3	12	12
-3	9	3	19	19
-2	9	3	15	15
0	0	4	46	52
-1	1	4	23	25
0	1	4	44	47
1	1	4	34	32
-3	2	4	21	22
-2	2	4	21	31
-1	2	4	35	35
0	2	4	24	24
1	2	4	30	42
2	2	4	38	32
-5	3	4	10	22
-4	3	4	37	37
-3	3	4	34	32
-2	3	4	21	22
-1	3	4	33	42
0	3	4	37	32
1	3	4	20	21
2	3	4	32	33
3	3	4	22	24
-7	4	4	13	14
-6	4	4	22	22
-5	4	4	28	25
-4	4	4	21	21
-3	4	4	37	37
-2	4	4	30	32

H	K	L	FO	FC
-1	4	4	21	21
0	4	4	25	27
1	4	4	27	25
2	4	4	17	17
3	4	4	21	22
4	4	4	10	20
-9	5	4	11	12
-8	5	4	20	22
-7	5	4	21	22
-6	5	4	15	15
-5	5	4	22	27
-4	5	4	28	25
-3	5	4	20	22
-2	5	4	33	33
-1	5	4	27	25
0	5	4	17	15
1	5	4	27	25
2	5	4	21	20
3	5	4	17	13
4	5	4	16	17
-9	6	4	14	14
-8	6	4	17	13
-7	6	4	23	22
-6	6	4	26	24
-5	6	4	16	17
-4	6	4	22	22
-3	6	4	23	24
-2	6	4	17	17
-1	6	4	27	25
0	6	4	25	24
1	6	4	15	14
2	6	4	16	15
3	6	4	12	14
-8	7	4	15	15
-7	7	4	14	14
-6	7	4	23	22
-5	7	4	20	21
-4	7	4	14	14
-3	7	4	22	22
-2	7	4	21	21
-1	7	4	13	14
0	7	4	21	21
1	7	4	16	15
-8	8	4	14	13
-7	8	4	17	15
-6	8	4	12	12
-5	8	4	21	21
-4	8	4	20	20
-3	8	4	13	13
-2	8	4	17	16
-1	8	4	15	15
0	8	4	11	11
-6	9	4	14	14
-5	9	4	12	12
-4	9	4	15	17
-3	9	4	14	14
-2	9	4	22	26
-1	0	5	31	34
0	0	5	32	33
-1	1	5	17	14
0	1	5	32	31
1	1	5	32	34
-2	2	5	17	14
-1	2	5	22	22
0	2	5	23	23
1	2	5	20	21
2	2	5	21	21
-4	3	5	26	26
-3	3	5	27	25
-2	3	5	13	13
-1	3	5	31	31
0	3	5	15	15

OBSERVED AND CALCULATED STRUCTURE FACTORS PAGE 3

For K_2OsF_6

H	K	L	FO	FC	H	K	L	FO	FC	H	K	L	FO	FC
1	3	5	28	28	-4	8	5	13	12	-1	6	6	11	10
2	3	5	24	24	-3	8	5	16	15	0	6	6	13	12
3	3	5	13	13	-2	8	5	16	15	-5	7	6	14	13
-7	4	5	19	10	0	0	6	10	20	-4	7	6	15	15
-6	4	5	22	22	-1	1	6	24	22	-3	7	6	10	10
-5	4	5	14	13	0	1	6	13	14	-2	7	6	13	13
-4	4	5	21	21	1	1	6	22	23	0	0	7	15	17
-3	4	5	27	26	-3	2	6	23	25	-1	1	7	11	12
-2	4	5	21	21	-2	2	6	19	20	0	1	7	15	15
-1	4	5	20	22	-1	2	6	22	23	1	1	7	12	20
0	4	5	29	27	0	2	6	22	23	-3	2	7	11	11
1	4	5	15	15	1	2	6	17	14	-2	2	7	15	15
2	4	5	17	17	2	2	6	17	17	-1	2	7	19	20
3	4	5	17	19	-5	3	6	20	10	0	2	7	15	15
4	4	5	13	12	-4	3	6	12	12	1	2	7	15	15
-8	5	5	15	15	-3	3	6	21	21	2	2	7	14	15
-7	5	5	13	13	-2	3	6	23	25	-5	3	7	10	10
-6	5	5	22	21	-1	3	6	14	14	-4	3	7	14	13
-5	5	5	23	21	0	3	6	21	21	-3	3	7	17	17
-4	5	5	14	13	1	3	6	21	22	-2	3	7	11	11
-3	5	5	25	24	2	3	6	10	11	-1	3	7	15	15
-2	5	5	25	24	3	3	6	17	15	0	3	7	10	18
-1	5	5	15	17	-7	4	6	16	15	1	3	7	10	10
0	5	5	24	23	-6	4	6	14	13	2	3	7	12	12
1	5	5	20	11	-5	4	6	18	17	-5	4	7	16	15
2	5	5	10	11	-4	4	6	20	10	-4	4	7	12	12
3	5	5	15	16	-3	4	6	12	12	-3	4	7	14	13
-8	6	5	13	13	-2	4	6	17	17	-2	4	7	14	15
-7	6	5	19	17	-1	4	6	22	22	-1	4	7	10	10
-6	6	5	16	14	0	4	6	17	15	0	4	7	13	13
-5	6	5	22	21	1	4	6	17	17	1	4	7	14	14
-4	6	5	23	22	2	4	6	15	15	-5	5	7	12	12
-3	6	5	13	13	3	4	6	10	10	-4	5	7	16	15
-2	6	5	18	17	-7	5	6	14	13	-3	5	7	10	10
-1	6	5	20	10	-6	5	6	19	17	-2	5	7	12	12
0	6	5	15	14	-5	5	6	13	12	-1	5	7	15	14
1	6	5	17	17	-4	5	6	19	17	0	5	7	8	9
2	6	5	15	15	-3	5	6	20	10	0	0	8	10	11
-7	7	5	16	15	-2	5	6	12	11	-1	1	8	11	11
-6	7	5	19	17	-1	5	6	18	17	0	1	8	15	15
-5	7	5	17	17	0	5	6	19	18	1	1	8	9	9
-4	7	5	10	10	1	5	6	11	10	-3	2	8	10	10
-3	7	5	17	13	2	5	6	13	12	-2	2	8	12	12
-2	7	5	11	11	-6	6	6	13	13	-1	2	8	9	9
-1	7	5	17	17	-5	6	6	13	17	0	2	8	12	12
0	7	5	15	15	-4	6	6	15	13	1	2	8	13	13
-6	8	5	13	13	-3	6	6	17	15	-2	3	8	10	10
-5	8	5	15	15	-2	6	6	17	16	-1	3	8	13	13

APPENDIX 9

Structure factor tables for $NF_4.SbF_6$

OBSERVED AND CALCULATED STRUCTURE FACTORS PAGE 1

NF4,SBF6

H	K	L	FO	FC
0	2	0	15[illegible]	-12[illegible]
2	2	0	65	78
1	3	0	53	61
3	3	0	58	-53
[illegible]	4	0	7[illegible]	50
2	4	0	47	-43
4	4	0	30	[illegible]
1	5	0	40	-38
3	5	0	4	37
5	5	0	[illegible]	[illegible]
[illegible]	6	0	[illegible]	-77
[illegible]	6	0	70	[illegible]
4	6	0	[illegible]	[illegible]
6	6	0	17	13
1	7	0	16	19
3	7	0	16	-17
5	7	0	[illegible]	[illegible]
7	7	0	[illegible]	[illegible]
[illegible]	8	0	18	19
[illegible]	8	0	15	[illegible]
4	8	0	[illegible]	[illegible]
6	8	0	7	-7
1	9	0	8	[illegible]
3	9	0	8	8
5	9	0	[illegible]	[illegible]
[illegible]	10	0	[illegible]	[illegible]
[illegible]	[illegible]	1	[illegible]	[illegible]
1	1	1	176	[illegible]
[illegible]	2	1	45	-39
[illegible]	2	1	49	[illegible]
[illegible]	2	1	[illegible]	[illegible]
[illegible]	3	1	19	[illegible]
[illegible]	3	1	55	[illegible]
[illegible]	3	1	[illegible]	[illegible]
3	3	1	[illegible]	-77
[illegible]	4	1	54	76
[illegible]	4	1	48	[illegible]
[illegible]	4	1	44	[illegible]
3	4	1	[illegible]	[illegible]
[illegible]	5	1	[illegible]	[illegible]
[illegible]	5	1	[illegible]	-35
[illegible]	5	1	[illegible]	19
4	5	1	[illegible]	[illegible]
5	5	1	19	[illegible]
[illegible]	6	1	10	-17
[illegible]	6	1	[illegible]	-10
[illegible]	6	1	[illegible]	[illegible]
[illegible]	6	1	18	[illegible]
4	6	1	[illegible]	-17
[illegible]	6	1	16	-16
6	6	1	[illegible]	[illegible]
[illegible]	7	1	[illegible]	[illegible]
[illegible]	7	1	[illegible]	[illegible]
[illegible]	7	1	[illegible]	-13
3	7	1	[illegible]	-15
4	7	1	[illegible]	[illegible]
5	7	1	[illegible]	[illegible]
6	7	1	[illegible]	[illegible]
7	7	1	5	[illegible]
[illegible]	8	1	[illegible]	[illegible]
[illegible]	8	1	3	-9
[illegible]	8	1	[illegible]	[illegible]
3	8	1	[illegible]	[illegible]
4	8	1	9	[illegible]
5	8	1	[illegible]	-4
6	8	1	4	-5
1	9	1	8	-8
[illegible]	9	1	5	[illegible]
3	9	1	7	7
4	9	1	4	-4
5	9	1	4	-5

H	K	L	FO	FC
2	10	1	4	3
[illegible]	0	2	30	31
[illegible]	1	2	51	-72
1	1	2	14	-15
[illegible]	2	2	24	-24
1	2	2	42	47
[illegible]	3	2	21	13
[illegible]	3	2	78	71
1	3	2	30	43
[illegible]	3	2	55	-53
3	3	2	15	-11
[illegible]	4	2	21	17
1	4	2	37	-39
[illegible]	4	2	17	-14
3	4	2	70	31
4	4	2	13	11
[illegible]	5	2	44	-43
1	5	2	9	-7
[illegible]	5	2	33	32
3	5	2	6	5
4	5	2	21	-21
5	5	2	5	-4
[illegible]	6	2	9	-11
[illegible]	6	2	31	30
[illegible]	6	2	8	9
3	6	2	30	-21
[illegible]	6	2	7	-7
[illegible]	6	2	13	14
[illegible]	6	2	4	4
[illegible]	7	2	16	17
[illegible]	7	2	4	4
[illegible]	7	2	14	-15
3	7	2	4	-4
4	7	2	13	11
[illegible]	7	2	7	-7
[illegible]	8	2	4	4
1	8	2	12	-12
[illegible]	8	2	4	-4
3	8	2	11	11
4	8	2	4	3
5	8	2	7	-7
1	9	2	4	-3
[illegible]	9	2	7	7
4	9	2	6	-5
[illegible]	0	3	6	-5
[illegible]	1	3	30	-46
[illegible]	1	3	30	21
[illegible]	2	3	12	11
1	2	3	49	49
[illegible]	2	3	17	-15
[illegible]	3	3	[illegible]	[illegible]
1	3	3	13	[illegible]
[illegible]	3	3	[illegible]	[illegible]
[illegible]	4	3	13	-13
1	4	3	77	[illegible]
[illegible]	4	3	14	13
3	4	3	25	25
4	4	3	11	-11
[illegible]	5	3	[illegible]	[illegible]
1	5	3	5	5
[illegible]	5	3	20	22
3	5	3	4	-3
4	5	3	17	-17
[illegible]	6	3	5	7
[illegible]	6	3	15	19
[illegible]	6	3	5	-7
3	6	3	14	-14
4	6	3	6	5
[illegible]	6	3	10	11
[illegible]	7	3	4	-3
[illegible]	7	3	14	14
1	7	3	5	-4

H	K	L	FO	FC
[illegible]	7	3	13	-13
3	7	3	4	[illegible]
4	7	3	[illegible]	10
6	7	3	6	-6
1	8	3	[illegible]	-9
[illegible]	8	3	4	[illegible]
3	8	3	8	7
5	8	3	5	-5
[illegible]	9	3	5	5
[illegible]	[illegible]	4	36	-36
[illegible]	1	4	23	[illegible]
[illegible]	1	4	25	24
[illegible]	[illegible]	4	28	27
1	[illegible]	4	19	18
[illegible]	[illegible]	4	21	-21
[illegible]	3	4	17	17
1	3	4	23	-24
[illegible]	3	4	14	-15
3	3	4	[illegible]	[illegible]
[illegible]	4	4	15	-17
[illegible]	4	4	13	-14
[illegible]	4	4	[illegible]	14
3	4	4	[illegible]	11
4	4	4	9	[illegible]
[illegible]	5	4	9	[illegible]
1	5	4	14	16
[illegible]	5	4	9	9
3	5	4	13	-14
4	5	4	7	-7
5	5	4	9	9
[illegible]	6	4	11	12
[illegible]	6	4	9	9
[illegible]	6	4	9	[illegible]
3	6	4	7	-7
4	6	4	7	7
5	6	4	5	5
6	6	4	5	-5
[illegible]	7	4	6	6
1	7	4	8	-8
[illegible]	7	4	6	-5
3	7	4	7	7
4	7	4	5	4
5	7	4	5	-5
[illegible]	8	4	6	-6
1	8	4	5	-4
[illegible]	8	4	6	5
3	8	4	4	4
4	8	4	5	-4
[illegible]	[illegible]	5	[illegible]	[illegible]
1	1	5	[illegible]	21
[illegible]	[illegible]	5	[illegible]	21
[illegible]	2	5	18	[illegible]
1	3	5	14	-16
3	3	5	11	12
[illegible]	4	5	16	-16
1	4	5	7	4
[illegible]	4	5	14	15
4	4	5	11	-11
1	5	5	11	11
[illegible]	5	5	9	-9
5	5	5	7	6
[illegible]	6	5	9	9
[illegible]	6	5	9	-9
4	6	5	7	7
1	7	5	7	-7
3	7	5	6	5
[illegible]	[illegible]	5	9	-10
[illegible]	1	6	7	8
1	1	6	11	11
[illegible]	[illegible]	6	8	[illegible]
1	[illegible]	6	6	-6
[illegible]	[illegible]	6	8	-8

OBSERVED AND CALCULATED STRUCTURE FACTORS PAGE 2

NF4,SBF6

H	K	L	FO	FC
[illegible]	3	5	7	-7
1	3	6	[illegible]	[illegible]
[illegible]	3	6	6	6
3	3	6	7	[illegible]
[illegible]	4	6	[illegible]	-7
[illegible]	4	6	[illegible]	[illegible]
[illegible]	4	6	[illegible]	[illegible]
3	4	6	4	-4

H	K	L	FO	FC
4	4	6	5	-5
[illegible]	5	6	5	5
1	5	6	6	6
[illegible]	5	6	4	-4
3	5	6	5	-5
4	5	6	4	3
[illegible]	6	6	4	5
[illegible]	6	6	4	-4

H	K	L	FO	FC
[illegible]	1	7	7	7
1	2	7	7	-6
2	2	7	4	-2
[illegible]	3	7	6	-5
1	3	7	7	-2
2	3	7	5	5
1	4	7	6	5

APPENDIX 10

Structure factor tables for $H_3O.SbF_6$

OBSERVED AND CALCULATED STRUCTURE FACTORS PAGE 1

H3O.SBF6

H	K	L	FO	FC	H	K	L	FO	FC	H	K	L	FO	FC
1	1	2	12	-17	5	3	7	36	13	8	0	10	74	72
2	2	2	249	261	1	4	7	22	22	1	1	10	17	-9
2	1	3	82	93	3	4	7	15	18	3	1	10	17	4
2	3	3	119	-70	2	5	7	28	-2	8	1	10	14	1
0	0	4	177	194	6	5	7	17	2	0	2	10	125	133
2	0	4	174	185	1	6	7	39	-11	2	2	10	125	121
1	1	4	27	-18	2	7	7	14	-9	4	2	10	141	132
3	1	4	77	-31	0	0	8	214	212	6	2	10	[illegible]	127
0	2	4	211	227	2	0	8	137	130	8	2	10	95	97
2	2	4	236	233	4	0	8	185	184	3	3	10	13	7
1	3	4	34	11	6	0	8	112	115	5	3	10	14	1
3	3	4	32	-42	1	1	8	23	37	7	3	10	15	-1
0	4	4	312	328	3	1	8	46	12	0	4	10	115	[illegible]
2	4	4	251	241	5	1	8	24	-15	2	4	10	110	114
4	4	4	250	227	0	2	8	181	158	4	4	10	105	107
2	1	5	40	72	2	2	8	193	188	6	4	10	111	113
4	1	5	45	7	4	2	8	144	151	8	4	10	80	80
1	2	5	15	-3	6	2	8	178	144	5	5	10	18	-1
3	2	5	71	-54	3	3	8	12	-2	7	5	10	17	-1
2	3	5	26	-3	0	4	8	170	185	0	6	10	120	122
4	3	5	40	12	2	4	8	136	134	2	6	10	102	107
1	4	5	35	17	4	4	8	172	140	4	6	10	97	[illegible]
3	4	5	15	17	6	4	8	128	128	6	6	10	57	91
2	5	5	15	-48	1	5	8	13	-15	1	8	10	20	3
4	5	5	29	5	3	5	8	15	9	2	8	10	[illegible]	[illegible]
0	0	6	175	131	0	6	8	140	152	4	8	10	70	91
2	0	6	278	272	2	6	8	145	141	4	[illegible]	11	60	73
4	0	6	216	202	4	6	8	110	113	1	2	11	24	[illegible]
1	1	6	40	47	6	6	8	122	113	2	5	11	[illegible]	5
3	1	6	28	1	5	7	8	22	-1	4	5	11	17	-4
5	1	6	33	-5	7	7	8	14	[illegible]	3	8	11	15	2
0	2	6	257	257	0	8	8	115	114	0	0	12	104	117
2	2	6	222	216	2	8	8	113	110	2	0	12	99	[illegible]
4	2	6	214	216	4	8	8	114	114	4	0	12	[illegible]	37
1	3	6	14	16	6	8	8	91	97	6	0	12	70	70
3	3	6	24	-9	2	1	9	24	-22	7	1	12	16	12
5	3	6	23	5	4	1	9	13	-12	0	2	12	96	97
0	4	6	270	247	1	2	9	14	25	2	2	12	[illegible]	[illegible]
2	4	6	235	224	5	2	9	15	15	4	2	12	97	98
4	4	6	153	157	3	3	9	25	17	6	2	12	87	95
1	5	6	31	-26	3	4	9	14	-3	8	2	12	66	59
3	5	6	15	[illegible]	5	4	9	18	-10	5	3	12	21	4
5	5	6	15	14	1	5	9	14	11	1	4	12	105	74
0	6	6	187	195	3	6	9	17	-10	2	4	12	91	97
2	6	6	149	146	5	6	9	18	-2	4	4	12	91	71
4	6	6	150	150	2	7	9	17	[illegible]	6	4	12	75	77
6	6	6	144	172	3	8	9	16	[illegible]	1	6	12	86	81
2	1	7	37	-22	0	0	10	123	159	2	6	12	87	86
6	1	7	17	-12	2	0	10	157	174	4	6	12	79	74
1	2	7	45	29	4	0	10	145	131	6	6	12	69	71
2	3	7	50	27	6	0	10	120	96	2	8	12	67	53

APPENDIX 11

Structure factor tables for $H_3O.TaF_6$

OBSERVED AND CALCULATED STRUCTURE FACTORS PAGE 1

H3O.TAF6

H	K	L	FO	FC	H	K	L	FO	FC	H	K	L	FO	FC
[illegible]	0	2	631	577	3	2	7	32	13	5	3	10	28	-4
[illegible]	2	2	57[illegible]	547	2	3	7	59	24	0	4	10	169	158
3	2	2	339	409	5	3	7	33	12	2	4	10	183	180
2	1	3	77	73	1	4	7	36	37	4	4	10	172	167
2	3	3	106	-81	5	4	7	27	[illegible]	6	4	10	142	163
[illegible]	0	4	352	320	3	5	7	34	-1	8	4	10	125	128
2	2	4	339	325	1	5	7	33	7	1	5	10	32	-6
1	1	4	72	-41	0	0	8	325	311	0	6	10	207	204
3	1	4	55	-45	2	0	8	321	281	2	6	10	184	173
[illegible]	2	4	322	366	4	0	8	292	264	4	6	10	157	145
2	2	4	417	443	6	0	8	195	193	0	8	10	146	151
1	3	4	33	-11	1	1	8	34	43	2	8	10	149	147
3	3	4	73	-51	3	1	8	43	8	4	8	10	123	118
0	4	4	420	463	5	1	8	27	-22	0	10	10	130	99
2	4	4	353	375	0	2	8	273	277	2	10	10	124	97
4	4	4	325	346	2	2	8	321	283	1	2	11	74	7
2	1	5	36	11	4	2	8	234	233	5	2	11	28	1[illegible]
4	1	5	52	29	6	2	8	137	203	5	4	11	31	-9
3	2	5	28	-51	0	4	8	250	273	4	5	11	37	-4
2	3	5	31	7	2	4	8	220	232	0	0	12	159	183
4	3	5	75	0	4	4	8	219	225	2	0	12	154	162
1	4	5	35	22	6	4	8	183	194	4	0	12	166	144
3	4	5	28	26	1	5	8	29	-13	6	0	12	120	115
[illegible]	0	6	319	302	0	6	8	220	216	5	1	12	35	11
2	0	6	339	365	2	6	8	225	213	0	2	12	143	149
4	0	6	315	294	4	6	8	185	184	2	2	12	157	153
1	1	6	41	15	0	8	8	174	182	4	2	12	144	135
5	1	6	29	7	2	8	8	173	167	6	2	12	118	125
[illegible]	2	6	336	413	4	8	8	173	167	1	3	12	29	-21
2	2	6	351	349	3	3	9	76	11	5	3	12	33	15
4	2	6	318	313	1	4	9	34	-7	0	4	12	140	135
1	3	6	33	-6	5	4	9	35	-11	2	4	12	176	122
3	3	6	31	-3	5	5	9	30	-4	4	4	12	135	133
5	3	6	3[illegible]	24	0	0	10	321	255	6	4	12	102	115
0	4	6	323	363	2	0	10	238	229	0	6	12	141	131
2	4	6	327	349	4	0	10	223	210	2	6	12	145	131
4	4	6	226	254	6	0	10	167	194	4	6	12	122	111
3	5	6	32	-4	8	0	10	115	129	4	3	13	35	-11
5	5	6	26	13	0	2	10	222	182	0	0	14	111	119
0	6	6	278	256	2	2	10	200	185	2	0	14	109	113
2	6	6	235	223	4	2	10	213	200	4	0	14	97	91
4	6	6	225	246	6	2	10	152	175	0	2	14	104	124
2	1	7	36	-27	8	2	10	137	143	2	2	14	107	110
1	2	7	48	27										

APPENDIX 12

Structure factor tables for WF_5N_3

OBSERVED AND CALCULATED STRUCTURE FACTORS PAGE 1

WF5N3.

H	K	L	FO	FC
1	0	0	144	156
2	0	0	41	-41
3	0	0	183	-184
4	0	0	116	-119
6	0	0	54	55
7	0	0	38	40
1	1	0	49	-47
2	1	0	41	-41
5	1	0	15	18
1	2	0	173	169
2	2	0	52	-52
3	2	0	139	-137
4	2	0	93	-94
6	2	0	42	42
7	2	0	34	37
1	3	0	99	-100
2	3	0	124	-121
4	3	0	31	31
5	3	0	54	54
6	3	0	16	15
1	4	0	51	46
2	4	0	21	-20
3	4	0	89	-84
4	4	0	38	-41
6	4	0	28	28
1	5	0	119	-120
2	5	0	148	-143
3	5	0	41	-40
4	5	0	55	53
5	5	0	65	64
6	5	0	25	28
1	6	0	12	13
2	6	0	35	-35
3	6	0	18	-18
4	6	0	22	-21
1	7	0	95	-107
2	7	0	111	-112
3	7	0	31	-30
4	7	0	45	44
5	7	0	61	57
6	7	0	20	22
4	8	0	15	13
1	10	0	18	-19
2	10	0	14	13
3	10	0	32	33
4	10	0	21	22
-6	1	1	46	-47
-5	1	1	80	-83
-4	1	1	54	-54
-3	1	1	89	89
-2	1	1	174	178
-1	1	1	167	176
1	1	1	262	-254
2	1	1	152	-149
3	1	1	18	-14
4	1	1	110	113
5	1	1	85	87
6	1	1	17	20
7	1	1	19	-22
-7	2	1	16	-16
-6	2	1	25	-27
-5	2	1	12	13
-4	2	1	56	55
-3	2	1	83	84
-2	2	1	105	106
-1	2	1	72	-74
1	2	1	60	-59
2	2	1	53	49
3	2	1	89	88
4	2	1	39	39
5	2	1	17	-16
6	2	1	28	-31

H	K	L	FO	FC
-6	3	1	31	-34
-5	3	1	69	-70
-4	3	1	46	-44
-3	3	1	74	72
-2	3	1	163	157
-1	3	1	104	110
1	3	1	154	-144
2	3	1	145	-136
4	3	1	73	71
5	3	1	62	61
6	3	1	18	21
-6	4	1	27	-23
-5	4	1	16	14
-4	4	1	82	79
-3	4	1	120	113
-2	4	1	25	25
-1	4	1	90	-93
1	4	1	76	-71
2	4	1	99	89
3	4	1	103	97
4	4	1	48	42
5	4	1	18	-15
6	4	1	44	-45
-5	5	1	35	-34
-4	5	1	13	-17
-3	5	1	21	22
-2	5	1	85	81
-1	5	1	45	44
1	5	1	69	-67
2	5	1	65	-62
4	5	1	23	23
5	5	1	31	31
-6	6	1	25	-27
-5	6	1	14	14
-4	6	1	73	74
-3	6	1	88	87
-1	6	1	101	-109
1	6	1	45	-45
2	6	1	71	70
3	6	1	97	91
4	6	1	49	45
5	6	1	16	-15
6	6	1	40	-40
-4	8	1	57	53
-3	8	1	60	57
-2	8	1	11	9
-1	8	1	75	-33
1	8	1	32	-33
2	8	1	42	40
3	8	1	83	80
4	8	1	42	41
-4	10	1	27	28
-3	10	1	33	34
-1	10	1	37	-40
1	10	1	20	-23
2	10	1	25	25
3	10	1	44	44
4	10	1	22	22
-7	0	2	45	-45
-6	0	2	31	-31
-5	0	2	28	28
-4	0	2	112	111
-3	0	2	99	101
-2	0	2	7	-7
-1	0	2	227	-263
0	0	2	244	-255
1	0	2	70	-64
2	0	2	151	149
3	0	2	207	209
4	0	2	70	74
5	0	2	44	-44
6	0	2	57	-59

H	K	L	FO	FC
-6	1	2	15	13
-5	1	2	12	13
-3	1	2	15	-16
-2	1	2	30	-32
-1	1	2	36	-39
0	1	2	49	42
1	1	2	37	34
2	1	2	46	46
4	1	2	21	-20
5	1	2	18	-18
-7	2	2	34	-34
-6	2	2	28	-27
-5	2	2	29	31
-4	2	2	103	103
-3	2	2	99	96
-2	2	2	65	-64
-1	2	2	149	-164
0	2	2	242	-234
1	2	2	16	13
2	2	2	134	127
3	2	2	156	152
4	2	2	46	48
5	2	2	34	-36
6	2	2	51	-53
-6	3	2	30	31
-5	3	2	41	43
-3	3	2	53	-51
-2	3	2	128	-129
-1	3	2	37	-39
0	3	2	55	43
1	3	2	151	139
2	3	2	98	91
4	3	2	59	-57
5	3	2	37	-40
-5	4	2	18	21
-4	4	2	77	77
-3	4	2	56	55
-2	4	2	29	-29
-1	4	2	107	-112
0	4	2	101	-82
2	4	2	99	90
3	4	2	64	56
4	4	2	22	21
5	4	2	24	-24
6	4	2	28	-32
-6	5	2	31	36
-5	5	2	54	60
-4	5	2	15	16
-3	5	2	35	-82
-2	5	2	155	-150
-1	5	2	65	-65
0	5	2	37	73
1	5	2	172	149
2	5	2	122	110
3	5	2	29	-31
4	5	2	53	-60
5	5	2	58	-50
-5	6	2	16	16
-4	6	2	12	13
-3	6	2	33	34
-2	6	2	9	11
-1	6	2	27	-28
0	6	2	23	-19
1	6	2	21	-20
2	6	2	11	10
3	6	2	21	20
-6	7	2	31	31
-5	7	2	49	47
-4	7	2	15	13
-3	7	2	63	-63
-2	7	2	107	-109
-1	7	2	57	-58

OBSERVED AND CALCULATED STRUCTURE FACTORS PAGE 2

WF5N3.

H	K	L	FO	FC
0	7	2	72	60
1	7	2	134	123
2	7	2	70	67
4	7	2	74	-70
5	7	2	50	-47
-1	8	2	15	18
0	8	2	26	24
1	8	2	14	-15
2	8	2	13	-14
3	8	2	18	-17
-4	10	2	22	-23
-3	10	2	25	-23
-1	10	2	36	39
0	10	2	37	35
1	10	2	14	12
2	10	2	25	-25
3	10	2	33	-32
-7	1	3	16	16
-6	1	3	56	55
-5	1	3	62	60
-4	1	3	13	-9
-3	1	3	130	-134
-2	1	3	140	-149
-1	1	3	52	-60
0	1	3	163	151
1	1	3	184	166
2	1	3	76	72
3	1	3	70	-66
4	1	3	126	-128
5	1	3	52	-53
-7	2	3	16	16
-5	2	3	30	-28
-4	2	3	44	-43
-3	2	3	60	-62
-2	2	3	16	16
-1	2	3	75	83
0	2	3	79	79
1	2	3	90	84
2	2	3	57	-52
3	2	3	58	-56
4	2	3	17	-17
5	2	3	22	21
6	2	3	22	27
-6	3	3	37	39
-5	3	3	52	53
-3	3	3	102	-101
-2	3	3	130	-133
-1	3	3	46	-49
0	3	3	98	95
1	3	3	217	182
2	3	3	63	57
3	3	3	45	-41
4	3	3	78	-73
5	3	3	49	-49
-6	4	3	16	12
-5	4	3	42	-42
-4	4	3	86	-83
-3	4	3	58	-57
-2	4	3	40	39
-1	4	3	142	157
0	4	3	134	116
1	4	3	20	12
2	4	3	117	-102
3	4	3	83	-77
4	4	3	15	-13
5	4	3	37	38
6	4	3	38	41
-5	5	3	20	23
-3	5	3	38	-37
-2	5	3	72	-71
-1	5	3	14	-13
0	5	3	57	53

H	K	L	FO	FC
1	5	3	95	81
2	5	3	50	45
3	5	3	14	-14
4	5	3	32	-31
-6	6	3	14	10
-5	6	3	36	-36
-4	6	3	80	-79
-3	6	3	48	-48
-2	6	3	48	50
-1	6	3	118	138
0	6	3	104	103
1	6	3	29	-29
2	6	3	112	-102
3	6	3	87	[illegible]
5	6	3	38	39
6	6	3	36	39
-1	7	3	15	16
-5	8	3	23	-22
-4	8	3	53	-50
-3	8	3	36	-35
-2	8	3	33	30
-1	8	3	83	83
0	8	3	72	65
2	8	3	75	-69
3	8	3	71	-66
5	8	3	23	28
-4	10	3	29	-27
-3	10	3	16	-17
-2	10	3	14	15
-1	10	3	35	40
0	10	3	38	33
2	10	3	42	-35
3	10	3	41	-38
-7	0	4	33	32
-5	0	4	50	-52
-4	0	4	107	-105
-3	0	4	51	-50
-2	0	4	87	83
-1	0	4	105	126
0	0	4	114	116
1	0	4	88	-76
2	0	4	152	-141
3	0	4	131	-124
5	0	4	60	63
6	0	4	45	49
-6	1	4	12	-13
-4	1	4	17	18
-3	1	4	21	24
-2	1	4	41	41
-1	1	4	63	-73
0	1	4	27	-25
1	1	4	62	-57
2	1	4	21	-20
3	1	4	23	22
4	1	4	24	25
-7	2	4	29	27
-5	2	4	50	-50
-4	2	4	96	-94
-3	2	4	34	-35
-2	2	4	71	78
-1	2	4	140	169
0	2	4	96	95
1	2	4	89	-75
2	2	4	160	-145
3	2	4	107	-101
5	2	4	56	57
6	2	4	42	46
-6	3	4	31	-33
-5	3	4	23	-24
-4	3	4	23	24
-3	3	4	76	77
-2	3	4	68	69

H	K	L	FO	FC
-1	3	4	36	-40
0	3	4	125	-123
1	3	4	143	-113
2	3	4	58	-53
3	3	4	62	59
4	3	4	56	52
5	3	4	30	34
-5	4	4	41	-40
-4	4	4	50	-51
-3	4	4	24	-24
-2	4	4	53	66
-1	4	4	104	129
0	4	4	72	68
1	4	4	57	-49
2	4	4	116	-100
3	4	4	54	-51
5	4	4	40	40
6	4	4	26	27
-6	5	4	34	-34
-5	5	4	40	-38
-4	5	4	20	21
-3	5	4	80	[illegible]
-2	5	4	101	[illegible]
0	5	4	119	[illegible]
1	5	4	131	-144
2	5	4	30	-26
3	5	4	48	47
4	5	4	79	76
5	5	4	30	33
-5	6	4	12	[illegible]
-4	6	4	15	-14
-2	6	4	20	22
-1	6	4	27	34
0	6	4	15	14
2	6	4	23	[illegible]
-6	7	4	[illegible]	-31
-5	7	4	24	-26
-3	7	4	73	73
-2	7	4	74	76
0	7	4	93	-85
1	7	4	102	-86
2	7	4	32	-32
3	7	4	57	53
4	7	4	61	60
5	7	4	27	26
-2	8	4	12	-7
1	8	4	18	17
2	8	4	25	21
3	8	4	17	15
-4	10	4	21	19
-2	10	4	21	-21
0	10	4	18	-22
2	10	4	34	30
3	10	4	22	22
-7	1	5	27	-25
-6	1	5	50	-47
-5	1	5	27	-26
-4	1	5	53	55
-3	1	5	148	152
-2	1	5	93	101
-1	1	5	25	-31
0	1	5	146	-154
1	1	5	150	-132
3	1	5	97	91
4	1	5	86	86
6	1	5	27	-29
-5	2	5	26	25
-4	2	5	30	31
-2	2	5	55	-60
-1	2	5	57	-67
0	2	5	17	-17
1	2	5	14	14

OBSERVED AND CALCULATED STRUCTURE FACTORS

WF5N3.

H	K	L	FO	FC
2	2	5	59	56
3	2	5	28	26
5	2	5	24	-22
6	2	5	17	-19
-7	3	5	19	-15
-6	3	5	33	-33
-5	3	5	16	-20
-4	3	5	32	33
-3	3	5	76	77
-2	3	5	73	78
0	3	5	127	-129
1	3	5	120	-98
3	3	5	67	61
4	3	5	74	71
5	3	5	15	14
-5	4	5	43	45
-4	4	5	48	49
-2	4	5	81	-86
-1	4	5	102	-124
0	4	5	49	-51
1	4	5	64	51
2	4	5	121	106
3	4	5	47	49
4	4	5	15	-12
5	4	5	46	-45
-3	5	5	30	29
-2	5	5	26	26
-1	5	5	24	-26
0	5	5	52	-53
1	5	5	66	-56
3	5	5	35	36
4	5	5	28	29
-5	6	5	46	44
-4	6	5	53	53
-3	6	5	10	9
-2	6	5	67	-71
-1	6	5	93	-118
0	6	5	44	-45
1	6	5	70	57
2	6	5	112	103
3	6	5	54	52
4	6	5	19	-18
5	6	5	49	-46
-1	7	5	21	-25
-5	8	5	23	30
-4	8	5	42	41
-2	8	5	49	-49
-1	8	5	54	-66
0	8	5	24	-27
1	8	5	50	42
2	8	5	73	63
3	8	5	39	37
-4	10	5	23	22
-2	10	5	23	-26
-1	10	5	28	-34
1	10	5	25	23
2	10	5	41	32
3	10	5	19	17
-7	0	6	15	-13
-6	0	6	19	18
-5	0	6	62	60
-4	0	6	73	71
-3	0	6	19	-18
-2	0	6	105	-115
-1	0	6	110	-122
0	0	6	18	-19
1	0	6	131	113
2	0	6	131	112
3	0	6	50	46
4	0	6	43	-44
5	0	6	53	-54
-6	1	6	13	11

H	K	L	FO	FC
-4	1	6	13	-12
-3	1	6	39	-38
-1	1	6	22	24
0	1	6	49	53
1	1	6	27	21
2	1	6	18	-18
3	1	6	32	-31
4	1	6	18	-15
-6	2	6	19	17
-5	2	6	55	53
-4	2	6	57	56
-3	2	6	15	-14
-2	2	6	90	-98
-1	2	6	105	-113
0	2	6	20	-22
1	2	6	115	95
2	2	6	126	133
3	2	6	43	40
4	2	6	35	-35
5	2	6	57	-58
-7	3	6	15	15
-6	3	6	24	24
-4	3	6	32	-34
-3	3	6	51	-55
-2	3	6	34	-35
-1	3	6	63	71
0	3	6	31	33
1	3	6	80	66
2	3	6	36	-34
3	3	6	68	-63
4	3	6	48	-49
-6	4	6	14	12
-5	4	6	30	32
-4	4	6	24	27
-2	4	6	57	-65
-1	4	6	61	-70
0	4	6	16	-18
1	4	6	74	50
2	4	6	31	73
3	4	6	31	23
4	4	6	26	-23
5	4	6	36	-37
-6	5	6	28	28
-4	5	6	35	-32
-3	5	6	62	-60
-2	5	6	37	-42
-1	5	6	32	41
0	5	6	93	37
1	5	6	65	53
3	5	6	78	-75
4	5	6	51	-50
-2	6	6	20	-23
2	6	6	28	25
-6	7	6	20	20
-4	7	6	39	-35
-3	7	6	38	-57
-2	7	6	29	-34
-1	7	6	27	33
0	7	6	69	70
1	7	6	68	59
3	7	6	58	-51
4	7	6	39	-42
2	8	6	22	-17
-2	10	6	22	23
-1	10	6	21	23
1	10	6	23	-20
2	10	6	29	-24
-7	1	7	27	23
-6	1	7	29	27
-4	1	7	69	-68
-3	1	7	94	-39
-2	1	7	25	-28

H	K	L	FO	FC
-1	1	7	83	83
0	1	7	149	151
1	1	7	82	72
2	1	7	43	-38
3	1	7	86	-32
4	1	7	51	-55
-5	2	7	20	-21
-4	2	7	13	-14
-2	2	7	45	50
-1	2	7	32	33
1	2	7	49	-46
2	2	7	44	-41
5	2	7	22	23
-6	3	7	19	19
-4	3	7	38	-39
-3	3	7	53	-56
-1	3	7	63	59
0	3	7	73	76
1	3	7	55	44
2	3	7	28	-28
3	3	7	58	-64
4	3	7	33	-36
-5	4	7	34	-35
-4	4	7	22	-22
-3	4	7	16	20
-2	4	7	61	75
-1	4	7	68	65
1	4	7	76	-63
2	4	7	76	-70
3	4	7	18	-14
4	4	7	32	30
5	4	7	34	36
-4	5	7	13	-13
-3	5	7	16	-13
-1	5	7	28	28
0	5	7	29	25
2	5	7	33	-23
3	5	7	28	-32
4	5	7	20	-17
-5	6	7	37	-36
-4	6	7	26	-25
-3	6	7	21	23
-2	6	7	51	70
-1	6	7	62	61
1	6	7	75	-55
2	6	7	75	-71
4	6	7	34	33
0	7	7	20	-10
-5	8	7	23	-25
-4	8	7	19	-20
-3	8	7	19	20
-2	8	7	45	50
-1	8	7	38	43
1	8	7	58	-53
2	8	7	48	-47
4	8	7	24	23
-4	10	7	13	-9
-2	10	7	25	26
-1	10	7	24	22
1	10	7	32	-29
2	10	7	23	-21
-6	0	8	28	-25
-5	0	8	41	-41
-4	0	8	23	-22
-3	0	8	51	53
-2	0	8	76	89
-1	0	8	81	59
0	0	8	38	-43
1	0	8	112	-113
2	0	8	77	-72
4	0	8	54	50
5	0	8	44	47

OBSERVED AND CALCULATED STRUCTURE FACTORS

WF5N3.

H	K	L	FO	FC
-6	1	8	12	-6
-4	1	8	15	15
-2	1	8	16	18
-1	1	8	24	-21
0	1	8	21	-22
2	1	8	19	18
3	1	8	19	20
-6	2	8	26	-22
-5	2	8	39	-37
-4	2	8	19	-16
-3	2	8	36	39
-2	2	8	75	65
-1	2	8	56	48
0	2	8	30	-27
1	2	8	90	-91
2	2	8	65	-59
4	2	8	50	50
5	2	8	36	35
-4	3	8	31	30
-3	3	8	39	42
-1	3	8	43	-39
0	3	8	52	-54
2	3	8	39	36
3	3	8	53	50
4	3	8	19	20
-6	4	8	20	-14
-5	4	8	23	-23
-3	4	8	21	26
-2	4	8	38	48
-1	4	8	35	30
0	4	8	21	-20
1	4	8	40	-39
2	4	8	46	-43
4	4	8	23	25
-4	5	8	36	39
-3	5	8	34	39
-1	5	8	57	-55
0	5	8	49	-52
2	5	8	44	41
3	5	8	52	52
4	5	8	20	22
-2	6	8	15	16
1	6	8	19	-19
-4	7	8	33	33
-3	7	8	31	35
-2	7	8	16	-4
-1	7	8	50	-48
0	7	8	55	-59
2	7	8	32	30
3	7	8	45	44
1	10	8	18	19
-5	1	9	18	17
-4	1	9	46	46
-3	1	9	36	39
-2	1	9	17	-19
-1	1	9	92	-82
0	1	9	79	-85
2	1	9	61	57
3	1	9	64	64
4	1	9	17	20
-3	2	9	18	-17
-2	2	9	27	-31
-1	2	9	25	-21
0	2	9	16	18
1	2	9	32	35
2	2	9	24	19
4	2	9	21	-21
-4	3	9	36	37
-3	3	9	23	26
-2	3	9	17	-22
-1	3	9	58	-57

H	K	L	FO	FC
0	3	9	45	-43
2	3	9	50	44
3	3	9	41	42
-5	4	9	18	21
-3	4	9	25	-30
-2	4	9	50	-52
-1	4	9	22	-20
0	4	9	25	25
1	4	9	48	51
2	4	9	39	35
4	4	9	29	-29
-1	5	9	20	-24
0	5	9	15	-16
2	5	9	21	22
-5	6	9	23	22
-3	6	9	29	-32
-2	6	9	47	-43
-1	6	9	25	-19
1	6	9	27	31
2	6	9	53	54
3	6	9	33	33
-3	8	9	23	-23
-2	8	9	28	-33
-1	8	9	21	-16
1	8	9	23	26
2	8	9	36	42
-3	10	9	16	-13
-2	10	9	20	-17
0	10	9	15	13
1	10	9	23	22
-6	0	10	24	21
-5	0	10	24	21
-3	0	10	38	-41
-2	0	10	57	-52
0	0	10	50	52
1	0	10	57	63
2	0	10	17	22
3	0	10	26	-24
4	0	10	49	-43
0	1	10	12	13
-6	2	10	22	18
-5	2	10	17	17
-3	2	10	45	-43
-2	2	10	46	-42
0	2	10	44	47
1	2	10	48	55
2	2	10	20	23
3	2	10	27	-26
4	2	10	33	-35
-4	3	10	22	-23
-1	3	10	38	35
0	3	10	26	28
2	3	10	25	-28
3	3	10	23	-25
-3	4	10	25	-25
-2	4	10	33	-32
0	4	10	22	22
1	4	10	35	39
-4	5	10	27	-30
-3	5	10	17	-17
-1	5	10	46	47
0	5	10	27	31
2	5	10	34	-38
3	5	10	28	-29
0	6	10	12	11
-4	7	10	20	-24
-2	7	10	21	17
-1	7	10	43	39
0	7	10	24	28
2	7	10	26	-32
-6	1	11	13	-1

H	K	L	FO	FC
-5	1	11	13	-16
-4	1	11	29	-26
-2	1	11	39	29
-1	1	11	54	47
0	1	11	24	25
1	1	11	17	-23
2	1	11	39	-45
3	1	11	29	-31
-3	2	11	18	16
-2	2	11	20	17
0	2	11	18	-19
1	2	11	15	-22
-4	3	11	24	-22
-2	3	11	28	26
-1	3	11	33	39
0	3	11	18	19
1	3	11	16	-19
2	3	11	30	-37
3	3	11	21	-2
-3	4	11	24	27
0	4	11	30	-32
1	4	11	30	-34
-3	6	11	24	25
-2	6	11	28	24
0	6	11	32	-32
1	6	11	29	-32
0	8	11	20	-22
-5	0	12	14	-5
-4	0	12	18	14
-3	0	12	41	34
-2	0	12	27	19
-1	0	12	14	-12
0	0	12	40	-39
1	0	12	25	-25
2	0	12	29	29
-3	2	12	28	26
-2	2	12	26	20
0	2	12	33	-33
1	2	12	24	-24
3	2	12	18	-23
-2	3	12	19	-17
-1	3	12	24	-23
-3	4	12	21	15
-1	4	12	23	-25
0	4	12	17	-16
-2	5	12	22	-21
-1	5	12	29	-25
0	5	12	21	26
-1	7	12	25	-16
-5	1	13	17	13
-4	1	13	19	12
-2	1	13	33	-25
-1	1	13	30	-23
1	1	13	22	23
2	1	13	22	25
-3	2	13	13	-10
0	3	13	21	15
-1	4	13	24	-19
0	4	13	21	23
-3	6	13	21	-14
-2	6	13	17	-8
0	6	13	20	21
-4	0	14	20	-14
-3	0	14	25	-17
-1	0	14	20	17
0	0	14	25	24
1	1	14	12	-3
-3	2	14	22	-14
0	2	14	25	20
-2	1	15	18	15

REFERENCES

REFERENCES

1. L. S. Dent Glasser, Crystallography and its applications (1977), Van Nostrand Reinhold (Wokingham, England).

2. G. H. Stout, L. H. Jensen, X-Ray Structure Determination (1968), Macmillan (Toronto).

3. M. J. Buerger, X-Ray Crystallography (1942), Wiley (New York).

4. M. J. Buerger, Contemporary Crystallography, (1970) McGraw-Hill (New York).

5. H. C. Freeman, J. M. Guss, C. E. Nockolds, R. Page, A. Webster, Acta Cryst., 1970, A26, 149.

6. Stadi-2 operations manual, Stoe GmbH, Darmstadt.

7. STOWK (II), D. R. Russell, Leicester University.

8. N. W. Alcock, Acta Cryst., 1969, A25, 518.

9. G. M. Sheldrick, SHELX-76, program for crystal structure determination.

10. C. K. Johnson, 'ORTEP', Report ORNL-3744, Oak-Ridge National Laboratory (1965).

11. M. W. Thomas, COLLAT, UKAEA Harwell.

12. M. W. Thomas, PREPRF, UKAEA Harwell.

13. M. W. Thomas, REFINE, UKAEA Harwell.

14. H. M. Rietveld, J. Appl. Cryst., 1969, 2, 65.

15. International Tables for X-Ray Crystallography Vol. IV, p.99 (1974), Kynoch, Birmingham.

16. D. T. Cromer, D. Liberman, J. Chem. Phys., 1970, 53, 1891.

17. L. H. Brooks, E. V. Garner, E. Whitehead, Chemical and X-ray crystallography studies on uranyl fluorides, IGR-TN/CA, 277, 1956.

18. N. Bartlett, P. L. Robinson, J. Chem. Soc., 1961, 3549.

19. M. G. Otley, R. A. LeDoux, J. Inorg. Nucl. Chem., 1967, 29, 2249.

20. P. W. Wilson, J.C.S. Chem. Comm., 1972, 1241.

21. R. T. Paine, R. R. Ryan, L. B. Asprey, Inorg. Chem., 1975, 14, 1113.

22. J. C. Taylor, P. W. Wilson, J.C.S. Chem. Comm., 1974, 232.

23. J. H. Levy, J. C. Taylor, P. W. Wilson, J. Inorg. Nucl. Chem., 1977, 39, 1989.

24. J. C. Taylor, P. W. Wilson, Acta Cryst., 1974, B30, 1701.

25. E. Jacob, W. Polligkeit, Z. Naturforsch., 1973, 28B, 120.

26. P. W. Wilson, J. Inorg. Nucl. Chem., 1974, 36, 303.

27. P. W. Wilson, ibid., p.1783.

28. K. W. Bagnall, J. G. H. du Preez, B. J. Gellatly, J. H. Holloway, J.C.S. Dalton, 1975, 1963.

29. R. Bougon, T. Bui Huy, P. Charpin, Inorg. Chem., 1975, 14, 1822.

30. P. Joubert, R. Bougon, Compt. rend., 1975, 280, C, 193.

31. P. Joubert, R. Bougon, B. Gaudreau, Can. J. Chem., 1978, 56, 1874.

32. P. Joubert, J. M. Weulersse, R. Bougon, B. Gaudreau, ibid., p.2546.

33. R. Bougon, J. Fawcett, J. H. Holloway, D. R. Russell, Compt. rend., 1978, 287, C, 423.

34. R. Bougon, J. Fawcett, J. H. Holloway, D. R. Russell, J.C.S. Dalton, 1979, 1881.

35. R. D. W. Kemmitt, M. Murray, V. M. McRae, R. D. Peacock, M. C. R. Symons, T. A. O'Donnell, J. Chem. Soc., 1968, 862.

36. A. J. Edwards, G. R. Jones, R. J. C. Sills, J.C.S. Chem. Comm., 1968, 1527.

37. B. Frlec, J. H. Holloway, J.C.S. Dalton, 1975, 535.

38. R. J. Gillespie, B. Landa, Inorg. Chem., 1973, 12, 1383.

39. J. Burgess, B. Frlec, J. H. Holloway, J.C.S. Dalton, 1974, 1740.

40. F. O. Sladky, P. A. Bulliner, N. Bartlett, J.C.S. (A), 1969, 2179.

41. G. J. Schrobilgen, J. H. Holloway, P. Granger, C. Brevard, Inorg. Chem., 1978, 17, 980.

42. D. E. McKee, C. J. Adams, A. Zalkin , N. Bartlett, J.C.S. Chem. Comm., 1973, 26.

43. D. E. McKee, C. J. Adams, N. Bartlett, Inorg. Chem., 1973, 12, 1722.

44. R. J. Gillespie, G. J. Schrobilgen, Inorg. Chem., 1974, 13, 2370.

45. P. Boldrini, R. J. Gillespie, P. R. Ireland, G. J. Schrobilgen, Inorg. Chem., 1974, 13, 1690.

46. R. J. Gillespie, G. J. Schrobilgen, Inorg. Chem., 1974, 13, 765.

47. G. L. Gard, G. H. Cady, Inorg. Chem., 1964, 3, 1745.

48. R. J. Gillespie, G. J. Schrobilgen, J.C.S. Chem. Comm., 1974, 90.

49. B. Frlec, J. H. Holloway, J.C.S. Chem. Comm., 1974, 89.

50. R. J. Gillespie, G. J. Schrobilgen, Inorg. Chem., 1976, 1, 22.

51. B. Frlec, J. H. Holloway, Inorg. Chem., 1976, 15, 1263.

52. A. J. Edwards, J. H. Holloway, R. D. Peacock, Proc. Chem. Soc., 1963, 275.

53. V. M. McRae, R. D. Peacock, D. R. Russell, J.C.S. Chem. Comm., 1969, 62.

54. J. Burgess, C. J. W. Fraser, V. M. McRae, R. D. Peacock, D. R. Russell, J. Inorg. Nucl. Chem., 1976, supplement 183.

55. D. E. McKee, Report 1973, L.B.L., 1814, 93, Nucl. Sci. Abst., 1973, 28(10), 26894.

56. F. Seel, O. Detmer, Z. anorg. allg. Chem., 1959, 301, 113.

57. A. J. Edwards, R. J. C. Sills, J. Chem. Soc. (A), 1970, 2697.

58. M. Schmeisser, W. Ludovici, Z. Naturforsch., 1965, 20b, 602.

59. A. A. Woolf, N. N. Greenwood, J. Chem. Soc., 1950, 2200.

60. A. J. Edwards, G. R. Jones, J. Chem. Soc. (A), 1969, 1467.

61. R. Bougon, T. Bui Huy, A. Codet, P. Charpin, R. Rousson, Inorg. Chem., 1974, 13, 690.

62. M. D. Lind, K. O. Christe, Inorg. Chem., 1972, 11, 608.

63. R. J. Gillespie, G. J. Schrobilgen, Inorg. Chem., 1974, 13, 1230.

64. A. J. Edwards, J. Chem. Soc. (A), 1972, 2325.

65. P. A. W. Dean, R. J. Gillespie, Can. J. Chem., 1971, 1736.

66. A. M. Qureshi, F. Aubke, Can. J. Chem., 1970, 3117.

67. G. M. Begun, A. C. Rutenberg, Inorg. Chem., 1967, 6, 2212.

68. K. O. Christe, W. Sawodny, Inorg. Chem., 1973, 12, 2879.

69. D. E. McKee, N. Bartlett, Inorg. Chem., 1973, 12, 2738.

70. B. K. Morrell, A. Zalkin, A. Tressaud, N. Bartlett, Inorg. Chem., 1973, 12, 2640.

71. A. J. Edwards, G. R. Jones, J. Chem. Soc. (A), 1969, 1651.

72. J. C. Taylor, P. W. Wilson, J. W. Kelly, Acta Cryst., 1973, B29, 7.

73. A. J. Edwards, P. Taylor, Chem. Comm., 1971, 1376.

74. A. J. Edwards, J. Chem. Soc., 1964, 717, 3714.

75. G. J. Kruger, C. W. F. T. Pistorius, A. M. Heyns, Acta Cryst., 1976, B32, 2916.

76. O. Ruff, F. Eisner, Ber., 1907, 40, 2926.

77. O. Ruff, F. Eisner, W. Heller, Z. Anorg. Chem., 1907, 52, 256.

78. E. E. Aynsley, G. Hetherington, P. L. Robinson, J. Chem. Soc., 1954, 1119.

79. R. T. Paine, R. R. Ryan, L. B. Asprey, Inorg. Chem., 1975, 14, 1113.

80. B. G. Ward, F. E. Stafford, Inorg. Chem., 1968, 7, 2569.

81. O. Von Schmitz-Dumont, I. Bruns, I. Heckmann, Z. Anorg. Chem., 1953, 271, 347.

82. K. F. Zmbov, O. M. Uy, J. L. Margrave, J. Phys. Chem., 1969, 73, 3008.

83. F. N. Tebbe, E. L. Muetterties, Inorg. Chem., 1968, 7, 172.

84. A. M. Noble, J. M. Winfield, J. Chem. Soc. (A), 1970, 501.

85. A. D. Webb, H. A. Young, J. Amer. Chem. Soc., 1950, 72, 3356.

86. G. H. Cady, G. B. Hargreaves, J. Chem. Soc., 1961, 1568.

87. L. E. Alexander, I. R. Beattie, A. Bukovszky, P. J. Jones, C. J. Marsden, G. J. van Schalkwyk, J.C.S. Dalton, 1974, 81.

88. A. J. Edwards, G. R. Jones, B. R. Steventon, Chem. Comm., 1967, 462.

89. R. T. Paine, R. S. McDowell, Inorg. Chem., 1974, 13, 2366.

90. R. J. Gillespie, "Molecular Geometry" Van Nostrand Reinhold, London, 1972.

91. A. J. Edwards, B. R. Steventon, J. Chem. Soc. (A), 1968, 2503.

92. A. J. Edwards, G. R. Jones, R. J. C. Sills, Chem. Comm., 1968, 1177.

93. I. R. Beattie, K. M. S. Livingstone, D. J. Reynolds, G. A. S. Ozin, J. Chem. Soc. (A), 1970, 1210.

94. A. J. Edwards, G. R. Jones, J. Chem. Soc. (A), 1968, 2074.

95. I. R. Beattie, D. J. Reynolds, Chem. Comm., 1968, 1531.

96. L. B. Asprey, R. R. Ryan, E. Fukushima, Inorg. Chem., 1972, 11, 3122.

97. G. B. Hargreaves, R. D. Peacock, J. Chem. Soc., 1958, 2170.

98. G. B. Hargreaves, R. D. Peacock, ibid., 1958, 4390.

99. J. H. Holloway, G. J. Schrobilgen, P. Taylor, Chem. Comm., 1975, 40.

100. P. A. Tucker, P. A. Taylor, J. H. Holloway, D. R. Russell, Acta Cryst., 1975, B31, 906.

101. G. B. Hargreaves, R. D. Peacock, J. Chem. Soc., 1960, 1099.

102. T. A. O'Donnell, K. A. Phillips, Inorg. Chem., 1972, 11, 2611.

103. O. Ruff, W. Kwasnik, Z. Anorg. Chem., 1934, 219, 65.

104. E. E. Aynsley, R. D. Peacock, P. L. Robinson, J. Chem. Soc., 1950, 1622.

105. R. T. Paine, Inorg. Chem., 1973, 12, 1457.

106. H. Selig, unpublished communication.

107. R. C. Burns, T. A. O'Donnell, A. B. Waugh, J. Fluorine Chem., 1978, 12, 505.

108. R. D. Peacock, N. Edelstein, J. Inorg. Nucl. Chem., 1976, 38, 771.

109. R. C. Burns, T. A. O'Donnell, Inorg. Nucl. Chem. Letters, 1977, 13, 657.

110. R. T. Paine, R. S. McDowell, Inorg. Chem., 1974, 13, 2366.

111. A. J. Edwards, G. R. Jones, J. Chem. Soc., 1968, 2511.

112. A. J. Edwards, cited by R. D. Peacock, Advan. Fluorine Chem., 1973, 7, 134.

113. A. J. Edwards, G. R. Jones, R. J. C. Sills, J. Chem. Soc., 1970, 2521.

114. B. Krebs, A. Muller, H. H. Beyer, Inorg. Chem., 1969, 8, 436.

115. R. D. W. Kemmitt, D. R. Russell, D. W. A. Sharp, J. Chem. Soc., 1963, 4408.

116. J. H. Burns, Acta Cryst., 1962, 15, 1098.

117. V. Gutmann, K. H. Jack, Acta Cryst., 1951, 4, 246.

118. N. Schrewelius, Z. Anorg. Chem., 1938, 238, 241.

119. G. Teufer, Acta Cryst., 1956, 9, 539.

120. H. Bode, H. Clausen, Z. Anorg. Chem., 1951, 265, 229.

121. H. Bode, H. V. Döhren, Acta Cryst., 1958, 11, 80.

122. M. A. Hepworth, K. H. Jack, G. J. Westland, J. Inorg. Nucl. Chem., 1956, 2, 79.

123. A. M. Heyns, C. W. F. T. Pistorius, Spectrochemica Acta, 1974, 30A, 99.

124. H. Bode, E. Voss, Z. Anorg. Chem., 1951, 264, 144.

125. H. Bode, Z. Anorg. Chem., 1951, 267, 62.

126. R. J. Gillespie, B. Landa, Inorg. Chem., 1973, 12, 1383.

127. O. L. Keller, Inorg. Chem., 1963, 2, 783.

128. J. Cox, J. Chem. Soc., 1956, 876.

129. H. Bode, G. Teufer, Z. Anorg. Chem., 1952, 268, 20.

130. G. Hargreaves, R. D. Peacock, J. Chem. Soc., 1957, 4212.

131. H. M. Rietveld, Acta Cryst., 1966, 20, 508.

132. H. M. Rietveld, Acta Cryst., 1967, 22, 151.

133. H. M. Rietveld, J. Appl. Cryst., 1969, 2, 65.

134. W. P. Klug, L. E. Alexander, X-Ray Diffraction Procedures, 1959, 2nd. Ed. p.251, New York, John Wiley.

135. G. Caglioti, A. Paoletti, F. P. Ricci, Nucl. Instrum., 1958, 3, 223.

136. M. W. Thomas, REFINE, UKAEA Harwell.

137. A. Bystrom, Arkiv Kem., 1943, 8, 17B.

138. I. Kay, Acta Cryst., 1961, 14, 80.

139. J. Leciewicz, Acta Cryst., 1961, 14, 66.

140. F. A. Wedgewood, UKAEA research group report, 1968, R-5802.

141. B. Cox, A. G. Sharpe, J. Chem. Soc., 1953, 1783.

142. J. L. Hoard, W. B. Vincent, J. Amer. Chem. Soc., 1939, 61, 2849.

143. G. R. Clark, D. R. Russell, Acta Cryst., 1978, B34, 894.

144. H. Bode, W. Wendt, Z. Anorg. Chem., 1952, 269, 165.

145. R. J. Williams, D. R. Dillin, W. O. Milligan, Acta Cryst., 1973, B29, 1369.

146. A. Zalkin, J. D. Forrester, D. H. Templeton, Acta Cryst., 1964, 17, 1408.

147. R. Hoppe, W. Dähne, Naturwiss., 1960, 47, 397.

148. Ch. Hebecker, H. G. Schnering, R. Hoppe, Naturwiss., 1966, 53, 154.

149. B. Cox, J. Chem. Soc., 1953, 197.

150. B. Cox, J. Chem. Soc., 1954, 3251.

151. R. D. Peacock, Prog. Inorg. Chem., 1960, 2, 193-249.

152. R. Hoppe, W. Liebe, W. Dähne, Z. Anorg. Allgem. Chem., 1961, 307, 276.

153. G. Siebert, R. Hoppe, Z. Anorg. Allgem. Chem., 1972, 391, 113.

154. R. Hoppe, H. Henkel, Z. Anorg. Chem., 1968, 359, 160.

155. G. Brunton, Acta Cryst., 1973, B29, 2294.

156. C. Cipriani, Rend. Soc. Mineral Ital., 1954, 10, 253; ibid., 1955, 11, 58.

157. D. H. Brown, K. R. Dixon, R. D. W. Kemmitt, J. Chem. Soc., 1965, 1559.

158. B. Cox, D. W. A. Sharp, A. G. Sharpe, J. Chem. Soc., 1956, 1242.

159. M. A. Hepworth, P. L. Robinson, G. J. Westland, J. Chem. Soc., 1958, 611.

160. G. Brunton, Acta Cryst., 1969, B25, 2164.

161. J. A. A. Ketelaar, Z. Krist., 1935, 92A, 155.

162. H. Bode, R. Brockmann, Z. Anorg. Chem., 1952, 269, 173.

163. R. Huss, W. Klemm, Z. Anorg. Allgem. Chem., 1950, 262, 25.

164. H. Bode, E. Voss, Z. Anorg. Chem., 1956, 286, 136.

165. N. Bartlett, J. W. Quail, J. Chem. Soc., 1961, 3728.

166. R. Hoppe, W. Klemm, Z. Anorg. Allgem. Chem., 1952, 268, 364.

167. D. P. Mellor, N. C. Stephenson, Aust. J. Sci. Res., 1951, 4A, 406.

168. A. G. Sharpe, J. Chem. Soc., 1953, 197.

169. H. Bode, G. Teufer, Acta Cryst., 1956, 9, 929.

170. R. Hoppe, B. Mehlhorn, Z. Anorg. Allgem. Chem., 1976, 425, 200.

171. S. Siegel, Acta Cryst., 1952, 5, 683.

172. J. L. Hoard, W. B. Vincent, J. Amer. Chem. Soc., 1942, 64, 1233.

173. R. Hoppe, B. Hofmann, Z. Anorg. Allgem. Chem., 1977, 436, 65.

174. R. D. Peacock, J. Chem. Soc., 1956, 1291.

175. E. Weise, Z. Anorg. Allgem. Chem., 1956, 283, 377.

176. H. Bode, G. Teufer, Z. Anorg. Allgem. Chem., 1956, 283, 18.

177. R. W. G. Wyckoff, J. H. Müller, Am. J. Sci., 1927, 13, 347.

178. B. Gossner, O. Kraus, Z. Krist., 1934, 88, 223.

179. E. O. Schlemper, W. C. Hamilton, J. Chem. Phys., 1966, 44, 2499; ibid., 45, 408.

180. B. K. Vajnstejn, M. M. Stasova, Kristollografija SSSR, 1956, 1, 311.

181. B. K. Vajnstejn, R. N. Kurdjumova, Kristollografija, 1958, 3, 29.

182. B. Cox, A. G. Sharpe, J. Chem. Soc., 1954, 1798.

183. R. W. G. Wyckoff, E. Posnjak, J. Am. Chem. Soc., 1921, 43, 2292.

184. W. C. Hamilton, Acta Cryst., 1965, 18, 502.

185. D. Pilipovich, United States patent 3,963,542, 1976.

186. W. C. Price, T. R. Passmore, D. M. Roessler, Discussions Faraday Soc., 1963, 35, 201.

187. J. N. Wilson. Paper presented at Symposium on Advanced Propellant Chemistry, Am. Chem. Soc., Detroit, Michigan, 1965.

188. K. O. Christe, J. P. Guertin, A. E. Pavlath, Inorg. Nucl. Chem. Letters, 1966, 2, 83.

189. K. O. Christe, J. P. Guertin, A. E. Pavlath, Inorg. Chem., 1966, 5, 1921.

190. W. E. Tolberg, R. T. Rewick, R. S. Stringham, M. E. Hill, Inorg. Nucl. Chem. Letters, 1966, 2, 79.

191. W. E. Tolberg, R. T. Rewick, R. S. Stringham, M. E. Hill, Inorg. Chem., 1967, 6, 1156.

192. S. M. Sinel'nikov, V. Ya. Rosolovskii, Dokl. Akad. Nauk. SSSR, 1970, 194, 1341.

193. V. Ya. Rosolovskii, V. I. Nefedov, S. M. Sinel'nikov, Izv. Akad. Nauk. SSSR, Ser. Khim., 1973, 7, 1445.

194. C. T. Goetschel, V. A. Campanile, R. M. Curtis, K. R. Loos, D. C. Wagner, J. N. Wilson, Inorg. Chem., 1972, 11, 1696.

195. K. O. Christe , R. D. Wilson, A. E. Axworthy, Inorg. Chem., 1973, 12, 2478.

196. K. O. Christe , C. J. Schack, R. D. Wilson, Inorg. Chem., 1976, 15, 1275.

197. S. P. Mishra, M. C. R. Symons, K. O. Christe , R. D. Wilson, R. I. Wagner, Inorg. Chem., 1975, 14, 1103.

198. K. O. Christe , R. D. Wilson, C. J. Schack, Inorg. Chem., 1977, 16, 937.

199. D. Clark, H. M. Powell, A. F. Wells, J. Chem. Soc., 1942, 642.

200. I. R. Beattie, K. M. S. Livingstone, G. A. Ozin, D. J. Reynolds, J. Chem. Soc., 1969, 958.

201. K. O. Christe , D. Pilipovich, Inorg. Chem., 1971, 10, 2803.

202. R. A. Pennemann, Inorg. Chem., 1967, 6, 431.

203. K. O. Christe , private communication.

204. H. Goldschmidt, O. Udby, Z. Physik. Chem., 1907, 60, 728.

205. A. Hantzsch, Z. Physik. Chem., 1908, 61, 257.

206. J. O. Lundgren, I. Olovsson, The Hydrogen Bond, Vol. II, Chapter 10, North-Holland Publishing Co., 1976, p.473.

207. J. O. Lundgren, J. M. Williams, J. Chem. Phys., 1973, 58, 788.

208. J. O. Lundgren, R. Tellgren, I. Olovsson, to be published.

209. J. M. Williams, The Hydrogen Bond, Vol. II, Chapter 14, North-Holland Publishing Co., 1976, p.656.

210. L. Basile, P. LaBonville, J. R. Ferraro, J. M. Williams, J. Chem. Phys., 1974, 60, 1981.

211. B. S. Ault, G. C. Pimentel, J. Phys. Chem., 1973, 77, 57.

212. B. Bonnet, J. Roziere, R. Fourcade, G. Mascherpa , Can. J. Chem., 1974, 52, 2077.

213. R. Bougon et al., private communication.

214. K. O. Christe , C. J. Schack, R. D. Wilson, Inorg. Chem., 1975, 14, 2224.

215. J. P. Masson, J. P. Desmoulin, P. Charpin, R. Bougon, Inorg. Chem., 1976, 15, 2529.

216. H. Selig, W. A. Sunder, F. A. Disalvo, W. E. Falconer, J. Fluorine Chem., 1978, 11, 39.

217. J. Strähle, K. Dehnicke, Z. Anorg. Chem., 1965, 338, 287.

218. K. Dehnicke, J. Strähle, Z. Anorg. Chem., 1965, 339, 171.

219. K. Dehnicke, J. Inorg. Nucl. Chem., 1965, 27, 809.

220. G. W. Fraser, M. Mercer, R. D. Peacock, J. Chem. Soc. (A), 1967, 1091.

221. G. W. Fraser, C. J. W. Gibbs, R. D. Peacock, J. Chem. Soc. (A), 1970, 1708.

222. A. M. Noble, J. M. Winfield, J. Chem. Soc. (A), 1970, 501; idem ibid, 2574.

223. F. Brinckman, R. B. Johannesen, L. B. Hardy, J. Fluorine Chem., 1972, 1, 493.

224. A. Majid, R. L. McLean, D. W. A. Sharp, J. M. Winfield, Z. Anorg. Chem., 1971, 385, 85.

225. A. Majid, D. W. A. Sharp, J. M. Winfield, I. Henley, J. Chem. Soc. (Dalton), 1973, 1876.

226. M. Winnewisser, R. L. Cook, J. Chem. Phys., 1964, 41, 999.

227. A. Mugnoli, C. Mariani, M. Simonetta, Acta Cryst., 1965, 19, 367.

228. R. L. Livingstone, C. N. Ramachandra Rao, J. Phys. Chem., 1960, 64, 756.

229. K. Kimura, K. Katada, S. H. Bauer, J. Am. Chem. Soc., 1966, 88, 416.